DESIGN, PREPARATION AND CHARACTERIZATION OF POLYMER INCLUSION MEMBRANES AS AN EMERGING TECHNIQUE FOR PRECONCENTRATION AND SPECIATION MEASUREMENTS

Ruben Vera Chamorro

Universitat de Girona

Doctoral Thesis

Design, preparation and characterization of polymer inclusion membranes as an emerging technique for preconcentration and speciation measurements

Ruben Vera Chamorro

2019

Doctoral programme in water science and technology

Supervised by:

Dr. Clàudia Fontàs

Dr. Enriqueta Anticó

Thesis submitted in fulfilment of the requirements for the degree of Doctor from the University of Girona.

Universitat de Girona

Dr. Clàudia Fontàs and Dr. Enriqueta Anticó, of the University of Girona,

WE DECLARE:

That the thesis entitled "Design, preparation and characterization of polymer inclusion membranes as an emerging technique for preconcentration and speciation measurements", presented by Ruben Vera Chamorro to obtain a doctoral degree, has been completed under our supervision and meets the requirements to qualify for an International Doctorate.

For all intents and purposes, we hereby sign this document.

Dr. Clàudia Fontàs

Dr. Enriqueta Anticó

Girona, 4 February of 2019

This thesis was financially supported by the Spanish Ministry of Economy and Competitiveness (MINECO) through the national research projects CTM2013-48967-C2-2-P, CTM2016-78798-C2-2-P (AEI/FEDER/UE), through a predoctoral research fellowship (BES-2014-068316), and through a grant for short-term stays (EEBB-I-17-12404).

“Come as you are, as you were

As I want you to be

As a friend, as a friend

As an old enemy

Take your time, hurry up

Choice is yours, don't be late

Take a rest as a friend

As an old memoria”

Nirvana (Nevermind, 1991)

Agraïments / Acknowledgements

Ara que malauradament s'acaba aquesta etapa, m'agradaria escriure unes paraules a totes aquelles persones amb les quals he tingut la sort de compartir bons moments i que han fet que aquest llarg viatge que m'ha portat a escriure una tesi hagi sigut completament especial.

En primer lloc m'agradaria agrair a les dues persones que principalment han fet possible que estigui ara escrivint tot això, a la Clàudia i l'Enriqueta. Gràcies Clàudia per haver-me donat l'oportunitat al 2012 (com passa el temps...), no només d'acceptar-me com el teu estudiant per a fer el treball experimental de final de carrera, amb el qual vaig començar a endinsar-me en el món de la investigació, sinó també per comptar amb mi pel projecte amb l'empresa Dena Desarrollos S.A i posteriorment oferir-me realitzar aquesta tesi amb la beca del ministeri. T'estaré sempre agraït no només per totes les oportunitats que m'has donat en aquest temps, sinó també per haver-me permès assistir a diversos congressos nacionals i internacionals i poder haver viscut durant prop de mig any a l'altra punta de món, on vaig aprendre moltíssimes coses. Moltes gràcies Enriqueta per totes les converses i moments viscuts al llarg d'aquesta tesi. Ha sigut una gran sort tenir-te també de directora d'aquesta tesi. A totes dues m'agradaria dir-vos que ha sigut realment gratificant poder compartir tot aquest temps junts, contagiant-me de la vostra passió pel que feu cada dia i haver après tan com he pogut de tot el que m'heu ensenyat.

També m'agradaria agrair a la resta de professors que formen l'àrea de química analítica i ambiental de la Universitat de Girona com son l'Eva Marguí, per tota l'ajuda rebuda durant el meu treball de final de carrera, a la Mònica per tots els dubtes i problemes resolts amb el vell i estimat ICP-OES, a la Victòria, la Nela i en Juanma per tota l'amabilitat rebuda durant tot aquests anys. No puc oblidar tampoc la gran amabilitat d'en Josep Galceran i tot el grup de recerca de Lleida així com de l'Olga Serra, amb els quals he tingut la sort de treballar en l'elaboració d'algunes de les publicacions d'aquesta tesi. No puedo olvidarme tampoco de Juana Benavente, a la que guardo un especial cariño por su amabilidad, cercanía y humildad lo cual ha hecho que trabajar con ella haya sido todo un placer. Gracias por tratarnos tan bien durante nuestra breve estancia en Málaga y ofrecerte para resolver cualquier duda.

També vull agrair als antics membres del grup de química analítica i ambiental amb els quals vaig coincidir a la meva primera etapa del doctorat, a la Dolors Companys, Mònica

Alonso, Anna Godayol i Ester Sagristà. Gràcies als grans consells de la Carme Valls i la Raquel Güell, els quals em van ajudar a decidir-me i encarar el doctorat de la millor manera. I que puc dir de l'Aida Garcia, des del primer moment que vam coincidir, sempre et vas disposar a ajudar-me amb qualsevol cosa, s'aprèn molt d'algú com tu. Gràcies per haver inaugurat la ruta Girona-Melbourne i per tots els consells i experiències compartides. Tampoc puc oblidar-me de membres d'altres àrees, amb els que he coincidit en sopars quan encara eren doctorands, com en Pep Antón, la Cristina Rosés o la Iteng Choi. A tots els anteriorment anomenats, us desitjo el millor en la vostra vida personal i professional.

I can't forget to mention two amazing guys that I also met right at the beginning of my thesis. It was a big pleasure to share things with you, Subha and Santanu. Subha, I still remember when you compared me with a bottle of wine in the acknowledgements of your thesis, I am extremely happy that everything is going awesome in your life. It is impossible to forget either all the discussions and tips provided by Santanu and I really appreciate all the knowledge you shared with me about India. I keep very nice memories from both of you and, although thousands of kilometres separate us, we are still in touch and it is always so nice to hearing from you. I wish you all the best for your future endeavours not only professionally but also in life!

Moreover, I also met a crazy Turkish guy that was an *incredible* discover. The *real perfect man*, as you used to say. We lived very funny moments inside the lab but also outside the university. Thanks for all the Turkish words you tried to teach me. I wish we could catch up soon.

Tampoc em puc oblidar de totes les persones que en un moment o altra han aparegut pels laboratoris d'analítica, ja sigui degut al treball final de grau, a pràctiques en empresa o a breus estades de doctorat. Tirant la vista enrere, m'adono que he viscut moments realment únics. Moltes gràcies a tots aquells amb els quals he compartit bons moments: Anna Ballesteros, Gerard Serrat, Andreu Llort, Vanessa Vivet, Eline Michielsen, Albert Solanas, Cristina Turón (x2), Michiel Vereeke, Adrià Casanovas, Ester López, Cristina Juanola, Clàudia Martínez (Clàudia Jr.), Eva Sigüenza, Eva Mateo, Silvia Montero, David Palma, Sindy Carolina, Ibrahim, Karima, Mouhamed Dekkouche, Rogerta Dalipi, Albert Salado, Miquel "*de Ses Illes*", Sergi Cot, Roger, Soetkin Leys, Donatella Chillè "*la calapacci*". D'altra banda, la calma i la pau del passadís es van veure afectats per 3 persones que van coincidir en el temps i en l'espai: l'Albert Rodríguez, en Gerard Samsó i la Cristina García. Encara avui, queden moltes paraules i expressions d'aquells dies: el velero, aúpa ahí, etc. Eskerrik asko a los tres!

També, cal destacar i recordar la gran feina de la "*comissió de festes del departament de química*" formada per l'Àngel Oliveras, la Cristina Camó, l'Ester Manrique i en Martí Wang. Ells van ser els responsables de molts dels dinars de nadal i primavera, organitzats al departament. Us desitjo el millor!

Un apartat d'aquests agraïments ha d'anar dirigit obligatòriament a la Laura Torrent i a la Gemma Elias. Laura, vam començar alhora aquest llarg camí que suposa fer un doctorat, hem patit, hem rigut, hem après noves paraules i hem crescut junts durant aquests anys. Gràcies per tots els moments viscuts. A tu Gemma, gràcies per totes les converses que hem tingut durant tots aquests anys i per totes les experiències que hem compartit junts. A totes dues us desitjo el millor a la vostra vida personal (que al final és la mes important) així com a la professional, us ho mereixeu!

De la mateixa manera voldria agrair a la Gemma Mostazo també coneguda per *little Gemma*, per tots els petits moments i totes les converses i riures que hem viscut, ha sigut genial compartir despatx tot aquests temps amb vosaltres!

I would also like to thank all the members of Kolev's research group from the University of Melbourne where I spent almost five months conducting a part of this thesis. I really appreciate all the kindness, sincere support and mentorship received during my stay. It was a real rewarding experience, which it has been extremely useful not only for the development of my thesis but also for my future life endeavours. Thanks to all the students of the research group: Lenka Sraj, Mason Bonacci, Justin Cheng, Charles Croft, Bosirul Hoque, Edward Nagul, Neda Nematollahi, Fidelis Nitti, Jonathan Peters, Syane Agacy and Madeline King. Of course I can't forget to thank Patrick Mornane for helping me out assembling the Flow analysis system, Yanlin Zhang who shared his wisdom and answered me hundreds of questions as well as he took me to collect river water samples and Inês G. S. Almeida, an incredible researcher, who is always ready to solve your upcoming problems. Thanks Inês for all the support received throughout the project, it was really special to catch up last year in Girona! I would also like to acknowledge the honorary staff, Robert W. Cattrall and Ian D. Mckelvie. Robert turns regular Thursdays into a special day because of the chocolate's tradition while taking a cup of coffee. An adorable tradition that I was lucky to join almost every week during my stay. Thanks Ian for all the useful tips and to strongly encourage me to visit different places while I was in Australia. Lastly, but no less important I would like to thank Spas for all the things you have done for me. I couldn't

have got a better supervisor for my international stay. I tried to learn as much as I could from one of the best researchers I have ever met. Your dedication and passion for your work are contagious and creates an incredible atmosphere in the whole research group. If I had to repeat an international stay I wouldn't have a doubt to join again your group. I will always remember my *ozzy* experience in such a lovely research group.

I would also like to highlight the good memories that I shared with Lucie Zelena, Victoria, Shaif Salik, Eri Makri, Prakhar Bhargava, Amer, Avi Gandhi, Muzay, Mayu Sasakura, Soumya Mukherjee, Shubham Rawal, Melissa Kennedy, Claudio Pacciarelli, Joshua Rhee and many others!! All the above-mentioned made my Melbourne experience amazing, thank you all!

A mis compañeros de la capital que conocí en Melbourne: Esther, Cecilia, José y Germán os deseo lo mejor en vuestros proyectos personales! No me cabe duda que en cuanto al tema profesional no hace falta que os desee suerte. Espero que nos podamos ver pronto todos en Madrid o Girona. ¡De momento ya he visto a Germán y Esther!

A vosaltres, Bernat Riera, Albert Manso i Ernest Iñigo, us podria dedicar un parell de fulls, però ho resumiré de forma breu, donant-vos les gràcies per ser-hi sempre. Espero i desitjo que l'amistat continuï per molts més anys. Gràcies també a la Laura "Gonfaus" i a la Julia per totes les converses i moments viscuts al llarg de tots aquests anys d'amistat.

Durant aquest doctorat també he après a donar importància als petits moments, a tot el que ens envolta el dia a dia i als detalls que sovint no acabem de valorar completament. Haver-te conegut Jordi Gascons ha sigut una de les millors coses que m'han passat mai. És molt gran tot el que transmets a la resta que t'envolta. Ha sigut un gran regal vital poder-te conèixer i compartir tants moments únics durant aquests anys. T'asseguro que sempre podràs comptar amb mi. També agrair a la Dolors, l'Amadeu i l'Enric per sempre haver tingut un tracte tan especial i afectuós amb mi. No puc deixar enrere a la Sandra, amb la qual he compartit infinitat d'instants durant tot aquest temps i que han fet que aquest doctorat fos molt més fàcil de portar endavant. Res de tot això hagués sigut possible sense la teva ajuda.

Ja per concloure, agrair a la meva família: pares, germà i avis, per tot el suport rebut durant tots aquests anys de formació, gràcies per tota l'ajuda i suport que m'heu anat donant al llarg d'aquests 28 anys. A vosaltres, Elsa i Ian, tan sols us desitjo que sigui quin sigui el

camí que escolliu quan sigueu grans, que hi poseu totes les ganes i empenta en fer allò que mes us agradi i motivi.

Moltes gràcies a tots, els que he anomenat i als que malauradament hagi pogut oblidar. I a tu, siguis qui siguis, gràcies per mirar-te aquesta tesi, encara que només siguin els agraïments, perquè representa una etapa de mes de quatre anys de la meva vida.

PUBLICATIONS LIST

This thesis meets all the requirements to be presented as a compendium of publications and has resulted in the publication of six scientific articles and one submitted.

R. Vera, C. Fontàs, E. Anticó, Titanium dioxide solid phase for inorganic species adsorption and determination: the case of arsenic, Environ. Sci. Pollut. Res. 24 (2017) 10939-10948.
DOI: https://doi.org/10.1007/s11356-016-7667-0
Impact factor: 2.800
Quartile: Q2

R. Vera, L. Gelde, E. Anticó, M.V. Martínez de Yuso, J. Benavente, C. Fontàs, Tuning physicochemical, electrochemical and transport characteristics of polymer inclusion membrane by varying the counter-anion of the ionic liquid Aliquat 336, J. Memb. Sci. 529 (2017) 87-94.
DOI: https://doi.org/10.1016/j.memsci.2017.01.055
Impact factor: 6.578
Quartile: Q1

R. Vera, C. Fontàs, J. Galceran, O. Serra, E. Anticó, Polymer inclusion membrane to access Zn speciation: Comparison with root uptake, Sci. Total Environ. 622-623 (2018) 316-324.
DOI: https://doi.org/10.1016/j.scitotenv.2017.11.316
Impact factor: 4.610
Quartile: Q1

R. Vera, S. Insa, C. Fontàs, E. Anticó, A new extraction phase based on a polymer inclusion membrane for the detection of chlorpyrifos, diazinon and cyprodinil in natural water samples, Talanta 185 (2018) 291-298.
DOI: https://doi.org/10.1016/j.talanta.2018.03.056
Impact factor: 4.244
Quartile: Q1

R. Vera, E. Anticó, C. Fontàs, The Use of a Polymer Inclusion Membrane for Arsenate Determination in Groundwater, Water 10 (2018) 1093.
DOI: https://doi.org/10.3390/w10081093
Impact factor: 2.069
Quartile: Q2

R. Vera, Y. Zhang, C. Fontàs, M.I.G.S Almeida, E. Anticó, R.W. Cattrall, S.D. Kolev, Automatic determination of arsenate in drinking water by flow analysis with dual membrane-based separation, Food Chem. 283 (2019) 232-238.
DOI: https://doi.org/10.1016/j.foodchem.2018.12.122
Impact factor: 4.946
Quartile: Q1

R. Vera, E. Anticó, N. Aranburu, C. Fontàs, First report on a solvent-free preparation of polymer inclusion membranes with an ionic liquid, React. Funct. Polym. (submitted).

ABBREVIATIONS LIST

2-FP2-NPE	2-fluorophenyl 2-nitrophenyl ether
A	Absorbance
ACA	Catalan Water Agency
ACN	Acetonitrile
AFM	Atomic force microscopy
AFS	Atomic fluorescence spectroscopy
AGNES	Absence of gradient Nernstian equilibrium stripping
AHS	Agricultural Health Study
Aliquat 336 / AlqCl	Methyltrioctylammonium chloride
AMPA	Aminomethylphosphonic acid
AOAC	Association of Official Analytical Chemists
AR	Absolute recovery
ASV	Anodic stripping voltammetry
ATR	Attenued total reflectance
BBPA	Bis(1-butylpentyl) adipate
BE	Binding energy
BLM	Biotic Ligand Model
BLM	Bulk liquid membrane
Bmim	1-butyl-3-methyl imidazolium
BuDC18C6	Di-tert-butylcyclohexano-18-crown-6
C	Concentration in the effluent measured
C_0	Initial concentration
CA	Cellulose acetate
CAB	Cellulose acetate butyrate
CAH	Cellulose acetate hydrogen phthalate
CAP	Cellulose acetate propionate
CCA	Chromated-copper-arsenate
CLE-AdCSV	Competitive ligand equilibration-adsorptive cathodic stripping voltammetry

Cmax	Maximum adsorption capacity
CMPO	Octyl(phenyl)-N,N-diisobutyl carbamoylmethyl phosphine oxide
CP	Chlorpyrifos
CPE	Cloud-point extraction
CTA	Cellulose triacetate
CTAB	Cetyltrimethylammonium bromide
CTB	Cellulose tributyrate
cv	Cultivated variety
Cyanex 272	Bis(2,4,4-trimethylpentyl)phosphinic acid
Cyanex 301	Bis(2,4,4-trimethylpentyl)dithiophosphinic acid
Cyanex 302	Bis(2,4,4-trimethylpentyl)monothiophosphinic acid
Cyanex 471X	Tri-isobutylphosphine sulfide
CYP	Cyprodinil
Cyphos 101	Trihexyl(tetradecyl)phosphonium chloride
Cyphos 104	Trihexyl(tetradecyl)phosphonium-(2,4,4-trimethylpentyl)phosphinate
D2EHDTPA	Di(2-ethylhexyl) dithiophosphoric acid
D2EHPA	Di(2-ethylhexyl) phosphoric acid
DBBP	Dibutyl butyl phosphonate
DBP	Dibutyphtalate
DBS	Dibutylsebacate
DDT	Dichlorodiphenyltrichloroethane
DEHA	bis(2-ethylhexyl) adipate
DGT	Diffusive gradient in thin-film gels
DMA	Dimethylarsinic acid
DMT	Donnan membrane techniques
DNNDS	Dinonylnaphthalene disulfonic acid
DNNS	Dinonylnaphthalene sulfonic acid
DOP	Dioctyl phthalate
DPC	Diphenylcarbazide
DSC	Differential scanning calorimetry

DSMA	Disodium methanearsonate
DTPA	Diethylenetriaminepentaacetic acid
DZ	Diazinon
e.g.	For example
EB	Ethyl benzoate
ECD	Electron capture detector
EDTA	Ethylenediaminetetraacetic acid
EDXRF	Energy dispersion X-ray fluorescence
EE	Extraction efficiency
EI	Electron impact
ELM	Emulsion liquid membrane
EPA	Environmental Protection Agency
Eq.	Equation
et.al	And others
EU	European Union
EXAFS	X-ray absoprtion fine structure
FA	Flow analysis
FAO	Food and Agriculture Organization
FDA	Fluorescein di-acetate
FIA	Flow Injection analysis
FIAM	Free Ion Activity Model
FTIR	Fourier transform infrared spectroscopy
GC	Gas chromatography
GC-ECD	Gas chromatography coupled to electron capture detector
GC-FPD	Gas chromatography coupled to flame photometric detector
GC-ITMS	Gas chromatography coupled to ion trap mass spectrometry
GC-NPD	Gas chromatography coupled to nitrogen phosphorous detector
GC-QqQ	Gas chromatography coupled to triple quadrupole mass spectrometry
GDC	Gas-diffusion cell
GFAAS	Graphite furnace atomic absorption spectrometry

GLYP	Glyphosphate
GW	Groundwater
h	Hours
ha	Hectare
HA	Humic acid
HF	Holow fibre
HG-AAS	Hydride generation atomic absorption spectrometry
HG-AFS	Hydride generation atomic fluorescence spectrometry
HG-ICP-OES	Hydrde generation inductively coupled plasma optical emission spectrometry
HPLC	High performance liquid chromatography
i.d.	Internal diameter
i.e.	Id est (that is)
IARC	International Agency for Research on Cancer
IC	Ion chromatography
ICP-AES	Inductively coupled plasma atomic emission spectrometry
ICP-MS	Inductively coupled plasma mass spectrometry
IDL	Instrumental detection limit
IL	Ionic liquid
IR	Infrared
IS	Impedance spectroscopy
ISE	Ion-selective electrode
IUPAC	International Union of Pure and Applied Chemistry
IV	Injection valve
J_{PIM}	PIM flux
J_{root}	Root flux
Kelex 100	7-(4-Ethyl-1-methyloctyl)-8-hydroxyquinoline
Kow	Octanol-water partitioning coefficient
LC	Liquid chromatography
LED	light emitting diode
LIX® 84-1	2-Hydroxy-5-nonylacetophenone oxime

LLE	Liquid-liquid extraction
LM	Liquid membrane
LOD	Limit of detection
LOQ	Limit of quantification
LPME	Liquid-phase microextraction
m/z	Mass to charge ratio
MDL	Method detection limit
ME	Matrix effect
MES	acid 2-(N-morpholino) ethanesulfonic
MMA	Monomethylarsonic acid
MRM	Multiresidue methods
MS	Mass spectrometry
MSMA	Monosodium methanearsonate
MW	Molecular weight
MWc	Critical entanglement molecular weight
n	number of replicates
NAA	Neutron activation analysis
NPD	Nitrogen phosphorous detector
NPOE	2-nitrophenyloctyl ether
NPOT	2-Nitrophenyl octanoate
NPPE	2-nitrophenylpentyl ether
OCs	Organochlorines
OPPs	Organophosphate pesticide
OPs	Organophosphates
PCL	Poli $\boldsymbol{\varepsilon}$-caprolactone
PDMS	Polydimethylsiloxane
PEEK	Polyetheretherketone
PEG-DA	Poly(ethylene glycol) diacrylate
PEG-DMA	Poly(ethylene glycol) dimethacrylate
pH_{pzc}	pH at the point of zero charge

PI	Propidium iodide
PIM	Polymer Inclusion Membrane
PLM	Permeation liquid membrane
POCIS	Polar organic chemical integrative sampler
PTFE	Poly(tetrafluoroethylene)
PVC	Poly(vinyl chloride)
PVDF-HFP	Poly(vinylidine fluoride-cohexafluoropropylene)
PVDF-TFE	Poly(vinylidene fluoride-co-tetrafluoroethylene)
PVP	Poly(vinylpyrrolidone)
R	Recovery
R^2	Coefficient of determination
RC	Reaction coil
RIMM	Reflection infrared mapping microscopy
RSD	Relative standard deviation
S/N	Signal noise ratio
SBSE	Stir-bar sorptive extraction
SCP	Stripping chronopotentiometry
SD	Standard deviation
SDDC	Silver diethyldithiocarbamate
SEM	Scanning electron microscope
SEM-EDS	Scanning electron microscope-energy dispersive spectroscopy
SFA	Segmented flow analysis
SGW	Simulated groundwater
SIA	Sequential injection analysis
SLM	Supported liquid membrane
SMX	Sulfamethoxazole
SPE	Solid-phase extraction
SPMD	Semipermeable membrane device
SPME	Solid-phase microextraction
SRM	Selected reaction monitoring mode

TBA	Tri-n-butylamine
TBEP	Tris(2- butoxyethyl) phosphate
TBP	Tri-n-butyl phosphate
TDA	Tri-n-decylamine
TDPNO	4-(1'-n-tridecyl)pyridine N-oxide
TE	Transport efficiency
TEHP	Tris-(2-ethylhexyl) phosphate
Tg	Transition temperature
TGA	Thermogravimetric analysis
THA	Tri-n-hexylamine
THF	Tetrahydrofuran
TIMM	Transmission infrared mapping microscopy
Tm	Melting temperature
TMS	Teorell-Meyer-Sievers
TOA	Tri-n-octyl amine
TOC	Total organic carbon
TODGA	N,N,N',N'-Tetraoctyl-3-oxapentanediamide
TOMA	Trioctylmethylammonium
TOPO	Tri-n-octyl phosphine oxide
TPU	Thermoplastic polyurethane
TWA	Time weight average
UAE	Ultrasonic assisted extraction
UV-Vis	Ultraviolet-visible
UN	United Nations
Unicef	United Nations Children's Fund
USA	United States of America
USD	United State Dollar
vs.	Versus
WFD	Water Framework Directive
WHO	World Health Organization

w/w	Weight by weight
XANES	X-ray absorption near-edge structure
XIC	Extracted-ion chromatogram
XPS	X-ray photoelectron spectroscopy
XRD	X-ray diffraction
XRF	X-ray fluorescence
Zincon	2-carboxy-2 '-hydroxy-5 '-sulfoformazylbenzene
LLME	Liquid-liquid microextraction
DLME	Dispersive liquid-liquid microextraction
SDME	Single drop microextraction

FIGURES LIST

TABLES LIST

TABLE OF CONTENTS

ABSTRACT

Water is essential for humankind not only for its direct consumption but also for its multiple applications in industry or agriculture, among others. The presence of undesirable substances or pollutants directly affects its quality. Therefore, it is of paramount importance to develop analytical methodologies which permit the detection and/or quantification of different species or compounds that can restrict their usage.

The research presented in this thesis is focused on the design, preparation and characterization of new analytical methodologies based on functionalized membranes for the preconcentration and speciation of pollutants in the aqueous environment.

Frequently, the direct analysis of environmental samples cannot be achieved due to the high complexity of the matrix, or because the concentration of the different compounds is found below the technique's detection limit. Thus, a previous preconcentration step is needed that allows separation and/or preconcentration in order to remove interferences and/or improve compound detection at low levels. It is also important to obtain information about the different chemical species present in the sample, as toxicity is often species-related. The design of devices which allow the miniaturization and automation of the whole process as well as enabling *in situ* analysis is also relevant.

Taking into account all the aforementioned aspects, in this thesis we have developed simple and innovative analytical methods based on polymer inclusion membranes (PIMs) for water sample treatment in order to facilitate its analysis. Hence, we have developed a PIM-based device, using Aliquat 336 as the carrier, which has allowed satisfactory arsenate determination in groundwater samples. Besides, an analogous membrane has been coupled into a flow analysis system allowing the online detection and determination of arsenate. Furthermore, the use of a commercial sorbent based on titanium dioxide, named Adsorbsia As600, has been explored and has shown great retention capacity towards both inorganic arsenic species. The use of minicolumns embedded with this sorbent has facilitated the detection of total arsenic in water samples.

We have focused not only on the preparation of PIMs but also on the characterization of physicochemical and electrochemical properties by modifying the ionic liquid (IL), using Aliquat 336 as a carrier. Depending on the hydrophilic nature of the membrane, the results have shown a direct impact on its efficiency in transport systems. Furthermore, in order to reduce the impact on the environment, a new PIM

preparation methodology has been developed that avoids the use of harmful solvents and at the same time uses polymers from renewable or biodegradable sources for the first time.

PIMs containing D2EHPA as the carrier, have been used as an emerging technique to conduct zinc speciation studies from a nutrient solution. Results have shown that the metal flow through the membrane is proportional to its free fraction, despite the presence of various organic ligands. Moreover, we have related PIM results with the internalization of metal in the roots of potato plants (*Solanum tuberosum*), showing that different processes intervene in the internalization of metal in plants that are not observed in chemical systems.

Finally, another innovative application of PIMs has been presented based on its satisfactory use as a sorbent for the preconcentration of three pesticides. The membrane used is only made up of polymer and plasticizer, without the addition of a carrier agent. This analytical methodology has facilitated the analysis of pesticides at trace levels in river water samples.

RESUM

L'aigua és un bé essencial i necessari per la humanitat, no només pel seu consum directe, sinó també pel seus usos industrials o agrícoles, entre d'altres. La presència de substàncies no desitjables o contaminants afecta directament la seva qualitat. Cal doncs, disposar de metodologies analítiques que permetin la seva anàlisi per tal de detectar i/o quantificar diferents espècies o compostos que poden limitar el seu ús.

La investigació que es presenta en aquesta tesi es centra en el disseny, la preparació i caracterització de noves metodologies analítiques basades en membranes funcionalitzades per a la preconcentració i l'especiació de contaminants al medi aquós.

Freqüentment, l'anàlisi directe de mostres ambientals no es pot dur a terme, ja sigui degut a la complexitat de la matriu o bé perquè la concentració dels compostos d'interès a analitzar, es troba per sota del límit de detecció de la tècnica. Per això, és necessària una etapa prèvia que permeti la separació i/o preconcentració per tal d'eliminar les interferències i/o millorar la seva detecció a nivells baixos de concentració. D'altra banda, també es important obtenir informació sobre les diferents espècies químiques presents a la mostra, ja que sovint la toxicitat hi està estretament relacionada. A més, es important dissenyar dispositius que permetin la miniaturització i automatització dels processos i que també permetin l'anàlisi in situ.

Tenint en compte tots els aspectes anteriorment anomenats, en aquesta tesi s'han desenvolupat mètodes analítics simples i innovadors basats en membranes d'inclusió polimèrica (PIMs) per al tractament de mostres d'aigua per tal de facilitar-ne la seva anàlisi. Així, s'ha desenvolupat un dispositiu basat en PIM, utilitzant Aliquat 336 com a agent portador, el qual ha permès la satisfactòria determinació d'arsenat en aigües subterrànies. També, una membrana similar s'ha acoblat en un sistema d'anàlisi en continu permetent la detecció i determinació online d'arsenat. D'altra banda, s'ha explorat la utilització d'un sorbent comercial basat en diòxid de titani, anomenat Adsorbsia As600, el qual ha demostrat una gran capacitat per la retenció d'ambdues formes d'arsènic inorgàniques. Així, utilitzant minicolumnes amb aquest sorbent s'ha facilitat la detecció d'arsènic total en mostres d'aigua.

S'ha fet èmfasi en la preparació de PIMs així com en la caracterització de les propietats fisicoquímiques i electroquímiques tot modificant el líquid iònic (LI), Aliquat 336 utilitzat com a agent portador. Els resultats obtinguts han demostrat que en funció el caràcter hidrofílic de la membrana té un impacte directe sobre la seva eficàcia en sistemes

de transport. També, per tal de reduir l'impacte sobre el medi ambient, s'ha desenvolupat una nova metodologia de preparació de PIMs que evita l'ús de dissolvents nocius i a la vegada s'han utilitzat, per primera vegada, polímers de fonts renovables o biodegradables.

Es presenta també l'ús de PIMs, contenint D2EHPA com a agent extractant, com a tècnica emergent per realitzar estudis d'especiació de zinc contingut en una dissolució nutrient. Els estudis han demostrat que el flux de metall a través de la membrana és proporcional a la fracció lliure d'aquest, tot i la presència de diversos lligands orgànics. Tanmateix, els resultats obtinguts amb PIM s'han relacionat amb la internalització de metall a les arrels de plantes de patata (*Solanum tuberosum*), demostrant que diferents processos intervenen en la internalització de metall a les plantes els quals no s'observen en sistemes químics.

Finalment, s'ha presentat una altra innovadora aplicació de les PIMs basada en la seva satisfactòria utilització com a sorbent per a la preconcentració de tres pesticides. La membrana utilitzada només està constituïda de polímer i plastificant, sense l'addició d'un agent portador. Aquesta metodologia analítica ha facilitat l'anàlisi de pesticides a nivells traça en mostres d'aigua de riu.

RESUMEN

El agua es un bien preciado y necesario para la humanidad, no solo por su consumo directo sino también por sus usos industriales o agrícolas, entre otros. La presencia de substancias no deseadas o contaminantes afecta directamente a su calidad. Por ello, se necesitan metologías analíticas que permitan su análisis para poder detectar y/o cuantificar las diferentes especies o compuestos que puedan limitar su uso.

La investigación que se presenta en esta tesis se centra en el diseño, la preparación y caracterización de nuevas metodologías analíticas basadas en membranas funcionalizadas para la preconcentración y especiación de contaminantes en medio acuoso.

Frecuentemente, el análisis directo de muestras ambientales no se puede llevar a cabo, debido a una alta complejidad de la matriz o bien porque la concentración de los compuestos de interés a ser analizados se encuentra por debajo del límite de detección de la técnica. Por ello, es necesaria una etapa previa que permita la separación y/o preconcentración para poder eliminar las interferencias y/o mejorar su detección a niveles bajos de concentración. Por otra parte, también es importante obtener información sobre las diferentes especies químicas presentes en la muestra, ya que la toxicidad está estrechamente relacionada en función de la especie. Además, es importante diseñar dispositivos que permitan la miniaturización y automatización de los procesos y que también permitan el análisis in situ.

Teniendo en cuenta todos los aspectos anteriormente mencionados, en esta tesis se han desarrollado métodos analíticos simples e innovadores basados en membranas de inclusión polimérica (PIM) para el tratamiento de muestra de agua con el fin de facilitar su análisis. De este modo se ha desarrollado un dispositivo basado en PIM, utilizando Aliquat 336 como agente portador, el cual ha permitido la satisfactoria determinación de arsenato en aguas subterráneas. También, una membrana similar ha sido acoplada en un sistema de análisis en continuo permitiendo la detección y determinación online de arsenato. Por otra parte, se ha explorado la utilización de un adsorbente comercial basado en dióxido de titanio, llamado Adsorbsia As600, el cual ha demostrado una alta capacidad para la retención de ambas formas inorgánicas de arsénico. De este modo, la utilización de minicolumnas conteniendo el adsorbente han facilitado la detección de arsénico total en muestras de agua.

Se ha hecho énfasis en la preparación de PIMs así como en la caracterización de las propiedades fisicoquímicas y electroquímicas mediante la modificación del líquido iónico (LI), Aliquat 336, utilizado como agente portador. Los resultados obtenidos han demostrado que en función del carácter hidrofílico de la membrana, este afecta directamente a su eficacia en sistemas de transporte. También, por tal de reducir el impacto sobre el medio ambiente, se ha desarrollado una nueva metodología de preparación de PIMs que evita la utilización de disolventes nocivos y a su vez utiliza por primera vez, polímeros de fuentes renovables o biodegradables.

Se presenta también el uso de PIMs, conteniendo D2EHPA como agente extractante, como técnica emergente para la realización de estudios de especiación de zinc en disoluciones nutrientes. Los estudios han demostrado que el flujo de metal a través de la membrana es proporcional a la fracción libre de este, aun con la presencia de diversos ligandos orgánicos. Del mismo modo, los resultados obtenidos con PIM se han relacionado con la internalización de metal en raíces de plantas de patata (*Solanum tuberosum*), demostrando que diferentes procesos intervienen en la internalización de metal en las plantas los cuales no se observan en sistemas químicos.

Finalmente, se ha presentado otra innovadora aplicación de las PIMs basada en su satisfactoria utilización como adsorbente para la preconcentración de tres pesticidas. La membrana utilizada solo está formada por polímero y plastificante, sin la adición de un agente portador. Esta metodología analítica ha facilitado el análisis de pesticidas a concentraciones traza en muestras de agua de río.

CHAPTER 1

General Introduction

Water is essential for humankind and its management throughout history has contributed to the development of our society. As one of our principal resources, its supply must be kept at a satisfactory level to avoid major impacts on people's well-being [1]. Nevertheless, an ever-increasing world population as well as industrial growth and development, have led to considerable pressure on the environment, threatening the integrity of freshwater resources. There is a finite supply of freshwater and only less than a half of one percent of all the water on earth is available, the largest reserve being groundwater. The remaining amount is seawater, stored frozen in polar ice or too inaccessible for practical usage [2]. Moreover, accessibility to clean water has been considered by organizations such as United Nations Children's Fund (UNICEF), the United Nations (UN) and the World Health Organization (WHO) as one of the biggest challenges of this century. In July 2010, the UN General Assembly recognized the human right to water and sanitation. Every human being should have access to enough water, which must be safe, acceptable, affordable and physically accessible [3,4].

Water scarcity can be defined as a situation in which insufficient water resources are available to satisfy long-term average requirements and similarly [5] as the overexploitation of water resources when demand for water is higher than water availability [6]. Nearly 20% of the world's population (1.2 billion people) live in areas of physical water scarcity [7] and this has an important impact on the socio-economic development and prosperity in many different countries [8]. Indeed, water is progressively being degraded in terms of quality, increasing the cost of treatment and threatening human and ecosystem health [7].

Safe drinking water, as defined by the WHO, is one that does not represent any significant risk to health over a lifetime of consumption, including different sensitivities that may occur at different life stages, such as infancy, early childhood or old age [9]. Therefore, one of the target goals of WHO included in the 2030 agenda for drinking water is to improve water quality by reducing pollution, eliminating dumping and minimizing the release of hazardous chemicals and materials, with the aim of reducing by half the proportion of untreated wastewater and substantially increasing recycling and safe reuse globally [10].

Waters must be free from pathogens and elevated levels of harmful pollutants in order to be considered safe for drinking purposes. At a global scale, the faecal matter (microbial contamination) and the amount of arsenic and fluoride are the highest priority parameters regarding the risk to human health [10]. Microbial contamination is a

universal concern, whereas the risk of contamination with arsenic and fluoride is greater in some parts of the world than others. Several countries have adopted national drinking water quality standards aligned with the ones reported by the WHO [9]. However, estimation of water quality is only available for 45% of the global population, which suggests that compliance with the standards is low in many developing countries [10,11].

In Europe, the legal tool of mandatory application to all members of the European Union (EU) is the European Water Framework Directive (WFD), namely Directive 2008/105/EC of the European Parliament and of the Council of 16 December 2008, which establishes the environmental quality standards in the field of water policy [12]. In accordance with this directive, groundwater represents the largest, less contaminated freshwater reserve of the EU [13]. In the particular case of Catalonia (Spain), the Catalan Water Agency (ACA) is the public entity of the Government of Catalonia in charge of water policies based on the WFD principles. All these organizations are of paramount importance in promoting the implementation of monitoring programs and improving fate and risk assessment tools and policies to control pollutants as a base for sustainable water resource management.

1.1 The occurrence and problem of pollutants in the environment

1.1.1 Oxyanions

An oxyanion is a chemical compound with a general chemical formula $A_xO_y^{z-}$, where A represents a chemical element and O an oxygen atom. A different number of oxyanions, such as nitrate, molybdate, selenite, selenate, chromate and arsenate, can be toxic to humans or wildlife at μg/L to mg/L concentrations [14]. Among all these elements, chromium and arsenic species have been extensively investigated in numerous works because of their carcinogenic potential, which poses a risk to human health. Taking into account they are charged molecules, they tend to be highly soluble in water [15].

1.1.1.1 Arsenic

Arsenic (As) was discovered and isolated for the first time by the German, Albertus Magnus in 1250 [16]. Arsenic is a metalloid known historically for its toxicity

and was extensively used as a poison in ancient Greece and Rome. It gained popularity among the royalty and nobility for its lack of colour, odour, or taste as well as its widespread occurrence in nature. Moreover, it has earned several nicknames throughout history such as the *"king of poisons"* or "*inheritance powder",* because of its use in disposing of spouses or relatives.

Arsenic is one of the most abundant and ubiquitous trace elements on earth, and it can be found in the air, natural waters, rocks and soils. It is mobilized through a combination of natural processes as well as through a range of anthropogenic activities [17]. The most important anthropogenic inputs are from smelter operations and fossil-fuel combustion. It is released into the atmosphere through inputs from wind erosion, volcanic emissions, low-temperature volatilization from soils, marine aerosols and pollution and is returned to the earth's surface by wet and dry deposition [18].

Arsenic belongs to group 15 and has the atomic number 33 on the periodic table, and its atomic weight is 74.92 unified atomic mass unit (u). It is placed between phosphorus and antimony and has more non-metal than metal characteristics, and therefore, tends to form more anions than cations species. In the environment, arsenic can be found in different chemical compounds, depending on oxidation states: As(V) (arsenate), As(III) (arsenite), As(0) (elemental As) and As(-III) (arsenide). The most common inorganic forms in aqueous medium are As(III) as $H_3AsO_3^0$, $HAsO_3^{2-}$ and $H_2AsO_3^-$ whereas As(V) is found as $H_3AsO_4^0$, $H_2AsO_4^-$, $HAsO_4^{2-}$ and AsO_4^{3-}. As(V) is predominant in oxygen-rich waters, whereas As(III) is the main species in reducing or anaerobic environments. Taking into account that As(III) is more toxic than As(V) species, waters from a reducing environment present a higher toxicity compared to those from oxidizing environments. The distribution of these inorganic species depends on the redox conditions, the biological activity and on the pH. The different species of arsenic depending on pH are shown in Figure 1.1 for both As(V) and As(III).

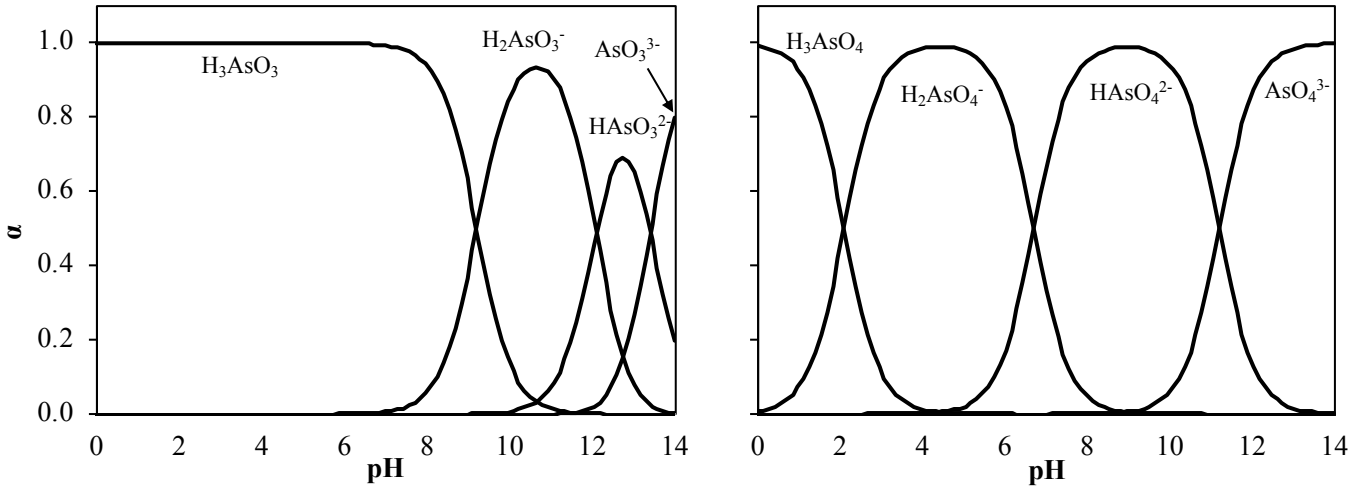

Figure 1.1 Speciation of arsenite (As(III)) and arsenate (As(V)) as a function of pH (arsenic concentration 1mM).

Inorganic arsenic compounds can be methylated by different living organisms such as bacteria, fungi, or yeasts, and be turned into organic compounds such as monomethylarsonic acid (MMA), dimethylarsinic acid (DMA), and gaseous derivatives of arsine [19]. These organic compounds are less toxic than the inorganic forms and they are likely to be found in living organisms as well as arsenobetaine (AsB), which is the main source of arsenic in fish and seafood [20]. These organic compounds are mostly common in waters affected by industrial pollution or influenced by biological activity [18]. The most toxic arsenic compound is arsine (AsH_3), which is a colourless toxic gas [8], followed by arsenites, arsenates and organic arsenic compounds.

The main source of arsenic mobilization in the environment comes from As-enriched minerals. The main arsenic ore is arsenopyrite (FeAsS), as it contains around 46% of arsenic by mass [21]. This mineral is found in thermal reservoirs and in some metamorphic and magmatic rocks. The principal mechanism of arsenic mobilization occurs due to the decomposition of FeAsS according to Eq. (1.1) [22]:

$$FeAsS + 13\ Fe^{3+} + 8H_2O = 14\ Fe^{2+} + SO_4^{2-} + 13\ H^+ + H_3AsO_4 \qquad (1.1)$$

FeAsS oxidation is catalyzed by ferrooxidans bacteria, which also oxidizes ferrous (Fe(II)) turning into ferric ion (Fe(III)).

The chemistry of arsenic and sulphur has some analogies, and therefore, there are many other sulphide minerals such as pyrite, galena, marcasite, chalcopyrite, among

others, which contain more than 10% As by mass [23]. Indeed, arsenic is also present in metal oxides and hydrous minerals either belonging to the mineral structure or as an adsorbed species. It is retained on the surface of manganese oxides, hydrous aluminum, calcite and hydrous iron oxides. Some examples of such kinds of oxide minerals are hematite, magnetite, ilmenite, Fe(II) oxides or Fe(III) oxyhydroxides [24–26]. Nevertheless, rich phosphate minerals are much less abundant than the above mentioned oxide minerals, so their contribution to As concentration in most sediments is minor [18].

In the case of Europe, the average concentration of arsenic in topsoil is estimated at 7.0 mg kg^{-1}, although background concentration can depend significantly on soil conditions [27]. The distribution of arsenic topsoil concentrations in Spain is shown in Figure 1.2.

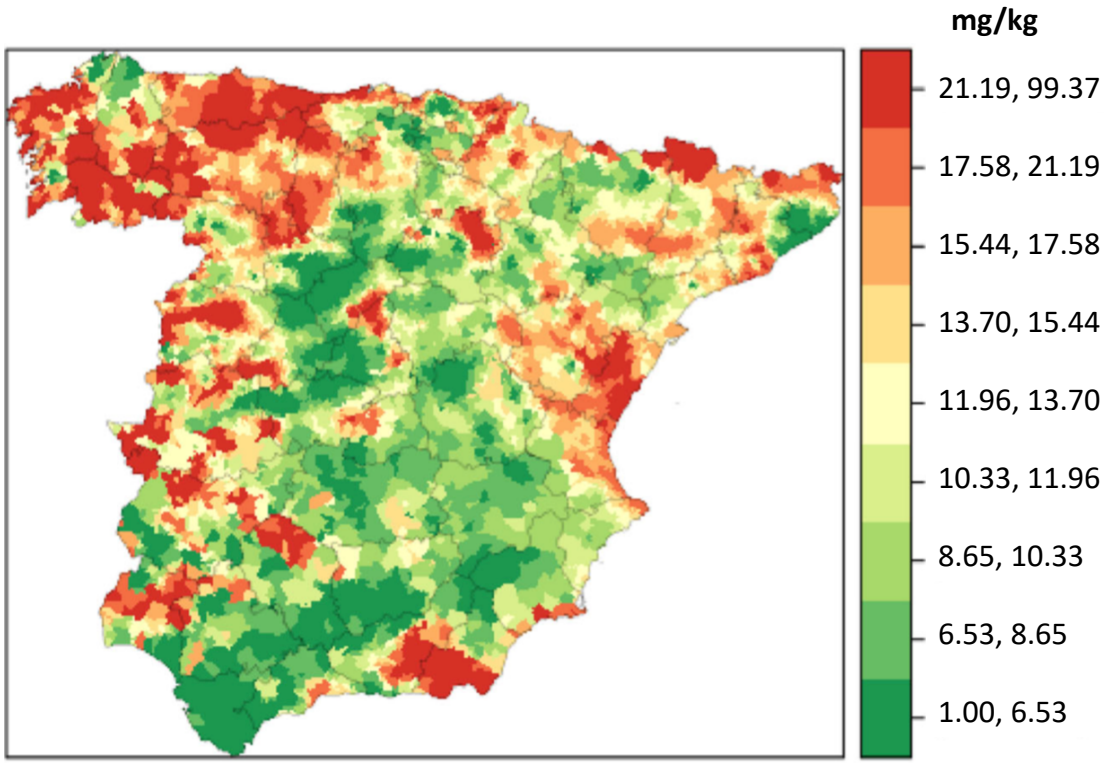

Figure 1.2 Distribution of arsenic in the Spanish topsoil [28].

A large number of aquifers all around the globe have been reported to bear high arsenic concentrations [18]. More than half of the world's population depends on groundwater as their drinking-water source and among this population (over 100 million people), groundwater represents their only available drinking-water source [29].

Elevated arsenic concentrations in groundwater have been found in 105 countries around the globe. One of the most severe threats is found in South-East Asia, such as in Bangladesh, India (especially in West Bengal), or in Vietnam, where over 100 million people are at risk of arsenic-related diseases due to groundwater contamination [30–32]. In these areas, polluted groundwater with an elevated arsenic content, is used for crop irrigation, such as rice or vegetables, and therefore, consumption of food grown in these soils causes a life-threatening problem for millions of people [27] (see Figure 1.3). Moreover, the presence of arsenic in different groundwaters has been identified in New Zealand, France, Chile, United States of America (USA) [29,33] and also in Spain [34].

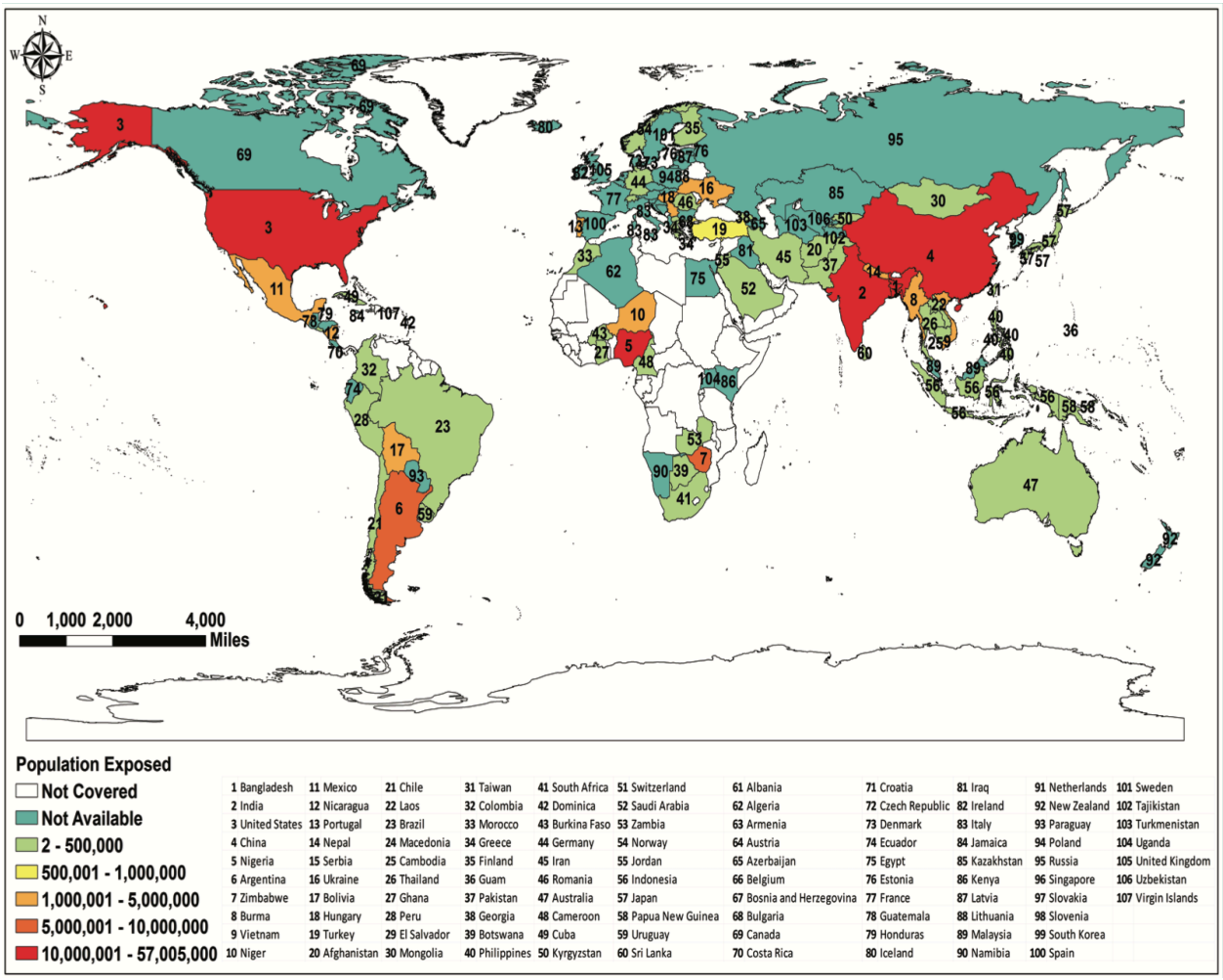

Figure 1.3 World population exposed to elevated levels of arsenic in groundwater [35].

- *Regulation and health implications*

The evidence of the toxicological effects of arsenic has led the maximum arsenic concentration for human consumption recommended by the WHO to be established at 10 μg L^{-1}. However, in many developing countries, the WHO has established a limit of 50 μg L^{-1}, as a result of economic constraints and the difficulty of analytical determination when arsenic is present at very low concentrations [9,10]. On applying the WHO guideline of 10 μg L^{-1}, more than 100 million people are at risk, and out of these more than 45 million people, mainly in developing countries in Asia, are at risk of being exposed to more than 50 μg L^{-1} [33]. On a minor scale, the presence of this pollutant has also been detected in different areas in the northeast of Catalonia (Spain). Hence, different municipalities have set up arsenic removal water treatment plants in order to achieve satisfactory levels based on the coprecipitation of arsenate with iron(III) salts [36,37].

Moreover, maximum levels of arsenic in food have been established by Commission Regulation (EU) No 2015/1006 [38], which was applicable from 1 January 2016 onwards. Apart from drinking water, grain-based processed products, such as wheat bread, rice, milk and dairy products, are the main sources of exposure for the general population in Europe. Children under 3 years of age are the most exposed to inorganic arsenic because they consume more rice-based products. Indeed, certain ethnic groups or people following a gluten-free diet, who have relatively higher intakes of rice, or are high consumers of algae-based products, can exceed their tolerable weekly intake of inorganic arsenic [39].

Inorganic arsenic compounds are classified by the International Agency for Research on Cancer (IARC) in Group 1 (carcinogenic to humans) on the basis of sufficient evidence for carcinogenicity in humans and limited evidence for carcinogenicity in animals [40]. The acute toxicity of arsenic compounds in humans is predominantly a function of their rate of removal from the body.

The regular consumption of water polluted with arsenic can cause skin, lung, bladder and kidney cancer, as well as changes in pigmentation, neurological disorders, muscle weakness, loss of appetite, nausea and diabetes [41]. Moreover, there is emerging evidence of negative impacts on foetal and infant development, as birth weight is reduced. Humans can be exposed to arsenic by inhalation, skin absorption, and ingestion of food and water. Inhalation may occur due to industrial emissions, tobacco smoke or gas from electricity-generating combustion plants. Regarding ingestion, studies have been carried

out in which the gastrointestinal tract rapidly absorbs arsenic, and its effects depend on the source of arsenic [42]. On the other hand, the risk associated with skin absorption is relatively low compared to that of ingestion.

- *Uses of arsenic*

Despite its toxicity, arsenic is still being used in various applications, although increasingly less over time. Arsenical pesticides and insecticides, such as lead arsenate, zinc arsenate, calcium arsenate, zinc arsenite, Paris green and magnesium arsenate, have been extensively used in numerous countries for decades until the development of dichlorodiphenyltrichloroethane (DDT) [43–45]. Among the different applications, arsenic-based pesticides have been used as herbicides, insecticides, cotton desiccants, defoliants, and soil sterilants. Inorganic arsenic pesticides were stopped being applied on USA crops in 1993. However, organic forms were allowed until 2009, when the Environmental Protection Agency (EPA) issued a cancellation order to eliminate and terminate gradually the use of organic arsenical pesticides by 2013. The only exception was monosodium methanearsonate (MSMA), a broadleaf weed herbicide, which is still allowed on cotton crops. Conversely, the herbicide disodium methanearsonate (DSMA, or cacodylic acid), used on cotton fields was banned under the aforementioned EPA organic arsenical product regulation [46,47]. Other organic arsenical products such as roxarsone or arsanilic acid are used as animal feed additives to increase weight gain, enhance productivity or disease control in the poultry and swine industries [48–51].

One of the main applications of this element has been as a preservative to protect wood from microorganisms, fungi and insects. These products consist of a mixture of arsenic oxides, chromium and copper. Chromated-copper-arsenate (CCA) has been extensively used for several years in Europe and North America [52]. In 2003, CCA's manufacturers voluntarily discontinued producing this compound for homeowner users, although no prohibition has been established and only recommendations to use the new generation of preservatives has been advised by the EPA [53].

In addition, gallium and indium arsenides (GaAs and InAs) are important semiconductor materials, which have different applications in laser devices, solar panels or light-emitting diodes (LEDs). Besides, arsenic is also used as an additive in lead alloys and, in small amounts, helps to inhibit brass corrosion [46,54].

1.1.1.2 Chromium

Chromium (Cr) was discovered in 1797 by the French chemist Nicholas Louis Vauquelin, who studied the composition of a mineral with an intense red colour discovered in a gold mine in Siberia. Its name comes from the Greek *chroma*, which means colour, because of the colouration of all its compounds, either as solids or dissolved [55]. Chromium belongs to group 6 of transition metals and has the atomic number 24 on the periodic table, and its atomic weight is 52.00 u. It can present different oxidation states, ranging from neutral Cr(0) to oxidized Cr(VI) species, Cr(VI) and Cr(III) being the most frequent oxidation states. In water environments, Cr(III) exists as Cr^{3+} and $Cr(OH)^{2+}$ cationic species or $Cr(OH)_3$ whereas Cr(VI) exists as various anionic species, such as $Cr_2O_7^{2-}$, $HCrO_4^-$ and CrO_4^{2-} [56,57]. Figure 1.4 depicts Cr(VI) speciation as a function of pH.

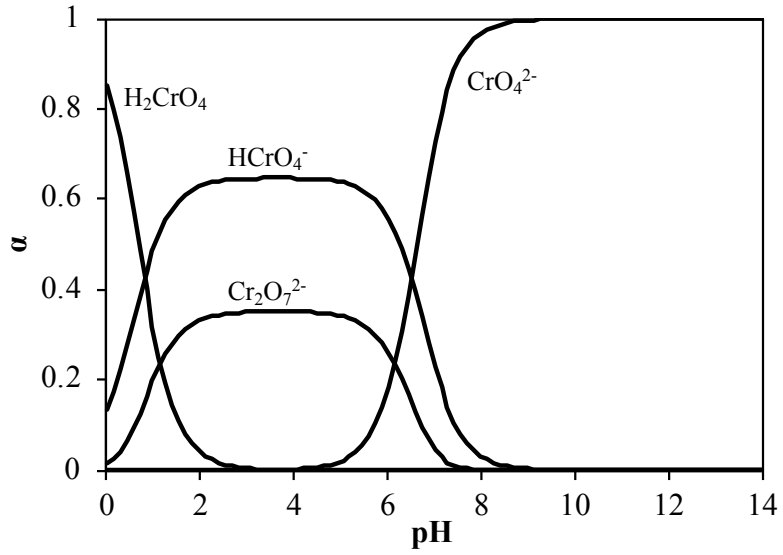

Figure 1.4 Speciation of chromate (Cr(VI)) as a function of pH (chromium concentration 1mM).

Chromium is relatively abundant in the Earth's crust, although its elemental form is very scarce. It is the Earth's 21st most abundant element and the 6th most abundant transition metal. The main chromium ore is iron(II) chromite, $FeCr_2O_4$, found mainly in South Africa (with 96% of the world's reserves), Russia and the Philippines. Less common sources include crocoite, $PbCrO_4$, and chrome ochre, Cr_2O_3. The gemstones emerald and ruby owe their colours to traces of chromium [55]. This element is present in a great variety of minerals and rocks with different origins (e.g., igneous, metamorphic,

sedimentary) and its oxidation state and isotope composition provide valuable information on the genesis, redox conditions and mineralization history of the Earth's materials [57].

The average concentration of chromium in ambient air is normally below 20 ng m^{-3}, although in indoor air areas with permitted cigarette smoking, this level can be increased by 10 to 400 times. Soils usually contain 10 to 90 mg Kg^{-1} and chromium levels in surface waters tend to oscillate between concentrations of less than 1 μg L^{-1} and up to about 30 μg L^{-1}, with an average value of 10 μg L^{-1} [58–60].

- *Regulation and health implications*

Cr(III) is considered an essential trace element for the proper functioning of living organisms, whereas Cr(VI) is highly toxic and can produce mutagenic and carcinogenic effects in humans. During wastewater treatment, the less toxic Cr(III) often changes its oxidation state and turns into a more toxic species, Cr(VI). The toxicity of Cr(VI), which has been reported to be 100-1000 times more toxic than Cr(III), is remarkable even at low concentrations. Therefore, the WHO recommends a maximum level of Cr(VI) of 5 μg L^{-1} in waste water. Moreover, many countries have regulations regarding the maximum permissible concentration of Cr(VI) and total chromium in natural or drinking water. In Spain, the permissible concentration of total chromium in drinking water is 50 μg L^{-1} [61].

- *Uses of chromium*

Nowadays, the global production of chromium is increasing as a result of the huge range of different applications of this element. A great number of chromium applications are related to enhancing the resistance of materials to physical and chemical agents. Some of these applications are leather tanning, metallurgy, metal finishing, pigments, wood protection, electroplating, catalysis and electrical and electronic equipment, or as a magnetic agent (in the manufacture of audio or video tapes), despite its toxicity [62]. However, the main industry that benefits from the advantages of this phenomenon is the galvanization industry, which makes coatings with a layer of chromium by means of an electrolytic process. This process generates large volumes of residual water with a high Cr(VI) content that must be treated [58]. Chromium can also enter drinking water supply

systems via corrosion inhibitors used in water pipes and containers or via contamination of underground water leaching from sanitary landfill [63].

Other frequent applications are based on its resistance, as in the production of stainless steel, which normally contains a minimum of 10.5% chromium (traditionally 11 or 12%). Thus, it has considerable corrosion resistance when compared to steels with a lower percentage of this element. Its corrosion resistance is due to the formation of a self-repairing passive layer of chromium oxide on the surface of stainless steel [64].

1.1.2 Zinc

Zinc (Zn), was first isolated by the German chemist Andreas Sigismund Marggraf in 1746. Zinc is considered a post-transition metal and a moderately reactive metal and strong-reducing agent. It belongs to group twelve and has the atomic number 30 on the periodic table, and its atomic weight is 65.39 u. As it presents a d subshell with 2s electrons, the divalent cation (Zn^{2+}) is its only naturally occurring oxidation state. However, the unusual oxidation state Zn(I) has also been reported [65]. Zinc can also exist in a neutral or uncharged species, Zn(0). Besides, it has relative stability and the ability to coordinate 4 or occasionally 6 ligands, and a capacity to act as a Lewis acid.

Zinc is the second most important transition metal in organisms after iron, and it is considered a micronutrient, present in all tissues, organs and fluids in the organism [66]. The relevance of zinc was first reported in 1869 due to its importance for the normal growth of the common bread mould fungus *Aspergillus niger* [67].

Zinc is one of the most abundant elements on earth, ranking in 23rd place [68]. Zinc sulphide is the main component of the mineral sphalerite, which is the principal zinc ore mineral in the world. Approximately 0.012% of the earth's crust is zinc [69]. The most quoted range of total zinc in normal soils in 10–300 mg kg^{-1} with a natural mean level of 50 mg kg^{-1}. However, total zinc content in soil depends upon the parent rock, weathering, organic matter, texture and pH [70]. Soils formed from basic rocks such as basalt present greater zinc content than those from acid rocks such as granite or gneisses. Zinc can be present in soils in a variety of chemical forms that can be classified in five different pools: water soluble, exchangeable, adsorbed, chelated or complexed zinc. Zinc is of paramount importance in terms of plant nutrition [70]. The factors that control the amount of zinc available for plants are the total zinc content, clay content, calcium carbonate content, redox conditions, and microbial activity in the rhizosphere, soil moisture status,

concentration of other trace elements, concentration of macro-nutrients, especially phosphorus and climate [71]. The contribution or combination of these factors can lead to a reduction in zinc availability, and, hence, produce poor zinc absorption in plants. Among the different types of crops, rice is the most affected by zinc deficiency [70].

In natural surface waters, zinc is frequently present below 10 μg L^{-1}, and ranges from 10 to 40 μg L^{-1} in groundwaters. However, zinc concentration can be much higher in tap water as a result of the corrosion of piping and fittings producing the leaching of zinc [72].

- *Regulation and health implications*

In the first edition of the WHO Guidelines for Drinking-water Quality (1984), a guideline value of 5.0 mg L^{-1} was established for zinc, based on an organoleptic evaluation, since it gives an undesirable astringent taste to water. Later, in the third edition of the Guidelines (2004), a level above 3 mg L^{-1} was reported as possibly not being acceptable to drinking waters. However, no health-based guideline value has been proposed for zinc in drinking water [72].

Either an excess or lack of this element can lead to several health problems (see Figure 1.5), as it is a crucial element for the survival of most organisms. Throughout, the twentieth century, the role of zinc as a nutrient and its importance in the activity of different enzymes was established [73]. The relevance of this element for human life was not reported until 1963, when zinc deficiency was related to being a major contributing factor in nutritional dwarfing and hypogonadism [74]. Zinc acts as a cofactor of more than 300 proteins, and is the only metal present in all six enzyme classes (oxidoreductase, transferase, hydrolases, lyases, isomerases and ligases) [75]. Therefore, zinc deficiency, especially in infants and young children, is a cause of great concern, generating thousands of deaths every year and affecting 2 billion people, according to the WHO. Moreover, it is estimated that 60–70% of the population in Asia and Sub-Saharan Africa might be at risk of low zinc intake [76]. The main zinc source is food such as poultry, fish and seafood, whole cereals, dairy products and red meat which represents the most available source of zinc to humans, whereas plants provide a lower bioavailability due to dietary fibre and phytic acid, which inhibit the absorption of zinc [77].

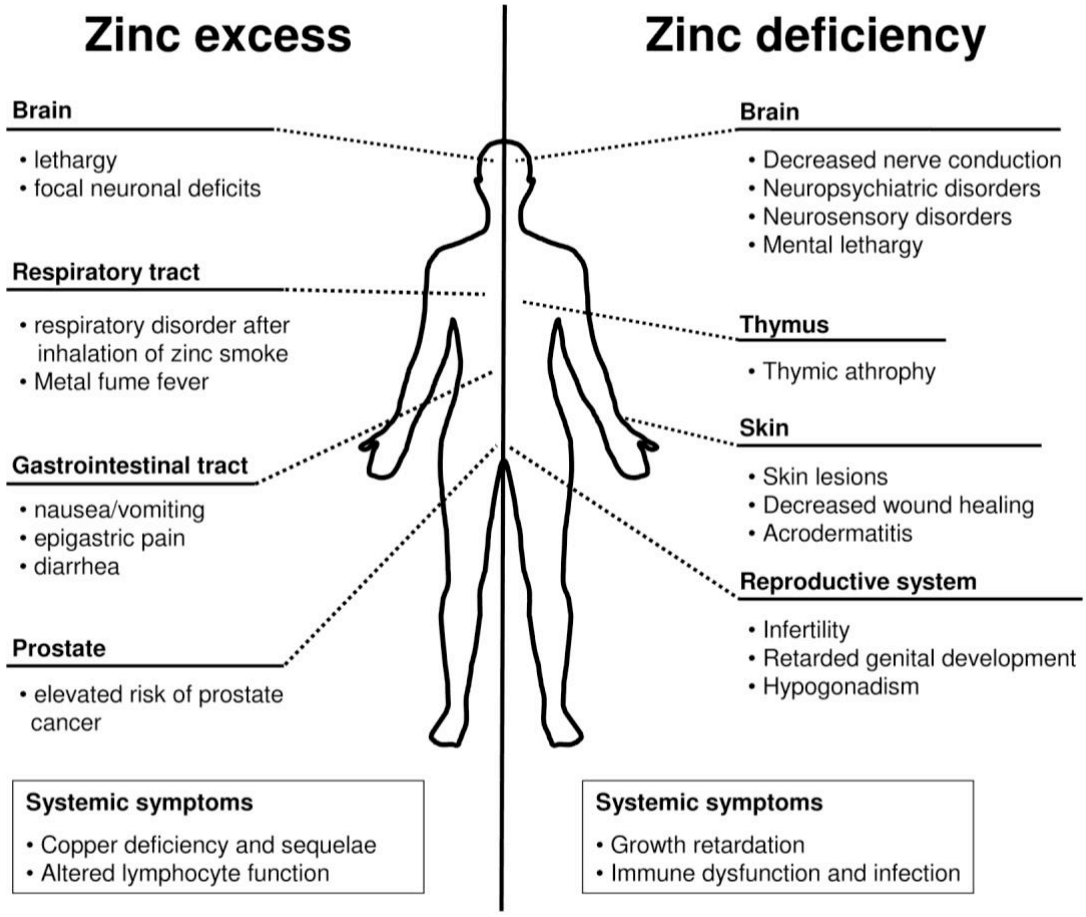

Figure 1.5 Effects of either a high (left side) or low zinc intake (right side) on human health [78].

- *Uses of zinc*

Considering tonnage production, it occupies the fourth position in the entire world's metal production, after iron, aluminium and cooper. About 75 % of this element is consumed as a metal used for galvanizing iron or steel to protect them from corrosion, for the production of corrosion-resistant alloys and brass, as a zinc-based die and as rolled zinc. The remaining 25 % is dedicated to the production of fertilizers or pesticides (zinc carbamate), to rubbers used as a white pigment (ZnO), and to various chemical and paint industries [68,72].

1.1.3 Pesticides

A pesticide is a chemical or biological substance designed to kill or retard the growth of pests that damage or interfere with the growth of crops, shrubs, trees, timber

and other vegetation desired by humans [79]. They act by interfering with a variety of biochemical and physiological processes that are common to a wide range of organisms.

The term pesticide includes, amongst others: herbicides, fungicides, insecticides, acaricides, nematicides, molluscicides, rodenticides, growth regulators, repellents and biocides. Therefore, target pests can include insects, plant pathogens, weeds, molluscs, nematodes (roundworms), and microbes that cause nuisances, spread disease or are vectors for disease [80,81].

Pesticides may be organic or inorganic compounds. Organic pesticides belong to a variety of substance classes, including N- and P-containing compounds. Based on their chemical family, the different molecules of organic pesticides may be grouped into classes, such as organophosphates, carbamates, pyrethroids or organochlorine compounds. Conversely, inorganic pesticides are copper or arsenic-containing products, or, to a lesser extent, zinc- and mercury-based compounds [82]. The different chemical families present diverse toxicities and environmental persistency as will be commented upon later.

In the context of the escalating challenges of population growth, placing pressure on energy resources, the environment and global food supplies, agrochemicals have gained an important role as they are used not only to protect crops but also to enhance crop yields [83]. From the 1940s onwards, a further increase in food production was allowed by the introduction of synthetic crop protection chemicals; in other words, the use of pesticides was advisable to maintain high levels of food production.

The use of pesticides is not equal across the world due not only to the cost of the chemicals (most of them patented), but also to the cost of manpower and the specific pests of each climatic/geographic region. The Food and Agriculture Organization (FAO) has computed the average application rates of pesticides per hectare (ha) of arable land, 6.5–60 kg/ha being the highest average values occurring in Asia and in some countries of South America. However, in North America and West Europe, the use of herbicides, intensively applied in agriculture and in urban areas, has experienced a boom in the last decades. In Asia, the use of herbicides has remained low and contrasts with the use of insecticides, which is still very high [84].

On a global scale, worldwide pesticide production increased at a rate of about 11% per year, from 0.2 million tons in 1950s to almost 6 million tons by 2005 [85]. The value of expenditure on pesticides in 2008 was 48.8 billion United State Dollar (USD) compared to 55.9 billion USD achieved in 2012. In that year, herbicides, including plant

growth regulators, were in first place and represented 44% of the total value, followed by insecticides, which accounted for about 29% of the total expenditure, fungicides (26%) and other pesticides, such as nematicides, fumigants, and other miscellaneous pesticides (1 %) [86]. The total quantity of pesticide sales in Europe for 2013 was close to 360,000 tonnes, and among the different EU Member States, Spain (19.5%), France (18.7%), Italy (13.8%), Germany (12.3%) and Poland (6.2%) accumulated up to 70.5% of EU pesticide sales [87].

Early synthetic pesticides developed to control agriculture pests, such as DDT, prohibited in 1972, or lindane (i.e. gamma-hexachlorocyclohexane, γ-HCH), prohibited in 2008, both belonging to the organochlorine class, were intensively used for the control of cattle ticks and human parasites in North America or Europe, and, despite their current prohibition, they are still popular food preservatives for sun-dried fish in South Asia and remain in use, sometimes illegally, to control malaria vectors and household pests in urban areas in the tropics [84]. The reason for the prohibition of the aforementioned pesticides is due to their persistence and to the fact that these compounds could give rise to harmful effects on human health or the environment. Persistence is defined by IUPAC [88] as the residence time of a chemical species in a specifically defined compartment of the environment and which presents bio-accumulative properties which contribute to spreading these compounds in the environment. Therefore, it is of paramount importance to control them in a wide variety of samples [89–91].

Nowadays, the EU aims to achieve a sustainable use of pesticides throughout the European Union through Directive 2009/128/EC. This Directive seeks to reduce the risks and impacts of pesticide use on human health and the environment, and promote the use of integrated pest management and alternative approaches or techniques, such as non-chemical alternatives to pesticides [92].

Pesticides can be introduced in the aquatic system due to different processes such as surface water runoff, rainwater or melted snow which can transport pesticides into deeper soil and into underground water supplies, accidental spills or irresponsible dumping of these kinds of chemicals, or by either an excessive or improper application of these products near freshwater sources [93]. Among the different economic sectors, agriculture represents the main cause of degradation of water resources since it demands the highest amount of fresh water (70% of world consumption) [94].

A great number of pesticides are included in the monitoring schedule of most western countries. However, the cost of analysis and the necessity to sample at critical

times of the year, linked to periods of pesticide use, produces a lack of extensive data [95]. According to the Stockholm Convention on Persistent Organic Pollutants, 9 of the 12 most dangerous and persistent organic chemicals are pesticides [96]. In Europe, the WFD has set 0.1 μg L^{-1} as the maximum concentration permitted for individual pesticides in waters intended to be used for drinking purposes [12]. However, it is still challenging for regulatory agencies to understand the potential effects of chemical mixtures on humans and the environment, and, although guidelines evaluating the possible effects from exposure to chemical mixtures have been provided, their implementation is difficult due to the complexity of mixtures that occur in the environment and the inadequacy of data on their toxicity [97].

In 2012, the European Commission released a communication on the combined effects of chemicals, to ensure that risks associated with chemical mixtures are properly understood and assessed, and to state the current limitations of evaluating compounds individually. It highlights that EU have strict policies for individual chemicals but their combination is rarely assessed [98].

With regard to human health risks, pesticides can pose a threat depending on how toxic they are, the amount present in water, and how much exposure occurs on a daily basis. Health effects depend on the type of pesticide; for example, in the case of organophosphates and carbamates, these kinds of compounds affect the nervous system. There are others that can cause skin or eye irritation and some can be carcinogenic [97].

The studies conducted as part of this thesis are focused on two organophosphate (OPs) insecticides, namely chlorpyrifos (CP) and diazinon (DZ), and one fungicide which belongs to the chemical class of aminopyrimidines, cyprodinil (CYP).

OPs emerged from wartime research on nerve gases. OPs block cholinesterase, the chemical that transfers nerve impulses across synapses, and so their effect is primarily on the nervous system. The advantage of OPs is that they are rapidly degraded in the environment to non-toxic secondary compounds, unlike organochlorines (OCs) [99].

CP is recognized as a priority pollutant by WFD [12], and considered hazardous to humans by the WHO, as more than 10,000 CP-related human deaths are reported per year [100]. In the case of DZ, it has been classified by IARC as "*probably carcinogenic to humans*". The Agricultural Health Study cohort has linked exposure to this pesticide with a higher risk of leukaemia. DZ-induced DNA or chromosomal damage in rodents and in human and mammalian cells in vitro [101].

Aminopyrimidines play an important role in biological processes, as the pyrimidine ring is present in several vitamins, nucleic acids and coenzymes. They interfere with the biosynthesis of methionine and other aminoacids and inhibit the secretion of hydrolytic enzymes. Nevertheless, fungi treated with these kinds of compounds tend to create resistance [102,103]. It has been reported that CYP is able to cause slight acute toxicity [104].

There are many difficulties linked to controlling pesticides as they are mainly found in low quantities in the environment. This is even more of a problematic issue in many developing countries as it requires highly flexible field and laboratory programs responding to periods of pesticide application, discrimination between those pesticides that appear as artifacts of historical use versus those that are currently being used, and the need for detection levels that have meaning for human health and ecosystem protection [97].

1.2 Determination of pollutants in waters

As previously explained, the aquatic environment might contain several metallic/metalloid species or other toxic pollutants due to both natural and anthropogenic activities. All these contaminants are increasingly under the spotlight and even though they might be present at trace levels, their adverse effects on animals, aquatic life and even humans are cause for great concern [105,106]. Therefore, it is of utmost relevance to employ very sensitive analytical techniques to satisfy environmental regulations.

1.2.1 Metal and metalloid determination

Depending on the cost, sample throughput, sensitivity and detection limit, concentration range, matrices, and regulation requirements, different instruments can be selected for a wide range of environmental applications.

Most inexpensive and widespread methodologies for the determination of metals and metalloids are based on colorimetric methods. In the case of **arsenic**, molybdenum blue, silver diethyldithiocarbamate (SDDC) or leuco malachite green methods are the most used. In the molybdenum blue method, As(V) reacts with Mo(VI) to form a

characteristic blue complex in which its typical absorbance can be measured with a spectrophotometer at 865 nm [107]. In the SDDC method, arsenic is reduced to arsine, which is absorbed in a SDDC solution prepared in chloroform or pyridine. The red-violet complex is formed as a result and measured at 510-525 nm [108]. The leuco-malachite green method is based on the reaction between arsenic and potassium iodide in acidic conditions to liberate iodine, which selectively oxidises leuco-malachite green into malachite green dye, measured at 617 nm [109].

The necessity to ensure sufficient detection limits has originated the combination of these colorimetric methods with other enrichment/preconcentration steps so as to enhance the applicability with environmental samples.

In the case of **chromium**, the most widely used spectrophotometric method is based on the selective reaction of diphenylcarbazide (DPC) with Cr(VI) at pH 1 [56], whereas in the case of **zinc**, the reagent (2-carboxy-2'-hydroxy-5'-sulfoformazylbenzene) (Zincon) has traditionally been used for its rapid determination [110].

Atomic spectroscopy and spectrometry techniques are the most popular for trace metal analysis, and they have been extensively employed for the determination of elements, such as the ones studied in this thesis (i.e. arsenic, chromium, zinc).

For instance, in the case of **arsenic**, a great number of highly sensitive analytical techniques have been employed to determine total arsenic in environmental samples at μg L^{-1} level, such as graphite furnace atomic absorption spectrometry (GFAAS) [111,112], hydride generation atomic absorption spectrometry (HG-AAS) [113–115], hydride generation atomic fluorescence spectrometry (HG-AFS) [116–119], neutron activation analysis (NAA) [120], inductively coupled plasma atomic emission spectrometry (ICP-AES) [121] or inductively coupled plasma mass spectrometry (ICP-MS) [122,123]. When using ICP-AES, arsenic determination can suffer from spectral interferences at high concentrations of titanium, iron, manganese or chromium due to vacuum ultraviolet lines (under 200 nm) and also high concentration of vanadium and chromium due to ultraviolet lines [124]. Conversely, ICP-MS provides higher precision and the capability to reach lower detection limits. However, samples with high amounts of chloride (Cl^-), can cause interference given that when chloride and argon combine in the plasma they form argon chloride ($^{40}Ar^{35}Cl$), which has similar mass to arsenic (^{75}As). These types of interferences can be overcome by using mathematical correction equations, high-resolution detectors or a collision/reaction cell [125,126]. In addition, arsenic can suffer from poor ionization in the plasma, which can cause a problem when

analysing low concentrations of arsenic in environmental samples. Some possibilities of enhancing the sensitivity of the analysis exist, such as the addition of a certain amount of methanol, ethanol or other C-containing compounds, to enhance the ionization of arsenic in the plasma [127]. Another approach is hydride generation, which is frequently used not only to avoid matrix interferences but also to enhance the detection limits of the method. It is based on the reaction of arsenic with a reducing reagent such as sodium borohydride to form a volatile arsenic hydride, which is then transported to the plasma, ensuring a more efficient sample introduction to the system [128].

The determination of **chromium** and **zinc** in liquid samples at low levels can also be achieved by means of spectroscopic techniques such as GFAAS, ICP-AES, ICP-MS or NAA [63,129]. In the case of chromium, various potential spectral interferences can occur at high concentrations of tungsten and cobalt when analysing by ICP-AES [130]. Moreover, the analysis of this metal by ICP-MS can also present some interferences specially when matrices contain high levels of chloride or carbon leading to the formation of polyatomic ions such as $^{35}Cl^{16}OH^+$, $^{40}Ar^{12}C^+$ or $^{37}Cl^{14}NH^+$, which interfere with the detection of ^{52}Cr [131]. These interferences can also be overcome using the aforementioned approaches as in the case of arsenic.

1.2.2 Pesticide determination

The correct selection of the methodology for the determination of pesticides depends on the sample matrix and on the structure and properties of the target compounds. Indeed, when considering the lowest permissible levels of pesticides in various matrices, it is highly important to select sensitive and selective analytical techniques. Conventional methods for pesticide determination are described by EPA and can be divided into three groups: (i) the ones based on the use of gas chromatography (GC) with selective detection (e.g. electron capture detector (ECD) or nitrogen phosphorous detector (NPD)), (ii) those which use gas chromatography mass spectrometry (GC-MS) and (iii) those which use liquid chromatography (LC) with fluorescent or diode array detection [132,133]. Nowadays, several multiresidue methods have been developed either based on GC or HPLC coupled to high-resolution mass spectrometry (HRMS) [134,135]. However, often due to long time analysis, effort required and the need for large volumes of organic solvents, these methods do not meet expectations and are, therefore, combined with different preconcentration techniques.

1.3 Speciation studies

The International Union of Pure and Applied Chemistry (IUPAC) defines speciation analysis as analytical activities of identifying and/or measuring the quantities of one or more individual chemical species in a sample. The different species can consider differences at the levels of isotopic composition, electronic or oxidation state, inorganic and organic compounds and their complexes, organometallic species, and macromolecular compounds and complexes [136].

Speciation studies can be achieved by means of chromatographic techniques. In such cases, separation is accomplished by chromatography (GC, HPLC, ion chromatography) or capillary electrophoresis (CE), and detection by sensitive spectroscopy or spectrometry techniques (ICP-AES and ICP-MS) resulting in hyphenated techniques. (IC). For instance, separation of **chromium** species (Cr(VI) and Cr(III)) is achieved by means of an anion-exchange column and detection with ICP-MS. Cr(III) cation is previously derivatized by the addition of a ligand that does not form a complex with Cr(VI) species [137]. In the case of **arsenic**, the use of an ion-pair reversed phase HPLC hyphenated with ICP-MS has allowed the separation and determination of eight arsenic species including As(III), As(V), MMA, DMA, trimethylarsinoxide (TMAO), tetramethylarsonium (Tetra), arsenocholine (AsC) and AsB [126].

Other approaches are based on the separation of the metal species from the solution by adsorption on a solid such as ion exchange or complexing resins or liquids supported on solids. Different strategies based on solid extraction can be performed to achieve speciation: i) the use of an adsorbent that retains the different species and then, the selective elution by using the appropriate elutant solutions [138]; ii) the use of functionalized sorbents that selectively retain one species while the other species remains in solution [139]; iii) the combination of a selective adsorption (under appropriate pH conditions of the medium) with a selective elution [140]. Many examples of different applications can be found in the literature. In the case of **chromium**, the use of chitosan-modified magnetic nanoparticles exhibit excellent adsorption performance for Cr(III) at pH 9 and total Cr (Cr(III) and Cr(VI)) at pH 6, thus allowing its speciation [141]. Another approach consists of the selective extraction of a Cr(VI)-APDC chelate by multiwalled carbon nanotubes (MWNTs). The total chromium content is determined by a previous oxidation of Cr(III) to Cr(VI) by using hydrogen peroxide [142]. In the case of **arsenic**, several methodologies have been reported [143,144], which allow the speciation of

inorganic arsenic species. Chen et al. [143] used ordered mesoporous silica micro-columns modified with 3-(2-aminoethylamino) propyltrimethoxysilane for inorganic arsenic speciation, since only As(V) was selectively adsorbed on the micro-column within the pH range 3–9, whereas Xiong et al. [144] used a micro-column packed with CTAB-modified alkyl silica sorbent where only the negatively charged As(V) was adsorbed at the studied pH. In both studies, the total inorganic arsenic was obtained after As(III) oxidation.

In effect, there are essential elements for living organisms, such as boron, silicon, selenium or zinc, which carry out important physiological functions, as they are part of different biologically relevant molecules. Living organisms obtain these dissolved trace metals from the soluble forms in sediments or water where they can be found in various chemical species, such as free ions, inorganic or organic complexes. However, not all metal species are available, and therefore, a lack or an excess of these elements can generate severe consequences for living organisms. In this context, availability can be defined as the fraction of the total metal in the water column or sediment compartments that is unbound, free, or available for uptake by an organism [145]. In the case of cationic metals the general consensus is that the concentration of the free metal ion is the best predictor for both metal bioaccumulation and toxicity in aquatic systems [146]. Information about the free metal ion or labile species can be obtained by means of different techniques. Electrochemical methods have been used for metal speciation, namely anodic stripping voltammetry (ASV), which is based on metal reduction at the mercury electrode at deposition potential [147], competitive ligand equilibration-adsorptive cathodic stripping voltammetry (CLE-AdCSV), which is an indirect method that detects an electrochemically active complex formed between a metal and a well-characterized organic ligand added to the sample [148], stripping chronopotentiometry (SCP), where ions are reduced at a constant potential for a fixed period of time and subsequently stripped to quantify the accumulated metal [149] and absence of gradient Nernstian equilibrium stripping (AGNES), which is specially designed for the analysis of free metal ions [150].

Other approaches have recently been developed, such as Donnan membrane techniques (DMT), diffusive gradient in thin-film gels (DGT), Chemcatcher® and liquid membranes (LMs) [151]. DMT is based on the distribution of metal ions among phases for the determination of free metal ion in non-perturbed samples [152]. In the case of DGT, the flux of metal ions through a porous gel matrix into an underlying layer of

complexing cation exchange beads is used for the quantification of the concentration of labile metals [153], whereas Chemcatcher® is formed by a chelating disk receiving phase overlaid with a cellulose acetate (CA) diffusion-limiting membrane for the accumulation by diffusion of the labile fraction of metals with minimal disturbance of the system [154]. In LM systems, the membrane is a liquid, which is immiscible with both the feed (i.e. donor) and stripping (i.e. receiving) solutions and serves as a semipermeable barrier between these two liquid or gas phases, allowing the selective transport of gases, ions or molecules [155]. Different types of LMs have been proposed, but the most used configuration for speciation studies consists of the organic phase impregnating the pores of a thin, macroporous hydrophobic support. Selectivity and transport efficiency in a LM can be improved by the addition of an extractant (i.e carrier). This technique has been used in different geometries such as flat-sheet membranes or as hollow fibre (HF). Bayen et al. [156] studied the flux of Ni species in the presence of different organic ligands, such as tartrate, glycine or oxalate, using a flat-sheet LM containing a mixture of 1,10-didecyl-1,10-diaza-18-crown-6 ether (22DD) and di(2-ethylhexyl)phosphoric acid (D2EHPA) in toluene/phenylhexane. They demonstrated that the proposed LM system was a reliable tool to measure free nickel concentrations in the presence or absence of ligands, rather than the total concentration of Ni. Likewise, Slaveykova et al. [157] also used a flat-sheet LM containing 22DD and lauric acid dissolved in a mixture of toluene/phenylhexane to meaure Pb fluxes in the absence and presence of tiron and nitrilotriacetic, iminodiacetic, malonic, citric, polyacrylic and fulvic acids. Other authors have used a LM using HF geometry in order to measure lower amounts of metal in the absence and presence of complexing agents. HF geometry allows us to measure down to 10^{-9} M of free Cd species compared to 10^{-8} M using a flat-sheet LM [158]. In the case of **zinc**, Gramlich et al. developed a LM, with a HF configuration, containing 22DD and lauric acid, for the measurement of free Zn species in the presence of organic ligands, such as ethylenediaminetetraacetate or citrate. However, when L-histidine was added, higher than calculated free Zn concentrations were measured suggesting that positively charged complexes contributed to the metal flux [159]. Moreover, other authors have reported an LM with HF configuration to determine free zinc concentration in three water samples from a mining area, reaching enrichment factors of around 700 in the stripping phase [160].

1.4 Separation and preconcentration processes

As previously stated, sample treatment is sometimes required not only to achieve very low limits of detection (in order to satisfy the corresponding environmental policy requirements), but also to remove matrix interferences.

One of the most traditional techniques for separation is liquid-liquid extraction (LLE) consisting of the transfer of a solute from one solvent to another, the two solvents being immiscible with each other. Water or an aqueous mixture and a non-polar organic liquid are frequently used as solvents. LLE comprises a step of mixing followed by a step of phase separation. Both steps are crucial in terms of solvent selection and modes of operation. Equilibrium is reached when the chemical potential of the extractable solute is the same in the two phases, leading to the definition of a "distribution coefficient" (K), which indicates the relative preference of the solute for the solvents, as shown in Eq. (1.2):

$$K = \frac{[A]_{org}}{[A]_{aq}} \qquad (1.2)$$

where $[A]_{org}$ and $[A]_{aq}$ are the equilibrium concentrations of the solute in the organic and aqueous phases, respectively. For the extraction of neutral compounds, the organic phase consists solely of a solvent. However, for ionic organic compounds or inorganic cations and anions, the presence of an additional compound, called extractant, is required. The proper selection of the extractant is a key parameter to achieve an efficient extraction. The extractant is responsible for binding with the species of interest by means of different mechanisms, such as ion exchange, solvation or chelation. A list of available extractants is further detailed in *section 1.5*.

LLE presents some advantages, such as ease of operation and simplicity of the method. However, LLE implies the use of high amounts of organic solvents (e.g., dichloromethane, hexane, petroleum ether, among others) and the risk of emulsion formation during agitation. This fact has led to the replacement of this extraction technique by other more environmentally-friendly alternatives [161]. This is the case of LMs where the small volume of organic phase encompasses the reduction of the amount of organic solvent employed and allows the use of expensive and tailor-made extractants [162,163]. LMs have been used for the separation and preconcentration of both organic

[164] and inorganic species [165]. For instance, in the case of organic compounds, LMs have been employed for the transport and preconcentration of the herbicide glyphosate and its main metabolite using a LM consisting of 0.2 M Aliquat 336 in dodecane modified with 4% dodecanol [166]. A LM with the same components was also used for the separation of **arsenic** species at pH= 13. Even though both As(III) and As(V) are present as anionic species at this basic pH and were quantitatively extracted by an anion-exchange mechanism by LLE, when using the LM and HCl as stripping phase only As(V) was transported due to differences in the extraction kinetics of arsenate and arsenite at this pH [167]. Besides, a LM with a HF geometry was also developed for the removal and preconcentration of **chromium** species, namely Cr(VI), using Aliquat 336 as carrier and a diluted HNO_3 solution as stripping. This methodology allowed both the separation and enrichment of the metal in the stripping phase [61].

Other techniques that are used to achieve both separation and preconcentration are liquid-phase microextraction (LPME), single drop microextraction (SDME), dispersive liquid-liquid microextraction or cloud-point extraction (CPE), amongst others. These techniques have been applied for the determination of different metallic species [168,169] as well as for the determination of organic compounds [170,171].

Another approach for the preconcentration of target species relies on the sorption of analytes on a solid sorbent (solid phase extraction, SPE). The solid phase usually consists of small porous particles of silica, with or without bonded organic chains, organic polymers and ion exchangers. Depending on the kind of solid phase employed, the extraction mechanism can be adsorption, partitioning or an ion exchange. Compared to LLE systems, solid sorbents are faster and provide high enrichment factors and they can also be used for the extraction of both organic and inorganic compounds. The most commonly used SPE sorbents reported in the literature for the determination of organic compounds are alkyl-bonded silicas, such as octacedcyl (C_{18}) or octyl-bonded silica, and copolymer sorbents like cross-linked polystyrene-divinylbenzene (PS-DVB) resins such as the Amberlite XAD series, in-house hypercross-linked polymeric sorbent and hydrophilic lipophilic balanced polymers, such as Oasis HLB, which form the monomers divinylbenzenevinylpyrrolidone (DVB) and N-vinylpyrrolidone. Different applications of these solid sorbents are reported in the literature [172].

However, these solid sorbents might not be well suited for the retention of species when these are polar or ionic, in particular in the case of inorganic compounds For this reason, they are modified with functional groups responsible for the extraction of the

target compound. As previously mentioned, different methodologies have been reported not only for the speciation but also for the preconcentration of inorganic **arsenic** species, which can be achieved by means of silica modified with 3-(2-aminoethylamino) propyltrimethoxysilane [143], or by using cetyltrimethylammonium bromide (CTAB)-modified alkyl silica [144], after the corresponding oxidation of As(III) to As(V). **Chromium** species have been extracted with PS-DVB functionalized with 2-Naphthol-3,6-disulfonic acid from waste waters by adjustment of the pH [173] or by using a polymeric sorbent containing aminocarboxylic groups [174]. Moreover, Cr(VI) species can be extracted and preconcentrated from water samples using activated alumina, tributyltin chloride immobilized on C_{18} cartridges, ion-exchange columns and DPC immobilized on silica [63]. **Zinc** has been extracted with XAD-4 loaded with APDC, or Chelex-100, where iminodiacetate functional groups are bound to polystyrene [175].

Other solid sorbents used for the extraction of inorganic species are based on the use of oxides such as alumina $A1_2O_3$ and magnesia MgO, among other oxide species. In the case of **arsenic** adsorption, different solid sorbents such as iron oxides or zero-valent iron [176,177], modified calcinated bauxite [178], hydrotalcite [179], and titanium dioxide (TiO_2) [180] among others [181], have also been used. An extensive list of different TiO_2-based materials for the adsorption of arsenic species can be found in the literature [182]. TiO_2 solid sorbent allows the adsorption of both inorganic arsenic species without a further oxidation step. This solid can act as a photocatalyst and adsorbent of As(III)/organic arsenic in the presence of UV light or sunlight irradiation or only as adsorbent in the absence of irradiation. TiO_2 has been used in different forms such as nanotubes, nanocrystalline particles, hydrous or granular or impregnated in chitosan beds, among others.

Solid-phase microextraction (SPME) was introduced in the early nineties by Professor Janusz Pawliszyn [183] as an alternative to SPE for the extraction of organic compounds. The commercial SPME device contains a fused silica fibre coated with a suitable stationary phase polymer, polydimethylsiloxane (PDMS), polyacrylate (PA), and also mixtures of polydimethylsiloxane and polydivinylbenzene (PDMS-DVB), carbowax and polydivinylbenzene (CW-DVB) being the most common [161]. This technique has been extensively used for the determination of different organic compounds [184,185]. Likewise, stir-bar sorptive extraction (SBSE) consisting of a magnetic stirrer coated with a thick layer of PDMS, where the target compounds are extracted, has been employed showing greater sorption capacity compared to SPME fibres [161,186].

Recently, other sorbent-based microextraction techniques have also been explored using magnetic molecularly imprinted polymers [187], silicone rods and silicone tubes [188] or HF [189].

1.5 Polymer Inclusion Membrane (PIM)

Among the different sample treatments, membrane-based processes have attracted noticeable attention as a valuable alternative to conventional separation processes [190]. In general, a membrane can be defined as a semipermeable barrier between two phases [191]. The membrane restricts the movement of the different molecules through various mechanisms such as size exclusion, differences between diffusion coefficients, electric charge, among others [192]. Membranes can be classified by the driving force that causes the flow of the analytes through the membrane [193]: pressure difference across the porous membrane (*i.e.* reverse osmosis, ultrafiltration, microfiltration, membrane gas and vapour separation), temperature difference across the membrane (*i.e.* membrane distillation), concentration difference across the membrane (*i.e.* dialysis, membrane extraction), electric potential difference across the membrane (*i.e.* electrodialysis) and chemical potential difference across the membrane (*i.e.* liquid membrane, LM). In contrast to osmotic, dialysis, filtration or size-exclusion type membranes, LMs rely on the action of a chemical agent to extract the solute of interest from an aqueous phase [162]. The carrier is usually solubilized in an organic solvent and different types of LMs have been described, depending on whether they only contain liquid phases or the liquid phase is retained in a polymeric support. Bulk liquid membrane (BLM) consists of a bulk aqueous feed and stripping phases separated by a bulk organic, water-immiscible liquid phase. Emulsion liquid membrane (ELM) is prepared from the mixture between the aqueous feed solution and an emulsion, which is formed by the stripping solution, an organic solution and the suitable surfactant. In this kind of membranes, the stripping solution is emulsified in an immiscible LM, which is dispersed in the feed solution allowing the mass transfer from the feed into the internal stripping phase. Supported liquid membranes (SLMs) are usually constituted with the mobile carrier and the organic solvent, in the pores of a solid microporous support, where it is retained by capillarity. SLMs have been extensively studied since they offer high transport rates and good

selectivity, although a lack of long-term stability hampers their use in many practical applications [194].

In contrast PIMs are a relatively novel type of self-supporting LMs entrapping the carrier in a base polymer matrix, which consists of a base polymer and in some cases may contain plasticizers and chemical modifiers [162].

The concept of PIM first appeared 50 years ago, and since then it has received several names such as polymer liquid, gelled liquid, polymeric plasticized, fixed-site carrier or solvent polymeric membrane [190]. Later, in 1987, Sugiura et al. [195] were the first to name this kind of membrane PIM. From then onwards, PIMs have been used in many different applications as they exhibit excellent stability and versatility and adequate mechanical properties. They are economically viable, and they also prevent the use of high amounts of toxic compounds, making them an environmentally friendly alternative [196]. The evolution of the number of published papers on PIMs since 2000, is shown in Figure 1.6.

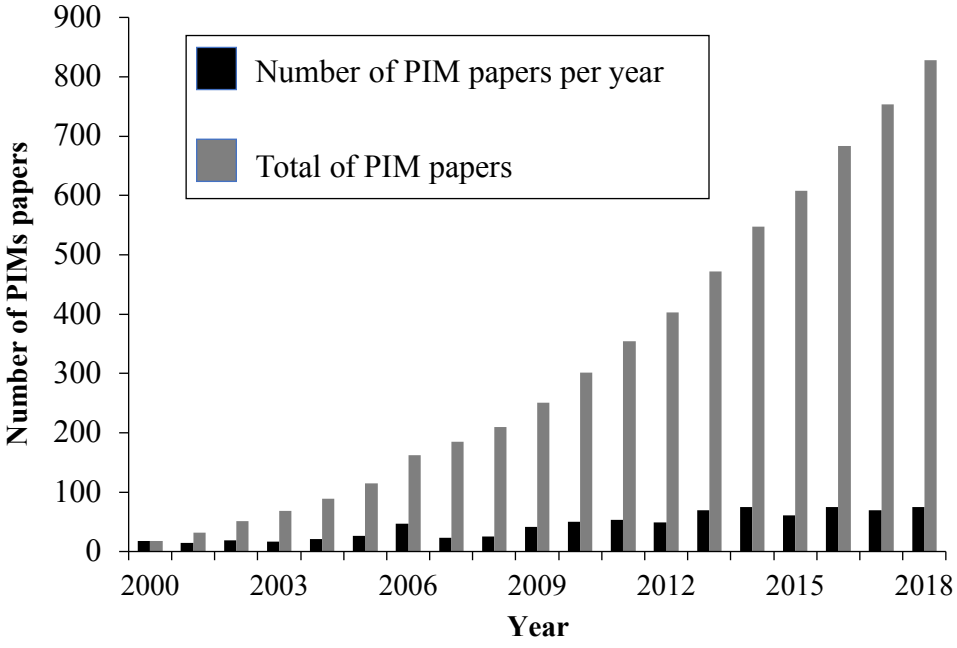

Figure 1.6 Evolution of the number of PIM papers (including reviews) from 2000 until 2018 (according to ISI web of Knowledge).

The transport mechanism in PIMs, as well as in other LMs containing a carrier, can be formally described as the simultaneous combination in a single stage of an extraction and a stripping operation in non-equilibrium conditions [165]. First the analyte,

which is initially found in the feed solution, reacts in the feed-membrane interface with the carrier, forming a lipophilic complex. Then, the complex diffuses across the membrane and is released at the membrane-stripping interface. This process is known as facilitated or carrier-mediated LM separation. In many cases, facilitated transport is combined with coupling counter- or co-transport of different ions through the liquid membrane [155,192]. A scheme of the transport of a cation (M^+) and the counter-transport of H^+ across a liquid membrane is depicted in Figure 1.7.

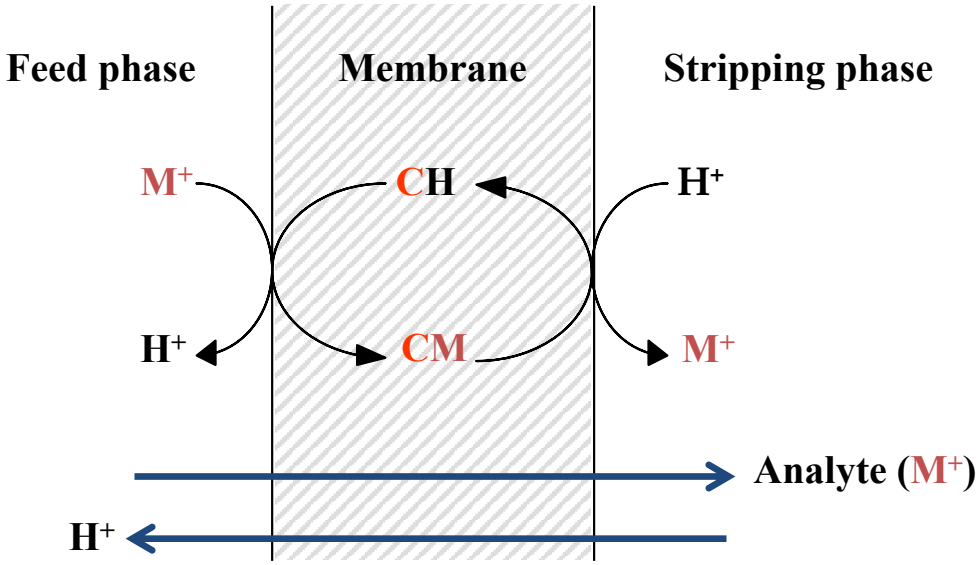

Figure 1.7 Mechanisms for maintaining electroneutrality during the transport of a cation (M+) and the counter-transport of H+ through a LM. C stands for the carrier.

The transport of cations can be achieved through different mechanisms: (i) co-transport of a counter-anion, (ii) counter-flux transport of H^+ (as shown in Figure 1.7) or (iii) the counter-flux transport of any other cation.

Metal species are transported across the membrane against their concentration gradient by "uphill" transport which will continue until all the metal species are transferred from the feed to the stripping side, provided the driving force of the process is kept constant [165].

Different authors [165,197] have proposed mathematical models to explain metal flux across the membrane comprising the different steps occurring during transport. At the steady-state, the diffusion through the aqueous boundary layer (J_a), the interfacial flux (J_b), and the membrane diffusion (J_c) are equal, and by further assuming linear

concentration gradients, the following equation (Eq. 1.3) is obtained for membrane flux (J), and permeability coefficient (P):

$$P = \frac{J}{C} = \frac{K_1}{K_1 \frac{d_a}{D_a} + K_{-1}\frac{d_0}{D_0} + 1} \quad (1.3)$$

where C stands for the time-dependent bulk concentration of metal species in the feed solution, K_1 and K_{-1} are the pseudo-first-order rate constants of the interfacial reactions, d_a and d_0 are the thickness of the aqueous and membrane diffusion layer, respectively. D_a and D_0 represent the aqueous and the membrane diffusion coefficient, respectively.

Equation (1.3) can be further simplified when interfacial chemical reactions are very fast and since the relationship of J with the concentration (C), the feed volume (V) and the membrane area (A) is (Eq. 1.4):

$$J = -\frac{dC}{dt} \cdot \frac{V}{A} \quad (1.4)$$

the resulting integrated form of the flux is (Eq. 1.5):

$$ln\frac{C}{C_0} = -\frac{A}{V}\,Pt \quad (1.5)$$

where C_0 is the value of C at time zero. Equations (1.3) and (1.5) are used to predict the permeation behaviour of LMs when feed solutions are relatively dilute in metal species [165].

Apart from the characterization of the membrane system by experimentally determining the permeability coefficient, LMs can provide different types of information by measuring the total concentration of the analyte in the stripping solution:

- At equilibrium, the corresponding concentration at the stripping phase is proportional to either the total concentration or to that of the free analyte species in the source solution, depending on the nature of the stripping phase and the volumes of stripping and feed phases.

- The flux through the membrane over a short accumulation time may provide the concentration of free analyte species, the whole of the labile complexes or lipophilic complexes depending on the characteristics of the device used [197].

Then, with the appropriate design of the membrane system, including chemical and physical parameters, LMs, can be used as a tool for preconcentration of analyte species, thus facilitating their determination, and they can also be used as sensors for speciation measurements. Both aspects have been indicated in previous sections.

1.5.1 PIM Components

Membrane properties depend essentially on the materials that comprise them and their structure. The choice of these components plays a fundamental role in the selectivity of the separation and in the stability of the membrane.

The **polymer** that constitutes the skeleton of the PIM consists of linear polymer strands and because there are no cross-links between these strands, they can be dissolved in a suitable organic solvent, where the polymer strands become separated. It plays a crucial role as it provides the membrane with mechanical strength due to a combination of intermolecular forces and the process of entanglement. Despite the absence of intermolecular covalent bonds, a very stable film is formed. Membrane flexibility is governed by the nature of the main polymer chain as well as the side chains. Depending on the saturation of the main chain, the bonds may rotate or not, and therefore, either a flexible or rigid chain will be generated. Indeed, the presence of aromatic or heterocyclic groups in the main chain reduces flexibility, but increases both thermal and chemical stability. Conversely, the presence of other elements such as oxygen or nitrogen increases the flexibility of the material. On the other hand, if the lateral groups are long, strong interactions will be generated between them, restricting the movement, and therefore decreasing flexibility.

The length of polymer chains, which is the number of repeating units, determines the properties of the material. The longer the chain, the more possibilities of interaction with other chains, and therefore the properties of the polymer will be different. Polymers contain a great number of chains and not all of them with the same molecular weight (MW). This is the reason why an average MW is given for each polymer. Polymer MW

is a key parameter that must be higher than the critical entanglement molecular weight (MW_c). MW variations above MW_c are expected to produce a negligible influence either on membrane performance or mechanical strength [198].

In terms of interaction between polymer chains, in the case of three-dimensional polymers, interactions are mostly covalent bonds, whereas in the case of side chains, interactions are hydrogen bonding, dispersion forces or dipole-dipole interactions. All these interactions are strongly related to the polymer's physical properties and to its permeability.

Another parameter that must be taken into account is the state of the polymer, whether crystalline, liquid or vitreous. Generally, a degree of crystallinity reduces permeability through the membrane, whereas it is enhanced with membrane elasticity. One characteristic of the polymers is the vitreous transition temperature (Tg), which is the gradual and reversible transition from which an amorphous polymer (not crystalline) turns from a rigid and relatively brittle state (vitreous state) into a viscous or rubbery state as the temperature is increased. In this state the free rotation of the polymer chains allows more flexible membranes. Besides, the degree of crystallinity determines the state of the polymer. Some polymers have regular structural units that allow the formation of crystals, since the chains can be packaged according to an ordered pattern. The presence of crystals clearly influences the mechanical and transport properties of the membrane.

If the polymer is amorphous, an increase in temperature above the Tg will cause a drastic modification to its chemical and physical properties. This change will also occur in crystalline polymers if we exceed the melting temperature (Tm). Nevertheless, if the temperature increase is too high, irreversible degradation (decomposition, oxidation, etc.) can be achieved.

Polymers used on PIM preparations are thermoplastic and among the great variety, poly(vinyl chloride) (PVC) and cellulose triacetate (CTA) are the two main polymers used in most of the investigations conducted so far. The widespread use of these two polymers is due to the fact that they provide a thin film through a simple procedure based on a solvent casting method and to the scarcity of information regarding the role of the base polymer [190]. The physical properties of different polymers used in PIM preparations are summarized in Table 1.1.

CTA is a polar and frequently highly crystalline polymer with a number of hydroxyl and acetyl groups that are capable of forming highly orientated hydrogen bonding. Moreover, CTA can be slightly hydrated and, thus, prone to acid hydrolysis. In

contrast, the group C-Cl in PVC is relatively polar and non-specific dispersion forces dominate the intermolecular interactions. Thus, PVC is an amorphous polymer with a small degree of crystallinity [190].

Besides PVC or CTA, a few other base polymers have been tested, such as cellulose derivatives (i.e. cellulose acetate propionate (CAP), cellulose acetate butyrate (CAB), and cellulose tributyrate (CTB)). Gardner et al. [199] compared the different cellulose derivates in terms of resistance against hydrolysis under alkaline or acidic conditions, finding that resistance to hydrolysis was enhanced with an increase in the alkyl chain, although the transport across the membrane decreased. Besides, Ocampo et al. [200], tested different PIMs based on CAP, CAB and cellulose acetate hydrogen phthalate (CAH) as polymers and dinonylnaphthalene sulfonic acid (DNNS) and dinonylnaphthalene disulfonic acid (DNNDS) as carriers. The PIM preparation was not possible using DNNS and only fragile membranes were obtained when DNNS was employed as the carrier.

In addition, more recently some PIMs have been prepared using poly(vinylidene fluoride-co-tetrafluoroethylene) (PVDF-TFE) [201,202] or poly(vinylidine fluoride-cohexafluoropropylene) (PVDF-HFP) [203,204] as the base polymers. PVDF is a thermoplastic fluoropolymer that shows good chemical resistance, because of the lack of reactive functional groups, and an excellent thermal and mechanical stability. All these advantages have made it an attractive base polymer for PIM preparations [205].

PVDF-HFP has been used for the preparation of cross-linking membranes with the aim of further reducing membrane leaching into the adjacent aqueous phases. The cross-linking process is based on the creation of a more tortuous and rigid environment in the PIM polymeric structure, which is achieved by treating PVDF-HFP with bisnucleophiles, such as diamines or bisphenols at an elevated temperature, or by irradiation (e.g., electron beam). As an alternative to these difficult approaches, PVDF-HFP can also be combined with a cross-linking oligomer such as poly(ethylene glycol) diacrylate (PEG-DA) [206] or poly(ethylene glycol) dimethacrylate (PEG-DMA) [207], in order to obtain a semi-interpenetrating polymer network. First, the polymer is dissolved in an organic solvent and later the solution is cast to obtain a film. Then, the film is treated either with heat or with ultraviolet light to induce the cross-linking of the oligomer leading to the distribution of PVDF-HFP chains in the membrane's three-dimensional network.

Although the cross-linking process leads to an increase in tortuosity and rigidity, which may cause an undesired effect by depleting membrane permeability, photo-

crosslinked PIMs have been successfully applied in thiocyanate transport showing a significant increase in both membrane stability and permeability in comparison to traditional PIMs [208].

Table 1.1 Physical properties of polymers frequently used in PIMs.

Polymer	Structure	MW used in PIMs (KDa)	MW_c	Tg (ºC)	Tm (ºC)	Characteristics
PVC	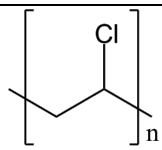	90-180[a]	12.7[a]	80[a]	na	Slightly crystalline, mostly amorphous
CTA	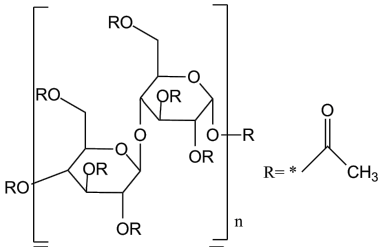	72-74[a]	17.3[a]	na	302[a]	Infusible, high degree of crystallinity, excellent strength
CTB	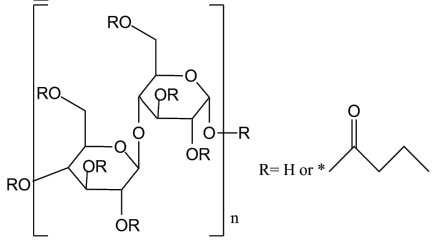	120[a]	47.4[a]	na	207[a]	Infusible, high degree of crystallinity, excellent strength
PVDF-HFP	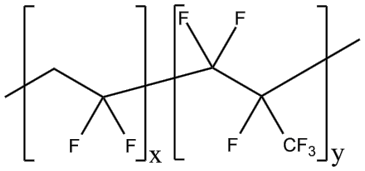	<400[b]	na	na	115-135[b]	Crystalline, thermoplastic copolymer

na: not available.

[a] Ref [190].

[b] Ref [209].

The **carrier** is usually a complexing agent or ion-exchanger responsible for binding the target species, facilitating its extraction into the PIM. Performance of the membrane system is strongly related to carrier characteristics. The general desirable characteristics for carriers are listed below [155]:

- High selectivity towards target species.
- High capacity of the target species to be extracted.

- High ability to complexate (to extract) a solute from an aqueous feed phase into a liquid membrane phase at feed-liquid membrane interface (high extraction or distribution, or partition constant).
- High ability of carrier-solute complex in a liquid membrane to be decomplexed and stripped into an aqueous stripping phase at the liquid membrane-stripping interface (high decomplexation or stripping constant).
- Rapid kinetics of formation (complexation) and destruction (decomplexation) of the complex on membrane interfaces.
- Rapid kinetics of diffusion of the carrier-solute complex through the liquid membrane (a measure of the diffusion rate, diffusion coefficient).
- Stability of the carrier.
- No side reactions.
- No irreversible or degradation reactions.
- Low solubility of the carrier into the adjacent aqueous phases.
- No complexation (coextraction) of water.
- It should be easily regenerated.
- Suitable physical properties, such as density, viscosity, surface tension.
- Low toxicity for biological systems and low corrosivity.
- Reasonable price at industrial applications

Although some authors have reported newly synthesized reagents, most of the research on PIMs has been conducted using commercially available solvent extraction reagents as carriers. The different carriers can be classified into four groups: basic, acidic and chelating, neutral or solvating and macrocyclic and macromolecular, examples of these group of compounds can be seen in Table 1.2.

Among the different basic carriers, fully substituted quaternary ammonium compounds (e.g., Aliquat 336), react as an anion exchanger forming an ion-pair with another metal anion or a complex metal anion present in the feed phase, whereas in the case of amine and other weak bases, the carrier must be firstly protonated to allow anion exchange [190].

Table 1.2 Classification and some examples of the different carriers used in PIMs studies.

Type of carriers		**Examples**
Basic	Quaternary amines	methyltrioctylammonium chloride (Aliquat 336)
	Tertiary amines	Tri-n-octyl amine (TOA), tri-n-decylamine (TDA), tri-n-butylamine (TBA), tri-n-hexylamine (THA), among other tri-alkyl amines
	Pyridine and derivatives	4-(1'-n-tridecyl)pyridine N-oxide (TDPNO)
Acidic	Hydroxyoximes	2-Hydroxy-5-nonylacetophenone oxime (LIX® 84-1)
	Hydroxyquinoline	7-(4-Ethyl-1-methyloctyl)-8-hydroxyquinoline (Kelex 100)
	β-Diketones	Benzoylacetone, dibenzoylacetone, benzoyltrifluoroacetone
	Alkyl phosphoric acids	Di(2-ethylhexyl) phosphoric acid (D2EHPA), Di(2-ethylhexyl) dithiophosphoric acid (D2EHDTPA), Bis(2,4,4-trimethylpentyl)phosphinic acid (Cyanex 272), Bis(2,4,4-trimethylpentyl)dithiophosphinic acid (Cyanex 301), Bis(2,4,4-trimethylpentyl)monothiophosphinic acid (Cyanex 302), Tri-isobutylphosphine sulfide (Cyanex 471X)
	Sulfonic and carboxylic acids	DNNS, DNNDS, Lauric acid, Lasalocid A
Neutral	Phosphoric acid esters	Tri-n-butyl phosphate (TBP)
	Phosphonic acid esters	Dibutyl butyl phosphonate (DBBP)
	Others	Octyl(phenyl)-N,N-diisobutyl carbamoylmethyl phosphine oxide (CMPO), N,N,N',N'-Tetraoctyl-3-oxapentanediamide (TODGA), Tri-n-octyl phosphine oxide (TOPO), polyethylene glycol
Ionic liquids (ILs)	Ammonium	methyltrioctylammonium chloride (Aliquat 336), methyltrioctylammonium thiosalicylate
	Phosphonium	Trihexyl(tetradecyl)phosphonium chloride (Cyphos 101), trihexyl(tetradecyl)phosphonium-(2,4,4-trimethylpentyl)phosphinate (Cyphos 104)
	Imidazolium	1-Butyl-3-methylimidazolium hexafluorophosphate, 1-octyl-3-methylimidazolium tetrafluoroborate
	Others	1-butyl-1-methylpyrrolidinium trifluoromethanesulfonate, 1-butyl-3-methylpyridinium tetrafluoroborate
Macrocyclic and macromolecular	Crown ethers and calixarenes	Di-tert-butylcyclohexano-18-crown-6 (BuDC18C6), DC18C6, imidazole azothiacrown ether, Meso-octamethyl-porphyrinogen (Calix[4]pyrrole), among others.
	Others	Bathophenanthroline, bathocuproine, poly(vinylpyrrolidone) (PVP)

Basic carriers are used for the extraction and/or transport of anionic complexes of heavy metals (e.g., As(V), Au(III), Cd(II), Co(II), Cr(VI), Cu(II), Ni(II), Pd(II), Pt(IV), Re(VII)), anions (e.g., I^-, SCN^-) and organic compounds (e.g., antibiotics, small saccharides, thiourea, among others)

Acidic carriers (e.g., alkyl phosphoric acids, sulfonic acids and carboxylic acids) are frequently used for the extraction and transport of metal cations (e.g., Zn(II), U(VI), Pb(II), Cd(II), Cr(III), Fe(III)), involving the exchange of the metal ion for protons of the carrier. Moreover, the group of compounds such as hydroxyoximes, hydroxyquinoline and β-Diketones, present both acidic and strong chelating properties.

Neutral and solvating carriers show a high selectivity towards actinides and lanthanides such as U(VI) and Ce(III). In the case of phosphoric and phosphonic acid esters, the mechanism is based on the replacement of the water molecules coordinated to the metallic cation by molecules of the carrier. The carrier D2EHPA has been incorporated in PIMs allowing the extraction of bivalent ions such as Zn(II), Cd(II) or Pb(II) [210]. This carrier has a hydrophobic character and good solubility in many organic solvents. Extraction with D2EHPA is based on a counter-transport mechanism; in this case, a crossed transport of protons and metallic ions takes place [211].

Another important group of carriers are **ionic liquids** (ILs), which are molten salts liquid at room temperature formed by an organic cation and an organic or inorganic anion. ILs present remarkable features, such as high ion conductivity, negligible vapour pressure, low volatility, non-flammability, high potential for recycling, high solvating capacity and high viscosity. However, they only attracted attention after the mid-1980s when ILs with a low melting temperature were presented as solvents for organic synthesis [212,213]. Since then a large amount of ILs have been reported with a great variety of structures and properties. The extensive range of combinations of cation and anion that ILs provide, permits an extensive variety of tunable interactions and applications [214,215]. In the late 1990s, the concept of task-specific ILs (TSILs) was introduced. TSILs are formed by ILs containing metal ion-ligating functional groups. They can be used both as the hydrophobic solvent and the extractant. One example of these compounds is Aliquat 336 which is classified as a basic carrier but also has properties related to ILs. Aliquat 336 is an affordable cation source of a new family of hydrophobic ILs [216]. This extractant has been incorporated in different PIM-based systems for the extraction and preconcentration of a wide range of target compounds such as oxyanions, anion metallic species or different organic compounds, as shown in the literature [196].

Moreover, Aliquat 336 allows the extraction of As(V) present in waters at neutral pH (mainly $H_2AsO_4^-$ and $HAsO_4^{2-}$) by an anion-exchange mechanism. As(III) is not transported under neutral pH conditions since it is mainly present as a neutral species (H_3AsO_3) and thus permits the speciation of arsenic inorganic species [217]. Moreover, Aliquat 336 also allows the extraction of Cr(VI) species at low pH as the predominant species is the anion $HCrO_4^-$ [218].

Finally, **macrocyclic and macromolecular** carriers bear high complexing selectivity toward metal ions as their structure can be tailored to a selected metal ion. The extraction is based on the recognition of the target compound. Besides, they also exhibit low water solubility, although they are expensive to synthesize and most of them are not commercially available.

The addition of **plasticizers** or modifiers increases membrane softness and flexibility. They are usually organic compounds that contain a hydrophobic alkyl skeleton with a polar group or more. However, the addition of these compounds is not mandatory when the carrier also presents plasticizing properties (e.g., Aliquat 336, D2EHPA and TBP). The addition of these compounds has also been shown to enhance metal flux across the membrane [219].

Plasticizers penetrate between polymer chains, which are held together by a combination of various types of attractive forces, and "neutralize" the polar groups of the polymer with their own polar groups or increase the distance between polymer molecules, reducing the strength of the intermolecular forces.

The Tg temperature of a plasticized membrane decreases as the amount of plasticizer increases. In general terms, this can produce an increase in the diffusion coefficient and therefore in membrane permeability. From a physicochemical point of view, individual molecular chains are connected to a polymeric membrane by a combination of various types of forces. As an example, Van der Waals forces are very frequent but weak and little specific. In addition, polar interactions, which are much stronger, only occur with the presence of polar centres in the molecule. These polar interactions increase the rigidity of membranes due to an unlikely three-dimensional structure that hampers the diffusion of the species of interest. Therefore, plasticizers are used to improve the flexibility and the compatibility between the membrane components

(i.e. base polymer, carrier and carrier/extracted species complex or ion-pair) [190,205,220].

The different physicochemical parameters of the plasticizers have a strong impact on the flux across the membrane. Polarity, which is related to the dielectric constant and viscosity of the plasticizer, is likely to be the main characteristic which affects the transport of PIM systems. Besides, the plasticizer's polarity influences the chemical potential of metal ion partitioning in the membrane, whereas increasing the viscosity of the plasticizer decreases the rate of transport, most likely by inhibiting diffusion [221]. Kozlowski and Walkowiak [222] obtained a linear correlation between the viscosity of the plasticizer and the Cr flux across polymeric membranes containing TOA as the carrier. Besides, some authors have attributed the success of nitrophenyl alkyl ethers in PIM studies, to their high dielectric constants despite their low viscosity [195,223]. However, certain caution must be adopted when attempting to correlate initial PIM flux values with the dielectric constant and viscosity of the plasticizer. It is worth mentioning that the resulting dielectric constant of the PIM itself depends on the dielectric constants from the carrier and the base polymer [205].

Despite the great variety of commercially available plasticizers, only a reduced number have so far been used in PIM studies, such as 2-nitrophenyloctyl ether (NPOE), 2-nitrophenylpentyl ether (NPPE), bis(2-ethylhexyl) adipate (DEHA), dibutyphtalate (DBP) or dibutylsebacate (DBS) [219]. Other examples of plasticizers with the corresponding physicochemical parameters are shown in Table 1.3.

Table 1.3 Physicochemical parameters of some PIM plasticizers (adapted from [205]).

Plasticizer	Dielectric constant (εr)	Viscosity (cP)
NPOE	24 (25°C)	11.1 (25°C)
NPPE	24 (na)	7.58 (na)
DEHA	5 (na)	13.7 (na)
DBP	6.58 (20°C)	16.6 (25°C)
Tris-(2-ethylhexyl) phosphate (TEHP)	4.8 (25°C)	13.1 (25°C)
DBS	4.54 (20°C)	9.5 (na)
Tris(2- butoxyethyl) phosphate (TBEP)	8.7 (na)	-
2-fluorophenyl 2-nitrophenyl ether (2-FP2-NPE)	50 (na)	13.0 (na)
Dioctyl phthalate (DOP)	5.22 (20°)	40.4 (na)
TBP	8.34 (20°)	3.32 (na)
Ethyl benzoate (EB)	6.20 (20°C)	-

2-Nitrophenyl octanoate (NPOT)	5.88 (na)	-
1-dodecanol	5.82 (30°C)	-
1-tetradecanol	4.42 (45°C)	-

na: temperature not available

The amount of plasticizer is also a crucial factor, as a low amount can lead to undesirable rigidity and brittleness being obtained. This phenomenon is commonly referred to as the "anti-plasticizing" effect. The minimum amount varies according to the plasticizer and the base polymer used. Conversely, the addition of a great amount of plasticizer is also problematic, since it can interfere in the membrane/aqueous phase interface, creating an additional barrier that limits the transport of the species of interest through the membrane. Therefore, an excess of plasticizer can produce a decrease in the mechanical resistance of the membrane, as well as a reduction in its transport efficiency [190].

1.5.2 Characteristics of PIMs

These aforementioned components are incorporated into a PIM by a relatively simple process. All components are dissolved using a suitable solvent, mixed, cast in a mould (e.g. a glass ring positioned on a flat glass plate or in a petri dish) and the solvent is allowed to evaporate. Once this has been achieved, a transparent, flexible and homogeneous film is left; this film is a PIM (see Figure 1.8).

Figure 1.8 PIM placed on a wooden plank.

Moreover, PIMs possess a dense structure, with no pores. This ease of fabrication makes PIMs particularly attractive for the development of low-cost separation technologies.

1.5.3 Characterization of PIMs

Several techniques have been used in PIM studies to provide information about the morphology and structure of the membranes, and to evaluate the resulting PIM composition, assess homogeneity or to check the presence of a micro-porous structure.

A great variety of different techniques has been used for PIM characterization, such as scanning electron microscopy (SEM), SEM-energy dispersive spectroscopy (SEM-EDS), atomic force microscopy (AFM), Fourier transform infrared spectroscopy (FTIR), transmission infrared mapping microscopy (TIMM), reflection infrared mapping microscopy (RIMM), X-ray photoelectron spectroscopy (XPS), X-ray diffraction (XRD), XRF, thermogravimetric analysis (TGA), differential scanning calorimetry (DSC), impedance spectroscopy (IS), elastic and contact angle measurements.

SEM, AFM and XPS are surface techniques, which provide information about the membrane morphology, such as how the carrier and/or the plasticizer are distributed within the base polymer. SEM images of PIM surfaces and cross-sections show the homogeneity and dense structure of this kind of membranes (see Figure 1.9 for a PIM composition of 50% CTA – 50% Aliquat 336).

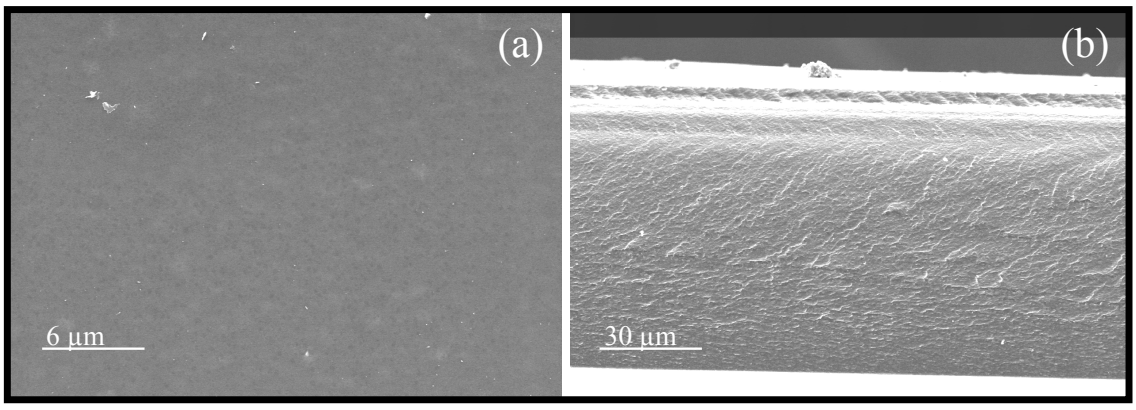

Figure 1.9 SEM images of PIMs consisting of 50% CTA–50% Aliquat 336: surface (a), cross-section (b).

Moreover, a combined analysis of SEM-EDS can be used to obtain semi-quantitative elemental results about very specific locations within an area of interest, as reported by Mercader-Trejo et al. [224], where the sulphur content of Cyanex 471X was monitored to demonstrate the homogeneous distribution of the carrier across the membrane. An analogous technique is XPS, which provides valuable quantitative and chemical state information from the surface of the membrane [225].

The use of AFM has been demonstrated as a useful technique for detecting the leaching of the carrier from a PVC-based PIM [226]. Moreover, this technique has also been used to compare the more homogeneous surface and smoother appearance of membranes plasticized with TBP compared to those plasticized with NPOE, correlating the smoother surface with an enhanced permeation [227].

FTIR analysis has been used to provide information about the interaction between the different PIM components. However, different studies have concluded that no covalent bonding takes place between the different constituents of the membrane; there are only weak interactions such as Van der Waals or hydrogen bonds [210,228].

Some authors have used the TIMM technique to obtain a distribution profile of the membrane components. Ansari et al. [229], found a slightly non-uniform distribution of the carrier TODGA in CTA-based PIMs, whereas De San Miguel et al. [230] used TIMMs maps to study the distribution of kelex 100 and NPOE. In addition, the analogous technique RIMM was used to study the distribution of the carrier D2EHPA in PIMs with different compositions, obtaining an increase in the extractant absorbance band with the increase in its concentration [231].

XRD examines the crystallinity of a sample. It provides information about the crystal structure(s) of the membrane, as well as the space group, lattice parameters, preferred orientation and crystallite size. It suggests that CTA-based PIMs containing crown ethers as carriers, and TBP or NPOE as plasticizers, present an amorphous structure [232,233]. Moreover, energy dispersion X-ray fluorescence (EDXRF) which is a non-destructive technique, has been used to directly quantify the amount of mercury adsorbed in a PIM without a further elution step [234]. This technique has also been employed to monitor the leaching of the carrier Aliquat 336 by determining the presence of chloride, before and after mass loss experiments, in CTA-based PIMs.

To understand the type of interaction between the base polymer and the different carriers as well as to provide information about the thermal degradation of the different PIM components, TGA has been employed as an effective technique [200,210]. TGA and

DSC analysis are frequently performed together in the same analysis. DSC experiments performed on PIMs showed variation on the Tg with the addition of a plasticizer to a CTA-based membrane. The presence of NPOE lowered the Tg compared to pure CTA, hence demonstrating the plasticizing effect of NPOE [221].

Another characterization technique used in PIMs studies so far is IS, which allows the determination of electrical parameters of materials, such as electrical resistance and capacitance, which are directly related to the electrical response of a particular material. The experimental set-up of this technique is shown in Figure 1.10.

Vazquez et al. [225] reported that an increase in the amount of the carrier Aliquat 336 clearly enhances both membrane dielectric constant and conductivity, regardless of the membrane supporting material. Membranes, either based on PVC or CTA with the same Aliquat 336 content, showed similar conductivity values and only slight differences were observed in the case of dielectric permeability.

Elasticity is a crucial parameter as previously stated. Therefore, different authors have performed elastic measurements on different PIM compositions. A clear softer and tougher character of the PVC-based membranes was obtained compared to CTA-based membranes and, in addition, elastic behaviour enhancement was observed with an increase of Aliquat 336 on both polymer-based membranes [225].

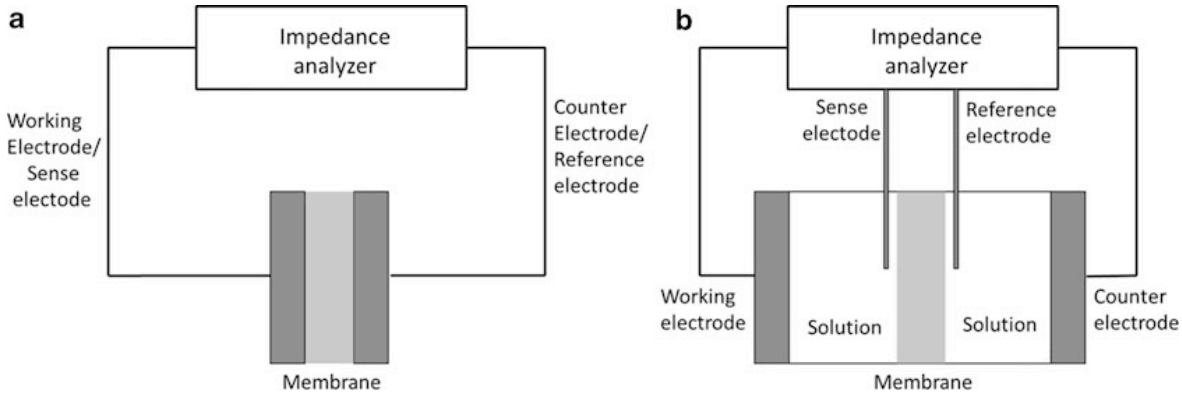

Figure 1.10 Experimental set-up of IS on membrane characterization using two probes (a) or four probes (b) [235].

The membrane's hydrophobic/hydrophilic character is also of paramount importance and can be determined by contact angle measurements. A high hydrophobicity of the PIM results in a more stable membrane [228]. However, higher contact angle values normally correspond to lower permeability values as found in the

literature [236], and thus, a compromise between stability and efficiency must be achieved.

1.5.4 Analytical applications of PIMs

PIMs were first used as sensing membranes in ion-selective electrodes (ISEs) and optodes about 50 years ago. From then onwards, PIMs have been used in different analytical applications such as sample preparation, sample preconcentration, electro-driven extraction, passive sampling, speciation studies, and incorporated into on-line and automated analysis systems and used as sorbents for different target compounds.

In 1970, a more suitable procedure for preparing the sensing membrane in ISEs was presented, by the immobilization of the organic phase in a PVC polymeric matrix. However, these were not termed as PIM, even though they were practically identical [237]. The main difference between polymer membranes used in ISEs and the ones used in PIM studies is the amount of extractant and plasticizers used in the membrane composition. In the case of ISEs, a concentration of the carrier (also called ionophore in this application) ranging from 1% to 2% in total weight is needed to achieve a fast ion exchange at the membrane/sample solution interface with a very low transport rate of the ion of interest. Conversely, in the case of PIMs, concentrations starting from 30% are normally used as both fast ion exchange and transport are required [219].

Nowadays, the research using polymer membranes in ISEs is focused on lowering the limits of detection and allowing this technique to provide reliable results down to picomole or even femtomole [238]. This research has led to highly stable and reproducible miniature sensing devices being obtained for monitoring purposes in clinical and environmental applications [196].

PIMs have also been broadly employed in optical chemical sensors, named optodes, since first reported in 1989 [239]. Optode sensing involves the formation of a coloured or fluorescent complex with the analyte and numerous recent works are listed in the following review [196].

PIMs have been demonstrated to be an effective tool for sample treatment, and different authors have employed them for the separation and preconcentration of various species of interest, such as metallic species or organic compounds. Likewise, our research group has effectively contributed to the separation and preconcentration of different

compounds using PIMs. In 2006, a novel method was reported for the separation and preconcentration of Cr(VI) from electroplating waste waters by means of an Aliquat 336-based PIM used as a sorbent. PIMs showed a higher degree of homogeneity in terms of metal distribution when compared to SLM [240].

In addition, a simple and effective procedure for both cadmium removal and separation, using an Aliquat 336-based PIM from either acidic or saline solutions, was also presented [241]. Besides, a PIM-based system was used for the separation and transport of inorganic As species (arsenite and arsenate) from aqueous solutions using a two-compartment transport cell (see Figure 1.11) [121]. Moreover, a different configuration was used for arsenate transport, where the volume of the stripping phase (5 mL) was lower than the volume of the feed phase (100 mL) and thus, allowed a preconcentration of arsenate. The resulting method was successfully applied for the determination of arsenate in groundwaters [217]. With regard to organic compounds, PIMs have successfully been applied for the transport and preconcentration of six different antibiotics (four sulphonamides and two tetracyclines) from environmental water samples [242].

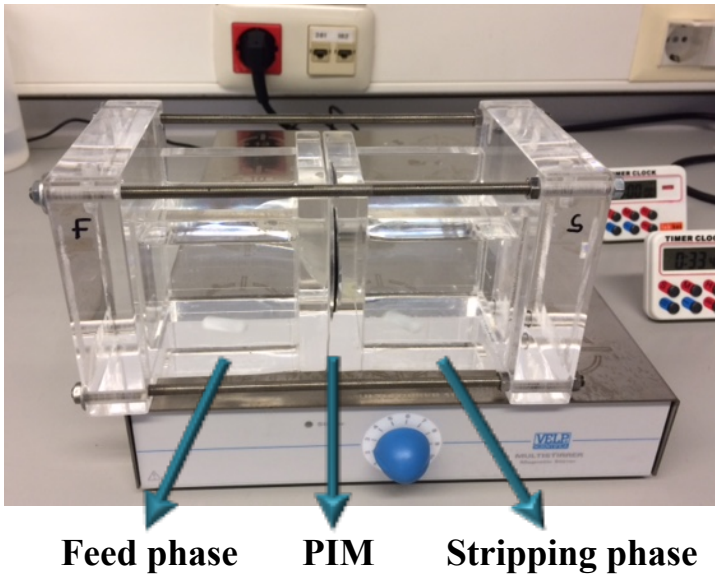

Figure 1.11 Two-compartment transport cell placed on a magnetic multistirrer.

Besides the above mentioned off-line configurations which involve two compartments separated by a PIM and where samples need to be manually collected from the stripping phase, PIMs have also been incorporated in on-line systems which use a

flow-through approach where both feed and stripping solutions flow past the PIM. In 2011, the first use of a PIM for on-line separation in FIA, involving simultaneous extraction and back-extraction, was reported. The optimal PIM composition consisted of 40% D2EHPA as the carrier, 10% DOP as the plasticizer and 50% PVC as the base polymer, and allowed the on-line determination of Zn(II) in aqueous samples in the presence of other metallic species [243]. Later, the same authors presented two different approaches involving temperature and sonication to improve the already existing FIA system by enhancing the overall mass transfer process in the PIM separation cell [244]. Moreover, the same research group presented a highly sensitive FA system for the trace determination of phosphate in natural waters, using a PIM containing Aliquat 336 as the carrier. The resulting method allowed the analysis of natural water samples containing concentrations of phosphate in the low μg L^{-1} range [245]. More recently, a PIM constituted by PVDF, Cyphos 101 and NPOE was used for the on-line extractive separation of V(V) prior to its spectrophotometric determination in a FIA system. The developed system allowed the determination of V(V) in water and dietary supplement samples [246].

PIMs have also been tested in electro-membrane extraction, where membrane extraction is driven by an electric field rather than facilitated transport. SLMs have traditionally been used in this application. However, due to their limited stability, the use of PIMs has emerged as an attractive alternative. The first electro-driven extraction using a PIM was presented by See and Hauser [247]. A CTA-based PIM containing Aliquat 336 and the plasticizer NPOE was used for the extraction and preconcentration of glyphosphate (GLYP) and aminomethylphosphonic acid (AMPA) from spiked river water samples. In this study, an enrichment factor of 26 was achieved. However, after the modification of continuously pumping the feed solution through its compartment, while the stripping solution was stagnant, greater enrichments were obtained for both compounds [248]. Schmidt-Marzinkowski et al. [249] reported an electro-driven extraction of perchlorate through a PIM without carrier, only containing NPOE and CTA, due to the high lipophilicity of this anion compared to others such as phosphate or sulphate. For the transport of less liphophilic anions, a PIM with a high content of extractant was needed. Even though most PIM studies are carried out with casting flat-sheet membranes, other configurations are also possible. As an example, Mamat and See [250] prepared a small cylindrical PIM with a hollow centre, where 20 μL of stripping phase were accommodated. This setup allowed the electroextraction of three basic drugs

(i.e. amphetamine, methamphetamine and 3,4-methylenedioxy-N-methylamphetamine) from human plasma samples through a PIM made of CTA as base polymer, D2EHPA as carrier and TEHP as plasticizer.

Passive sampling involves the exposure of sampling devices for extended periods of time (from days to weeks) within the aquatic system of interest (e.g. lake, river or drain) to provide time weight average (TWA) concentration data. Passive samplers (e.g. Chemcatcher®, semipermeable membrane devices (SPMDs), DGT, polar organic chemical integrative samplers (POCISs)) present some limitations, such as a need for calibration in order to correlate the amount of analyte accumulated in the receiving phase with its TWA concentration in the same sample. However, this comparison is not easy due to different environmental factors (e.g. temperature, flow pattern, biofouling) that can modify the diffusion of the target compound across the semi-permeable barrier. Moreover, the stripping phase of the sampler is frequently a resin or sorbent which requires a further elution step. This disadvantage can be overcome with the use of PIMs, as the stripping solution is an aqueous solution and can, therefore, be directly analysed. PIMs incorporated in a device (see Figure 1.12) have been used for the passive sampling of different inorganic species (e.g. Zn(II), NH_4^+) and organic compounds (e.g. sulfamethoxazole) in environmental samples. For instance, Almeida et al. [251] presented a novel passive sampler which contained acidic stripping solution and was separated from the feed solution by a PIM made of PVC as the base polymer and D2EHPA as the carrier. The developed passive sampler was used to measure TWA concentration of Zn(II) from urban waters. The same author also reported a passive sampler for the TWA concentration of total ammonia (i.e. molecular ammonia and the ammonium cation) in freshwaters (e.g. stormwater drain and creek water), using a PIM composed of PVC as the base polymer, DNNS as the carrier and 1-tetradecanol as the plasticizer. In effect, an acidic solution was also used as stripping phase.

García-Rodríguez et al [252], reported for the first time a PIM-based passive sampler for the monitoring of sulfamethoxazole. The PIM was composed of CTA, Aliquat 336 and NPOE, and allowed the transport of sulfamethoxazole from different environmental samples (i.e. groundwater, river water and wastewater) towards a sodium chloride stripping solution.

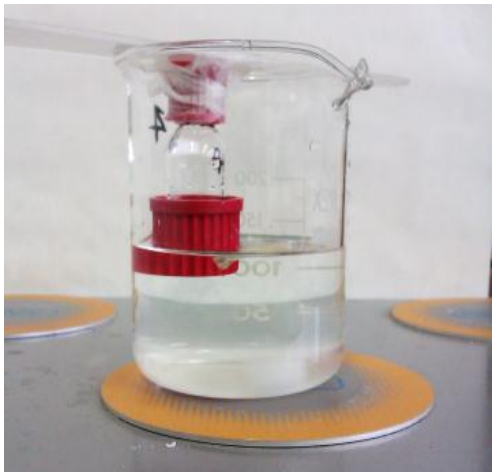

Figure 1.12 PIM-based device used for preconcentration and passive sampling of different target compounds.

In recent years, the applicability of PIMs as solid sorbents for the extraction of different metallic species has also been explored. PIMs have been used to entrap metallic species as a preconcentration procedure before EDXRF analysis. For instance, Fontàs et al. [240] reported a PIM made either of PVC or CTA and containing the extractant Aliquat 336 for the selective enrichment of Cr(VI) in the PIM from electroplating water samples. Likewise, a PIM made of CTA and containing the same extractant and plasticizer as the previously mentioned work, was employed for the preconcentration of cadmium from complex liquid samples such as seawater, followed by the direct analysis of the membrane with EDXRF [253]. More recently, Elias et al. [234], developed an effective PIM-based sorbent to facilitate mercury extraction from different types of water such as river, seawater, groundwater, and tap water. Interestingly, mercury collected in the PIM-based sorbent was shown to be stable for at least 6 months after metal extraction.

Furthermore, the effect of sonication and membrane composition was also evaluated for the extraction of Au(III) from hydrochloric acid solutions. The optimal PIM composition contained PVC, Aliquat 336 and 1-dodecanol. The authors reported an enhancement of Au(III) extraction due to sonication, which eliminates the stagnant diffusion layer near the membrane/solution interface, and thus, increases metal extraction [254]. Besides, a PIM-based sorbent made of PVC and containing Aliquat 336 provided an attractive alternative to conventional solvent extraction methods for the separation of Co(II) from Ni(II). These membranes showed a high selectivity towards Co(II), even with the presence of Ni(II) and other base metal ions, such as Fe(III) and Cd(II) [255].

Despite all the above mentioned uses and applications of PIMs for analytical purposes, it is expected that ongoing research will expand the applicability of these membranes and broaden their use for different purposes due to the advantages and feasibility they present.

References

[1] F.R. Rijsberman, Water scarcity: Fact or fiction?, Agric. Water Manag. 80 (2006) 5–22.

[2] M. Barlow, T. Clarke, Blue Gold: The Battle against Corporate Theft of the World's Water. Earthscan, London (UK), (2002).

[3] United Nations (UN), Resolution adopted by the General Assembly on 28 July 2010- 64/292. The human right to water and sanitation, (2010). http://www.un.org/es/comun/docs/?symbol=A/RES/64/292&lang=E (accessed April 10, 2018).

[4] United Nations (UN), Global Issues of Water- The right to water, (n.d.). http://www.un.org/en/sections/issues-depth/water/ (accessed April 10, 2018).

[5] European Union (EU), Addressing the Challenge of Water Scarcity and Droughts in the European Union, Communication from the Commission to the European Parliament and the Council, Eur. Comm., DG Environ., Brussels, 2007.

[6] A.F. Van Loon, H.A.J. Van Lanen, Making the distinction between water scarcity and drought using an observation-modeling framework, Water Resour. Res. 49 (2013) 1483–1502.

[7] H. Cooley, N. Ajami, M.-L. Ha, V. Srinivasan, J. Morrison, K. Donnelly, J. Christian-Smith, Global water governance in the 21st century. Pacific Institute, Oakland, 2013.

[8] J. Schewe, J. Heinke, D. Gerten, I. Haddeland, N.W. Arnell, D.B. Clark, R. Dankers, S. Eisner, B.M. Fekete, F.J. Colón-González, S.N. Gosling, H. Kim, X. Liu, Y. Masaki, F.T. Portmann, Y. Satoh, T. Stacke, Q. Tang, Y. Wada, D. Wisser, T. Albrecht, K. Frieler, F. Piontek, L. Warszawski, P. Kabat, Multimodel assessment of water scarcity under climate change, Proc. Natl. Acad. Sci. 111 (2014) 3245–3250.

[9] World Health Organization (WHO). Guidelines for Drinking-water quality, 4th edition., 2017.

[10] WHO/UNICEF, Safely managed drinking water - thematic report on drinking water. Geneva (Switzerland), (2017) 1–56.

[11] WHO/UNICEF, Progress on drinking water, sanitation and hygiene: 2017 update and SDG baselines, Geneva (Switzerland), 2017.

[12] Directive 2008/105/EC of the European Parliament and of the Council of 16 December 2008 on environmental quality standards in the field of water policy, (2008).

[13] A. Jurado, E. Vàzquez-Suñé, J. Carrera, M. López de Alda, E. Pujades, D. Barceló, Emerging organic contaminants in groundwater in Spain: A review of sources, recent occurrence and fate in a European context, Sci. Total Environ. 440 (2012) 82–94.

[14] G. Montes-Hernandez, N. Concha-Lozano, F. Renard, E. Quirico, Removal of oxyanions from synthetic wastewater via carbonation process of calcium hydroxide: Applied and fundamental aspects, J. Hazard. Mater. 166 (2009) 788–795.

[15] H. Rüdel, C. Díaz Muñiz, H. Garelick, N.G. Kandile, B.W. Miller, L. Pantoja Munoz, W.J.G.M. Peijnenburg, D. Purchase, Y. Shevah, P. van Sprang, M. Vijver, J.P.M. Vink, Consideration of the bioavailability of metal/metalloid species in freshwaters: experiences regarding the implementation of biotic ligand model-based approaches in risk assessment frameworks, Environ. Sci. Pollut. Res. 22 (2015) 7405–7421.

[16] K.R. Henke, Arsenic. Environmental Chemistry, Health Threats and Waste Treatment, John and Wiley & Sons Ltd., West Sussex, UK, 2009.

[17] I. Villaescusa, J.-C. Bollinger, Arsenic in drinking water: sources, occurrence and health effects (a review), Rev. Environ. Sci. Bio/Technology. 7 (2008) 307–323.

[18] P.L. Smedley, D.G. Kinniburgh, A review of the source, behaviour and distribution of arsenic in natural waters, Appl. Geochemistry. 17 (2002) 517–568.

[19] M. Bissen, F.H. Frimmel, Arsenic - A review. Part I: Occurrence, toxicity, speciation, mobility, Acta Hydrochim. Hydrobiol. 31 (2003) 9–18.

[20] A. Navas-Acien, K.A. Francesconi, E.K. Silbergeld, E. Guallar, Seafood intake and urine concentrations of total arsenic, dimethylarsinate and arsenobetaine in the US population, Environ. Res. 111 (2011) 110–118.

[21] D.K. Nordstrom, Arsenic, antimony, selenium, tellurium and bismuth, in: C. Young (Ed.), Minor elements 2000. Society for mining, Metallurgy and Exploration, 2000: pp. 21–30.

[22] A. Garcia-Sanchez, E. Alvarez-Ayuso, Arsenic in soils and waters and its relation to geology and mining activities (Salamanca Province, Spain), J. Geochemical Explor. 80 (2003) 69–79.

[23] W.H. Baur, B.M.H. Onishi, Arsenic, in: K.H. Wedepohl (Ed.), Handb. Geochemistry, Springer-Verlag, Berlin, 1969: pp. 33-A-1-33-0–5.

[24] J.M. Brannon, W.H. Patrick, Fixation, Transformation, and Mobilization of Arsenic in Sediments, Environ. Sci. Technol. 21 (1987) 450–459.

[25] S. Goldberg, R.A. Glaubig, Anion Sorption on a Calcareous, Montmorillonitic Soil—Arsenic, Soil Sci. Soc. Am. J. 52 (1988) 1297.

[26] B.A. Manning, S. Goldberg, Modeling Competitive Adsorption of Arsenate with Phosphate and Molybdate on Oxide Minerals, Soil Sci. Soc. Am. J. 60 (1996) 121–131.

[27] R. Singh, S. Singh, P. Parihar, V.P. Singh, S.M. Prasad, Arsenic contamination, consequences and remediation techniques: A review, Ecotoxicol. Environ. Saf. 112 (2015) 247–270.

[28] O. Núñez, P. Fernández-Navarro, I. Martín-Méndez, A. Bel-Lan, J.F. Locutura, G.

López-Abente, Arsenic and chromium topsoil levels and cancer mortality in Spain, Environ. Sci. Pollut. Res. 23 (2016) 17664–17675.

[29] J.O. Nriagu, P. Bhattacharya, A.B. Mukherjee, J. Bundschuh, R. Zevenhoven, R.H. Loeppert, Arsenic in soil and groundwater: an overview, in: P. Bhattacharya, A.B. Mukherjee, J. Bundschuh, R. Zevenhoven, R.H. Loeppert (Eds.), Arsen. Soil Groundw. Environ., Elsevier, Amsterdam, 2007: pp. 3–60.

[30] R. Bhattacharyya, D. Chatterjee, B. Nath, J. Jana, G. Jacks, M. Vahter, High arsenic groundwater: Mobilization, metabolism and mitigation - An overview in the Bengal Delta Plain, Mol. Cell. Biochem. 253 (2003) 347–355.

[31] M. Kumar, M.M. Rahman, A.L. Ramanathan, R. Naidu, Arsenic and other elements in drinking water and dietary components from the middle Gangetic plain of Bihar, India: Health risk index, Sci. Total Environ. 539 (2016) 125–134.

[32] D. Chakraborti, M.M. Rahman, S. Ahamed, R.N. Dutta, S. Pati, S.C. Mukherjee, Arsenic groundwater contamination and its health effects in Patna district (capital of Bihar) in the middle Ganga plain, India, Chemosphere. 152 (2016) 520–529.

[33] P. Ravenscroft, H. Brammer, K. Richards, Arsenic Pollution: A Global Synthesis, Wiley-Blackwell, Oxford, 2009.

[34] A. Navarro, X. Font, M. Viladevall, Geochemistry and groundwater contamination in the La Selva geothermal system (Girona, Northeast Spain), Geothermics. 40 (2011) 275–285.

[35] S.K. Singh, E.A. Stern, Global Arsenic Contamination: Living With the Poison Nectar, Environ. Sci. Policy Sustain. Dev. 59 (2017) 24–28.

[36] X. Valeri, Setcases aconsella no beure aigua de la xarxa per causa del nivell d´arsènic, Diariv de Girona. (2014). http://www.diaridegirona.cat/comarques/2014/08/23/setcases-aconsella-no-beure-aigua/684343.html.

[37] Ajuntament de Caldes de Malavella- Planta potabilitzadora-depuradora, (n.d.). http://www.caldesdemalavella.cat/planta-potabilitzadora-depuradora (accessed April 23, 2018).

[38] Commission regulation (EU) 2015/1006 of 25 June 2015 amending regulation (EC) No. 1881/2006 as regards maximum levels of inorganic arsenic in foodstuff, (2015).

[39] European Commission - Arsenic in food, (n.d.). https://ec.europa.eu/food/safety/chemical_safety/contaminants/catalogue/arsenic_en (accessed April 25, 2018).

[40] International Agency for Research on Cancer (IARC). Monographs on the Evaluation of Cancerogenic Risks to Humans, Lyon, (2002).

[41] T.S.Y. Choong, T.G. Chuah, Y. Robiah, F.L. Gregory Koay, I. Azni, Arsenic toxicity, health hazards and removal techniques from water: an overview, Desalination. 217 (2007) 139–166.

[42] G.K.H. Tam, S.M. Charbonneau, F. Bryce, C. Pomroy, E. Sandi, Metabolism of inorganic arsenic (^{74}As) in humans following oral ingestion, Toxicol. Appl. Pharmacol. 50 (1979) 319–322.

[43] H. Garelick, H. Jones, A. Dybowska, E. Valsami-Jones, Arsenic Pollution Sources- Reviews of Environmental Contamination Volume 197: International Perspectives on Arsenic Pollution and Remediation, in: Springer New York, New York, NY, 2008: pp. 17–60.

[44] S. Wang, C.N. Mulligan, Occurrence of arsenic contamination in Canada: Sources, behavior and distribution, Sci. Total Environ. 366 (2006) 701–721.

[45] L.L. Embrick, K.M. Porter, A. Pendergrass, D.J. Butcher, Characterization of lead and arsenic contamination at Barber Orchard, Haywood County, NC, Microchem. J. 81 (2005) 117–121.

[46] International Agency for Research on Cancer (IARC), Arsenic, metals, fibres, and dusts: A review of human carcinogens, (2012). https://www.ncbi.nlm.nih.gov/books/NBK304375/pdf/Bookshelf_NBK304375.pdf (accessed April 25, 2018).

[47] Environmental Protection Agency (EPA). Organic Arsenicals; Product Cancellation Order and Amendments to Terminate Uses (EPA–HQ– OPP–2009–0191; FRL–8437–7), (2009).

[48] Environmental Protection Agency (EPA). National Primary Drinking Water Regulations: Arsenic and Clarifications to Compliance and New Source Contaminants Monitoring; Proposed Rule [40 CFR Parts 141 and 142]Fed Regist, (2000) 38888–38983.

[49] Environmental Protection Agency (EPA). Revised Reregistration Eligibility Decision for MSMA, DSMA, CAMA, and Cacodylic Acid (EPA 738-R-06–021), (2006).

[50] Food and Drug Administration (FDA). Roxarsone (21CFR558.530), (2008) 500–503.

[51] Food Drug Administration (FDA). Arsanilic acid (21CFR558.62), (2008) 413–414.

[52] J.A. Hingston, C.D. Collins, R.J. Murphy, J.N. Lester, Leaching of chromated copper arsenate wood preservatives: A review, Environ. Pollut. 111 (2001) 53–66.

[53] United States Environmental Protection Agency (EPA)- Chromated arsenicals (CAA), (n.d.). https://www.epa.gov/ingredients-used-pesticide-products/chromated-arsenicals-cca (accessed September 8, 2018).

[54] E. Claesson, O. Rod, The effect of alloying elements on the corrosion resistance of brass, Mater. Sci. Technol. 32 (2016) 1794–1803.

[55] D. Mohan, C.U. Pittman, Activated carbons and low cost adsorbents for remediation of tri- and hexavalent chromium from water, J. Hazard. Mater. 137 (2006) 762–811.

[56] H. Chen, Y.-Y. Zhang, K.-L. Zhong, L.-W. Guo, J.-L. Gu, L. Bo, M.-H. Zhang, J.-R. Li, Selective sampling and measurement of Cr(VI) in water with polyquaternary ammonium salt as a binding agent in diffusive gradients in thin-films technique., J. Hazard. Mater. 271 (2014) 160–5.

[57] J. Farkaš, V. Chrastný, M. Novák, E. Čadkova, J. Pašava, R. Chakrabarti, S.B. Jacobsen, L. Ackerman, T.D. Bullen, Chromium isotope variations ($\delta^{53/52}$Cr) in mantle-derived sources and their weathering products: Implications for environmental studies and the evolution of $\delta^{53/52}$Cr in the Earth's mantle over geologic time, Geochim. Cosmochim. Acta. 123 (2013) 74–92.

[58] E. Merian, Metals and their compounds in the environment: occurrence, analysis, and biological relevance, New York: VCH Publishers, (1991).

[59] Agency for toxic substances & disease registry, (n.d.). https://www.atsdr.cdc.gov/toxprofiles/tp7-c2.pdf (accessed May 23, 2018).

[60] B.K. Mandal, R. Vankayala, L. Uday Kumar, Speciation of Chromium in Soil and Sludge in the Surrounding Tannery Region, Ranipet, Tamil Nadu, ISRN Toxicol. 2011 (2011) 1–10.

[61] R. Güell, E. Anticó, V. Salvadó, C. Fontàs, Efficient hollow fiber supported liquid membrane system for the removal and preconcentration of Cr(VI) at trace levels, Sep. Purif. Technol. 62 (2008) 389–393.

[62] J. Konczyk, C. Kozlowski, W. Walkowiak, Removal of chromium(III) from acidic aqueous solution by polymer inclusion membranes with D2EHPA and Aliquat 336, Desalination. 263 (2010) 211–216.

[63] V. Gómez, M.P. Callao, Chromium determination and speciation since 2000, TrAC - Trends Anal. Chem. 25 (2006) 1006–1015.

[64] Aalco Metals Limited, Stainless Steel - General Information - Alloying Elements in Stainless Steel, (n.d.). http://www.aalco.co.uk/datasheets/Stainless-Steel_Alloying-Elements-in-Stainless-Steel_98.ashx (accessed May 25, 2018).

[65] G. Parkin, Zinc-Zinc Bonds: A New Frontier, Science. 305 (2004) 1117–1118.

[66] H. Kozlowski, A. Janicka-Klos, J. Brasun, E. Gaggelli, D. Valensin, G. Valensin, Copper, iron, and zinc ions homeostasis and their role in neurodegenerative disorders (metal uptake, transport, distribution and regulation), Coord. Chem. Rev. 253 (2009) 2665–2685.

[67] J. Raulin, Chemical studies on vegetation, Ann. Sci. Nat. 11 (1869) 93–99.

[68] United States Geological Survey (USGS). Zinc Statistics and Information, (n.d.). https://minerals.usgs.gov/minerals/pubs/commodity/zinc/ (accessed June 5, 2018).

[69] W. Yawar, K. Naeem, P. Akhter, I. Rehana, M. Saeed, Assessment of three digestion procedures for Zn contents in Pakistani soil by flame atomic absorption spectrometry, J. Saudi Chem. Soc. 14 (2010) 125–129.

[70] A. Sharma, B. Patni, D. Shankhdhar, S.C. Shankhdhar, Zinc - An Indispensable Micronutrient, Physiol. Mol. Biol. Plants. 19 (2013) 11–20.

[71] B.J. Alloway, Zinc in soils and crop nutrition, International Zinc Association, Brussels, Belgium, 2008.

[72] World Health Organization (WHO). Chemical hazards in drinking-water: Zinc, (n.d.). http://www.who.int/water_sanitation_health/water-quality/guidelines/chemicals/zinc/en/ (accessed June 6, 2018).

[73] B.L. O'Dell, P.G. Reeves, Zinc Status and Food Intake, in: C.F. Mills (Ed.), Zinc Hum. Biol., Springer London, London, 1989: pp. 173–181.

[74] A.S. Prasad, J.A. Halsted, M. Nadimi, Syndrome of iron deficiency anemia, hepatosplenomegaly, hypogonadism, dwarfism and geophagia, Am. J. Med. 31 (1961) 532–546.

[75] N. Gupta, H. Ram, B. Kumar, Mechanism of Zinc absorption in plants: uptake, transport, translocation and accumulation, Rev. Environ. Sci. Biotechnol. 15 (2016) 89–109.

[76] R. Prasad, Zinc in soils and in plant, human and animal nutrition, Indian J. Fertil. 2 (2006) 103–119.

[77] S. Das, A. Green, Importance of zinc in crops and human health, J. SAT. Agric. Res. 11 (2016) 31–40.

[78] L.M. Plum, L. Rink, H. Hajo, The essential toxin: Impact of zinc on human health, Int. J. Environ. Res. Public Health. 7 (2010) 1342–1365.

[79] R. Bhadekar, S. Pote, V. Tale, B. Nirichan, Developments in Analytical Methods for Detection of Pesticides in Environmental Samples, Am. J. Anal. Chem. 02 (2011) 1–15.

[80] European Comission (EC)- Pesticides, (n.d.). https://ec.europa.eu/food/plant/pesticides_en (accessed May 28, 2018).

[81] R.C. Gilden, K. Huffling, B. Sattler, Pesticides and Health Risks, J. Obstet. Gynecol. Neonatal Nurs. 39 (2010) 103–110.

[82] R. Jayaraj, P. Megha, P. Sreedev, Organochlorine pesticides, their toxic effects on living organisms and their fate in the environment, Interdiscip. Toxicol. 9 (2016) 90–100.

[83] F.P. Carvalho, Agriculture, pesticides, food security and food safety, Environ. Sci. Policy. 9 (2006) 685–692.

[84] F.P. Carvalho, Pesticides, environment, and food safety, Food Energy Secur. 6 (2017) 48–60.

[85] Food and Agriculture Organization (FAO), (n.d.). http://www.fao.org/faostat/en/#home (accessed May 30, 2018).

[86] United States Environmental Protection Agency (EPA)-Pesticides Industry Sales and Usage, 2008-2012 Market estimates, (n.d.). https://www.epa.gov/sites/production/files/2017-01/documents/pesticides-industry-sales-usage-2016_0.pdf (accessed May 30, 2018).

[87] Forti, R., Henrard, M. (eds.). Agriculture, forestry and fishery statistics, Luxembourg, EU, (2015).

[88] R. Greenhalgh, R. Baron, J. Desmoras, R. Engst, H. Esser, W. Klein, Definition of Persistence in Pesticide Chemistry, Int. Union Pure Appl. Chem. 52 (1980) 2563–66.

[89] E. Herrero-Hernández, M.S. Andrades, A. Álvarez-Martín, E. Pose-Juan, M.S. Rodríguez-Cruz, M.J. Sánchez-Martín, Occurrence of pesticides and some of their degradation products in waters in a Spanish wine region, J. Hydrol. 486 (2013) 234–245.

[90] Z. Likudis, V. Costarelli, A. Vitoratos, C. Apostolopoulos, Determination of pesticide residues in olive oils with protected geographical indication or designation of origin, Int. J. Food Sci. Technol. 49 (2014) 484–492.

[91] A. Lozano, S. Uclés, A. Uclés, C. Ferrer, A.R. Fernández-Alba, Pesticide Residue Analysis in Fruit- and Vegetable-Based Baby Foods Using GC-Orbitrap MS, J. AOAC Int. (2018) 374–382.

[92] European Comission (EC)-Sustainable use of pesticides, (n.d.). https://ec.europa.eu/food/plant/pesticides/sustainable_use_pesticides_en (accessed September 15, 2018).

[93] ATS environmental services- Pesticides in drinking water, (n.d.). http://www.atsenvironmental.com/residential/water/contaminants/list/pesticides/ (accessed May 31, 2018).

[94] Organisation for Economic Cooperation and Development (OECD)- Water use in agriculture, (n.d.). http://www.oecd.org/agriculture/water-use-in-agriculture.htm (accessed May 31, 2018).

[95] E.D. Ongley, Control of water pollution from agriculture - FAO irrigation and drainage paper 55, in: FAO, 1996.

[96] Stockholm convention on persistent organic pollutants, (2001). http://www.pops.int (accessed June 1, 2018).

[97] Safe Drinking Water Fundation (SDWF)- Pesticides and water pollution, (n.d.). https://www.safewater.org/fact-sheets-1/2017/1/23/pesticides (accessed May 30, 2018).

[98] A. Kienzler, S.K. Bopp, S. van der Linden, E. Berggren, A. Worth, Regulatory assessment of chemical mixtures: Requirements, current approaches and future perspectives, Regul. Toxicol. Pharmacol. 80 (2016) 321–334.

[99] J. Pretty, The pesticide detox: Towards a more sustainable agriculture, Routledge, London (UK), 2012.

[100] R. Vera, S. Insa, C. Fontàs, E. Anticó, A new extraction phase based on a polymer inclusion membrane for the detection of chlorpyrifos, diazinon and cyprodinil in natural water samples, Talanta. 185 (2018) 291–298.

[101] K.Z. Guyton, D. Loomis, Y. Grosse, F. El Ghissassi, L. Benbrahim-Tallaa, N.

Guha, C. Scoccianti, H. Mattock, K. Straif, Carcinogenicity of tetrachlorvinphos, parathion, malathion, diazinon, and glyphosate, Lancet Oncol. 16 (2015) 490–491.

[102] N. Petsikos-Panayotarou, E. Markellou, A.E. Kalamarakis, D. Kyriakopoulou, N.E. Malathrakis, In vitro and in vivo activity of cyprodinil and pyrimethanil on Botrytis cinerea isolates resistant to other botryticides and selection for resistance to pyrimethanil in a greenhouse population in Greece, Eur. J. Plant Pathol. 109 (2003) 173–182.

[103] B. Forster, T. Staub, Basis for use strategies of anilinopyrimidine and phenylpyrrole fungicides against Botrytis cinerea, Crop Prot. 15 (1996) 529–537.

[104] C.C. Fang, F.Y. Chen, C.R. Chen, C.C. Liu, L.C. Wong, Y.W. Liu, J.G.J. Su, Cyprodinil as an activator of aryl hydrocarbon receptor, Toxicology. 304 (2013) 32–40.

[105] A. Pal, K.Y.H. Gin, A.Y.C. Lin, M. Reinhard, Impacts of emerging organic contaminants on freshwater resources: Review of recent occurrences, sources, fate and effects, Sci. Total Environ. 408 (2010) 6062–6069.

[106] S. Rist, B. Carney Almroth, N.B. Hartmann, T.M. Karlsson, A critical perspective on early communications concerning human health aspects of microplastics, Sci. Total Environ. 626 (2018) 720–726.

[107] D.L. Johnson, M.E.Q. Pilson, Spectrophotometric determination of arsenite, arsenate, and phosphate in natural waters, Anal. Chim. Acta. 58 (1972) 289–299.

[108] M.H. Arbab-Zavar, M. Hashemi, Evaluation of electrochemical hydride generation for spectrophotometric determination of As(III) by silver diethyldithiocarbamate, Talanta. 52 (2000) 1007–1014.

[109] H. Revanasiddappa, B. Dayananda, T. Kumar, A sensitive spectrophotometric method for the determination of arsenic in environmental samples, Environ. Chem. Lett. 5 (2007) 151–155.

[110] J.A. Platte, V.M. Marcy, Photometric Determination of Zinc with Zincon: Application to Water Containing Heavy Metals, Anal. Chem. 31 (1959) 1226–1228.

[111] R. Kashanaki, H. Ebrahimzadeh, M. Moradi, B. Hazer, T. Duan, X. Zhang, J. Dědina, D.J. Thomas, M. Stýblo, Ultrasound-assisted supramolecular solvent microextraction coupled with graphite furnace atomic absorption spectrometry for speciation analysis of inorganic arsenic, Anal. Methods. 9 (2017) 3121–3127.

[112] V.N. Alves, T.S. Neri, S.S.O. Borges, D.C. Carvalho, N.M.M. Coelho, Determination of inorganic arsenic in natural waters after selective extraction using Moringa oleífera seeds, Ecol. Eng. 106 (2017) 431–435.

[113] G.M. dos Santos, D. Pozebon, C. Cerveira, D.P. de Moraes, Inorganic arsenic speciation in rice products using selective hydride generation and atomic absorption spectrometry (AAS), Microchem. J. 133 (2017) 265–271.

[114] M.L. Susko, M.S. Bloom, I.A. Neamtiu, A.A. Appleton, S. Surdu, C. Pop, E.F. Fitzgerald, D. Anastasiu, E.S. Gurzau, Low-level arsenic exposure via drinking

water consumption and female fecundity - A preliminary investigation, Environ. Res. 154 (2017) 120–125.

[115] H.I. Ulusoy, M. Akçay, S. Ulusoy, R. Gürkan, Determination of ultra trace arsenic species in water samples by hydride generation atomic absorption spectrometry after cloud point extraction, Anal. Chim. Acta. 703 (2011) 137–144.

[116] G. Chen, B. Lai, X. Mao, T. Chen, M. Chen, Continuous Arsine Detection Using a Peltier-Effect Cryogenic Trap to Selectively Trap Methylated Arsines, Anal. Chem. 89 (2017) 8678–8682.

[117] W. Zhang, Y. Qi, D. Qin, J. Liu, X. Mao, G. Chen, C. Wei, Y. Qian, Determination of inorganic arsenic in algae using bromine halogenation and on-line nonpolar solid phase extraction followed by hydride generation atomic fluorescence spectrometry, Talanta. 170 (2017) 152–157.

[118] H. Luo, X. Wang, R. Dai, Y. Liu, X. Jiang, X. Xiong, K. Huang, Simultaneous determination of arsenic and cadmium by hydride generation atomic fluorescence spectrometry using magnetic zero-valent iron nanoparticles for separation and pre-concentration, Microchem. J. 133 (2017) 518–523.

[119] X.P. Lu, X.A. Yang, L. Liu, H.H. Hu, W.B. Zhang, Selective and sensitive determination of As(III) and tAs in Chinese herbal medicine samples using L-cysteine modified carbon paste electrode-based electrolytic hydride generation and AFS analysis, Talanta. 165 (2017) 258–266.

[120] P. Avino, G. Capannesi, A. Rosada, Ultra-trace nutritional and toxicological elements in Rome and Florence drinking waters determined by Instrumental Neutron Activation Analysis, Microchem. J. 97 (2011) 144–153.

[121] R. Güell, E. Anticó, S.D. Kolev, J. Benavente, V. Salvadó, C. Fontàs, Development and characterization of polymer inclusion membranes for the separation and speciation of inorganic As species, J. Memb. Sci. 383 (2011) 88–95.

[122] C. Fontàs, R. Vera, A. Batalla, S.D. Kolev, E. Anticó, A novel low-cost detection method for screening of arsenic in groundwater, Environ. Sci. Pollut. Res. 21 (2013) 11682–8.

[123] R. Vera, C. Fontàs, E. Anticó, Titanium dioxide solid phase for inorganic species adsorption and determination: the case of arsenic, Environ. Sci. Pollut. Res. (2016) 1–10.

[124] K.M. Attar, K. Alam, Spectral interferences on arsenic and mercury prominent emission lines in vacuum inductively coupled plasma-atomic emission spectrometry and use of methanol vapor as optical filter for spectral order sorting, Spectrochim. Acta Part B At. Spectrosc. 45 (1990) 221–232.

[125] V. Dufailly, L. Noël, T. Guérin, Optimisation and critical evaluation of a collision cell technology ICP-MS system for the determination of arsenic in foodstuffs of animal origin, Anal. Chim. Acta. 611 (2008) 134–142.

[126] K. Nan, M. He, B. Chen, Y. Chen, B. Hu, Arsenic speciation in tree moss by mass spectrometry based hyphenated techniques, Talanta. 183 (2018) 48–54.

[127] E.H. Larsen, S. Sturup, Carbon-enhanced inductively coupled plasma mass spectrometric detection of arsenic and selenium and its application to arsenic speciation, J. Anal. At. Spectrom. 9 (1994) 1099–1105.

[128] P. Montoro Leal, E. Vereda Alonso, M.M. López Guerrero, M.T.S. Cordero, J.M. Cano Pavón, A. García de Torres, Speciation analysis of inorganic arsenic by magnetic solid phase extraction on-line with inductively coupled mass spectrometry determination, Talanta. 184 (2018) 251–259.

[129] S. Ata, F.H. Wattoo, M. Ahmed, M.H.S. Wattoo, S.A. Tirmizi, A. Wadood, A method optimization study for atomic absorption spectrophotometric determination of total zinc in insulin using direct aspiration technique, Alexandria J. Med. 51 (2015) 19–23.

[130] M. Archer, R.I. McCrindle, E.R. Rohwer, Analysis of cobalt, tantalum, titanium, vanadium and chromium in tungsten carbide by inductively coupled plasma-optical emission spectrometry, J. Anal. At. Spectrom. 18 (2003) 1493–1496.

[131] Z.L. Chen, M. Megharaj, R. Naidu, Removal of interferences in the speciation of chromium using an octopole reaction system in ion chromatography with inductively coupled plasma mass spectrometry, Talanta. 73 (2007) 948–952.

[132] United States Environmental Protection Agency (EPA). Standardized Analytical Methods for Environmental Restoration Following Homeland Security Events—Revision 5.0; EPA-United States Environmental Protection Agency: Cincinnati, OH, USA, (2009).

[133] D. Barceló, Environmental Protection Agency and other methods for the determination of priority pesticides and their transformation products in water, J. Chromatogr. A. 643 (1993) 117–143.

[134] L. Alder, K. Greulich, G. Kempe, B. Vieth, Residue analysis of 500 high priority pesticides: better by GC-MS or LC-MS/MS?, Mass Spectrom. Rev. 25 (2006) 838–865.

[135] M.M. Gómez-Ramos, C. Ferrer, O. Malato, A. Agüera, A.R. Fernández-Alba, Liquid chromatography-high-resolution mass spectrometry for pesticide residue analysis in fruit and vegetables: Screening and quantitative studies, J. Chromatogr. A. 1287 (2013) 24–37.

[136] A. Gonzalvez, M.L. Cervera, S. Armenta, M. de la Guardia, A review of non-chromatographic methods for speciation analysis, Anal. Chim. Acta. 636 (2009) 129–157.

[137] Z.L. Chen, M. Megharaj, R. Naidu, Speciation of chromium in waste water using ion chromatography inductively coupled plasma mass spectrometry, Talanta. 72 (2007) 394–400.

[138] A.C. Sahayam, Speciation of Cr(III) and Cr(VI) in potable waters by using activated neutral alumina as collector and ET-AAS for determination, Anal. Bioanal. Chem. 372 (2002) 840–842.

[139] H. Filik, M. Doğutan, R. Apak, Speciation analysis of chromium by separation on a 5-palmitoyl oxine-functionalized XAD-2 resin and spectrophotometric

determination with diphenylcarbazide, Anal. Bioanal. Chem. 376 (2003) 928–933.

[140] S. Cathum, C. Brown, W. Wong, Determination of Cr^{3+}, CrO_4^{2-}, and Cr_2O7^{2-} in environmental matrixes by high-performance liquid chromatography with diode-array detection (HPLC-DAD), Anal. Bioanal. Chem. 373 (2002) 103–110.

[141] C. Cui, M. He, B. Chen, B. Hu, Chitosan modified magnetic nanoparticles based solid phase extraction combined with ICP-OES for the speciation of Cr(III) and Cr(VI), Anal. Methods. 6 (2014) 8577–8583.

[142] M. Tuzen, M. Soylak, Multiwalled carbon nanotubes for speciation of chromium in environmental samples, J. Hazard. Mater. 147 (2007) 219–225.

[143] D. Chen, C. Huang, M. He, B. Hu, Separation and preconcentration of inorganic arsenic species in natural water samples with 3-(2-aminoethylamino) propyltrimethoxysilane modified ordered mesoporous silica micro-column and their determination by inductively coupled plasma optical emission, J. Hazard. Mater. 164 (2009) 1146–1151.

[144] C. Xiong, Y. Qin, B. Hu, On-line separation/preconcentration of V(IV)/V(V) in environmental water samples with CTAB-modified alkyl silica microcolumn and their determination by inductively coupled plasma-optical emission spectrometry, J. Hazard. Mater. 178 (2010) 164–170.

[145] D.M. Di Toro, C.D. Kavvadas, R. Mathew, P.R. Paquin, The persistence and availability of metals in aquatic environments, Internatio Council on Metals and Environment (ICME), Ottawa, Canada, 2001.

[146] C.M. Zhao, P.G.C. Campbell, K.J. Wilkinson, When are metal complexes bioavailable?, Environ. Chem. 13 (2016) 425–433.

[147] G. Kefala, A. Economou, A. Voulgaropoulos, M. Sofoniou, A study of bismuth-film electrodes for the detection of trace metals by anodic stripping voltammetry and their application to the determination of Pb and Zn in tapwater and human hair, Talanta. 61 (2003) 603–610.

[148] C.M.G. van den Berg, P.J.M. Buckley, Z.Q. Huang, M. Nimmo, An Electrochemical Study of the Speciation of Copper, Zinc and Iron in Two Estuaries in England, Estuar. Coast. Shelf Sci. 22 (1986) 479–486.

[149] R. Matarese Palmieri, L. La Pera, G. Di Bella, G. Dugo, Simultaneous determination of Cd(II), Cu(II), Pb(II) and Zn(II) by derivative stripping chronopotentiometry in Pittosporum tobira leaves: A measurement of local atmospheric pollution in Messina (Sicily, Italy), Chemosphere. 59 (2005) 1161–1168.

[150] D. Aguilar, C. Parat, J. Galceran, E. Companys, J. Puy, L. Authier, M. Potin-Gautier, Determination of free metal ion concentrations with AGNES in low ionic strength media, J. Electroanal. Chem. 689 (2013) 276–283.

[151] M. Pesavento, G. Alberti, R. Biesuz, Analytical methods for determination of free metal ion concentration, labile species fraction and metal complexation capacity of environmental waters: A review, Anal. Chim. Acta. 631 (2009) 129–141.

[152] E.J.J. Kalis, L. Weng, F. Dousma, E.J.M. Temminghoff, W.H. Van Riemsdijk, Measuring Free Metal Ion Concentrations in Multicomponent Solutions Using the Donnan Membrane Technique Measuring Free Metal Ion Concentrations in Multicomponent Solutions Using the Donnan Membrane Technique, Enviromental Sci. Technol. 40 (2006) 955–961.

[153] A. Gramlich, S. Tandy, E. Frossard, J. Eikenberg, R. Schulin, Diffusion limitation of zinc fluxes into wheat roots, PLM and DGT devices in the presence of organic ligands, Environ. Chem. 11 (2014) 41–50.

[154] I.J. Allan, J. Knutsson, N. Guigues, G.A. Mills, A.-M. Fouillac, R. Greenwood, Chemcatcher® and DGT passive sampling devices for regulatory monitoring of trace metals in surface water, J. Environ. Monit. 10 (2008) 821.

[155] V.S. Kislik, ed., Liquid membranes, Principles & Applications in Chemical Separations & Wastewater treatment, Elsevier Science, Oxford (UK), 2010.

[156] S. Bayen, K.J. Wilkinson, J. Buffle, The permeation liquid membrane as a sensor for free nickel in aqueous samples, Analyst. 132 (2007) 262–267.

[157] V.I. Slaveykova, N. Parthasarathy, J. Buffle, K.J. Wilkinson, Permeation liquid membrane as a tool for monitoring bioavailable Pb in natural waters., Sci. Total Environ. 328 (2004) 55–68.

[158] S. Bayen, I. Worms, N. Parthasarathy, K. Wilkinson, J. Buffle, Cadmium bioavailability and speciation using the permeation liquid membrane, Anal. Chim. Acta. 575 (2006) 267–273.

[159] A. Gramlich, S. Tandy, V.I. Slaveykova, A. Duffner, R. Schulin, The use of permeation liquid membranes for free zinc measurements in aqueous solution, Environ. Chem. 9 (2012) 429–437.

[160] C. Fontàs, E. Anticó, V. Salvadó, Design of a Hollow Fiber Supported Liquid Membrane System for Zn Speciation in Natural Waters, Membranes (Basel). 8 (2018) 88.

[161] J. Stocka, M. Tankiewicz, M. Biziuk, J. Namie, Green Aspects of Techniques for the Determination of Currently Used Pesticides in Environmental Samples, Int. J. Mol. Sci. (2011) 7785–7805.

[162] A.M. St John, S.D. Kolev, C. Fontàs, Polymer inclusion membranes for the separation of uranium and arsenic from dilute aqueous solutions, in: A. Figoli, J. Hoinkis, J. Bundschuh (Eds.), Membr. Technol. Water Treat. Remov. Toxic Trace Elem. with Emphas. Arsenic, Fluoride Uranium (Sustainable Water Dev., CRC Press, Boca Raton, 2016: pp. 179–200.

[163] E. Anticó, Estudis de sistemes líquid-líquid i sòlid-líquid en processos de separació de metalls valuosos, Pd(II) i Y(III), Tesi Doctoral, Universitat Autònoma de Barcelona, 1995.

[164] L.C. Branco, J.G. Crespo, C.A.M. Afonso, Studies on the selective transport of organic compounds by using ionic liquids as novel supported liquid membranes, Chemistry. 8 (2002) 3865–71.

[165] P.R. Danesi, Separation of Metal Species by Supported Liquid Membranes, Sep. Sci. Technol. 19 (1984) 857–894.

[166] C. Rios, V. Salvadó, M. Hidalgo, Facilitated transport and preconcentration of the herbicide glyphosate and its metabolite AMPA through a solid supported liquid-membrane, J. Memb. Sci. 203 (2002) 201–208.

[167] R. Güell, C. Fontàs, V. Salvadó, E. Anticó, Modelling of liquid-liquid extraction and liquid membrane separation of arsenic species in environmental matrices, Sep. Purif. Technol. 72 (2010) 319–325.

[168] M.A. Aguirre, E.J. Selva, M. Hidalgo, A. Canals, Dispersive liquid-liquid microextraction for metals enrichment: A useful strategy for improving sensitivity of laser-induced breakdown spectroscopy in liquid samples analysis, Talanta. 131 (2015) 348–353.

[169] P. Biparva, A.A. Matin, Microextraction Techniques as a Sample Preparation Step for Metal Analysis, At. Absorpt. Spectrosc. 258 (2012) 62–88.

[170] H. Farahani, Y. Yamini, S. Shariati, M.R. Khalili-Zanjani, S. Mansour-Baghahi, Development of liquid phase microextraction method based on solidification of floated organic drop for extraction and preconcentration of organochlorine pesticides in water samples., Anal. Chim. Acta. 626 (2008) 166–73.

[171] L. Fu, X. Liu, J. Hu, X. Zhao, H. Wang, X. Wang, Application of dispersive liquid-liquid microextraction for the analysis of triazophos and carbaryl pesticides in water and fruit juice samples., Anal. Chim. Acta. 632 (2009) 289–95.

[172] A. Andrade-Eiroa, M. Canle, V. Leroy-Cancellieri, V. Cerdà, Solid-phase extraction of organic compounds: A critical review (Part I), TrAC Trends Anal. Chem. 80 (2016) 655–667.

[173] B.C. Mondal, D. Das, A.K. Das, Synthesis and characterization of a new resin functionalized with 2-naphthol-3,6-disulfonic acid and its application for the speciation of chromium in natural water, Talanta. 56 (2002) 145–152.

[174] I. Kubrakova, T. Kudinova, A. Formanovsky, N. Kuzmin, Determination of Chromium(III) and Chromium(VI) in River Water by Electrothermal Atomic Absorption Spectrometry After Sorption Preconcentration in a Microwave Field, Analyst. 119 (1994) 2477–2480.

[175] P. Su-Cheng, Pre-concentration efficiency of chelex-100 resin for heavy metals in seawater. Part 2. Distribution of Heavy Metals on a Chelex-100 Column and Optimization of the Column Efficiency by a Plate Simulation Method, Anal. Chim. Acta. 211 (1988) 271–280.

[176] S. Bhowmick, S. Chakraborty, P. Mondal, W. Van Renterghem, S. Van den Berghe, G. Roman-Ross, D. Chatterjee, M. Iglesias, Montmorillonite-supported nanoscale zero-valent iron for removal of arsenic from aqueous solution: Kinetics and mechanism, Chem. Eng. J. 243 (2014) 14–23.

[177] J.C. Hsu, C.J. Lin, C.H. Liao, S.T. Chen, Removal of As(V) and As(III) by reclaimed iron-oxide coated sands, J. Hazard. Mater. 153 (2008) 817–826.

[178] S. Ayoob, A.K. Gupta, P.B. Bhakat, Analysis of breakthrough developments and modeling of fixed bed adsorption system for As(V) removal from water by modified calcined bauxite (MCB), Sep. Purif. Technol. 52 (2007) 430–438.

[179] G.P. Gillman, A simple technology for arsenic removal from drinking water using hydrotalcite, Sci. Total Environ. 366 (2006) 926–931.

[180] M.Z. López Paraguay, J.A. Cortes, J.F. Pérez-Robles, M.T. Alarcón-Herrera, Adsorption of Arsenite from Groundwater Using Titanium Dioxide, Clean - Soil, Air, Water. 42 (2014) 713–721.

[181] D. Mohan, C.U. Pittman, Arsenic removal from water/wastewater using adsorbents-A critical review, J. Hazard. Mater. 142 (2007) 1–53.

[182] X. Guan, J. Du, X. Meng, Y. Sun, B. Sun, Q. Hu, Application of titanium dioxide in arsenic removal from water: A review, J. Hazard. Mater. 215–216 (2012) 1–16.

[183] C. Arthur, J. Pawliszyn, Solid phase microextraction with thermal desorption using fused silica optical fibers, Anal. Chem. 62 (1990) 2145–2148.

[184] D. García-Rodríguez, A.M. Carro, R. Lorenzo, F. Fernández, R. Cela, Determination of trace levels of aquaculture chemotherapeutants in seawater samples by SPME-GC-MS/MS., J. Sep. Sci. 31 (2008) 2882–90.

[185] K. Korba, L. Pelit, F.O. Pelit, K.V. Ozdokur, H. Ertaş, A.E. Eroğlu, F.N. Ertaş, Preparation and characterization of sodium dodecyl sulfate doped polypyrrole solid phase micro extraction fiber and its application to endocrine disruptor pesticide analysis, J. Chromatogr. B. 929 (2013) 90–6.

[186] J.M.F. Nogueira, Stir-bar sorptive extraction: 15 years making sample preparation more environment-friendly, TrAC Trends Anal. Chem. 71 (2015) 214–223.

[187] F. Zare, M. Ghaedi, A. Daneshfar, A. Ostovan, Magnetic molecularly imprinted polymer for the efficient and selective preconcentration of diazinon before its determination by high-performance liquid chromatography, J. Sep. Sci. 38 (2015) 2797–803.

[188] A. Martin, C. Margoum, J. Randon, M. Coquery, Silicone rubber selection for passive sampling of pesticides in water, Talanta. 160 (2016) 306–313.

[189] R. Montes, I. Rodríguez, E. Rubí, M. Ramil, R. Cela, Suitability of polypropylene microporous membranes for liquid- and solid-phase extraction of halogenated anisoles from water samples, J. Chromatogr. A. 1198–1199 (2008) 21–6.

[190] L. Nghiem, P. Mornane, I. Potter, J. Perera, R. Cattrall, S. Kolev, Extraction and transport of metal ions and small organic compounds using polymer inclusion membranes (PIMs), J. Memb. Sci. 281 (2006) 7–41.

[191] A. Figoli, Chapter 7 - Liquid Membrane in Gas Separations, in: V.S.B.T.-L.M. Kislik (Ed.), Liq. Membr., Elsevier, Amsterdam, 2010: pp. 327–356.

[192] C. Fontàs, Disseny i Caracterització de Sistemes de Membrana Líquida per al Transport de Metalls del Grup del Platí, Tesi Doctoral, Universitat de Girona, 2001.

[193] Matsuura T, Synthetic membranes and membrane separation processes. Boca Raton, USA: CRC Press, (1994).

[194] B. Pospiech, W. Kujawski, Ionic liquids as selective extractants and ion carriers of heavy metal ions from aqueous solutions utilized in extraction and membrane separation, Rev Chem Eng. 31 (2015) 179–191.

[195] M. Sugiura, M. Kikkawa, S. Urita, Effect of Plasticizer on Carrier-Mediated Transport of Zinc Ion through Cellulose Triacetate Membranes, Sep. Sci. Technol. 22 (1987) 2263–2268.

[196] M.I.G.S. Almeida, R.W. Cattrall, S.D. Kolev, Polymer inclusion membranes (PIMs) in chemical analysis - A review, Anal. Chim. Acta. 987 (2017) 1–14.

[197] J. Buffle, N. Parthasarathy, L. Djane, L. Matthiasson, Permeation liquid membranes for field analysis and speciation of trace compounds in waters, in: J. Buffle, G. Horvai (Eds.), Situ Monit. Aquat. Syst. Chem. Anal. Speciat., John and Wiley & Sons Ltd., West Sussex, UK, 2000: pp. 407–493.

[198] J. Rais, C. V Mason, K.D. Abney, Use of PVC Plasticized Membranes for Uptake of Radioactive Cesium and Strontium, Sep. Sci. Technol. 32 (1997) 951–969.

[199] J.S. Gardner, J.O. Walker, J.D. Lamb, Permeability and durability effects of cellulose polymer variation in polymer inclusion membranes, J. Memb. Sci. 229 (2004) 87–93.

[200] A.L. Ocampo, J.C. Aguilar, E. Rodríguez de San Miguel, M. Monroy, P. Roquero, J. de Gyves, Novel proton-conducting polymer inclusion membranes, J. Memb. Sci. 326 (2009) 382–387.

[201] L. Guo, Y. Liu, C. Zhang, J. Chen, Preparation of PVDF-based polymer inclusion membrane using ionic liquid plasticizer and Cyphos IL 104 carrier for Cr(VI) transport, J. Memb. Sci. 372 (2011) 314–321.

[202] L. Guo, J. Zhang, D. Zhang, Y. Liu, Y. Deng, J. Chen, Preparation of poly(vinylidene fluoride-co-tetrafluoroethylene)-based polymer inclusion membrane using bifunctional ionic liquid extractant for Cr(VI) transport, Ind. Eng. Chem. Res. 51 (2012) 2714–2722.

[203] Y.Y.N. Bonggotgetsakul, R.W. Cattrall, S.D. Kolev, Recovery of gold from aqua regia digested electronic scrap using a poly(vinylidene fluoride-co-hexafluoropropene) (PVDF-HFP) based polymer inclusion membrane (PIM) containing Cyphos® IL 104, J. Memb. Sci. 514 (2016) 274–281.

[204] Y. O'Bryan, R.W. Cattrall, Y.B. Truong, I.L. Kyratzis, S.D. Kolev, The use of poly(vinylidenefluoride-co-hexafluoropropylene) for the preparation of polymer inclusion membranes. Application to the extraction of thiocyanate, J. Memb. Sci. 510 (2016) 481–488.

[205] M.I.G.S. Almeida, R.W. Cattrall, S.D. Kolev, Recent trends in extraction and transport of metal ions using polymer inclusion membranes (PIMs), J. Memb. Sci. 415–416 (2012) 9–23.

[206] Y.J. Wang, D. Kim, The effect of F127 addition on the properties of PEGDA/PVdF

cross-linked gel polymer electrolytes, J. Memb. Sci. 312 (2008) 76–83.

[207] L. Zhao, H. Zhang, X. Li, C. Zhao, X. Yuan, Modification of Electrospun Poly(vinylidene fluoride-co-hexafluoropropylene) Membranes Through the Introduction of Poly(ethylene glycol) Dimethacrylate, J. Appl. Polym. Sci. 111 (2009) 3104–3112.

[208] Y. O'Bryan, Y.B. Truong, R.W. Cattrall, I.L. Kyratzis, S.D. Kolev, A new generation of highly stable and permeable polymer inclusion membranes (PIMs) with their carrier immobilized in a crosslinked semi-interpenetrating polymer network . Application to the transport of thiocyanate, J. Memb. Sci. 529 (2017) 55–62.

[209] Poly(vinylidene fluoride-co-hexafluoropropylene)- Sigma Aldrich, (n.d.). https://www.sigmaaldrich.com/catalog/product/aldrich/427160?lang=es&region=ES (accessed October 5, 2018).

[210] O. Kebiche-Senhadji, L. Mansouri, S. Tingry, P. Seta, M. Benamor, Facilitated Cd(II) transport across CTA polymer inclusion membrane using anion (Aliquat 336) and cation (D2EHPA) metal carriers, J. Memb. Sci. 310 (2008) 438–445.

[211] M. Resina, J. Macan, J. De Gyves, M. Mu, Zn(II), Cd(II) and Cu(II) separation through organic–inorganic Hybrid Membranes containing di (2-ethylhexyl) phosphoric acid or di-(2-ethylhexyl) dithiophosphoric acid as a carrier, J. Memb. Sci. 268 (2006) 57–64.

[212] S.E. Fry, N.J. Pienta, Effects of Molten Salts on Reactions. Nucleophilic Aromatic Substitution by Halide Ions in Molten Dodecyltributylphosphonium Salts1, J. Am. Chem. Soc. 107 (1985) 6399–6400.

[213] J.A. Boon, J.A. Levisky, J.L. Pflug, J.S. Wilkes, Friedel-Crafts Reactions in Ambient-Temperature Molten Salts, J. Org. Chem. 51 (1986) 480–483.

[214] P.S. Kulkarni, L.C. Branco, J.G. Crespo, M.C. Nunes, A. Raymundo, C.A.M. Afonso, Comparison of physicochemical properties of new ionic liquids based on imidazolium, quaternary ammonium, and guanidinium cations., Chemistry. 13 (2007) 8478–88.

[215] A. Stojanovic, B.K. Keppler, Ionic Liquids as Extracting Agents for Heavy Metals, Sep. Sci. Technol. 47 (2012) 189–203.

[216] J.-P. Mikkola, P. Virtanen, R. Sjöholm, Aliquat 336®—a versatile and affordable cation source for an entirely new family of hydrophobic ionic liquids, Green Chem. 8 (2006) 250.

[217] C. Fontàs, R. Vera, A. Batalla, S.D. Kolev, E. Anticó, A novel low-cost detection method for screening of arsenic in groundwater., Environ. Sci. Pollut. Res. 21 (2014) 11682–8.

[218] O. Kebiche-Senhadji, S. Tingry, P. Seta, M. Benamor, Selective extraction of Cr(VI) over metallic species by polymer inclusion membrane (PIM) using anion (Aliquat 336) as carrier, Desalination. 258 (2010) 59–65.

[219] S.D. Kolev, M.I.G.S. Almeida, R.W. Cattrall, Polymer Inclusion membranes, in:

Handb. Membr. Sep. Chem. Pharm. Food Biotechnol. Appl., CRC Press, Boca Raton, New York (United States), 2015: pp. 721–737.

[220] M. Resina, Desenvolupament de noves membranes per a la millora de la seva estabilitat, Tesi Doctoral, Universitat Autònoma de Barcelona, 2008.

[221] C. Fontàs, R. Tayeb, M. Dhahbi, E. Gaudichet, F. Thominette, P. Roy, K. Steenkeste, M.P. Fontaine-Aupart, S. Tingry, E. Tronel-Peyroz, P. Seta, Polymer inclusion membranes: The concept of fixed sites membrane revised, J. Memb. Sci. 290 (2007) 62–72.

[222] C.A. Kozlowski, W. Walkowiak, Transport of Cr(VI), Zn(II), and Cd(II) Ions Across Polymer Inclusion Membranes with Tridecyl(pyridine) Oxide and Tri-n-Octylamine, Sep. Sci. Technol. 39 (2004) 3127–3141.

[223] C. Fontàs, R. Tayeb, S. Tingry, M. Hidalgo, P. Seta, Transport of platinum(IV) through supported liquid membrane (SLM) and polymeric plasticized membrane (PPM), J. Memb. Sci. 263 (2005) 96–102.

[224] F.E. Mercader-Trejo, E.R. de San Miguel, J. de Gyves, Mercury(II) removal using polymer inclusion membranes containing Cyanex 471X, J. Chem. Technol. Biotechnol. 84 (2009) 1323–1330.

[225] M.I. Vázquez, V. Romero, C. Fontàs, E. Anticó, J. Benavente, Polymer inclusion membranes (PIMs) with the ionic liquid (IL) Aliquat 336 as extractant: Effect of base polymer and IL concentration on their physical–chemical and elastic characteristics, J. Memb. Sci. 455 (2014) 312–319.

[226] L. Wang, W. Shen, Chemical and morphological stability of Aliquat 336 / PVC membranes in membrane extraction : A preliminary study, Sep. Purif. Technol. 46 (2005) 51–62.

[227] A. Bhattacharyya, P.K. Mohapatra, P.A. Hassan, V.K. Manchanda, Studies on the selective Am^{3+} transport, irradiation stability and surface morphology of polymer inclusion membranes containing Cyanex-301 as carrier extractant, J. Hazard. Mater. 192 (2011) 116–123.

[228] A. Kaya, C. Onac, H.K. Alpoguz, A. Yilmaz, N. Atar, Removal of Cr(VI) through calixarene based polymer inclusion membrane from chrome plating bath water, Chem. Eng. J. 283 (2016) 141–149.

[229] S.A. Ansari, P.K. Mohapatra, V.K. Manchanda, Cation transport across plasticized polymeric membranes containing N,N,N',N'-tetraoctyl-3-oxapentanediamide(TODGA) as the carrier, Desalination. 262 (2010) 196–201.

[230] E.R. De San Miguel, A. V. Garduño-García, J.C. Aguilar, J. De Gyves, Gold(III) transport through polymer inclusion membranes: Efficiency factors and pertraction mechanism using Kelex 100 as carrier, Ind. Eng. Chem. Res. 46 (2007) 2861–2869.

[231] E. Rodríguez de San Miguel, M. Monroy-Barreto, J.C. Aguilar, A.L. Ocampo, J. de Gyves, Structural effects on metal ion migration across polymer inclusion membranes: Dependence of membrane properties and transport profiles on the weight and volume fractions of the components, J. Memb. Sci. 379 (2011) 416–

425.

[232] P.K. Mohapatra, D.S. Lakshmi, A. Bhattacharyya, V.K. Manchanda, Evaluation of polymer inclusion membranes containing crown ethers for selective cesium separation from nuclear waste solution, J. Hazard. Mater. 169 (2009) 472–479.

[233] O. Arous, M. Amara, H. Kerdjoudj, Selective Transport of Metal Ions Using Polymer Inclusion Membranes Containing Crown Ethers and Cryptands, Arab. J. Sci. Eng. 35 (2010).

[234] G. Elias, E. Marguí, S. Díez, C. Fontàs, Polymer Inclusion Membrane as an Effective Sorbent to Facilitate Mercury Storage and Detection by X-ray Fluorescence in Natural Waters, Anal. Chem. 90 (2018) 4756–4763.

[235] E. Fontananova, Impedance Spectroscopy, Membrane Characterization by BT - Encyclopedia of Membranes, in: E. Drioli, L. Giorno (Eds.), Springer Berlin Heidelberg, Berlin, Heidelberg, 2016: pp. 1025–1027.

[236] A. Yilmaz, G. Arslan, A. Tor, I. Akin, Selectively facilitated transport of Zn(II) through a novel polymer inclusion membrane containing Cyanex 272 as a carrier reagent, Desalination. 277 (2011) 301–307.

[237] G.J. Moody, R.B. Oke, J.D.R. Thomas, A calcium-sensitive electrode based on a liquid ion exchanger in a poly(vinyl chloride) matrix, Analyst. 95 (1970) 910–918.

[238] E. Bakker, E. Pretsch, Potentiometric sensors for trace-level analysis, TrAC Trends Anal. Chem. 24 (2005) 199–207.

[239] S.S.S. Tan, P.C. Hauser, N.A. Chaniotakis, G. Suter, W. Simon, Anion-selective optical sensors based on a coextraction of anion-proton pairs into a solvent-polymeric membrane, Chimia (Aarau). 43 (1989) 257–261.

[240] C. Fontàs, I. Queralt, M. Hidalgo, Novel and selective procedure for Cr(VI) determination by X-ray fluorescence analysis after membrane concentration, Spectrochim. Acta - Part B At. Spectrosc. 61 (2006) 407–413.

[241] N. Pont, V. Salvadó, C. Fontàs, Selective transport and removal of Cd from chloride solutions by polymer inclusion membranes, J. Memb. Sci. 318 (2008) 340–345.

[242] A. Garcia-Rodríguez, V. Matamoros, S.D. Kolev, C. Fontàs, Development of a polymer inclusion membrane (PIM) for the preconcentration of antibiotics in environmental water samples, J. Memb. Sci. 492 (2015) 32–39.

[243] L.L. Zhang, R.W. Cattrall, S.D. Kolev, The use of a polymer inclusion membrane in flow injection analysis for the on-line separation and determination of zinc, Talanta. 84 (2011) 1278–1283.

[244] L.L. Zhang, R.W. Cattrall, M. Ashokkumar, S.D. Kolev, On-line extractive separation in flow injection analysis based on polymer inclusion membranes : A study on membrane stability and approaches for improving membrane permeability, Talanta. 97 (2012) 382–387.

[245] E.A. Nagul, C. Fontàs, I.D. McKelvie, R.W. Cattrall, S.D. Kolev, The use of a

polymer inclusion membrane for separation and preconcentration of orthophosphate in flow analysis, Anal. Chim. Acta. 803 (2013) 82–90.

[246] M.R. Yaftian, M.I.G.S. Almeida, R.W. Cattrall, S.D. Kolev, Flow injection spectrophotometric determination of V(V) involving on-line separation using a poly(vinylidene fluoride-co-hexafluoropropylene)-based polymer inclusion membrane, Talanta. 181 (2018) 385–391.

[247] H.H. See, P.C. Hauser, Electric field-driven extraction of lipophilic anions across a carrier-mediated polymer inclusion membrane., Anal. Chem. 83 (2011) 7507–7513.

[248] H.H. See, S. Stratz, P.C. Hauser, Electro-driven extraction across a polymer inclusion membrane in a flow-through cell, J. Chromatogr. A. 1300 (2013) 79–84.

[249] S.-M. Julia, S.H. Heng, H.P. C., Electric Field Driven Extraction of Inorganic Anions Across a Polymer Inclusion Membrane, Electroanalysis. 25 (2013) 1879–1886.

[250] N.A. Mamat, H.H. See, Development and evaluation of electromembrane extraction across a hollow polymer inclusion membrane, J. Chromatogr. A. 1406 (2015) 34–39.

[251] M.I.G.S. Almeida, C. Chan, V.J. Pettigrove, R.W. Cattrall, S.D. Kolev, Development of a passive sampler for Zinc(II) in urban pond waters using a polymer inclusion membrane., Environ. Pollut. 193 (2014) 233–9.

[252] A. Garcia-Rodríguez, C. Fontàs, V. Matamoros, M.I.G.S. Almeida, R.W. Cattrall, S.D. Kolev, Development of a polymer inclusion membrane-based passive sampler for monitoring of sulfamethoxazole in natural waters. Minimizing the effect of the flow pattern of the aquatic system, Microchem. J. 124 (2016) 175–180.

[253] E. Marguí, C. Fontàs, K. Van Meel, R. Van Grieken, I. Queralt, M. Hidalgo, High-energy polarized-beam energy-dispersive X-ray fluorescence analysis combined with activated thin layers for cadmium determination at trace levels in complex environmental liquid samples, Anal. Chem. 80 (2008) 2357–2364.

[254] Y.Y.N. Bonggotgetsakul, M. Ashokkumar, R.W. Cattrall, S.D. Kolev, The use of sonication to increase extraction rate in polymer inclusion membranes. An application to the extraction of gold(III), J. Memb. Sci. 365 (2010) 242–247.

[255] A.H. Blitz-Raith, R. Paimin, R.W. Cattrall, S.D. Kolev, Separation of cobalt(II) from nickel(II) by solid-phase extraction into Aliquat 336 chloride immobilized in poly(vinyl chloride), Talanta. 71 (2007) 419–423.

CHAPTER 2

Objectives

The overall aim of this study is to develop new analytical methodologies for the preconcentration and speciation measurements of both inorganic and organic compounds. This general aim will be met by achieving the following specific objectives:

- To design, prepare and characterize polymer inclusion membranes using ionic liquids or specific carriers as a separation technique to be used for preconcentration and speciation measurements.

- To investigate the effect of modifications of the commercial ionic liquid Aliquat 336 as well as new routes of PIM preparations on physicochemical membrane characteristics and performance.

- To explore PIMs incorporated in a special device as well as in a flow technique to facilitate arsenic determination.

- To establish a transport model for the measurement of zinc speciation from a nutrient solution using PIMs as an emerging technique and its comparison with root uptake.

- To use PIMs made up of a polymer and a plasticizer as an extracting sorbent to preconcentrate pesticides from natural river samples prior to their determination.

CHAPTER 3

Results

3.1 Development of new analytical methodologies for arsenic determination

---

The contents of this section are based on the following studies:

R. Vera, E. Anticó, C. Fontàs, The Use of a Polymer Inclusion Membrane for Arsenate Determination in Groundwater, Water 10 (2018) 1093.

R. Vera, Y. Zhang, C. Fontàs, M.I.G.S. Almeida, E. Anticó, R.W. Cattrall, S.D. Kolev, Automatic determination of arsenate in drinking water by flow analysis with dual membrane-based separation, Food Chem. 283 (2019) 232-238.

R. Vera, C. Fontàs, E. Anticó, Titanium dioxide solid phase for inorganic species adsorption and determination: the case of arsenic, Environ. Sci. Pollut. Res. 24 (2017) 10939–10948.

3.1.1 The Use of a Polymer Inclusion Membrane for Arsenate Determination in Groundwater

Abstract

A polymer inclusion membrane (PIM) containing the ionic liquid methyltrioctylammonium chloride (Aliquat 336) as the carrier has been used satisfactorily for the preconcentration of arsenate present in groundwater samples, allowing its determination by a simple colorimetric method. The optimization of different chemical and physical parameters affecting the membrane performance allowed its applicability to be broadened. The transport of As(V) was not affected by the polymer used to make the PIM (cellulose triacetate (CTA) or poly(vinyl chloride) (PVC)) nor the thickness of the membrane. Moreover, the use of a 2 M NaCl solution as a stripping phase was found to allow the effective transport of arsenate despite the presence of other major anions in groundwater. Using the PIM for the analysis of different groundwaters spiked at 100 μg L^{-1} resulted in recoveries from 79% to 124% after only 5 h of contact time. Finally, the validated PIM-based method was successfully applied to the analysis of waters containing naturally occurring arsenate.

Introduction

Arsenic is a well-known pollutant that is present in high levels in soil and water in different countries around the world [1]. The World Health Organization (WHO) has set an upper limit of 10 μg L^{-1} in a guideline for concentrations in drinking water [2]. Due to the high toxicity of arsenic even at low concentrations, it is of paramount importance to perform routine analyses to monitor this pollutant in waters. Of the different separation techniques, functionalized membranes have attracted considerable attention as a valuable technology for many analytical purposes in recent years. This is the case of polymer inclusion membranes (PIMs), which are non-porous functionalized membranes that consist of a polymer, a plasticizer, and an extractant. These membranes are transparent, flexible and stable, and have been used in many applications such as sensing, both ion-selective electrodes (ISE) and optodes, sample pre-treatment (separation and pre-concentration), and electro-driven extraction. PIMs have also been used as passive samplers deploying the membrane device for a 7-day period without reporting any

drawback due to membrane fouling [3–5]. With the proper selection of the carrier, these membranes can effectively transport different species, such as inorganic pollutants [5], organic compounds [6] and metallic species [7].

In a previous study [8], a PIM made of cellulose triacetate (CTA) as the polymer and Aliquat 336 as the carrier was used for the transport of arsenate from aqueous natural samples to an 0.1 M NaCl stripping solution. Arsenate was transported through the membrane by the formation of the ion-pair [$(R_3R'N^+)_2HAsO_4^{2-}$], which was released in the stripping compartment by exchanging arsenate with the chloride present in this phase [8]. Under neutral pH conditions, inorganic As(III) transport was negligible since it is mainly present as a neutral species and, thus, the developed PIM allowed the quantitative separation of both inorganic As species. Moreover, it was found that even though other anions present in natural waters were also transported (e.g., chloride, phosphate, nitrate, sulphate and carbonate), As(V) transport efficiency was not hampered. The developed PIM-based separation system was later implemented in a special device, incorporating a PIM made of 69% (w/w) poly(vinyl chloride) (PVC) as the base polymer and 31% (w/w) Aliquat 336 as the carrier, which allowed the preconcentration of arsenate, thus providing easy arsenate detection by means of the formation of a blue complex [9]. This method provided a working range from 20 μg L^{-1} to 120 μg L^{-1} As(V) in ultrapure water, and a limit of detection (LOD) of 4.5 μg L^{-1} after 24 h of contact time using 5 mL 0.1 M NaCl as the stripping phase. It was successfully applied in the analysis of different waters from the Pyrenees region with low conductivity values. These two previous works allows us to establish the conditions for the effective transport of inorganic As(V) in a transport cell (without preconcentration) [8], and to apply the membrane system in a PIM-based device to allow As(V) preconcentration and detection with good results after 24 h contact time for water samples bearing low conductivity [9].

In the present study, in order to extend the applicability of this separation system, we have evaluated and optimized the chemical and physical parameters that can affect the PIM-based device, such as membrane composition, stripping phase characteristics, and membrane thickness, in order to accomplish the preconcentration of arsenic species in a more convenient timescale and to broaden the applicability of the method to more complex groundwater (GW) samples.

Methods

Reagents and Solutions

Stock solution (100 mg L^{-1}) of As(V) was prepared from solid $Na_2HAsO_4 \cdot 7H_2O$ purchased from Merck (Darmstadt, Germany). Working solutions of arsenate in ultrapure water and GW were prepared by dilution of the corresponding stock solution. Sodium chloride, obtained from Fluka (Bern, Switzerland), was used to prepare the stripping solution. Calibration standards of arsenic were prepared using the Spectrascan standard solution for atomic spectroscopy (Teknolab, Drıbak, Norway).

The extractant Aliquat 336 and the polymer PVC were purchased from Sigma-Aldrich (Steinheim, Germany) and CTA from Acros Organics (Geel, Belgium). The organic solvents tetrahydrofuran (THF) and chloroform ($CHCl_3$) (Panreac, Castellar del Vallès, Spain) were used to prepare the polymeric films.

Simulated groundwater (SGW) was prepared by dissolving 0.17 g of $NaHCO_3$, 0.22 g of $CaCl_2 \cdot 6H_2O$ (Panreac, Castellar del Vallès, Spain) and 0.07 g of Na_2SO_4 (Merck, Darmstadt, Germany) in 1 L of ultrapure water.

All reagents and solvents were of analytical reagent grade. Ultrapure water from a MilliQ Plus water purification system (Millipore Ibérica S.A., Madrid, Spain) was used to prepare all solutions.

Colorimetric Detection of As(V)

The determination of As(V) preconcentrated in the stripping phase was performed using the molybdenum blue method, which is based on the formation of an arsenomolybdate complex. The reagent solutions were prepared in accordance with the latest, improved version of the method [10]. Ammonium molybdate was prepared by dissolving 5.2 g of $(NH_4)_6Mo_7O_{24} \cdot 4H_2O$ (Scharlau, Barcelona, Spain) and 8.8 mg of potassium antimonyl tartrate, $K(SbO)C_4H_4O_6 \cdot 0.5H_2O$ (Merck, Darmstadt, Germany) in 30 mL of 9 M sulphuric acid and diluted with deionized water to 50 mL in a volumetric flask. A solution 10% (w/v) of ascorbic acid (Panreac, Castellar del Vallès, Spain), which was used as a reductant, was prepared daily. The reagents were added to As(V) samples or standard solutions in accordance with the recommended procedure. To account for the matrix effect, standard solutions were prepared both in ultrapure water and 2 M NaCl.

Polymer Inclusion Membrane (PIM) Preparation

PIMs were prepared by dissolving either CTA (200 mg) or PVC (400 mg) and the appropriate volume of a 0.5 M Aliquat 336 solution in chloroform or in THF, respectively. The solution was poured into a 9.0 cm diameter flat-bottom glass Petri dish which was set horizontally and covered loosely. The solvent was allowed to evaporate over 24 h at room temperature and the resulting film was then carefully peeled off the bottom of the Petri dish and circular 2.5 cm^2 pieces were cut from its central section and used in the experiments. PIMs of different thicknesses were prepared by reducing proportionally the total mass of polymer and Aliquat 336.

All PIM compositions are given in mass percentages for each component.

Preconcentration Experiments and Calibration Curve

The schematics and the whole set-up of the PIM-based device used in the preconcentration experiments are described elsewhere [11]. The device incorporates the PIM with an area of 2.5 cm^2 and contains the stripping solution. This device is immersed 1 cm in a vertical position in 100 or 50 mL of a water sample containing arsenic and placed on a magnetic stirrer. After a predetermined contact time, the device was removed from the solution and a selected volume of the stripping solution (usually 2 mL) was taken for the colorimetric analysis.

Arsenic transport efficiency (TE) was determined by using Eq. (3.1):

$$\mathrm{TE}(\%)=\frac{[As]_{strip\,(t)}}{[As]_{feed\,(0)}}\frac{1}{Vr}\times 100 \qquad (3.1)$$

where $[\mathrm{As}]_{\mathrm{strip(t)}}$ denotes the arsenic concentration in the stripping compartment at the end of the contact time, whereas $[\mathrm{As}]_{\mathrm{feed(0)}}$ is the initial arsenic concentration in the water sample. The volume ratio between the feed solution and stripping solutions is denoted by *Vr*.

The calibration curve for the preconcentration method was prepared by using the final selected conditions in accordance with the TE results (50 mL of aqueous feed solution, 2.5 mL of 2 M NaCl as the stripping phase and 5 h contact time).

All experiments were conducted at 22 ± 1 ºC, and were done per duplicate as minimum. Standard deviation (SD) is shown for each case with the corresponding number of replicates (n).

Apparatus

A Cary ultraviolet-visible (UV-Vis) (Agilent Technologies, Tokyo, Japan) instrument was used to measure the absorbance of As(V) complex at λ = 845 nm.

Arsenic concentration in the source solution of two GW samples with naturally occurring arsenic was measured using an inductively coupled plasma optical emission spectroscopy system (Agilent 5100 Vertical Dual View ICP-OES, Agilent Technologies, Tokyo, Japan).

PIM thickness was measured using a Digimatic Micrometer 0–25 mm (Mitutoyo, Takatsu-ku Japan).

The pH and conductivity values were determined with a Crison Model GLP 22 pH meter and Ecoscan, Entech Instruments, portable conductimeter, respectively. A magnetic multistirrer 15 (Fischer Scientific, Hampton, NH, USA) was also used.

Water Samples

Seven GW samples were collected from different locations in north-east Catalonia (Spain). Table 3.1 indicates the location of the different sampling spots as well as the main chemical characteristics of the different waters. GW samples 1–5 do not contain As and were used to study the effect of the water matrix by adding arsenate at different concentrations. GW samples 6 and 7 contained naturally occurring arsenic. All waters were used without any treatment (filtration or pH adjustment) except for sample GW7, which was brought to neutral pH by adding HCl.

Table 3.1 Characteristics and georeferences of the water samples used in this study.

Samples	Georeferences of Sampling Point (Coordinates)	pH	Conductivity ($\mu S\ cm^{-1}$)	Ions ($mg\ L^{-1}$)							Arsenic Concentration ($\mu g\ L^{-1}$)
				$[NO_3^-]$	$[Cl^-]$	$[SO_4^{2-}]$	$[HCO_3^-]$	$[Na^+]$	$[Mg^+]$	$[Ca^+]$	
GW1 (Pujarnol)	42° 6′ 16.907″ N Lat., 2° 42′ 34.64″ E Long.	7.21	684	1.2	15.4	63.9	269	19.0	30.1	96.1	n.f.
GW2 (Mongai)	41° 47′ 59.047″ N Lat., 0° 57′ 38.832″ E Long.	7.76	470	9.5	15	38.3	n.m.	10.8	14.9	68.9	n.f.
GW3 (St. Hilari)	41° 53′ 16.46″ N Lat., 2° 31′ 11.867″ E Long.	7.98	275	21.9	11.4	8.7	172	16.6	9.0	50.0	n.f.
GW4 (Cerdanya)	42° 21′ 16.059″ N Lat., 1° 42′ 17.742″ E Long.	7.5	423	0.3	4.3	2.5	349	11.4	13.2	70.7	n.f.
GW5 (Setcases)	42° 22′ 22.208″ N Lat., 2° 18′ 3.026″ E Long.	7.56	110	3.3	0.9	8.0	88	3.7	2.7	23.6	n.f.
GW6 (Cerdanya)	42° 22′ 16.393″ N Lat., 1° 40′ 41.159″ E Long.	7.5	236	2.2	2.7	12.4	140	n.m.	n.m.	n.m.	67.1
GW7 (Cerdanya)	42° 22′ 12.595″ N Lat., 1° 40′ 54.456″ E Long.	9.69	185	0.4	2.2	11.8	n.m.	n.m.	n.m.	n.m.	70.4
SGW	-	7.5	459	n.a.	71	47.0	123	70.2	n.a.	40.3	n.a.

n.m.: not measured; n.a.: not added; n.f.: not found.

Results and discussion

Parameters Affecting the Preconcentration System

Stripping composition

As reported in our previous study [9], As(V) transport through the PIM containing Aliquat 336 is based on an anionic exchange in which the chloride present in the striping phase is the driving force behind the up-hill transport of the arsenate anion. Despite other anions such as sulphate or nitrate also being transported through the PIM, the effectiveness of the system was not affected as long as the total concentration of anions in GW did not exceed the chloride concentration in the stripping solution. However, the applicability of the method was severely hampered in the case of water samples with high conductivity. Thus, to broaden the application of this PIM-based preconcentration system, we tested the use of a 2 M NaCl solution instead of 0.1 M NaCl, maintaining all the other experimental parameters (e.g., PIM: 69% PVC – 31% Aliquat 336 (w/w), time: 24 h, feed volume: 100 mL and stripping volume: 5 mL). The results are presented in Figure 3.1 as As(V) transport efficiency for both ultrapure water and GW1 and the two stripping solution compositions tested. It is worth mentioning that the conductivity of GW1 (648 μS) is between 2–6 times higher than the conductivity of natural waters studied in our previous work (in the 120–194 μS range) [9]. As can be observed, As(V) transport efficiency is dramatically affected if 0.1 M NaCl is used as the stripping phase, since only 34% of arsenate is transported. TE for GW1 increases up to 70% when the concentration of NaCl in the stripping phase is increased to 2 M. Similar results were observed in the work of Garcia-Rodríguez et al. [12], where the same PIM device was used for the monitoring of sulfamethoxazole (SMX) in natural waters, where a 2 M NaCl solution allowed a more efficient mass transfer across the membrane than an 0.5 M NaCl solution. Hence, a stripping phase consisting of a 2 M NaCl solution was fixed for subsequent experiments.

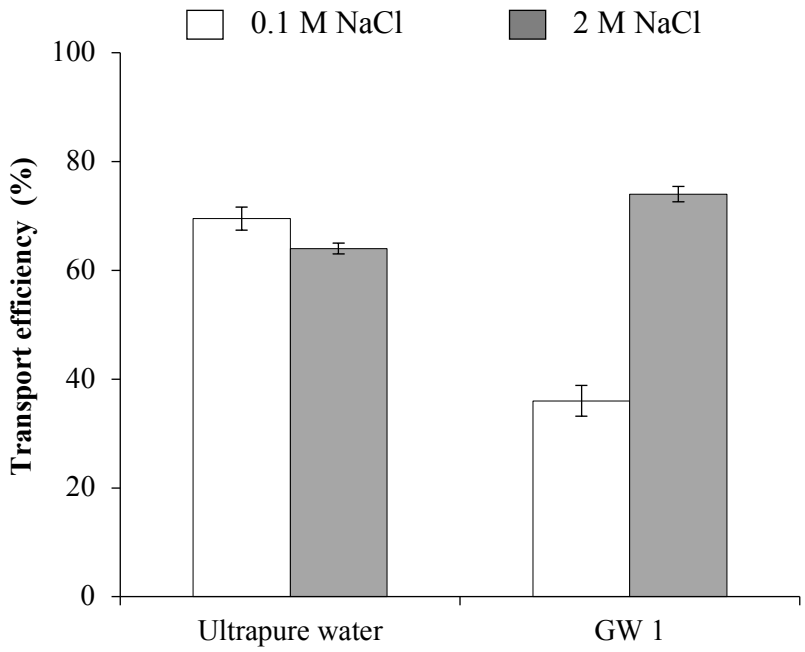

Figure 3.1 The effect of NaCl concentration used as a stripping solution on As(V) transport in both ultrapure and groundwater GW1 (spiked at 100 μg L^{-1} As(V)). Polymer inclusion membrane (PIM): 69% poly(vinyl chloride) (PVC) – 31% Aliquat 336 (w/w); time: 24 h; feed volume: 100 mL; stripping volume: 5 mL. (n=2).

Contact Time and Sample and Stripping Volume

As(V) transport was assessed by varying the volume of both feed and stripping solutions (volume ratio fixed at 20) and using two different water samples, ultrapure and GW1. As shown in Figure 3.2, better transport efficiencies are obtained for both water samples tested, when 50 mL volumes for the feed and 2.5 mL for the stripping solution (50/2.5) were used in the PIM-based device system after 24 h contact time.

Moreover, As(V) transport efficiencies at 5 h and 24 h are compared in the same figure. It can be observed that TE are higher when the contact time is 24 h but satisfactory results, around 60% of TE, are also obtained at a time as short as 5 h. In our previous work [9], at a contact time of 5 h and using 0.1 M NaCl as the stripping phase and the 100/5 volumes, the TE obtained was around 20%. Besides, at 5 h contact time, the difference in terms of As(V) transport between the two different water samples is negligible. Therefore, 50/2.5 volumes for feed and stripping solutions and a contact time of 5 h were selected for further experiments.

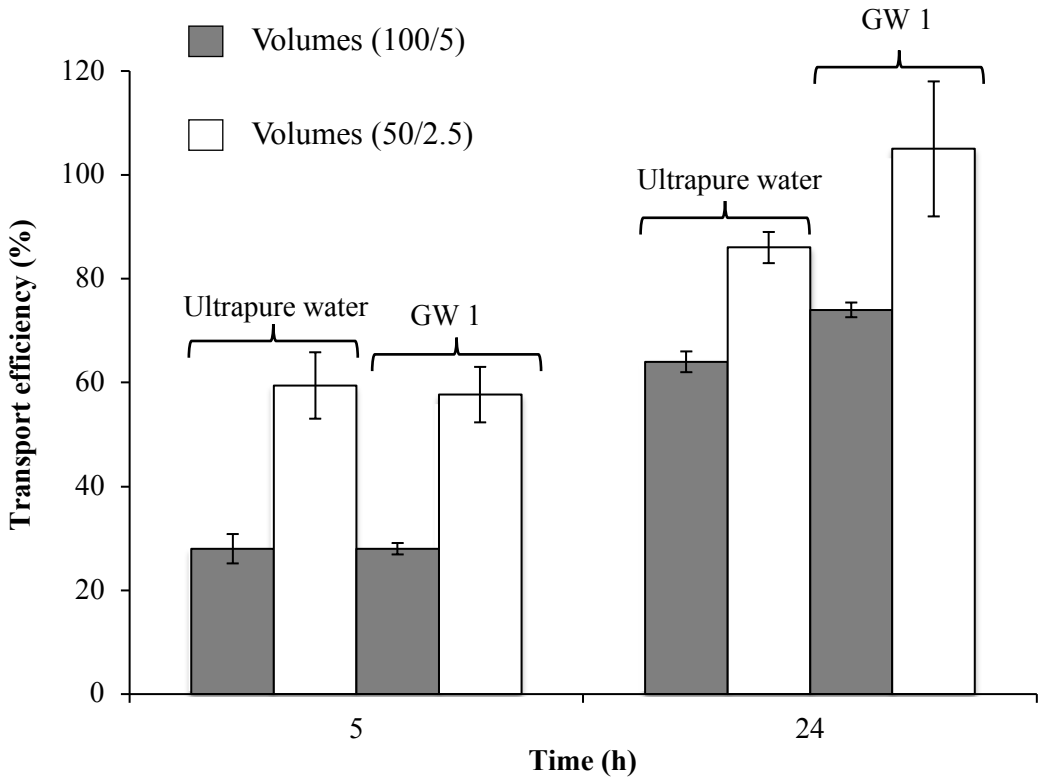

Figure 3.2 As(V) transport efficiency using a PIM-device with different volumes as feed and stripping solutions in both ultrapure and GW1 (spiked at 100 µg L^{-1} As(V)), after 24 h (a) and 5 h (b) contact time (n=2). PIM composition was 69% PVC – 31% Aliquat 336 (w/w) and 2 M NaCl was used as the stripping phase.

Membrane Characteristics

As reported by other authors [8,12], transport efficiency can be affected by both the amount of extractant in the PIM and the nature of the polymer. Therefore, various membrane compositions with different thickness were studied in terms of arsenate preconcentration in the stripping phase, after a 5 h contact time. As can be seen in Table 3.2, there was only slight variation for the different PIM compositions even though different polymers were employed. These results are in concordance with other publications where similar results were obtained with PIMs prepared with the two polymers, CTA and PVC [13,14].

Table 3.2 Effect of membrane composition and thickness on As(V) preconcentration in the stripping phase (n=3). Feed composition: 100 μg L^{-1} As(V) in GW1 (50 mL).

Polymer	PIM Composition (w/w)	Thickness (μm)	[As] stripping (μg L^{-1}) (± SD)
Poly(vinyl chloride) (PVC)	69% PVC–31% Aliquat 336	60	1160 (± 58)
		30	940 (± 94)
	50% PVC–50% Aliquat 336	96	900 (± 45)
		39	840 (± 53)
Cellulose triacetate (CTA)	70% CTA–30% Aliquat 336	38	880 (± 18)
	52% CTA–48% Aliquat 336	45	1060 (± 85)
		25	940 (± 19)

Additionally, different authors have reported the great influence of PIM thickness when metal transport is rate-limited by the diffusion of the metal across the membrane [15–17]. However, the reduction of the membrane thickness, using the PIM-based device under the selected conditions, did not enhance the As(V) preconcentration, which can be explained by diffusion through the membrane not being the only rate-limiting factor as diffusion in the acceptor solution is also involved [11].

The fact that only slight differences are obtained in terms of arsenate preconcentration using different PIMs composition highlights the great sturdiness of the system under these experimental conditions. PIM with a composition of 52% CTA – 48% Aliquat 336 (w/w) and a thickness of 45 μm was used in further experiments since the amount of reagents necessary to prepare PIMs made of CTA is smaller than PIMs based on PVC.

It should be noted that the preconcentration system provides an arsenate enrichment of around 10 times the initial concentration in the feed solution, which is a clear improvement in facilitating the detection of arsenate in polluted GW samples at low levels.

Analytical Application of the PIM-device

Effect of Water Matrix

The matrix composition of the calibration standards must be considered for the application of the PIM-based preconcentration system in the determination of As(V) as this is a critical point which can affect the TE and, consequently, the sensitivity of the method. For this reason, different water samples, GW1 to GW5 and SGW, were tested (see Table 3.1 for composition) under the selected experimental conditions. As(V) transport efficiencies are compared in Table 3.3, where values ranging from 53% up to 72% for GW1–4 and a value of 81% for GW5 are presented. The highest TE of GW5 is clearly related to the lowest conductivity value, which enables higher arsenate transport across the PIM. Our results support the hypothesis that the accuracy of the method might be compromised by the matrix composition used for the preparation of the calibration standards and the conductivity of the target water sample. As SGW presents an intermediate TE between GW1 and GW5, this is finally selected for the calibration and validation of the PIM-based device method.

Table 3.3 Comparison of the different GW samples on arsenate transport efficiency with the proposed PIM-based method (n=2).

Water Sample	**Conductivity (µS cm^{-1})**	**Amount of As(V) Added (µg L^{-1})**	**TE (%) (± SD)**
GW1	684	100	53 (± 8)
GW2	470	100	65 (± 6)

GW3	275	100	72 (± 6)
GW4	423	100	66 (± 23)
GW5	110	100	81 (± 11)
SGW	459	100	63 (± 8)

Analytical Parameters

Under selected conditions, the proposed PIM-based method was applied to standards containing As(V) in the range of 10 μg L^{-1} to 150 μg L^{-1} in SGW. Figure 3.3 shows the absorbance measured for each standard plotted versus known concentrations of As(V) in the initial feed phase, and a straight line was fitted to measured points by the least-square method. Parameters of the resulting calibration curve are also included in Figure 3.3. The fact that the regression coefficient was higher than 0.99 indicates a good linearity throughout the studied working range. It is worth mentioning that the LOD of 7 μg L^{-1} is in concordance with the maximum permitted in drinking waters set at 10 μg L^{-1} by the WHO [2], and acceptable relative standard deviation (RSD) values (below 20%) at two different levels (i.e., 10% at 30 μg L^{-1} and 13% at 100 μg L^{-1}) are also obtained.

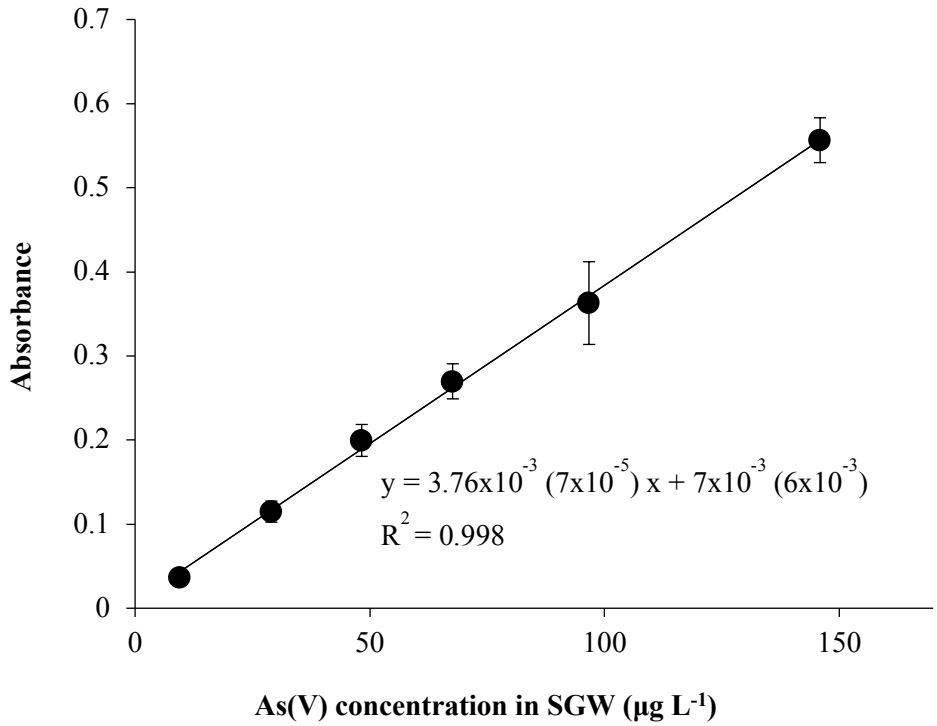

Figure 3.3 Calibration curve obtained with the PIM-based method. PIM, 52% CTA – 48% Aliquat 336 (w/w) (n=3). Feed solution, 50 mL of different As(V) concentrations in simulated groundwater (SGW); stripping solution 2.5 mL 2 M NaCl.

Recovery values of the proposed PIM-based method were calculated taking into account the calculated As(V) content based on the concentration found in the stripping and using the equation shown in Figure 3.3, in relation to the spiked level of different GW with 100 µg L^{-1} As(V). The results are collected in Table 3.4, where it can be seen that recovery values range from 79% up to 124% with the highest recovery corresponding to GW5.

Table 3.4 Effect of water sample on As(V) recovery (n=2).

Water Sample	As(V) Recovery (%) (± SD)
GW1	79 (± 13)
GW2	98 (± 10)
GW3	109 (± 9)
GW4	100 (± 35)
GW5	124 (± 17)

All recovery values and standard deviations obtained using our proposed PIM-based device method can be considered satisfactory taking into account the μg L^{-1} concentration level, as reported in the guidelines for standard method performance requirements [18].

Application to Contaminated Groundwater (GW) Samples

The proposed method was used to analyse two naturally occurring arsenate GW samples from Catalonia (north-east Spain). A comparison between the direct analysis of the water sample by inductively coupled plasma optical emission spectroscopy (ICP-OES) and the proposed PIM-based device method is presented in Table 3.5. The good agreement shows that the method is suitable for the determination of As(V) in GW samples.

Table 3.5 As(V) concentration in GW samples determined by the ICP-OES reference method and the proposed PIM-based device method (n=2).

Water Sample	As Concentration Measured (μg L^{-1}) (± SD)	
	ICP-OES	**PIM-based Device**
GW6	67 ± 2	82 (± 2)
GW7	70 ± 3	67.4 (± 0.5)

Conclusions

An effective and simple methodology has been proposed employing a device incorporating a PIM made of 52% CTA – 48% Aliquat 336 (w/w) and using the volumes of 50 mL and 2.5 mL for the feed and stripping solutions, respectively. The selection of a 2 M NaCl solution as the stripping phase and 5 h contact time resulted in TE around 53–81%. The type of polymer and the membrane thickness do not seem to influence the transport results under the studied experimental conditions. The use of an SGW as a matrix for the preparation of calibration standards enabled an improvement of the analytical parameters for the determination of As(V) in GWs with different chemical compositions. The results obtained for the PIM-based method of two GW samples naturally containing As(V) is in concordance with the ICP-OES analysis. Hence, it is demonstrated that the proposed method can be used as an attractive alternative for the determination of arsenate within a range of different aqueous matrices with different conductivities.

References

[1] I. Villaescusa, J.-C. Bollinger, Arsenic in drinking water: sources, occurrence and health effects (a review), Rev. Environ. Sci. Bio./Technol. 7 (2008) 307-323.

[2] World Health Organization (WHO). Guidelines for drinking-water quality, 4th ed, WHO, Geneva, 2011.

[3] M.I.G.S. Almeida, R.W. Cattrall, S.D. Kolev, Polymer inclusion membranes (PIMs) in chemical analysis - A review, Anal. Chim. Acta. 987 (2017) 1–14.

[4] M.I.G.S. Almeida, C. Chan, V.J. Pettigrove, R.W. Cattrall, S.D. Kolev, Development of a passive sampler for Zinc(II) in urban pond waters using a polymer inclusion membrane, Environ. Pollut. 193 (2014) 233–9.

[5] M.I.G.S. Almeida, A.M.L. Silva, R. a Coleman, V.J. Pettigrove, R.W. Cattrall, S.D. Kolev, Development of a passive sampler based on a polymer inclusion membrane for total ammonia monitoring in freshwaters, Anal. Bioanal. Chem. 408 (2016) 3213–22.

[6] A. Garcia-Rodríguez, V. Matamoros, S.D. Kolev, C. Fontàs, Development of a polymer inclusion membrane (PIM) for the preconcentration of antibiotics in environmental water samples, J. Membr. Sci. 492 (2015) 32–39.

[7] N. Pont, V. Salvadó, C. Fontàs, Selective transport and removal of Cd from chloride solutions by polymer inclusion membranes, J. Membr. Sci. 318 (2008) 340–345.

[8] R. Güell, E. Anticó, S.D. Kolev, J. Benavente, V. Salvadó, C. Fontàs, Development and characterization of polymer inclusion membranes for the separation and speciation of inorganic As species, J. Membr. Sci. 383 (2011) 88–95.

[9] C. Fontàs, R. Vera, A. Batalla, S.D. Kolev, E. Anticó, A novel low-cost detection method for screening of arsenic in groundwater, Environ. Sci. Pollut. Res. 21 (2014) 11682–8.

[10] S. Tsang, F. Phu, M.M. Baum, G.A. Poskrebyshev, Determination of phosphate/arsenate by a modified molybdenum blue method and reduction of arsenate by $S_2O_4^{2-}$, Talanta. 71 (2007) 1560–1568.

[11] R. Vera, C. Fontàs, J. Galceran, O. Serra, E. Anticó, Polymer inclusion membrane to access Zn speciation: Comparison with root uptake, Sci. Total Environ. 622–623 (2018) 316–324.

[12] A. Garcia-Rodríguez, C. Fontàs, V. Matamoros, M.I.G.S. Almeida, R.W. Cattrall,

S.D. Kolev, Development of a polymer inclusion membrane-based passive sampler for monitoring of sulfamethoxazole in natural waters. Minimizing the effect of the flow pattern of the aquatic system, Microchem. J. 124 (2016) 175–180.

[13] M.I. Vázquez, V. Romero, C. Fontàs, E. Anticó, J. Benavente, Polymer inclusion membranes (PIMs) with the ionic liquid (IL) Aliquat 336 as extractant: Effect of base polymer and IL concentration on their physical–chemical and elastic characteristics, J. Membr. Sci. 455 (2014) 312–319.

[14] O. Kebiche-Senhadji, S. Tingry, P. Seta, M. Benamor, Selective extraction of Cr(VI) over metallic species by polymer inclusion membrane (PIM) using anion (Aliquat 336) as carrier, Desalination. 258 (2010) 59–65.

[15] J. Konczyk, C. Kozlowski, W. Walkowiak, Removal of chromium(III) from acidic aqueous solution by polymer inclusion membranes with D2EHPA and Aliquat 336, Desalination. 263 (2010) 211–216.

[16] P.K. Mohapatra, D.S. Lakshmi, A. Bhattacharyya, V.K. Manchanda, Evaluation of polymer inclusion membranes containing crown ethers for selective cesium separation from nuclear waste solution, J. Hazardous Mater. 169 (2009) 472–479.

[17] S.P. Kusumocahyo, T. Kanamori, K. Sumaru, S. Aomatsu, H. Matsuyama, M. Teramoto, T. Shinbo, Development of polymer inclusion membranes based on cellulose triacetate: Carrier-mediated transport of cerium(III), J. Membr. Sci. 244 (2004) 251–257.

[18] AOAC Official Methods of analysis, Guidelines for standard method performance requirements Appendix F, AOAC International, 2012, pp. 1–17.

3.1.2 Automatic determination of arsenate in drinking water by flow analysis with dual membrane-based separation

Abstract

The sequential application of a polymer inclusion membrane (PIM), composed of poly(vinylidenefluoride-co-hexafluoropropylene) and the anionic extractant Aliquat 336, and a microporous polytetrafluoroethylene (PTFE) gas-permeable membrane was utilized for the first time to develop a flow analysis (FA) system, for the automatic determination of trace levels of arsenate (As(V)) in drinking water as arsine. The system incorporated a flow-through extraction cell for separation and preconcentration of arsenate and a gas-diffusion cell for the separation of arsine prior to its spectrophotometric determination based on the discoloration of a potassium permanganate solution. Under optimal conditions the FA system is characterized by a limit of detection of 3 μg L^{-1} As(V) and repeatability of 1.8% (n=5, 25 μg L^{-1} As(V)) and 2.8% (n=5, 50 μg L^{-1} As(V)). The newly developed FA method was successfully applied to the determination of arsenate in drinking water samples in the μg L^{-1} concentration range.

Introduction

Arsenic is a naturally occurring toxic element, which is present in natural waters around the world [1]. Inorganic species, such as arsenate (As(V)) and arsenite (As(III)), are the most common and toxic forms of arsenic found in aquatic systems [2]. Arsenic is considered a leading pollutant since it is often found at elevated levels in natural waters and long-term exposure to its forms have been associated with skin, lung, urinary tract, kidney, and liver cancer [3]. Therefore, the World Health Organization (WHO) has set the guideline concentration for arsenic in drinking water at 10 μg L^{-1} [4]. It should be pointed out that arsenic in drinking water is present very often almost entirely as arsenate (As(V)) [5,6]. The low regulated level of arsenic and its complex chemistry represent a challenge from an analytical point of view. Hence, a great number of highly sensitive analytical techniques have been developed and employed for the determination of arsenic in environmental samples, namely graphite furnace atomic absorption spectrometry

(GFAAS) [7], hydride generation atomic absorption spectrometry (HG-AAS) [8], hydride generation atomic fluorescence spectrometry (HG-AFS) [9], inductively coupled plasma atomic emission spectrometry (ICP-OES) [10], and inductively coupled plasma mass spectrometry (ICP-MS) [2,11]. These techniques provide the sensitivity required to directly measure arsenic concentrations in water samples at the μg L^{-1} level. However, the techniques mentioned above require expensive equipment and highly trained laboratory technicians.

Flow injection analysis (FIA) is a technique suitable for performing analysis on-line in an automatic fashion and it is highly efficient in minimizing both reagent and sample consumption as well as the overall analysis time and associated costs [12,13]. Different detection techniques have been successfully applied in FIA systems for the determination and speciation of arsenic (e.g., voltammetry [14], amperometry [15,16], chemiluminescence [17], or spectrophotometry [18-20]. A great number of spectrophotometric methods for arsenic are based on the method proposed by Johnson and Pilson [21], in which an arsenomolybdenum blue complex is formed. However, this method is affected by severe interferences from silicate or phosphate, often present in arsenic samples, which impose serious limitations on the applicability of this method. To avoid the interference of phosphate and silicate, some authors have used an anion-exchange column to retain the interfering anions [22,23] or optimized the molybdenum blue method to improve its selectivity for arsenate over phosphate, as reported by Dhar et al. [24]. Rupasinghe et al. [19] and Toda et al. [25] have reported on the development of FIA systems based on hydride generation where arsenic is converted into arsine followed by bleaching an oxidant acceptor $KMnO_4$ solution. The concentration of arsenic in many water samples is at trace level and preconcentration is often required.

Membrane-based extraction procedures involving liquid membranes have emerged as promising alternatives to ion-exchange based separation and preconcentration where retention and stripping of the analyte take place sequentially. In liquid membrane-based separation the extraction and back-extraction of the analyte from a donor aqueous stream into an acceptor aqueous stream occur simultaneously. Supported liquid membranes (SLMs), which are considered as the most frequently used type of liquid membranes at present, have been used successfully in the determination of arsenate in drinking water [26]. However, in this type of membranes the membrane liquid phase, consisting of an extractant and diluent, is retained in the micrometre size pores of a hydrophobic polymeric membrane and this leads to leaching of the membrane liquid

phase into the donor and acceptor aqueous phases, thus causing potential deterioration in the performance of the SLM [27].

Recently, polymer inclusion membranes (PIMs) have been shown to have a better stability than SLMs [28]. PIMs are casted from a solution of a base polymer, extractant and in some cases plasticizer or modifier in a suitable solvent [28,29]. The reason behind their superior stability compared to SLMs stems from the fact that the membrane liquid phase of PIMs (i.e., extractant and plasticizer/modifier) is retained between the entangled polymer chains of the base polymer, thus minimizing significantly its leaching to the adjacent aqueous solutions. The base polymer provides mechanical strength to the PIM, while the extractant (carrier) is responsible for the extraction/transport of the chemical species of interest. The plasticizer or modifier are often added to the PIM composition to provide elasticity or increased solubility of the extracted species in the membrane liquid phase, respectively [29]. PIMs have been successfully employed in flow analysis (FA) systems for the on-line separation and preconcentration of Zn(II) [30,31], orthophosphate [32] and vanadium(V) [33].

The present paper reports on the development of a spectrophotometric FA system implementing on-line preconcentration of arsenate using a PIM consisting of poly(vinylidene fluoride-co-hexafluoropropylene) (PVDF-HFP) and Aliquat 336 followed by on-line generation of arsine which diffuses across a gas-permeable membrane into a permanganate solution causing its discoloration. To the best of our knowledge this is the first use of a PIM in an FA system for the determination of arsenate in drinking waters at low μg L^{-1} levels and the first coupling of on-line membrane-based extractive separation with on-line membrane-based gas-diffusion separation.

Experimental

Reagents and solutions

All reagents and solvents used in this study were of analytical reagent grade. The polymers PVDF-HFP (Aldrich, USA) and poly(vinyl chloride) PVC (Fluka, Italy), the extractant Aliquat 336 (Aldrich, USA), and the modifier 1-tetradecanol (Aldrich, USA) were used as constituents of the PIMs studied. Tetrahydrofuran (THF) without a stabilizer, purchased from VWR (Australia), was used as the membrane casting solvent. The acceptor solution used in the PIM-based separation step contained 0.1 mol L^{-1} NaCl

(Chem-Supply, Australia) as the stripping reagent for arsenate. The reduction of As(V) to As(III) was conducted using a reductant solution composed of 4 mol L^{-1} HCl (32%, RCI Labscan, Thailand), 1% (w/v) KI (Aldrich, USA), and 0.5% (w/v) ascorbic acid (AA) (Ajax Finechem, Australia). The sodium borohydride reagent stream used for arsine generation contained 0.5% (w/v) $NaBH_4$ and 0.05 mol L^{-1} NaOH (Chem-Supply, Australia). Arsine was absorbed and oxidized in the gas-diffusion acceptor stream containing 0.2 mmol L^{-1} $KMnO_4$ (Chem-Supply, Australia) and 0.05 mol L^{-1} NaOH (Chem-Supply, Australia).

The interference studies were performed with working solutions prepared by dilution of stock solutions containing 500 mg L^{-1} $H_2PO_4^-$, Cl^-, NO_3^-, HCO_3^-, or SO_4^{2-}. These stock solutions were prepared by dissolving Na_2HPO_4 (BDH, Australia), NaCl, $NaNO_3$ (Ajax, Australia), $NaHCO_3$ (Chem-Supply, Australia), or Na_2SO_4 (Chem-Supply, Australia) in ultrapure water (≥18.2 MΩ cm, Millipore, Synergy 185, France), used in the preparation of all aqueous solutions.

Instrumentation

On-line spectrophotometric detection was conducted with a Pharmacia Novaspec II UV-Vis spectrophotometer (Pharmacia Biotech, Sweden) fitted with a flow-through cell made of quartz (10 mm optical path length, Starna, UK). The spectrophotometer was interfaced with a PowerChrom 280 (Model ER280) data recording system linked to a PC and run by the Chart software package (eDAQ, Australia).

The PIMs thickness was measured using an optical microscope (Model LH50A, Olympus, Japan) with a calibrated lens (Carton Optical Ind., Japan).

For method validation the samples were also analysed after off-line pre-reduction with a solution containing a mixture of 1% (w/v) KI and 0.5% (w/v) ascorbic acid by inductively coupled plasma optical emission spectrometry (ICP-OES, Model Optima 4300 DV, Perkin-Elmer) incorporating a home-made hydride generation unit.

Flow Analysis (FA) manifold

The FA manifold developed in the present study for arsenate preconcentration, separation and detection involving hydride generation is depicted in Figure 3.4.

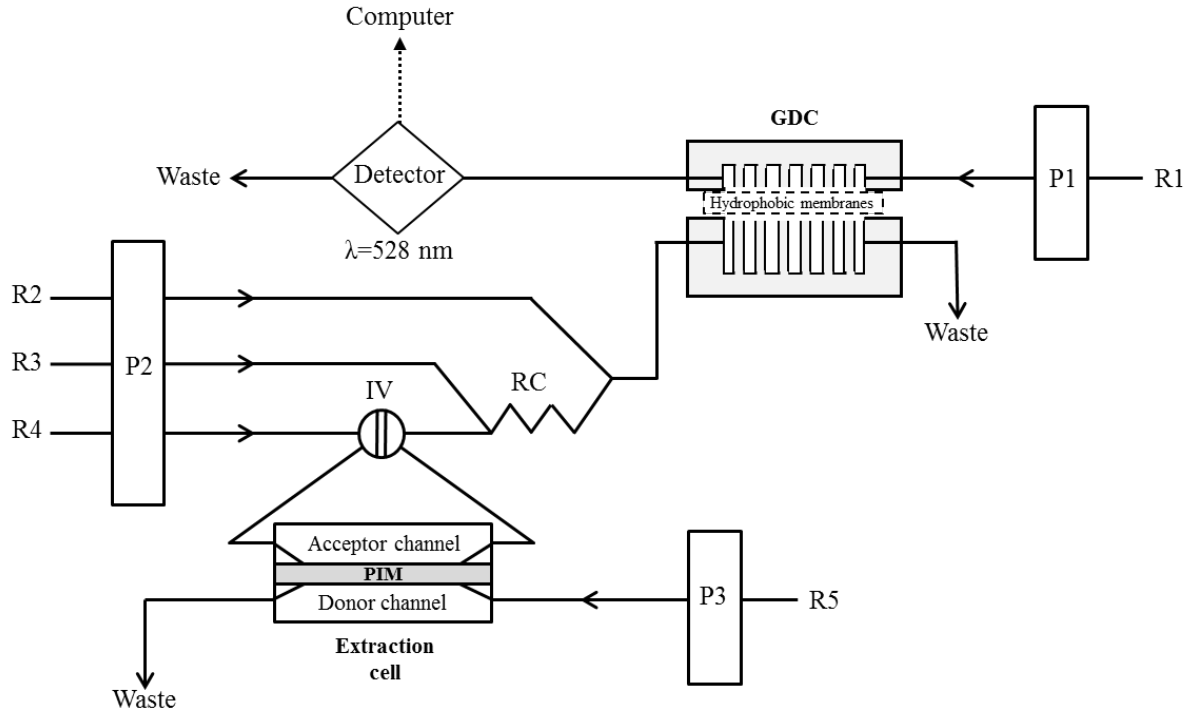

Figure 3.4 Schematic representation of the FA manifold. P1-P3: peristaltic pumps; R1: gas-diffusion acceptor stream (0.2 mM M $KMnO_4$, 0.05 M NaOH); R2: $NaBH_4$ stream (0.5% (w/v) $NaBH_4$, 0.05 mol L^{-1} NaOH); R3: reductant stream (4 M HCl, 1% (w/v) KI, 0.5% (w/v) ascorbic acid); R4: PIM acceptor stream (0.1 M NaCl); R5: PIM donor stream; RC: reaction coil; IV: injection valve; GDC: gas-diffusion cell; PIM: polymer inclusion membrane.

The system consisted of three four-channel peristaltic pumps, i.e., Pump 1 and Pump 2 (Model VS4, Watson Marlow Alitea, Sweden) and Pump 3 (Gilson Minipuls-3, France). All the pumps were fitted with Tygon tubing of suitable internal diameter (TACS, USA). Polytetrafluoroethylene (PTFE) tubing of 0.5 mm *i.d.* was used throughout the manifold, except for the gas-diffusion acceptor stream outlet tubing, which was of 3 m length and 0.3 mm i.d. to provide sufficient back-pressure. The latter was required to prevent the diffusion of H_2, generated by the decomposition of $NaBH_4$, across the hydrophobic membranes and the paper filter of the gas-diffusion cell (GDC, Figure 3.5a) into Stream R1 where it would have interfered with the analytical measurements. The following hydrophobic microporous membranes were used in the present study: Durapore ® and Surevent ® membranes (Merck Millipore, USA), PTFE membranes (Reece, Australia), and polypropylene membranes (Chemplex, Zimbadwe). The flow rates of all streams were measured gravimetrically by weighing the mass of water of known temperature pumped through the corresponding tubing over a 5 min period. On-

line preconcentration of arsenate was performed using a home-made extraction cell similar to the one described previously by us [31], which consisted of two Perspex blocks (150 mm length, 30 mm width and 15 mm height, each) clamped together by stainless steel screws. The two channels of the extraction cell were serpentine shaped and were 157, 1 and 0.25 mm in length, width and depth, respectively. Arsine was separated in a homemade GDC (Figure 3.5) made of Perspex and identical to the one used previously by us [34] where arseine diffused from the gas-diffusion donor stream (Streams R2+R3+R4, Figure 3.4) across an assembly of a filter paper disc (No. 54, Whatman, Britain) sandwiched between two hydrophobic microporous membranes (Figure 3.5a) into the gas-diffusion acceptor stream (Stream R1). The filter paper was used as a physical support for the hydrophobic membranes, which otherwise could have stretched as a result of the pressure difference between the two channels of the GDC (Figure 3.5a) thus changing the channels' volume and impacting negatively on repeatability. The shape of the two channels of identical width and length (Figure 3.5b), i.e., 1.8 mm and 100 mm, respectively, ensured efficient mixing of the gas-diffusion donor and acceptor streams which improved the generation, trans-membrane transfer and oxidation of arsine in the gas-diffusion acceptor stream (Stream R1) [34]. The depths of the acceptor and the donor channels were 0.5 and 6 mm, respectively, and the corresponding volumes were 90 μL and 1080 μL, respectively. This volume difference coupled with appropriately selected flow rates of Streams R1 – R4 allowed a degree of preconcentration of arsenic as arsine in the gas-diffusion acceptor stream (Stream R1).

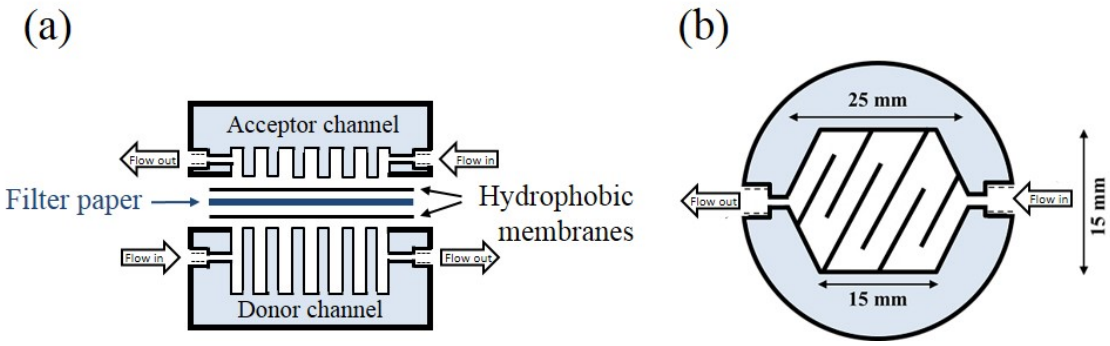

Figure 3.5 Schematic representation of the GDC used in the on-line separation of arsine. (a) Cross-section (donor and acceptor channels depths - 6 and 0.5 mm, respectively) and (b) top view of one of the halves of the GDC.

FA procedure

The standard/sample solution (Stream R5, Figure 3.4) was propelled for a predetermined period of time through the donor channel of the extraction cell where a PIM separated the sample (donor) stream (Stream R5) from the acceptor stream (Stream R4). The acceptor stream was stopped for a predetermined stop-flow time during the sample passage through the donor channel of the extraction cell to allow preconcentration of arsenate in the static acceptor solution located in the acceptor channel of the cell. At the end of the stop-flow time, the acceptor stream (R4) was re-started and arsenate was reduced to arsenite by merging the acceptor stream of the extraction cell (R4) with a reagent stream (R3) containing HCl, KI and ascorbic acid. Subsequently, arsine was generated by merging the combined R4+R3 stream with a sodium borohydride stream (R2). The generated arsine in the combined stream R4+R3+R2 diffused across the hydrophobic membranes and the filter paper of the GDC (Figure 3.5a) into its acceptor solution (R1) where it was oxidised by $KMnO_4$ resulting in a decrease in the permanganate absorbance, monitored continuously at 528 nm in the spectrophotometric measuring cell of the manifold. In all measurements the analytical signal recorded was the maximum decrease in $KMnO_4$ absorbance relative to the baseline level.

Optimisation of the FA method

The optimization of the reaction coil (RC) length (Figure 3.4) and the flow rate of Stream R1 and the selection of the most appropriate hydrophobic gas-diffusion membrane was carried out in a FA system similar to the one shown in Figure 3.4 where the extraction cell was replaced with an injection valve with a 500 μL sample loop. The standards injected in these experiments contained 1000 μg L^{-1} As(V).

The suitability of different PIM compositions was tested in the FA manifold shown in Figure 1 using a stop-flow procedure in which 5 mL of a 1000 μg L^{-1} As(V) standard solution was propelled at a flow rate of 0.2 mL min^{-1} through the donor channel of the extraction cell. The influence of the stop-flow time and the flow rate of Stream R5 was studied by propelling a standard solution containing 500 μg L^{-1} As(V) through the donor channel of the extraction cell.

PIM preparation

PVC-based PIMs containing 70% (w/w) PVC and 30% (w/w) Aliquat 336 were prepared by dissolving 180 mg of Aliquat 336 in 18 mL of THF, followed by slow addition of 420 mg of PVC into the casting solution, which was constantly stirred to avoid aggregation of the polymer. Finally, the resulting mixture was poured into a 16.5 cm in diameter glass ring sitting on a flat glass plate. The ring was covered with filter paper and a watch glass to slow down the evaporation of THF in the next 15 h after which the resulting PIM was carefully peeled from the glass plate [11,32].

PIMs containing 1-tetradecanol as a modifier were also prepared by the casting method outlined above. However, in this case 60 mg of this compound and 120 mg of Aliquat 336 were dissolved in the casting solution together with 420 mg of PVC and the corresponding PIMs contained 70% (w/w) PVC, 20% (w/w) Aliquat 336 and 10% (w/w) 1-tetradecanol.

The PVDF-HFP-based membranes were prepared following the procedure described by O'Bryan et al. [35]. In this method, 700 mg of PVDF-HFP and 300 mg of Aliquat 336 were dissolved in 8 mL of THF at 50 °C and the mixture was mechanically stirred until the complete dissolution of all PIM components. The casting solution was then spread onto a glass plate using a casting knife with 0.5 mm depth setting [35]. The glass plate was covered with an aluminium tray to allow the slow evaporation of THF in the next 48 h after which the membrane was peeled from the glass plate.

Interference studies

The effect of common anions in appropriately selected concentration ranges (i.e., 0.15 mg L^{-1} – 140 mg L^{-1} in the case of $H_2PO_4^-$ and 1.0 mg L^{-1} – 40 mg L^{-1} in the case of NO_3^-, Cl^-, HCO_3^-, and SO_4^{2-}) on the analytical signal for a 0.05 mg L^{-1} (0.67 μmol L^{-1}) As(V) standard was studied.

Sample analysis

Spiked with arsenate at the μg L^{-1} level tap and mineral water samples were analysed by both the newly developed FA method and ICP-OES. The tap water was obtained from Melbourne's public water supply, and the commercial mineral waters analysed were: Voss Still Water (Norway), Woolworths Mountain Spring Water

(Australia) and Icelandic Spring Water (Iceland). All samples were analysed by the standard addition method, involving at least 3 standard additions, and the measurements were performed in triplicate (unless otherwise stated).

Results and discussion

Optimization of the FA system parameters

The optimization range and the initial and optimal values for each of the design and operational parameters of the newly developed FA system investigated in this study are summarized in Table 3.6 in the order in which the optimization was done. The initial value of a parameter was the value used in the experiments prior to the optimization of this parameter. The compositions of the Streams R1 (0.2 mmol L^{-1} $KMnO_4$ and 0.05 mol L^{-1} NaOH), R2 (0.5% (w/v) $NaBH_4$ and 0.05 mol L^{-1} NaOH) and R3 (4 M HCl + 1% KI (w/v) + 0.5% (w/v) ascorbic acid) were selected on the basis of the results obtained in an earlier study involving the determination of arsenic by a gas-diffusion/hydride generation approach [34]. To simplify the operation of the FA system, Streams R2, R3 and R4 were kept at the same flow rate of 0.12 mL min^{-1}.

Table 3.6 Optimization of the FA system for the determination of As(V).

Parameter	Range studied	Initial value	Optimal value
Reaction coil length (m)	0 – 3.00	2.50	0.25
Stream R1 flow rate (mL min^{-1})	0.06 – 0.46	0.24	0.06
Gas-diffusion membrane	Polypropylene		
	Durapore®		SureVent®
	SureVent®		
	PTFE		
PIM composition (% w/w)	70 PVC, 30 A336		
	70 PVC, 20 A336, 1 1-TD		70 PVDF-HFP, 30 A336
	70 PVDF-HFP, 30 A336		
[NaCl] in R4 (mol L^{-1})	0.05 – 0.2	0.1	0.1
Stream R5 flow rate (mL min^{-1})	0.2 – 3.0	0.2	2.5

Stop-flow time of the acceptor stream of the extraction cell (min)	2 – 30	25	15

A336 – Aliquat 336, 1-TD – 1-tetradecanol

Effect of the reaction coil length, flow rate of Stream R1 and type of the gas-diffusion membrane

As mentioned earlier, the influence of these parameters was studied in an FA system, similar to the one shown in Figure 3.4, where the extraction cell was replaced with an injection valve with a 500 μL sample loop.

The length of the reaction coil (RC, Figure 1), where Streams R3 and R4 were merged, was varied between 0 m (*i.e.*, no reaction coil) and 3 m. The RC length affected both the efficiency of mixing between the two streams mentioned above and the dispersion of arsenic in the donor stream of the GDC. As expected, a longer RC enhanced arsenic dispersion which offset any increase in the analytical signal due to better mixing between Streams R3 and R4. The highest analytical signal was obtained when the length of the RC was 0.25 m and this length of the RC was used in the subsequent experiments. The percentage of As(V) converted into As(III) under these experimental conditions was calculated as equal to 70%, by comparing the analytical signals for standards containing 1000 μg L^{-1} of either As(III) or As(V).

As expected, higher analytical signals were recorded when lower flow rates of Stream R1 were used due to the fact that arsine generated in the RC was transferred into a smaller volume of the $KMnO_4$ acceptor solution of Stream R1. Experiments involving stopping Stream R1 during arsine generation were also conducted but they resulted in unstable baseline due to the transfer of greater and irreproducible amounts of H_2 into the static $KMnO_4$ solution located in the acceptor channel of the GDC (Figure 3.4). In addition, no enhancement in the analytical signal was observed. Hence, 0.06 mL min^{-1} was selected as the optimal flow rate of Stream R1 since this was the lowest flow rate that could be reproducibly maintained by Peristaltic pump P1.

Four different hydrophobic microporous membranes (i.e., Durapore®, SureVent®, PTFE, and polypropylene membranes) were compared with respect to their permeability to arsine, estimated on the basis of the corresponding analytical signal values. In each case the two channels of the gas-diffusion cell were separated by two membrane layers and a filter paper disc sandwiched between them. When the Durapore®

membrane was tested a rapid formation of a brown stain on both membrane surfaces was observed due to manganese dioxide formation, and for this reason this membrane was discarded. The average analytical signals based on 10 replicate measurements of a 1000 μg L^{-1} As(V) standard for the remaining three membranes were 0.081 ± 0.004 for the polyprolylene membrane, 0.101 ± 0.004 for the PTFE membrane, and 0.102 ± 0.004 for the SureVent® membrane. Although no significant difference between the last two membranes was obtained, the baseline was not very stable when using the PTFE membrane, possibly due to its malleability. SureVent® membrane was selected for further use because it was slightly thicker and more robust than the PTFE membrane and no issues with baseline stability were observed.

Effect of the PIM and the compositions of Stream R4

Fontàs et al. [11], reported on the successful use of a PIM composed of the base polymer PVC and the carrier Aliquat 336 for the preconcentration of arsenate in groundwater samples. The optimal composition of this PIM, i.e., 70% (w/w) PVC and 30% (w/w) Aliquat 336, was determined in a previous study by the same research team [10]. In this and other studies [10,36] 0.1 M NaCl was found to be the most suitable receiving solution for arsenate. The separation of arsenate using an Aliquat 336-based PIM involves the extraction of the $HAsO_4^{2-}$ anion from the sample solution into the PIM, followed by the diffusion of the corresponding adduct of this anion with the quaternary alkylammonium cation of Aiquat 336 (A^+) across the membrane and the back-extraction of $HAsO_4^{2-}$ into the acceptor solution containing NaCl as the stripping reagent [10]. The equilibrium, described by Eq. (3.2), is shifted to the right (extraction into the PIM) at the sample solution/PIM interface and to the left (back-extraction into the acceptor solution) at the PIM/acceptor solution interface.

$$HAsO_4^{2-} + 2(A^+Cl^-)_{PIM} \leftrightarrows [(A^+)_2HAsO_4^{2-}]_{PIM} + 2Cl^- \qquad (3.2)$$

The PIM and the receiving solution, mentioned above, were initially used in the newly developed FA system for the on-line preconcentration of As(V). However, the analytical signals obtained in 3 consecutive measurements of a 1000 μg L^{-1} As(V) standard (0.09, 0.08, 0.03) were relatively low. The poor repeatability was most likely due to the leaching of the PIM liquid phase consisting of Aliquat 336 into the adjacent

aqueous phases. Therefore, other PIM compositions were explored.

One of them was the composition reported by Cho et al. [37] for the extraction of thiocyanate from weakly alkaline aqueous solutions which consisted of 20% (w/w) Aliquat 336, 10% (w/w) 1-tetradecanol and 70% (w/w) PVC. This study demonstrated that the addition of a modifier (e.g., 1-tetradecanol) of a very low water solubility reduced significantly the leaching of the PIM liquid phase. However, the analytical signal achieved with this PIM composition (i.e., 0.041, 0.017, 0.023), though higher than the one for the PIM composed of only 70% (w/w) PVC and 30% (w/w) Aliquat, also showed poor repeatability.

O'Bryan et al. [35] demonstrated that PVDF-HFP-based PIMs containing 30% (w/w) Aliquat 336 and 70% (w/w) PVDF-HFP exhibited a significantly higher extraction and back-extraction rates for thiocyanate and higher stability compared to PVC-based PIMs containing the same concentration of liquid phase. This PIM provided much higher analytical signal (i.e., 0.173, 0.173, 0.172) and excellent repeatability and therefore was used in the subsequent experiments.

The concentration of NaCl in Stream R4 was varied between 0.05 and 0.20 mol L^{-1}. As expected, the analytical signal increased with increasing the NaCl concentration up to 0.1 mol L^{-1} after which no further signal enhancement was observed. Therefore, 0.1 mol L^{-1} was selected as the optimal NaCl concentration in Stream R4.

Effect of the flow rate of Stream R5 and the stop-flow time for Stream R4

It can be expected that the analytical signal will depend heavily on both the flow rate of Stream R5 and the stop-flow time (i.e., duration of the sample flow through the extraction cell) because these two parameters determine the sample volume and its contact time with the PIM. The individual effects of these two parameters on the analytical signal are not independent of each other and for this reason their combined effect was studied and the results are presented in Figure 3.6. It was observed that, independently of the flow rate of Stream R5, the analytical signal increased rapidly with increasing the stop-flow time up to 15 min and then it started gradually to level off. Also, it was observed that independently of the stop-flow time, the analytical signal increased with increasing the flow rate of Stream R5 up to 2.5 mL min^{-1} after which it started decreasing. Therefore, 2.5 mL min^{-1} was selected as the optimal flow rate. The analytical signal did not increase significantly for stop-flow times greater than 15 min (e.g., an

increase in the stop-flow time from 15 to 25 min resulted in only 10% increase in the analytical signal) and this value was selected as the optimal stop-flow time.

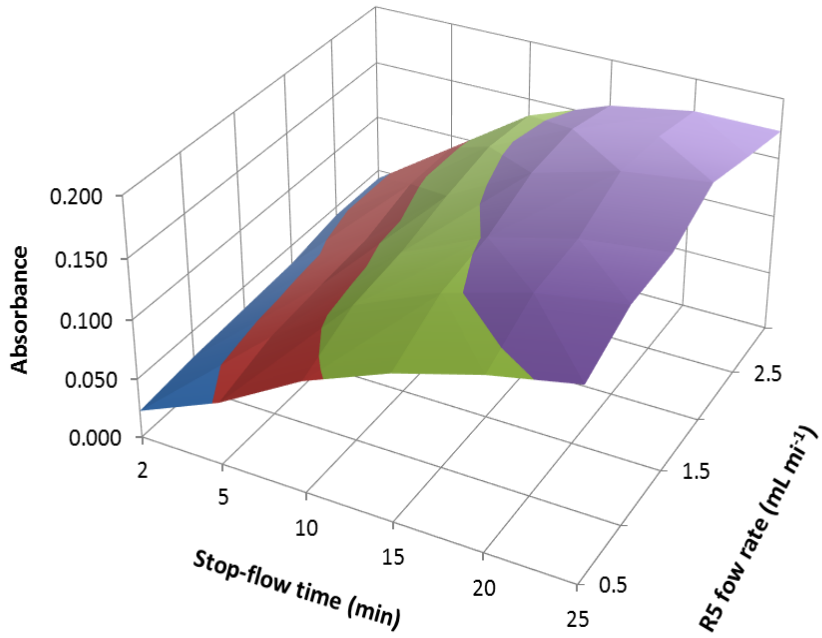

Figure 3.6 Influence of the stop-flow flow time and the flow rate of Stream R5 on the analytical signal for a 500 μg L^{-1} As(V) standard.

Interference studies

The presence of common anions in natural water (e.g., $H_2PO_4^-$, Cl^-, NO_3^-, HCO_3^-, and SO_4^{2-}) which can compete with the extraction of arsenate [11], makes it necessary to investigate their potential interference. No interference effects associated with these anions were expected in the arsine generation, trans-membrane transport and detection steps. Figure 3.7 shows the normalized analytical signal as a function of the logarithm of the concentration ratio between each one of the anions mentioned above and arsenate. The normalized analytical signal was calculated as a fraction of the analytical signal in the absence of interfering ions. Interference effects were observed only when the concentration of the interfering ions exceeded by 2 orders of magnitude the arsenate concentration (i.e., 50 μg L^{-1}). In the presence of significant interference effects, the standard addition method should be used.

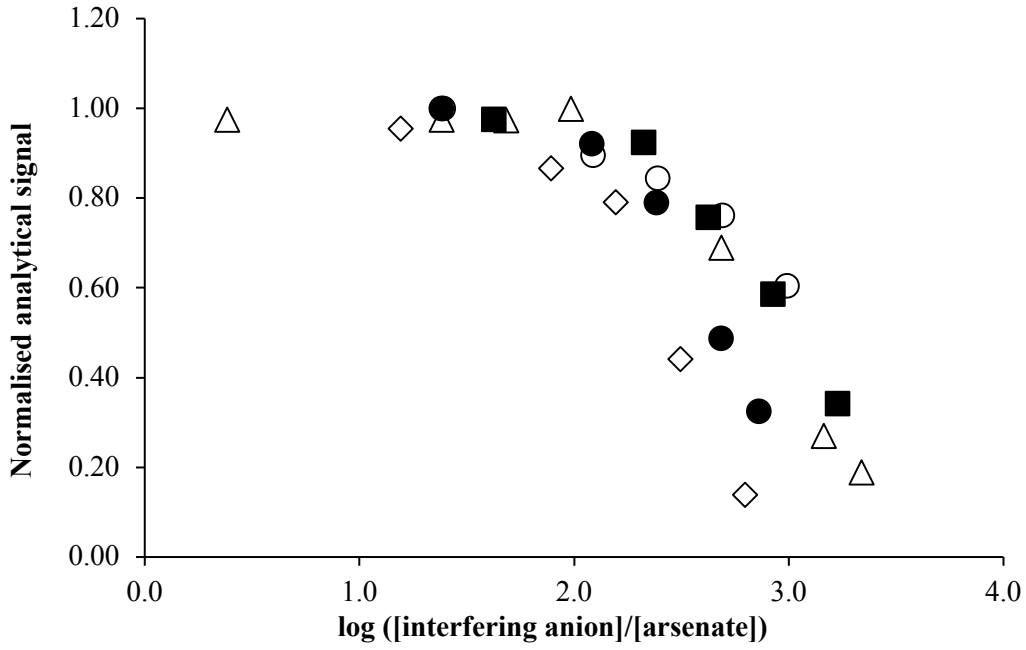

Figure 3.7 Effect of the concentration of $H_2PO_4^-$ (△), NO_3^- (●), SO_4^{2-} (◇), HCO_3^- (○), and Cl^- (■) on the normalised analytical signal for a 0.67 μmol L^{-1} (50 μg L^{-1}) As(V) standard.

Analytical figures of merit

Under optimal conditions (Table 3.6) the newly developed FA method is characterised by a linear range of 5.0-65 μg L^{-1} As(V) described by the following calibration equation: $A = (8.94\times10^{-4} \pm 1.77\times10^{-5}) \times C$ (R^2=0.998), based on 5 different As(V) standards, where A is the absorbance and *C* is the As(V) concentration in μg L^{-1}.

The method repeatability, expressed as the relative standard deviation (RSD) of 5 replicate measurements, was calculated as equal to 1.8% for 25 μg L^{-1} and 2.8% for 50 μg L^{-1} As(V), respectively. The limit of detection (LOD) of 3.0 μg L^{-1} was calculated as the analyte concentration corresponding to an analytical signal equal to the blank signal plus three standard deviations of the blank [38]. The sample solution was propelled for 15 min through the PIM extraction cell while the acceptor solution was stagnant, resulting in a sampling rate of 2.8^{-1}.

The newly developed FA method provides better sensitivity for the determination of As(V) than other spectrophotometric FA methods (e.g., 51 μg L^{-1} [18] and 21 μg L^{-1} [34]) and sensitivity comparable to that provided by FA methods utilizing bulky and expensive atomic optical detectors (e.g., atomic fluorescence detector - 0.61 μg L^{-1} [39] and atomic absorption detector – 0.5 μg L^{-1} [40].

Analysis of drinking water samples

As mentioned earlier, in most cases arsenic in drinking water consist almost entirely of As(V) [5,6] and therefore the newly developed method was validated by determining the As(V) concentration in 4 drinking water samples using the standard addition method (Table 3.7). The standard addition method was used instead of the calibration curve method because of the high concentrations of common anions relative to the As(V) concentration. All standard additions curves were characterised by excellent linearity ($R^2 \geq 0.997$) and the repeatability of the slopes of replicate samples (n=4) expressed as RSD was 5.6%. The As concentration in the spiked samples was also determined by HG-ICP-OES using the calibration curve method. There was no statistically significant difference at the 95% confidence level between the results obtained by both methods (Table 3.7).

Table 3.7 As(V) concentration in spiked drinking water samples determined by the newly developed FA method and HG-ICP-OES.

Sample	**Spiked As(V) concentration ($\mu g\ L^{-1}$)**	**Measured As(V) concentration ± SD ($\mu g\ L^{-1}$)**	
		FA (n=3)	HG-ICP-OES (n=3)
Tap water	6.0	6.5 ± 0.5	6.6 ± 0.4
	10.0	9.1 ± 0.7	10.5 ± 0.8
	15.0	14.0 ± 2.0*	15.8 ± 0.9
Voss mineral water	6.00	5.5 ± 0.5	6.4 ± 0.5
	10.0	10.0 ± 1.0*	10.5 ± 0.4
Spring mineral water	9.00	8.3 ± 0.8	9.4 ± 0.6
	20.0	21.0 ± 2.0*	21.6 ± 0.6
Icelandic mineral water	15.0	13.9 ± 0.9	13.7 ± 0.5
	25.0	22.0 ± 2.0*	25.0 ± 2.0

* experiments performed in duplicate

Conclusions

The hydride generation FA system for the determination of arsenate in drinking waters at low μg L^{-1} levels, developed as part of the current study, utilizes for the first time PIM-based on-line extractive separation of arsenate from the sample matrix which is subsequently reduced to arsine, detected spectrophotometrically after its on-line gas-diffusion separation. Under optimal conditions the FA system is characterized by an LOD of 3.0 μg L^{-1} and a repeatability, expressed as RSD, of 1.8% (n=5, 25 μg L^{-1}) and 2.8% (n=5, 50 μg L^{-1}). Lower limits of detection could be potentially achieved by using longer stop-flow times of the extraction cell acceptor solution, i.e., larger sample volumes. Common anions, such as phosphate, nitrate, sulphate, carbonate, and chloride, were found to interfere in the PIM-based separation process only at a concentrations 100 times higher than that of arsenate. The newly developed FA system allowed the accurate determination of arsenate in drinking water spiked with As(V) at the low μg L^{-1} level using the multi-point standard addition method. Since arsenic in most drinking waters is almost entirely composed of arsenate, it can be expected that the FA system, mentioned above, would be applicable for total arsenic determination of drinking water.

References

[1] I. Villaescusa, J.-C. Bollinger, Arsenic in drinking water: sources, occurrence and health effects (a review), Rev. Environ. Sci. Bio./Technol. 7 (2008) 307-323.

[2] R. Vera, C. Fontas, E. Antico, Titanium dioxide solid phase for inorganic species adsorption and determination: the case of arsenic, Environ. Sci. Pollut. Res. 24(12) (2017) 10939–10948.

[3] M. Bissen, F.H. Frimmel, Arsenic - A review. Part I: Occurrence, toxicity, speciation, mobility, Acta Hydrochim. Hydrobiol. 31 (2003) 9–18.

[4] World Health Organization (WHO). Guidelines for drinking-water quality, 4th ed, WHO, Geneva, 2011.

[5] S. Döker, M. Yılmaz, Speciation of Arsenic in Spring, Well, and Tap Water by High-performance Liquid Chromatography–Inductively Coupled Plasma–Mass Spectrometry, Anal. Lett. 51(1-2) (2018) 254–264.

[6] I. Komorowicz, D. Barałkiewicz, Determination of total arsenic and arsenic species in drinking water, surface water, wastewater, and snow from Wielkopolska, Kujawy-Pomerania, and Lower Silesia provinces, Poland, Environ. Monit. Assess 188 (2016) 504.

[7] V.N. Alves, T.S. Neri, S.S.O. Borges, D.C. Carvalho, N.M.M. Coelho, Determination of inorganic arsenic in natural waters after selective extraction using Moringa oleífera seeds, Ecological Engineering 106 (2017) 431-435.

[8] M.L. Susko, M.S. Bloom, I.A. Neamtiu, A.A. Appleton, S. Surdu, C. Pop, E.F. Fitzgerald, D. Anastasiu, E.S. Gurzau, Low-level arsenic exposure via drinking water consumption and female fecundity - A preliminary investigation, Environ. Res. 154 (2017) 120–125.

[9] G. Chen, B. Lai, X. Mao, T. Chen, M. Chen, Continuous Arsine Detection Using a Peltier-Effect Cryogenic Trap to Selectively Trap Methylated Arsines, Anal. Chem. 89 (2017) 8678–8682.

[10] R. Güell, E. Anticó, S.D. Kolev, J. Benavente, V. Salvadó, C. Fontàs, Development and characterization of polymer inclusion membranes for the separation and speciation of inorganic As species, J. Membr. Sci. 383 (2011) 88–95.

[11] C. Fontàs, R. Vera, A. Batalla, S.D. Kolev, E. Anticó, A novel low-cost detection method for screening of arsenic in groundwater, Environ. Sci. Pollut. Res. 21 (2013) 11682–8.

[12] M. Valcarcel, M.D. Luque de Castro, Flow-Injection Analysis: Principles and Applications, Ellis Horwood, Chichester, 1987.

[13] V. Cerda, J.M. Estela, On-line sample pretreatment: dissolution and digestion, in: S.D. Kolev, I.D. McKelvie (Eds.), Advances in Flow Injection Analysis and Related Techniques, Elsevier, Amsterdam, 2008, pp. 129–158.

[14] A.G. Fogg, N.K. Bsebsu, Differential-pulse voltammetric determination of phosphate as molybdovanadophosphate at a glassy carbon electrode and assessment of eluents for the flow injection voltammetric determination of phosphate, silicate, arsenate and germanate, Analyst 106(1269) (1981) 1288–

1295.

[15] J.R. Farrell, P.J. Iles, Y.J. Yuan, Determination of arsenic by hydride generation gas diffusion flow injection analysis with electrochemical detection, Anal. Chim. Acta 334 (1996) 193–197.

[16] T. Rupasinghe, T.J. Cardwell, R.W. Cattrall, S.D. Kolev, Determination of arsenic in industrial samples by pervaporation flow injection with amperometric detection, Anal. Chim. Acta 652 (2009) 266–271.

[17] C. Lomonte, M. Currell, R.J.S. Morrison, I.D. McKelvie, S.D. Kolev, Sensitive and ultra-fast determination of arsenic(III) by gas-diffusion flow injection analysis with chemiluminescence detection, Anal. Chim. Acta 583 (2007) 72–77.

[18] W. Boonjob, M. Miró, S.D. Kolev, On-line speciation analysis of inorganic arsenic in complex environmental aqueous samples by pervaporation sequential injection analysis, Talanta 117 (2013) 8–13.

[19] T. Rupasinghe, T.J. Cardwell, R.W. Cattrall, I.D. Potter, S.D. Kolev, Determination of arsenic by pervaporation-flow injection hydride generation and permanganate spectrophotometric detection, Anal. Chim. Acta 510 (2004) 225–230.

[20] T. Rupasinghe, T.J. Cardwell, R.W. Cattrall, M.D. Luque de Castro, S.D. Kolev, Pervaporation-flow injection determination of arsenic based on hydride generation and the molybdenum blue reaction, Anal. Chim. Acta 445 (2001) 229–238.

[21] D.L. Johnson, M.E.Q. Pilson, Spectrophotometric determination of arsenite, arsenate, and phosphate in natural waters, Anal. Chim. Acta 58 (1972) 289–299.

[22] W. Frenzel, F. Titzenthaler, S. Elbel, Selective determination of arsenite by flow injection spectrophotometry, Talanta 41 (1994) 1965–1971.

[23] Y. Narusawa, Flow-injection spectrophotometric determination of silicate, phosphate and arsenate with on-line column separation, Anal. Chim. Acta 204 (1988) 53–62.

[24] R.K. Dhar, Y. Zheng, J. Rubenstone, A. Van Geen, A rapid colorimetric method

for measuring arsenic concentrations in groundwater, Anal. Chim. Acta 526 (2004) 203–209.

[25] K. Toda, T. Ohba, Highly Sensitive Flow Analysis of Trace Level Arsenic in Water Based on Vaporization-collection In-line Preconcentration, Chem. Lett. 34 (2005) 176–177.

[26] M.A. Kamyabi, A. Aghaei, Electromembrane extraction and spectrophotometric determination of As(V) in water samples, Food Chem. 212 (2016) 65–71.

[27] M.I.G.S. Almeida, R.W. Cattrall, S.D. Kolev, Polymer inclusion membranes (PIMs) in chemical analysis - A review, Anal. Chim. Acta 987 (2017) 1–14.

[28] M.I.G.S. Almeida, R.W. Cattrall, S.D. Kolev, Recent trends in extraction and transport of metal ions using polymer inclusion membranes (PIMs), J. Membr. Sci. 415–416 (2012) 9–23.

[29] L.D. Nghiem, P. Mornane, I.D. Potter, J.M. Perera, R.W. Cattrall, S.D. Kolev, Extraction and transport of metal ions and small organic compounds using polymer inclusion membranes (PIMs), J. Membr. Sci. 281 (2006) 7–41.

[30] L.L. Zhang, R.W. Cattrall, M. Ashokkumar, S.D. Kolev, On-line extractive separation in flow injection analysis based on polymer inclusion membranes : A study on membrane stability and approaches for improving membrane permeability, Talanta 97 (2012) 382–387.

[31] L.L. Zhang, R.W. Cattrall, S.D. Kolev, The use of a polymer inclusion membrane in flow injection analysis for the on-line separation and determination of zinc, Talanta 84 (2011) 1278–1283.

[32] E.A. Nagul, C. Fontàs, I.D. McKelvie, R.W. Cattrall, S.D. Kolev, The use of a polymer inclusion membrane for separation and preconcentration of orthophosphate in flow analysis, Anal. Chim. Acta 803 (2013) 82–90.

[33] M.R. Yaftian, M.I.G.S. Almeida, R.W. Cattrall, S.D. Kolev, Flow injection spectrophotometric determination of V(V) involving on-line separation using a poly(vinylidene fluoride-co-hexafluoropropylene)-based polymer inclusion membrane, Talanta 181 (2018) 385–391.

[34] Y. Zhang, M. Miró, S.D. Kolev, Hybrid flow system for automatic dynamic fractionation and speciation of inorganic arsenic in environmental solids, Environ. Sci. Technol. 49 (2015) 2733–2740.

[35] Y. O'Bryan, R.W. Cattrall, Y.B. Truong, I.L. Kyratzis, S.D. Kolev, The use of poly(vinylidenefluoride-co-hexafluoropropylene) for the preparation of polymer inclusion membranes. Application to the extraction of thiocyanate, J. Membr. Sci. 510 (2016) 481–488.

[36] R. Güell, C. Fontàs, E. Anticó, V. Salvadó, J.G. Crespo, S. Velizarov, Transport and separation of arsenate and arsenite from aqueous media by supported liquid and anion-exchange membranes, Sep. Purif. Technol. 80 (2011) 428–434.

[37] Y. Cho, C. Xu, R.W. Cattrall, S.D. Kolev, A polymer inclusion membrane for extracting thiocyanate from weakly alkaline solutions, J. Membr. Sci. 367 (2011) 85–90.

[38] J.C. Miller, J.N. Miller, Statistics and chemometrics for Analytical Chemistry, Pearson Education Limited, Harlow, Essex England, 2010.

[39] A. Caballo-Lopez, M.D. Luque de Castro, Hydride generation-pervaporation-atomic fluorescence detection prior to speciation analysis of arsenic in dirty samples, J. Anal. At. Spectrom. 17 (2002) 1363–1367.

[40] Y. Zhang, S.B. Adeloju, Flow injection-hydride generation atomic absorption spectrometric determination of selenium, arsenic and bismuth, Talanta 76(4) (2008) 724-730.

3.1.3 Titanium dioxide solid phase for inorganic species adsorption and determination: the case of arsenic

Abstract

We have evaluated a new titanium dioxide (Adsorbsia As600) for the adsorption of both inorganic As(V) and As(III) species. In order to characterize the sorbent, batch experiments were undertaken to determine the capacities of As(III) and As(V) at pH 7.3, which were found to be 0.21 and 0.14 mmol g^{-1}, respectively. Elution of adsorbed species was only possible using basic solutions, and arsenic desorbed under batch conditions was 50% when 60 mg of loaded titanium dioxide was treated with 0.5 M NaOH solution. Moreover, its use as a sorbent for solid-phase extraction and preconcentration of arsenic species from well waters has been investigated, without any previous pretreatment of the sample. Solid-phase extraction was implemented by packing several minicolumns with Adsorbsia As600. The method has been validated showing good accuracy and precision. Acceptable recoveries were obtained when spiked waters at 100–200 μg L^{-1} were measured. The presence of major anions commonly found in waters did not affect arsenic adsoption, and only silicate at 100 mg L^{-1} level severely competed with arsenic species to bind to the material. Finally, the measured concentrations in water samples containing arsenic from the Pyrinees (Catalonia, Spain) showed good agreement with the ICP-MS results.

Introduction

Arsenic is an element found in the earth's crust. Its concentration in most rocks ranges from 0.5 to 2.5 mg/kg, though higher concentrations are found in finer-grained argillaceous sediments and phosphorites [1]. Arsenic is mobilized by natural weathering reactions, biological activity, geochemical reactions, volcanic emissions and other anthropogenic activities. Moreover, it was commonly used as part of the formulation of different pesticides used in agriculture [2]. Its occurrence in groundwater has been reported mainly in Bangladesh, China, India, Chile, Argentina, Mexico, Taiwan, Vietnam, and the USA, but also in several regions of Europe [3]. Arsenic is recognized to be carcinogenic and long-term drinking water exposure causes pigmentation changes,

skin thickening, neurological disorders, muscular weakness, loss of appetite, and nausea [4]. For this reason, the World Health Organization (WHO) fixed a limit concentration of arsenic in drinking waters at 10 μg L^{-1} [5]. From the chemical point of view, arsenic in waters can be encountered as inorganic or organic species and also in different oxidation states, e.g. As(V) and the more toxic As(III). Under reducing conditions, As(III) is prevalent while As(V) is the major species present under oxidizing atmospheres [3].

Due to the great toxicity of arsenic and the low levels that are permitted in drinking water, it has become necessary to develop highly sensitive methods for its monitoring. Besides atomic fluorescence spectroscopy (AFS), graphite furnace atomic absorption (GFAAS), hydride generation atomic absorption (HGAAS), and inductively coupled plasma-mass spectrometry (ICP-MS) [6,7], which require significant investment and trained personnel, simpler methodologies such as colorimetry can be employed [8], which are usually preceded by a preconcentration step. Solvent extraction and sorption on solid supports [9,10] are a good alternative for arsenic preconcentration. The affinity of As(V) to adsorb on solid phases has been well documented for removal purposes [11]. High elimination efficiency is obtained using iron oxides or zero-valent iron [12,13], modified calcinated bauxite [14], hydrotalcite [15], and titanium dioxide [16-20] among others. In fact, the arsenic removal from groundwater for drinking purposes is mainly based on such adsorption phases.

The behaviour of titanium dioxide (TiO_2) as a photocatalyst and for arsenic removal has been extensively reviewed by Guan et al. [21]. It has been applied in different forms, such as nanocrystalline particles, nanotubes, hydrous and granular, impregnated in chitosan beads, and based bimetal adsorbents. The authors discuss the capability of TiO_2 to oxidize As(III) to As(V), emphasizing the key role of crystal morphology and specific surface area to ensure an efficient removal of arsenic from water. Adsorption capacities at pH 7 ranging from 83 to 2.05 mg g^{-1} (1.094 to 0.027 mmol g^{-1}) were reported for hydrous TiO_2 (anatase) and TiO_2 impregnated in chitosan beads, respectively [21].

For analytical purposes, different solid phases have been suggested to preconcentrate arsenic, including the use of ion exchangers and chemically functionalized sorbents. Ion exchangers and aluminosilicate disposable cartridges have been exploited for field speciation of arsenic contemplating the pH dependence of arsenic species to enable selective preconcentration. The procedure employed consists of the selective retention of As(V) when a volume of water sample is passed through the disposable cartridge. The analysis of the filtered sample allows the As(III) concentration to be

determined, while total arsenic is determined from an independent non-filtered sample [22,23] or through a previous oxidation/reduction step [24,25]. Additionally, anion and cation exchangers have also been successfully applied for the speciation of organic and inorganic arsenic [26].

Ordered mesoporous silica modified with 3-(2-aminoethylamino) propyltrimethoxysilane [27] and CTAB-modified alkyl silica [28] has also been employed for arsenic preconcentration. The formation of arsenic complexes that are later entrapped in a solid sorbent has been exploited by Pozebon et al. [29]. In their research, ammonium diethyl dithiophosphate was used for the complexation of As(III) and a C-18 bonded silica gel microcolumn was used for the sorption; As(V) was then determined after being reduced using potassium iodide together with ascorbic acid. Other approaches are based on the preconcentration and separation of arsenic species in a knotted reactor coupled to hydride generation atomic fluorescence spectrometry [30].

The reported use of TiO_2 with or without modifiers for analytical purposes is, to the best of our knowledge, limited to Chen et al. [31], Huang et al. [32] and Liang and Liu [33]. Chen et al. [31] use a PTFE microcolumn filled with TiO_2 nanotubes for the speciation of inorganic arsenic in environmental water samples by ICP-MS. In Huang et al. [32], dimercaptosuccinic acid-modified TiO_2 and inductively coupled plasma optical emission spectrometry is used for the online separation of arsenic species. The detection limit (LOD) reached for the offline mode is rather low (0.1 μg L^{-1}) due to the higher enrichment factor (50), and speciation is accomplished by choosing the most appropriate working pH. Liang et al. have reported the speciation analysis of inorganic arsenic in water samples by using a nanometre TiO_2 immobilized on silica gel and graphite furnace atomic absorption spectrometry [33]. Only As(III) could be adsorbed quantitatively on the sorbent in the 9.5– 10.5 pH range. The LOD is 24 ng L^{-1} with an enrichment factor of 50. The present research aimed to investigate the use of Adsorbsia As600, a commercial-grade TiO_2, as an adsorbent for arsenic in analytical applications. The solid can be easily obtained and it has been fully characterized for the adsorption and preconcentration of arsenic species prior to their determination using ICP-OES. The analytical parameters and the application of the designed system to the determination of arsenic in well waters are shown.

Experimental

Reagents and solutions

Stock solutions (100 mg L^{-1}) of As(V) and As(III) were prepared from $Na_2HAsO_4 \cdot 7H_2O$ (Merck) and $NaAsO_2$ (Fluka) solids, respectively. Solutions of As(V) in ultrapure water were prepared by dilution of the corresponding stock solutions and the resulting pH was 7.3. However, to obtain this pH in the case of As(III), acidification with HCl was required. Sodium hydroxide (Panreac) was used to prepare the elution solution. Calibration standards of As were prepared using the Spectrascan standard solution for atomic spectroscopy (Teknolab). All reagents and solvents were of analytical reagent grade and distilled water was purified through a Milli-Q Plus system (Millipore).

Commercial TiO_2 Adsorbsia As600 was purchased from the manufacturer (Dow). This sorbent is designed as a single-use adsorbent for the treatment of drinking water. It is selective for oxyanions such as arsenate, chromate and selenite, but it also shows a strong affinity for lead and other heavy metals. According to the information supplied, the material consists of granulated TiO_2 media with particle size ranging from 250 to 1180 μm and a specific surface area of 250 $m^2\ g^{-1}$. The solid was cleaned with high purity water and air-dried before being used, and only particles with a particle size from 500 to 900 μm were selected.

Instruments

A sequential inductively coupled plasma atomic emission spectrometer (Liberty RL, Varian, Mulgrave, Vic., Australia) was used to determine the total concentration of As in the aqueous solutions at λ = 228 nm. The detection limit in 0.1 M NaCl medium was 300 μg L^{-1} of As.

A quadrupole-based ICP-MS system (Agilent 7500c, Agilent Technologies, Tokyo, Japan) equipped with an octopole collision reaction cell was used for arsenic determination in natural water samples. The isotope ^{75}As was selected and special conditions in the reaction cell (3 mL min^{-1} H_2 + 0.5 mL min^{-1} He) were employed to avoid spectral interferences due to the presence of chloride in water samples. The anionic composition of the water samples was determined by an ion chromatograph (IC) DIONEX IC5000 equipped with an autosampler AS-AP, a conductivity detector, and an IonPac® AS18 anion-exchange column (4 × 250 mm) with the AG Guard column (4 ×

50 mm).

X-ray diffraction measurement was performed on a Bruker D8Advance equipment using Cu Kalpha radiation, in transmission mode. X-ray fluorescence (XRF) spectra were obtained with a Bruker S2Ranger, equipped with a Pd tube and Spectra EDX software.

Isoelectric point measurements were performed dispersing the sample (previously grinded to a particle size <100 μm) in water (0.1% w/v) and modifying its pH by adding small volumes of HCl and NaOH solutions. At each pH point, the zeta potential of the sample was measured using the ZetaSizer Nano ZS (Malvern Instruments).

The pH and conductivity values of the water samples were determined with a Crison Model GLP 22 pH meter and an Ecoscan portable conductometer (Entech Instruments), respectively.

A Gilson peristaltic pump (Pacisa, Barcelona, Spain) was used to load the arsenic solutions into the minicolumn.

A rotary mixer (Labinco) was used in experiments where rotatory agitation was necessary.

Determination of the capacity of the adsorbent

Batch experiments

To evaluate the capacity of Adsorbsia As600 following a batch procedure, 20 mL of As solution (10 mg L^{-1}) was contacted with 0.06 g of the sorbent at different predetermined times (1 h for As(V) and 24 h for As(III)) in stoppered glass tubes. The mixture was filtered and the solution was analysed to determine the arsenic concentration in the filtrate. This process was repeated by using fresh solution until saturation was reached.

Flow experiments

Two types of packed columns were prepared depending on the purpose. For determining breakthrough curves, the solid granules (0.2 g or 0.8 g) were packed in a glass column with 0.6 cm *i.d.* A solution containing 20 mg L^{-1} As(V) at the working pH was pumped through the column at a flow rate of 1 mL min^{-1}. The arsenic concentration

in the effluent was continuously monitored to obtain the breakthrough curves. For preconcentration purposes, 60 mg of Adsorbsia As600 was packed into a self-made minicolumn consisting of a micropipette tip, plugged with a small portion of glass wool at both ends, and then connected to a flow system. The amount of sorbent in the minicolumn took into account the capacity of Adsorbsia As600 towards As(V) and As(III). This amount is similar to the amount of solid phase in commercial ion exchange cartridges [34]. In this case, 0.5 and 1 mL min^{-1} were tested as flow rates.

Selecting the elution conditions

The elution of adsorbed As(V) and As(III) was studied under batch and flow conditions. Considering previously reported results, HCl, NaCl and NaOH solutions were tested as elutant in batch mode [31,35,36]. For batch experiments, the loaded sorbent (0.1 g) was contacted with 20 mL of the tested solution to evaluate the percentage of As(V) and As(III) eluted, with a contact time of 24 h.

Elution under flow conditions with the sorbent packed in the glass column was also investigated, for which 0.2 g of loaded sorbent was contacted with 0.1 M NaOH solution at 1 mL min^{-1}, and the arsenic concentration in the effluent was continuously monitored. Elution curves were then plotted using these data.

For the elution of arsenic loaded in the 60-mg minicolumn, 2–4 mL of 0.5M NaOH solution was used at a flow rate of 0.5 and 1 mL min^{-1}.

Interference from major ions

Competitive experiments were designed with samples containing nitrate, sulphate, chloride, hydrogen carbonate, phosphate and silicate at the highest concentration level found in the non-contaminated natural water samples. Fifty millilitres of spiked water was used containing 200 μg L^{-1} As(V) at pH 7.3, percolated trough the Adsorbsia As600 minicolumn, and elution was performed with 2 mL of 0.5 M NaOH solution. Both loading and elution flow rate were 1 mL min^{-1}.

Calibration curve and method validation

Solutions (50 mL) containing As in ultrapure water at different concentrations from 50 to 500 μg L^{-1} were passed through the minicolumn at a flow rate of 1 mL min^{-1}. The loaded As was eluted with 2 mL of 0.5 M NaOH solution and ICP-OES signal intensity was measured. A calibration curve was obtained by plotting the signal intensity vs. the arsenic content in the ultrapure water solutions.

The method was validated by checking the linearity in the selected working range, the limit of detection, the repeatability (n=3), and also by performing recovery experiments at a concentration level of 200 μg L^{-1} of both As(V) and As(III). The limit of detection of the method was calculated as the concentration giving a signal equal to the intercept of the calibration curve plus three times the standard deviation of the intercept [37], under the final experimental conditions.

Water Samples

Water samples containing naturally occurring arsenic and others without arsenic were collected in the north of Catalonia (Spain). The samples were analysed and their composition is given in Table 3.8. Three different wells at both Lles and Setcases, villages in the foothills of the Pyrenees, were sampled. At Caldes, the water was collected from a hot spring. Unless otherwise stated, 50 mL of water samples were percolated trough the Adsorbsia As600 minicolumn, then eluted with 2 mL of 0.5 M NaOH solution and finally, the arsenic signal was measured. The amount of arsenic in the samples was obtained by interpolating the intensity value in the experimental calibration plot.

All experiments were at least performed in duplicate. The temperature was kept within the range 22 ± 2 °C.

Table 3.8 Characteristics of the water samples used for this study.

Sample	Conductivity	pH	Si	Cl	SO_4^{2-}	NO_3^-	HCO_3^-	As (μg L^{-1})[a]
S1_Pujarnol	527	8.37	5.7	15.4	63.8	1.8	268.5	nd
S2_Setcases	110	7.56	5.7	0.9	8.0	3.3	811.3	nd
S3_Caldes	3450	7.14	34.5	569.9	41	<LOQ	2037.3	59
S4_Lles	164	8.6	21.2	2.8	13.6	2.1	139.7	80

Concentrations are given in mg L^{-1}, except for As, which is in μg L^{-1}. Conductivity is in μS cm^{-1}

nd not detected

[a]Determined with ICP-MS under the conditions specified in the text

Results and discussion

Fundamentals and sorption capacity of Adsorbsia As600

In this study, we have analysed the adsorption of inorganic arsenic species present in water samples using Adsorbsia As600, a commercial-grade TiO_2. The chemical composition of the material was investigated by means of X-ray diffraction (XRD) and XRF. XRD data showed that the granules are made of TiO_2 in the crystalline form of anatase and that they also contain a small proportion of gypsum. With respect to the size, the granules are aggregates of nanocrystals of 7-nm average size according to the results of the calculation made using the peak width and the Debye-Scherrer equation [38]. XRF gave semiquantitative data on the elemental composition of the adsorbent: 91.9% of TiO_2, 4.25% of SO_3, and 3.05% of CaO were found. Zeta potential measurements revealed that the isoelectric point of the adsorbent was around 5.8–6.

The mechanism of the interaction of As(V) and As(III) with TiO_2 has been investigated by several authors. Jegadeesan et al. [39] used extended X-ray absorption fine structure (EXAFS) and X-ray absorption near-edge structure (XANES) to determine that As(V) and As(III) form bidentate inner-sphere complexes with amorphous TiO_2 at neutral pH. Pena et al. [40] and Jing et al. [41] have reported bidentate binuclear complexes for As(V) adsorption on nanocrystalline TiO_2 and on granular TiO_2. Moreover, Jing et al. [42] employed the CD-MUSIC modelling to describe the inorganic As adsorption on TiO_2. The model emphasizes the importance of the surface complex

structure and of the charge distribution at the interface.

Inorganic arsenic species in the aqueous solution are neutral or anionic, according to the corresponding pKa values and the pH of the sample [2]. At the pH range of the tested water samples, $H_2AsO_4^-$, $HAsO_4^{2-}$ and H_3AsO_3 are the predominant species while the primary anatase nanoparticles include the neutral species $TiOH^0$ and the negatively charged TiO^-. Then, the formation of the following bidentate complexes has been postulated [21]:

$$2\ TiOH + H_2AsO_4^- \leftrightarrow [(TiO)_2\ldots.AsO_4]^- + 2\ H_2O$$

$$2\ TiOH + HAsO_4^{2-} \leftrightarrow [(TiO)_2\ldots.AsO_4]^- + H_2O + OH^-$$

$$2\ TiOH + H_3AsO_3 \leftrightarrow [(TiO)_2\ldots.AsO_3]^- + 2\ H_2O + H^+$$

Whether As(III) is oxidized to As(V) or not, when adsorbed on TiO_2, is still an issue not fully understood and different opinions have been reported [16,41,43].

We have investigated the experimental capacity of Adsorbsia As600 for arsenic species under batch conditions. A value of 0.14 mmol g^{-1} (10.1 mg g^{-1}) and 0.21 mmol g^{-1} (16.5 mg g^{-1}) at pH 7.3 was obtained for As(V) and As(III), respectively. These values agree with those reported in the literature (see Table 3.9) for a similar working pH and taking into account the particle size and the specific surface area [39,40,43,44]. Moreover, the fact that TiO_2 solid phase is efficient for both the retention of As(V) and As(III) at pH 7.3 gives it a clear advantage over sorbents based on an ion exchange mechanism, in which only species present as anions can interact with the solid phase [45].

In addition, we could observe from these experiments that the complete removal of the arsenic species was accomplished in less than 2 h.

The capacity under flow conditions (flow rate 1 mL min^{-1}) was also investigated and the breakthrough curves we obtained are shown in Figure 3.8. It can be observed in Figure 3.8a, b that breakthrough volumes are reached very early for As(V) and As(III) (9 and 13 mL, respectively), and in both cases, the concentration of arsenic in the effluent increases linearly with the volume of solution. Similar curve shapes are shown in the work of Zeng et al. [46], and they explain this behaviour as arsenic removal being mass transport-limited. In Figure 3.8c,when the amount of Adsorbsia As600 is increased until 0.8 g, a breakthrough volume of about 100 mL is obtained. The increase of breakthrough volume is explained by the increase in the surface area providing more binding sites. It is also worth mentioning that the stoichiometric capacity of the column was not reached in any of the cases.

Table 3.9 Arsenic adsorption capacity by TiO_2 based materials.

Crystal morphology	Properties			Adsorption capacity (C)		Reference
	Particle size (nm)	Specific surface area (m^2g^{-1})	pHpzc	Cmax (mg g^{-1})	Experimental conditions	
Nanocrystaline	6	330	5.8	As(V), >36.5	pH 7.0, T=21-25 ºC	[40]
				As(III), >36.5	pH 7.0, T=21-25 ºC	
Amorphous		409	4.5	As(V), 19.0[a]	pH 7.0	[39]
				As(III), 66.8[a]	pH 7.0	
Anatase	10.5	141.3	NA	As(V), 18.0[a]	pH 7.0	[44]
				As(III), 15.1[a]	pH 7.0	
Rutile and anatase	30-50	15.63	6.3	As(III), 6.32[a]	pH 7.0, T=25 ºC	[43]
Titanate nanotubes	13	312.59	4.8	As(III), 59.5[a]	pH 7.0, T = 25 ºC	[43]
Anatase	7	250	5.8-6	As(V), 10.1	pH 7.3	This work
				As(III), 16.5	pH 7.3	

[a] Maximum capacity calculated from Langmuir isotherm

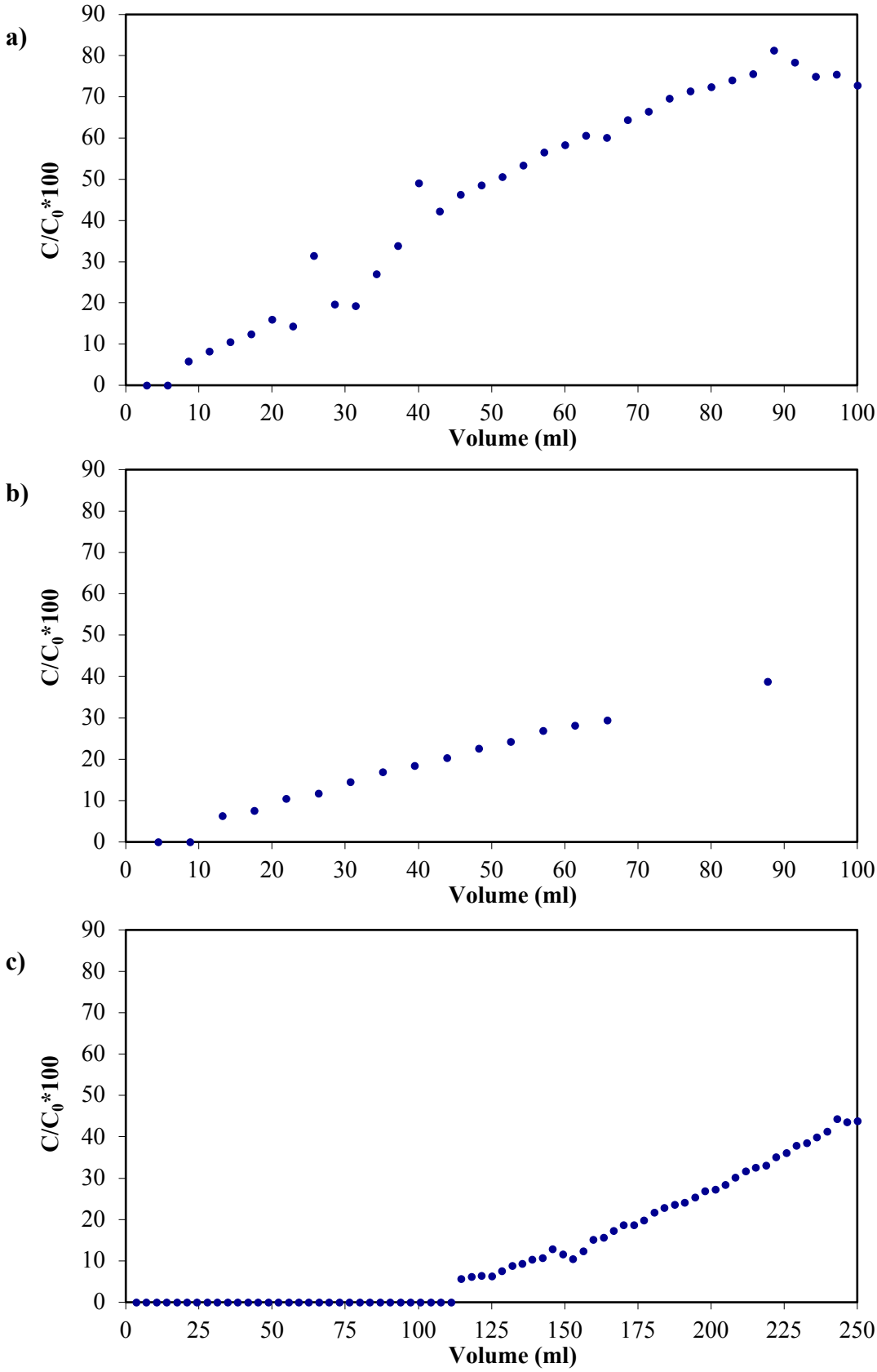

Figure 3.8 Breakthrough curves obtained for Adsorbsia As600 when a solution containing 20 mg L^{-1} of arsenic was pumped through the column. (a) As(V), 0.2 g of adsorbent; (b) As(III), 0.2 g

of adsorbent; (c) As(V), 0.8 g of adsorbent. Flow rate 1 mL min^{-1}. C is the concentration of arsenic in the effluent measured with ICP-OES; Co is the concentration of the feed solution (20 mg L^{-1}).

Elution experiments

From the different elutants, we observed that only NaOH solutions allow the recovery of loaded arsenic with recoveries of 44 and 87% with 0.1 and 1 M NaOH, respectively. The same percentage of elution was achieved for As(V) as well as for As(III). However, the collected solution presented a slight turbidity when 1 M NaOH was used, indicating that the strong base solution probably damages the solid. It is worth mentioning that for As(V) and 0.1 M NaOH recovery after 1 h is about 80% of the total arsenic recovered after 24 h. However, for As(III), this percentage is lower at about 50%.

The elution curve obtained under flow conditions (flow rate 1 mL min^{-1}) is shown in Figure 3.9. From the cumulative elution data, it can be calculated that only about 60% of As(V) is recovered after a volume of 100 mL of 0.1 M NaOH is passed through the loaded sorbent. This percentage decreases until 30% for a volume of 10 mL. In Figure 3.9, it can be seen that the maximum concentration in the elution solution was reached for a volume of about 7 mL, and that at this point, the value C/Co takes a value of 1.8 (Co is the initial concentration, 20 mg L^{-1}). A similar elution profile, not shown here, was found for As(III).

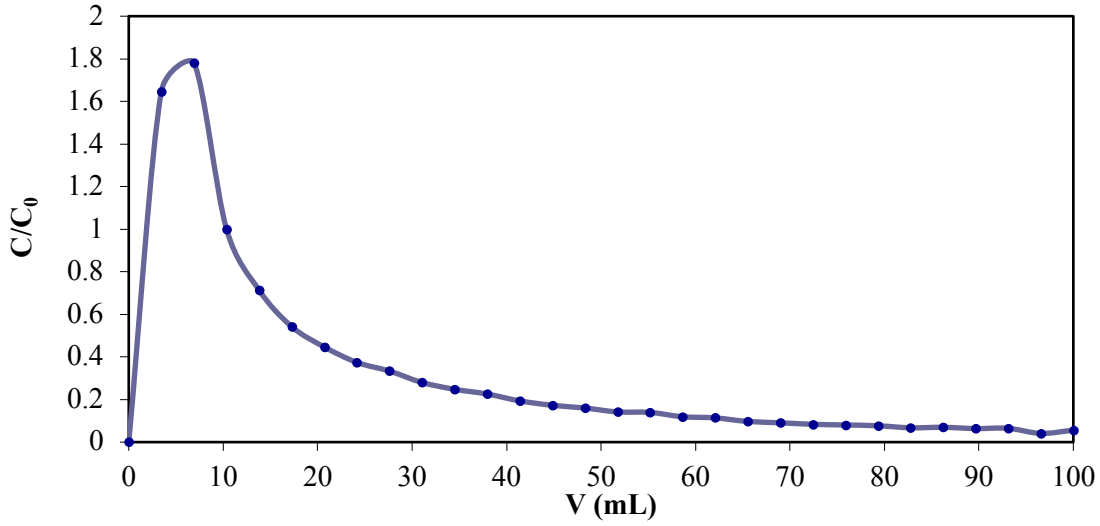

Figure 3.9 Elution isoplane for As(V) loaded Adsorbsia As600 sorbent (0.2 g). NaOH solution (0.1 M) was used for the elution and the flow rate was 1mL min^{-1}. C is the concentration of

arsenic in the effluent measured with ICP-OES; Co is the concentration of the feed solution used for loading the sorbent (20 mg L^{-1}).

The fact that the recovery is not quantitative and that the desorption kinetics are slow are clear drawbacks of this adsorbent when its use is intended for analytical purposes. In order to improve the results, we tested 0.5 M NaOH as an intermediate solution for both As(V) and As(III). In this case, an elution efficiency of 51% was obtained after 1 h contact time under batch conditions. This intermediate concentration was chosen as a compromise for further experiments.

Preconcentration with a minicolumn filled with Adsorbsia As600: the effect of eluent volume and flow rate

The influence of eluent volume and flow rate was studied by pumping 50 mL of 200 μg L^{-1} As(V) through the solid at a flow rate of 1mL min^{-1}. Under these conditions, all the arsenic was retained in the TiO_2 phase. After that, 2 and 4 mL of 0.5M NaOH were pumped through the solid and we obtained a percentage of arsenic eluted of 27 and 40%, respectively. These values are much lower than those obtained under batch conditions, which may be explained by the flow conditions affecting the contact between the loaded sorbent and the NaOH solution. In spite of the higher percentage of arsenic eluted with 4 mL, 2 mL was selected for further experiments in order to avoid sample dilution and to obtain a higher enrichment factor.

Similar experiments were performed for As(III) and we observed that, for this species, the percentage of arsenic eluted was only 13% (see Table 3.10). In order to improve this value, the effect of flow rate was studied and we observed that when the loading flow rate was decreased to 0.5 mL min^{-1}, improvement was obtained neither for As(V) nor for As(III). However, when the elution was evaluated at 0.5 mL min^{-1}, the percentage of As(III) eluted increased to 28%, indicating that this is a critical parameter especially for As(III).

Table 3.10 Influence of elution flow rate: concentration of arsenic in the elution solution (n=2). Standard deviation given in brackets.

Flow rate	Theoretical[a] (mg L^{-1})	Found[b] (mg L^{-1})
As(V)		
1 mL min^{-1}	5	1.4 (0.2)
0.5 mL min^{-1}	5	1.26 (0.09)
As(III)		
1 mL min^{-1}	5	0.64 (0.10)
0.5 mL min^{-1}	5	1.29 (0.20)

Spiked ultrapure sample (50 mL) containing 0.2 mg L^{-1} As(V) or As(III)

[a] The theoretical value is taken as the expected value in the 2 mL 0.5 M NaOH solution used for elution, assuming an elution efficiency of 100%

[b] The found value is that measured with ICP-OES directly in the 2 mL 0.5 M NaOH solution used for elution

Interference from the anions presents in water samples

The composition of water samples, in particular the presence of other ions, is of paramount importance for preconcentration purposes when the columns have a limited amount of solid phase. In particular, interference due to major anions is a limiting parameter when anion exchangers, in particular commercial cartridges, are intended to be used. For this reason, As(V) preconcentration was evaluated in the presence of the major anions commonly found in waters. The results for the percentage of arsenic eluted are presented in Figure 3.10, and the comparison with ultrapure water without anions can also be observed.

The percentage of arsenic eluted for the TiO_2 sorbent (60 mg) remains constant when 50 mg L^{-1} nitrate, 100 mg L^{-1} sulphate, 100 mg L^{-1} chloride and 500 mg L^{-1} hydrogen carbonate are present. Only silicate at 100 mg L^{-1} prevents the adsorption of As(V). These results indicate that the presence of common anions in water samples at high concentrations, except silicate, does not interfere with the adsorption of arsenic. This is another advantage with respect with ion exchangers, which require the use of a great excess of the sorbent due to the lack of selectivity.

Additional experiments were carried to check the interference from phosphate. Mixtures of As(V) at 200 μg L^{-1} and phosphate (0.6 and 2 mg L^{-1} P) in ultrapure water

were prepared, and it was found that the percentage of arsenic eluted was of 22.4 and 20%, respectively. These values are slightly lower than the value obtained in ultrapure water (27%). Although this result cannot be considered satisfactory, it is worth mentioning that 0.6 mg L^{-1} phosphate (P) is a rather high concentration for this species in well waters.

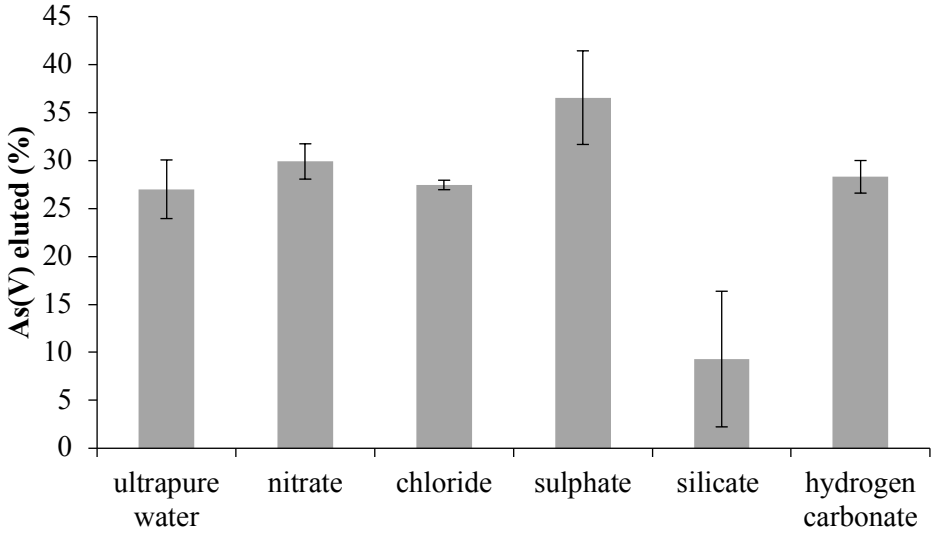

Figure 3.10 Study of the interference from major anions in As(V) adsorption. Sixty milligrams of solid phase packed in a minicolumn. The volume of the solution percolated through the column was 50 mL and the flow rate was 1 mL min−1. The concentration values tested were 50mg L^{-1} nitrate, 100 mg L^{-1} sulphate, 100 mg L^{-1} chloride and 500 mg L^{-1} hydrogen carbonate. As(V) concentration was 200 µgL^{-1} at pH 7.3.

Analytical performance of the method

As described in the *Calibration curve and method validation* section, a calibration set was prepared and the collected elution solution was measured with ICP-OES after preconcentration with Adsorbsia As600. The intensity values were plotted against the amount of As in the solutions and fitted to a lineal function. The linearity was checked by residual analysis, showing a random distribution of residuals. The coefficient of determination (R^2) was 0.993 and a detection limit of 40 µg L^{-1} for a sample volume of 50 mL was obtained (equivalent to 2 µg loaded arsenic). Repeatability (n=3) was also evaluated for an ultrapure water sample spiked with 200 µg L^{-1} As(V) and taken to the

whole procedure. The relative standard deviation (RSD) obtained was 19%, which can be considered acceptable within the concentration range studied [37]. For this sample, the recovery value obtained was 108%. For As(III), we obtained an RSD of 14% and 102% recovery. The values obtained make it clear that the preconcentration system followed by ICP-OES measurement provides a satisfactory system for arsenic determination. It is worth mentioning that a unique calibration curve is used for both As(V) and As(III), with it only being necessary to modify the elution flow rate, and that no previous oxidation of As(III) is needed, making this procedure much easier than the others reported in the literature [25].

Determination of arsenic in water samples

Different water samples, some spiked with 100 or 200 μg L^{-1} As(V) and others containing natural arsenic, were tested and the results compared with the theoretical concentration (values from ICP-MS plus As(V) added in spiked samples). The results are presented in Table 3.11, where it can be seen that the recovery results are satisfactory except for the water sample from Caldes (S3). This result is not surprising considering the complexity of this water matrix as shown in Table 3.8. When the amount of solid sorbent is increased from 60 to 120 mg, then the behaviour of the preconcentration system can be considered acceptable. Preconcentration with Adsorbsia As600 was applied to S4, and also, good results were found considering the arsenic concentration level in the sample.

Table 3.11 Concentration values and recovery (R) results for spiked water samples (n=2) measured with the present method.

Sample[b]	Initial[c] (μg L^{-1})	Added (μg L^{-1})	Found (μg L^{-1})	R (%)
S1	-	200	280	140 (14)
S1	-	100	120	95 (18)
S2	-	200	260	130 (8)
S2	-	100	120	94 (39)
S3	59	200	150	58 (7)

S3*	59	200	190	73 (16)
S4	80	-	90(1)	

For S3 which contains natural arsenic, the recovery values were calculated by taking into account both, natural and spiked arsenic

[a]120 mg of adsorbent used

[b]Identification as in Table 1

[c]Taken from Table 1

Finally, a water sample (50 mL) spiked at 10 μg L^{-1}, the WHO regulated level, was measured and a value of 11.3 μg L^{-1} was obtained.

Thus, we can conclude that the solid allows the preconcentration and determination of arsenic present in natural waters and that the composition of the matrix has little influence.

Conclusions

We have evaluated the adsorption behaviour of the commercial material Adsorbsia As600, for As(V) and As(III), and a capacity of 0.14 and 0.21 mmol g^{-1}, respectively, was obtained at pH 7.3. We have established the setup and the experimental conditions for using this TiO_2 sorbent for As(V) and As(III) preconcentration prior to its determination with ICP-OES. Good recoveries with acceptable reproducibility were obtained for waters containing As(V) when using 2 mL of 0.5 M NaOH solution for the elution at a flow rate of 1 mL min^{-1}. It was also observed that for As(III), the elution flow rate should be decreased to 0.5 mL min^{-1}. As an advantage over other As determination techniques, the developed method can be used for the determination of As(V) and As(III) at μg L^{-1} level without any previous oxidation step or coupling with the well-known hydride generation technique.

References

[1] A. Leónard, Arsenic, in E. Merian (Ed), Metals and their compounds in the environment. Occurrence, analysis and biological relevance, VCH Verlagsgesellschaft mbH, Weinheim, 1991, pp. 751–774.

[2] I. Villaescusa, J.-C. Bollinger, Arsenic in drinking water: sources, occurrence and health effects (a review), Rev. Environ. Sci. Bio./Technol. 7 (2008) 307–323.

[3] P.L. Smedley, D.G. Kinniburgh, A review of the source, behaviour and distribution of arsenic in natural waters, Appl. Geochem. 17 (2002) 517–568.

[4] T.S.Y. Choong, T.G. Chuah, Y. Robiah, F.L.G Koay, I. Azni, Arsenic toxicity, health hazards and removal techniques from water: an overview, Desalination 217 (2007) 139–166.

[5] World Health Organization (WHO). Arsenic in drinking water, WHO Factsheet 210, 3rd ed, WHO, Geneva, 1993.

[6] J.L. Gómez-Ariza, D. Sánchez-Rodas, I. Giráldez, E. Morales, A comparison between ICP-MS and AFS detection for arsenic speciation in environmental samples, Talanta 51 (2000) 257–268.

[7] T. Kubota, T. Yamaguchi, T. Okutani, Determination of arsenic content in natural water by graphite furnace atomic adsorption spectrometry after collection as molybdoarsenate on activated carbon, Talanta 46 (1998) 1311–1319.

[8] E.A. Nagul, I.D. McKelvie, P. Worsfold, S.D Kolev, The molybdenum blue reaction for the determination of orthophosphate revisited: opening the black box, Anal. Chim. Acta 890 (2015) 60–82.

[9] M.M. Bradley, L.M Siperko, M.D. Porter, Colorimetric-solid phase extraction method for trace level determination of arsenite in water, Talanta 86 (2011) 64–70.

[10] T. Okazaki, W. Wang, H. Kuramitz, N. Hata, S. Taguchi, Molibdenum blue spectrophotometry for trace arsenic in ground water using a soluble membrane filter and calcium carbonate column, Anal. Sci. 29 (2013) 67–72.

[11] D.Jr. Mohan, C.U. Pittman, Arsenic removal from water/wastewater using adsorbents-a critical review, J. Hazard. Mat. 142 (2007) 1–53.

[12] S. Bhowmick, S. Chakraborty, P. Mondal, W. Van Renterghem, S. Van den Berghe, G. Roman-Ross, D. Chatterjee, M. Iglesias, Montmorillonite-supported nanoscale zero-valent iron for removal of arsenic from aqueous solution: kinetics

and mechanism, Chem. Eng. J. 243 (2014) 14–23.

[13] J-C. Hsu, C-J. Lin, C-H. Liao, S-T. Chen, Removal of As (V) and As (III) by reclaimed iron-oxide coated sands, J. Hazard. Mat. 153 (2008) 817–826.

[14] S. Ayoob, A.K. Gupta, P.B. Bhakat, Analysis of breakthrough developments and modeling of fixed bed adsorption system for As (V) removal from water by modified calcinated bauxite (MCB), Sep. Purif. Tech. 52 (2007) 430–438.

[15] G.P. Gillman, A simple technology for arsenic removal from drinking water using hydrotalcite, Sci. Total Environ. 366 (2006) 926–931.

[16] Z.Ö. Kocabaş-Atakh, Y. Yürüm, Synthesis and characterization of anatase nanoadsorbent and application in removal of lead, copper and arsenic from water, Chem. Eng. J. 225 (2013) 625–635.

[17] M.Z. López Paraguay, J. Apolinar Cortés, J.F. Pérez-Robles, M.T. Alarcón Herrera, Adsorption of arsenite from groundwater using titanium dioxide, Clean-soil, air, water 42 (2014) 713–721.

[18] J. Guo, X. Cai, Y. Li, R. Zhai, S. Zhou, P. Na, The preparation and characterization of a three-dimensional titanium dioxide nanostructure with high surface hydroxyl group density and high performance in water treatment, Chem. Eng. J. 221 (2013) 342–352.

[19] K.K. Gupta, N.L. Singh, A. Pandey, S.K. Shukla, S.N. Upadayay, V. Mishra, P. Srivastava, N.P. Lalla, P.K. Mishra, Effect of anastase/rutile TiO_2 phase composition on arsenic adsorption, J. Dispers. Sci. Technol. 34 (2013) 1043–1052.

[20] S.L. Wu, W.T. Hu, X.B. Luo, F. Deng, K. Yu, S.L. Luo, L.X. Yang, X.M. Tu, G.S. Zeng, Direct removal of aqueous As (III) and As (V) by amorphous titanium dioxide nanotube arrays, Environ. Tech. 34 (2013) 2285–2290.

[21] X. Guan, J. Du, X. Meng, Y. Sun, B. Sun, Q. Hu, Application of titanium dioxide in arsenic removal from water: a review, J. Hazard. Mat. 215–216 (2012) 1–16.

[22] X. Meng, W. Wang, Speciation of arsenic by disposable cartridges, Third international conference on arsenic exposure and health effects, San Diego

(California), 1998.

[23] W.H. Ficklin, Separation of arsenic (III) and arsenic (V) in ground waters by ion-exchange, Talanta 30 (1983) 371–373.

[24] N.B. Issa, V.N. Rajaković-Ognjanović, B.M. Jovanović, L.V. Rajaković, Determination of inorganic arsenic species in natural waters- benefits of separation and preconcentration on ion exchange and hybrid resins, Anal. Chim. Acta 673 (2010) 185–193.

[25] K. Jitmanee, M. Oshima, S. Motomizu, Speciation of arsenic (III) and arsenic (V) by inductively coupled plasma-atomic emission spectrometry coupled with preconcentration system, Talanta 66 (2005) 529–533.

[26] M.J. Watts, J. O'Reilly, A.L. Marcilla, R.A. Shaw, N.I. Ward, Field based speciation of arsenic in UK and Argentinean water samples, Environ. Geochem. Health 32 (2010) 479–490.

[27] D. Chen, C. Huang, M. He, B. Hu, Separation and preconcentration of inorganic arsenic species in natural water samples with 3-(2- aminoethylamino) propyltrimethoxysilane modified ordered mesoporous silica micro-column and their determination by inductively coupled plasma optical emission spectrometry, J. Hazard. Mat. 164 (2009) 1146–1151.

[28] C. Xiong, M. He, B. Hu, On-line separation and preconcentration of inorganic arsenic and selenium species in natural water samples with CTAB-modified alkyl silica microcolumn and determination by inductively coupled plasma-optical emission spectrometry, Talanta 76 (2008) 772–778.

[29] D. Pozebon, V.L. Dressler, J.A. Gomes Neto, A.J. Curtius, Determination of arsenic (III) and arsenic (V) by electrothermal atomic spectrometry after complexation and sorption on a C-18 bonded silica column, Talanta 45 (1998) 1167–1175.

[30] X.P. Yan, X.B. Yin, X.W. He, Y. Jiang, Flow injection on-line sorption preconcentration coupled with hydride generation fluorescence spectrometry for determination of (ultra) trace amounts of arsenic (III) and arsenic (V) in natural water samples, Anal. Chem. 74 (2002) 2162–2166.

[31] S.Z. Chen, X. Guo, Y. He, D. Lu, Titanium dioxide nanotubes for speciation of inorganic arsenic in environmental water samples by ICP-MS, Atom. Spectrosc. 34 (2013) 113–118.

[32] C. Huang, B. Hin, Z. Jiang, Simultaneous speciation of inorganic arsenic and antimony in natural waters by dimercaptosuccinic acid modified mesoporous titanium dioxide micro-column on-line separation and inductively coupled plasma emission spectrometry determination, Spectrochim. Acta B 62 (2007) 454–460.

[33] P. Liang, R. Liu, Speciation analysis of inorganic arsenic in water samples by immobilized nanometer titanium dioxide separation and graphite furnace atomic absorption spectrometric determination, Anal. Chim. Acta 602 (2007) 32–36.

[34] Waters. http://www.waters.com/waters/en_US/Oasis-Sample-Extraction-Products (accessed September 10, 2015).

[35] R. Güell, C. Fontàs, V. Salvadó, E. Anticó, Modelling of liquid-liquid extraction and liquid membrane separation of arsenic species in environmental matrices, Sep. Pur. Technol. 72 (2010) 319–325.

[36] R. Güell, E. Anticó, S.D. Kolev, J. Benavente, V. Salvadó, C. Fontàs, Development and characterization of polymer inclusion membranes for the separation and speciation of inorganic As species, J. Membr. Sci. 383 (2011) 88–95.

[37] AOAC Official Methods of analysis, Guidelines for standard method performance requirements Appendix F, AOAC International, 2012, pp. 1–17.

[38] B.D. Cullity, S.R. Stock, Elements of X-ray diffraction, 3rd ed, Prentice Hall, Upper Saddle River (New Jersey), 2001.

[39] G. Jegadeesan, S.R. Al-Abed, V. Sundaram, H. Choi, K.G. Scheckel, D.D. Dionysiou, Arsenic sorption on TiO_2 nanoparticles: size and crystalline effects, Water Res. 44 (2010) 965–973.

[40] M. Pena, X.G. Meng, G.P. Korfiatis, C.Y. Jing, Adsorption mechanism of arsenic on nanocrystalline titanium dioxide, Environ. Sci. Technol. 40 (2006) 1257–1262.

[41] C. Jing, X. Meng, E. Calvache, G. Jiang, Remediation of organic and inorganic

arsenic contaminated groundwater using a nanocrystalline TiO_2-based adsorbent, Environ. Pollut. 157 (2009) 2514–2519.

[42] C. Jing, X. Meng, S. Liu, S. Baidas, R. Patraju, C. Christodoulatos, G.P. Korfiatis, Surface complexation of organic arsenic on nanocrystalline titanium dioxide, J. Colloid Interface Sci. 290 (2005) 14–21.

[43] H.Y. Niu, J.M. Wang, Y.L. Shi, Y.Q. Cai, F.S. Wei, Adsorption behavior of arsenic onto protonated titanate nanotubes prepared via hydrothermal method, Microporous Mesoporous Mater. 122 (2009) 28–35.

[44] Z. Xu, X. Meng, Size effects of nanocrystalline TiO_2 on As(V) and As(III) adsorption and As(III) photooxidation, J. Hazard. Mat. 168 (2009) 747–752.

[45] C.E. Meloan, Chemical separations. Principles, techniques and experiments, in techniques in analytical chemistry, Wiley-Interscience Publications, New York, 1999.

[46] H. Zeng, M. Arashiro, D.E. Giammar, Effects of water chemistry and flow rate on arsenate removal by adsorption to an iron oxide-based sorbent, Water Res. 42 (2008) 4629–4636.

3.2 Advances on PIMs

The contents of this section are based on the following studies:

R. Vera, L. Gelde, E. Anticó, M.V. Martínez de Yuso, J. Benavente, C. Fontàs, Tuning physicochemical, electrochemical and transport characteristics of polymer inclusion membrane by varying the counter-anion of the ionic liquid Aliquat 336, J. Memb. Sci. 529 (2017) 87-94.

R. Vera, E. Anticó, J.I. Eguiazábal, N. Aranburu, C. Fontàs, First report on a solvent-free preparation of polymeric membranes with an ionic liquid, React. Funct. Polym. (submitted).

3.2.1 Tuning physicochemical, electrochemical and transport characteristics of polymer inclusion membrane by varying the counter-anion of the ionic liquid Aliquat 336

Abstract

Polymer inclusion membranes (PIMs) have been prepared using cellulose triacetate (CTA) as polymer and derivatives of the commercial ionic liquid (IL) Aliquat 336, trioctyl methylammonium chloride (AlqCl), as extractants. The different ILs were prepared by exchanging chloride anion from AlqCl for other more lipophilic anions, obtaining IL derivatives $AlqNO_3$ and AlqSCN. PIMs containing these extractants at two different concentrations (30% and 60%) were prepared and characterized using X-ray photoelectron spectroscopy (XPS), infrared spectroscopy (FTIR), thermogravimetric analysis (TGA), contact angle and impedance spectroscopy to obtain information on the material properties of both the surface and bulk membranes. The IL counter-anion affects the membrane's electrical parameters (dielectric constant and conductivity) as well as its hydrophobic character, which also depends on the IL concentration in the PIM formulation. Passive transport across the different PIMs using HCl and NaCl aqueous solutions was also considered, and the results obtained seem to be directly related to the hydrophilic/hydrophobic character of the studied membranes.

Introduction

Membrane-based processes attract significant attention as a valuable technology for many industries. Besides membrane systems that exclude compounds due to pore size, there is great interest in the development of functionalized membranes, for which the separation is based on the chemical affinity of the target compound with the ligand or functional group present in the membrane. Among this type of functionalized membranes, polymer inclusion membranes (PIMs) have shown themselves to be useful for the separation of a wide variety of compounds from anions or metallic species to small organic molecules [1]. These membranes can be classified as a type of liquid membranes where the extractant or carrier is entrapped within a polymeric matrix, normally made of cellulose triacetate (CTA) or polyvinyl chloride (PVC). The role of the polymer is to

provide mechanical strength to the membrane, and a plasticizer is sometimes added to improve the elasticity and to modify the membrane's diffusion characteristics [2]. There is increasing interest in PIMs thanks to their easy preparation, low cost, versatility, good chemical resistance and high efficiency, which is closely related to the carrier incorporated in the membrane. A large number of extractants can be used in PIMs [3], many of which are commercially available. This is the case of the ionic liquid (IL) Aliquat 336 (a trioctylmethyl ammonium chloride), which has been proved to successfully transport analytes as different as metals [4–6], antibiotics [7] or nutrients [8]. Moreover, this extractant possesses the unique properties of ILs such as low vapour pressure, high electrical conductivity and ion mobility as well as good chemical and thermal stability [9]. It is important to consider that PIMs prepared with this IL are flexible and mechanically stable using both CTA and PVC polymers, so the use of a plasticizer is not mandatory [10].

Aliquat 336 has also shown itself to be a versatile cation source to prepare new hydrophobic ionic liquids by combining a trioctylmethyl ammonium (TOMA) cation with a number of anions prepared by means of simple replacement of the chloride anion in Aliquat 336. Mikkola et al. show in [11] the preparation and characterization of 12 new ILs containing both inorganic and organic anions. Kogelnig et al. describe in [12] the greener synthesis of three new ammonium ionic liquids also prepared from Aliquat 336: TOMA thiosalicylate, TOMA benzoate, and TOMA hexanoate, and studied their performance as extracting agents for cadmium.

Some Aliquat 336 derivatives have also been included in PIMs, such as in the work of Sakay et al. [13], where PIMs were made with PVC as a polymer, 2-nitrophenyl octyl ether as a plasticizer and different TOMA derivatives as carriers incorporating acetate, nitrate and perchlorate as anions. The resulting membranes were tested for the transport of thiourea, and it was found that the transport efficiency of this organic molecule was dependent on the anion accompanying TOMA, following the trend acetate > chloride > nitrate > > perchlorate. Even though a different behaviour was evidenced depending on the counter anion, PIMs were not characterized to understand the effects that these modifications have on membrane properties.

Thus, the aim of this work is to explore if slight changes in the formulation of the IL affect membrane characteristics that, in turn, can modify transport properties. To this end, we have chosen nitrate and thiocyanate anions to be exchanged by the chloride existing in Aliquat 336, and PIMs have been prepared with these ILs at two different

concentrations (30% IL and 60% IL, weight percentage) and fixing CTA as the polymer. A thorough characterization of the PIMs has been undertaken using different techniques to establish whether or not the physicochemical and electrochemical properties of the membranes are affected by the variation of the counter-anion of Aliquat 336. Thus, membranes were studied using techniques such as infrared spectroscopy (FTIR) and thermogravimetric analysis (TGA) to understand the type of interaction between the base polymer and the different ILs. These techniques have shown their effectiveness in the analysis of different PIMs, as reported in [14–16]. Contact angle measurements were used to provide information on the hydrophobic/hydrophilic character of the PIMs. These data are of great importance since hydrophobicity has been reported as increasing membrane stability [17]. The chemical characterization of the surface of the PIMs was performed by X-ray photoelectron spectroscopy (XPS) to assess whether or not the presence of the ILs on the surface of the membrane was dependent on the IL composition. This fact may be directly related to the ability of the carrier to interact with the target analyte, and, ultimately, with the efficiency of the membrane [18]. Besides these physicochemical parameters, the electrical behaviour of the polymeric membranes was also investigated using impedance spectroscopy (IS) to shed light on their ability to transport charged species. This technique has been successfully applied to characterize supported liquid membranes containing ILs [19], and to PIMs containing different plasticizers and Cyanex 272 as a carrier [20], as well as in our previous work dealing with PIMs made of CTA and Aliquat 336 [10]. Moreover, Salar- García et al. proposed a new method based on IS to calculate the internal resistance of PIMs including three different ILs to predict their behaviour as novel proton exchange membranes [21]. Finally, diffusive transport of ions has been studied with PIMs in contact with electrolyte solution, i.e. HCl and NaCl, to understand how transport/rejection characteristics of the membranes are affected by the nature of the counter-anion.

Experimental

Reagents and solutions

The extractant Aliquat 336 (AlqCl) and the polymer CTA were purchased from Fluka Chemie. $CHCl_3$ (Panreac) was used to dissolve the polymer and the ILs. NaSCN and $NaNO_3$ (Panreac, Spain) were used as anions source to prepare the new ILs. A 0.1N

$AgNO_3$ solution was used as an indicator of chloride presence in the aqueous solution. HCl (Panreac) and NaCl (Merck) were used for transport experiments.

PIM preparation

First, nitrate and thiocyanate salts of TOMA ($AlqNO_3$ and AlqSCN) were prepared, respectively, as follows: 5 mL of a 0.5 M AlqCl solution in $CHCl_3$ were contacted with 7–8 mL of a 2 M $NaNO_3$ or NaSCN and left stirring for 2–3 h inside 25 mL glass tubes. This procedure was repeated several times until the aqueous phase gave no white precipitation of AgCl with a solution of $AgNO_3$ [13]. The resulting chloroform solution was used to prepare the corresponding PIM.

Each membrane was prepared dissolving 200 mg of CTA in chloroform (5 h) and adding the corresponding volume of the chloroform solution of AlqCl, $AlqNO_3$ or AlqSCN to finally obtain an IL content of 30% and 60% (w/w) in the PIM. This solution was left to stir for 2 h more, and, after this time, the solution was poured into a 9.0 cm diameter flat bottom glass Petri dish, which was set horizontally and covered loosely. The solvent was allowed to evaporate over 24 h at room temperature, and the resulting film was then carefully peeled off from the bottom of the Petri dish and taken for further studies.

Thus, the resulting membranes were 70% CTA+30% IL (30% AlqCl, 30% $AlqNO_3$, 30% AlqSCN samples), or 40% CTA+60% IL (60% AlqCl, 60% $AlqNO_3$ and 60% AlqSCN samples).

IR spectroscopy

IR spectra were obtained with the aid of a diamond attenuated total reflectance (ATR) accessory on an Agilent Cary 630 FTIR spectrometer.

TGA analysis

The thermogravimetric analysis and differential scanning calorimetry (DSC) were performed using a Mettler Toledo TGA/DSC combined instrument. A sample of about

10 mg was used and a heating cycle from 30 to 650 °C at a heating rate of 10 °C/min under nitrogen atmosphere (40 mL min^{-1}).

Contact angle

Changes in the hydrophobic character of the membrane surfaces associated to both the composition of IL and its content were determined from contact angle measurements, which were performed by the tensile drop method using distilled water drops of 5 μL and a Teclis T2010 instrument equipped with a video system. Measurements were carried out on both membrane faces.

XPS measurements

A Physical Electronics spectrometer (PHI 5700) with X-ray Mg Kα radiation (300 W, 15 kV, 1253.6 eV) as the excitation source was used. High-resolution spectra were recorded at a given take-off angle of 45° by a concentric hemispherical analyzer operating in the constant pass energy mode at 29.35 eV, using a 720 μm diameter analysis area. Accurate ± 0.1 eV binding energies were determined with respect to the position of the adventitious C *1s* peak at 285.0 eV, and the residual pressure in the analysis chamber was maintained below 5×10^{-7} Pa during data acquisition. Membranes were mounted on a sample holder without adhesive tape and kept overnight at high vacuum in the preparation chamber before being transferred to the analysis chamber of the spectrometer for testing. Each spectral region was scanned several sweeps until a good signal-to-noise ratio was observed. PHI ACCESS ESCA-V6.0F software package was used for acquisition and data analysis. Membrane samples were irradiated for a maximum time of 20 min to reduce possible X-ray damage. A Shirley-type background was subtracted from the signals. To determinate more accurately the binding energy (BE) of the different element core levels, recorded spectra were fitted by Gauss–Lorentz curves following the methodology detailed elsewhere [22]. Atomic concentration (A.C.) percentages of the characteristic elements on the membranes surfaces were determined taking into account the corresponding area sensitivity factor [23] for the different measured spectral regions.

IS measurements

The test cell used for impedance spectroscopy measurements of the studied PIMs consists of a Teflon support on which two Pt electrodes were placed and screwed down (Pt-electrode//Membrane//Pt-electrode system). The electrodes were connected to a Frequency Response Analyzer (FRA, Solartron 1260, England) and 100 data points were recorded for frequency (f) ranging between 1 Hz and 107 Hz, at a maximum voltage of 0.01 V. These measurements were performed at room conditions (relative humidity ≈65% and temperature of 25 ± 2 °C).

The impedance of a system is a complex number, $Z=Z_{real}+j\ Z_{img}$, which can be separated into real and imaginary parts by algebra rules. For simple systems Z_{real} and Z_{img} are related to the electrical resistance (R) and the capacitance (C) by the following expressions (Eq. 3.3):

$$Z_{real} = (R/[1 + (\omega RC)^2]); \qquad Z_{img} = - (\omega R^2 C/[1 + (\omega.RC)^2]) \qquad (3.3)$$

where ω represents the angular frequency ($\omega = 2\pi f$). In the case of non-homogeneous systems, a non-ideal capacitor or constant phase element, Q(ω), is usually used instead of C; where $Q(\omega) = Y_o(j\omega)^{-n}$, Y_o is the inverse of the impedance ($Y_o = 1/Z$), and *n* is an experimental parameter ($0 \leq n \leq 1$). The fit of the impedance curves derived from the experimental data, obtained from a broad range of frequencies and using equivalent-circuits as models, permits the estimation of the electrical resistance and capacitance values associated to each membrane sample [24].

Membrane potentials

The membrane potential (ΔΦmbr) or the equilibrium electrical potential difference at both sides of a membrane, separating two solutions of the same electrolyte but different concentrations (C1 and C2), were obtained from the cell potential (ΔE). These potentials were measured with NaCl solutions and using two reversible Ag/AgCl electrodes connected to a digital voltmeter (Yokohama 7552, 1 GΩ input resistance) in a dead-end test cell similar to that described in [18]; the NaCl solutions were stirred at 540 rpm to minimize the concentration-polarization at the membrane surfaces. Measurements were performed at room temperature (25 ± 2) ºC and neutral pH by keeping the NaCl concentration constant at one side of the membrane (C_f) and gradually changing the

concentration of the solution at the other side (C_v, between 0.002 M and 0.1 M). $\Delta\Phi_{mbr}$ values were obtained by subtracting the calculated electrode potential ($\Delta\Phi_{elect} = (RT/F).\ln(C_v/C_f)$) from the measured cell potential values, in other words, $\Delta\Phi_{mbr} = \Delta E - \Delta\Phi_{elect}$ [24].

Study of HCl permeation though the PIMs

A similar two-compartment dead-end cell [25] was used to investigate the transport of 1 M HCl from the feed compartment to the stripping phase (ultrapure water). The exposed membrane area was 11.5 cm^2 and continuous stirring of both compartments was maintained during the experiment. The pH variation in the stripping solution was monitored using a pH-meter and a glass electrode.

Results and discussion

Physicochemical characterization of PIMs

Chemical differences in the surface of the studied PIMs were obtained by the XPS technique, which gives information on the elements present on the surface of a given sample by analysing the XPS spectra. Figure 3.11 shows the C *1s* and N *1s* core level spectra obtained for the three 30% IL membranes, as well as the spectrum corresponding to the 60% AlqCl sample for comparison. The signal of C *1s* (Figure 3.11 (a)) obtained for the three membranes with the same IL content only shows small differences between the samples. In all cases, two different peaks at binding energies (BE) of 285.0 eV, which correspond to aliphatic chains plus adventitious carbon, and 288.5–289.0 eV for the COO bond of CTA can clearly be observed. Moreover, a shoulder at 286.5–287 eV for the C-OH and C-O-C cellulose bonds was also obtained [26], and the relative intensity of this shoulder seems to decrease with the increase of the IL content in the membranes. However, the comparison of the N *1s* signal (Figure 3.11 (b)) shows some differences depending on the IL, with a common peak at 402.0 eV associated to the quaternary nitrogen of the cationic part of Aliquat 336, while the contribution of nitrogen associated to NO_3^- (at 406.4 eV) and thiocyanate (at 397.3 eV) can also be observed in $AlqNO_3$ and AlqSCN samples, respectively.

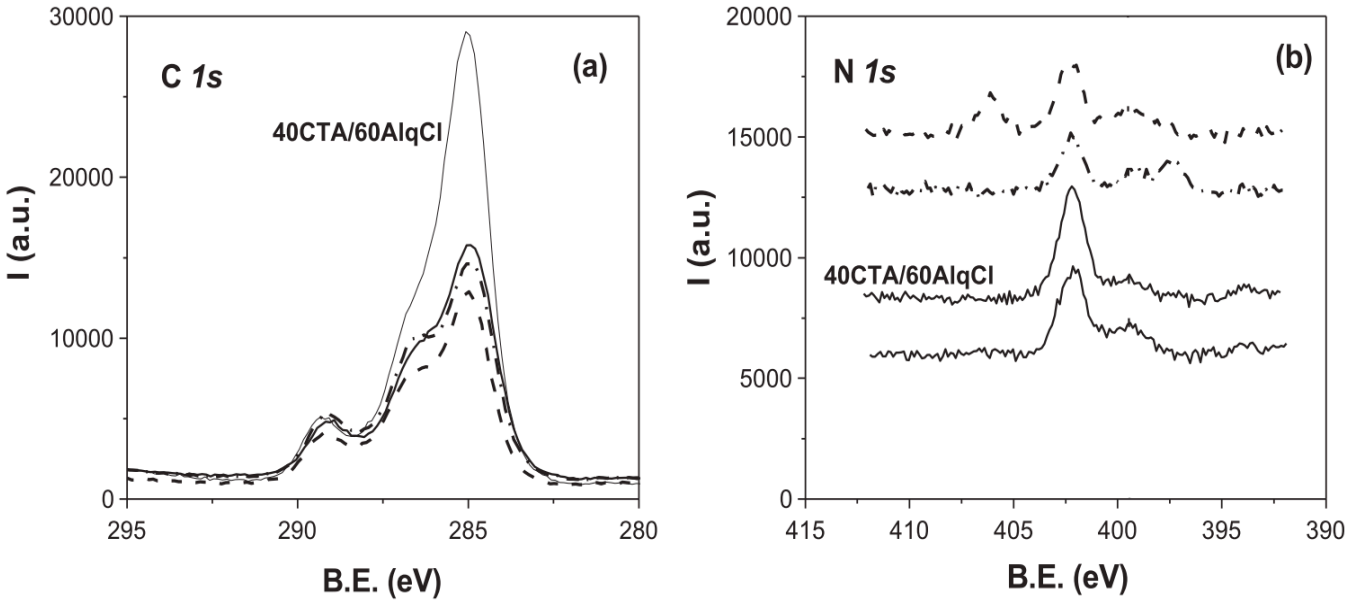

Figure 3.11 Core level spectra for 30% AlqCl (solid line), 30% $AlqNO_3$ (dashed line) and 30% AlqSCN (dashed-dot line) PIMs. (a) C *1s* and (b) N *1s*.

Average values of the atomic concentration percentages (A.C.%) of characteristic PIM elements found on both surfaces of each membrane are given in Table 3.12. These results show a good correlation between membrane formulation and the A.C.% of IL characteristic elements (Cl, N and S) as well as their increase when the IL content in the PIM increases. Moreover, the relatively small interval of error for the values found indicates that the chemical composition in both surfaces is not affected by external factors related to the PIMs preparation. These results also show that all the ILs investigated are present in the surface of the membranes, independently of the nature of the counter-anion. Hence, it is expected that it will be possible in all cases for the extraction reaction in the interface aqueous solution-membrane surface to take place.

Table 3.12 Average values of the atomic concentration percentages of the characteristic elements of the PIMs found on both membrane surfaces.

PIM		<C> (%)	<O> (%)	<N> (%)	<Cl> (%)	<S> (%)
AlqCl	30%	71.3 ± 0.4	27.0 ± 0.5	0.9 ± 0.2	0.7 ± 0.1	----
	60%	85.6 ± 1.1	8.8 ± 0.9	2.7 ± 0.2	2.4± 0.2	----
$AlqNO_3$	30%	73.2 ± 0.3	24.4 ± 0.3	1.6 ± 0.1	----	----
	60%	81.1 ± 1.2	13.5 ± 0.6	4.0 ± 0.2	----	----
AlqSCN	30%	71.5 ± 0.2	25.5 ± 0.1	1.5 ± 0.1	----	0.9 ± 0.1
	60%	86.0 ± 1.5	6.2 ± 1.1	4.5 ± 0.3	----	2.5 ± 0.2

[a]Small percentages of Si (from the petri-dish) were also found on some samples.

IR spectroscopy was used to give information on chemical bulk differences among the studied membranes. FTIR spectra are shown in Figure 3.12 for the 60% IL-PIMs. As reported previously [10], the main observed bands are those of the individual constituents of the membrane. The band at 1235 cm^{-1}, which corresponds to the TOMA group in Aliquat 336, appears in all membrane compositions as well as the absorption bands at 1747 and 1041 cm^{-1}, which correspond to the C=O and C-O-C groups in the CTA polymer. Moreover, some characteristic bands of the anion accompanying the quaternary ammonium group can also be observed. This is the case of the absorption band at 2048 cm^{-1} in Figure 3.12 (c), which corresponds to the –N-C-S of the thiocyanate anion, and the intense band at 1300–1400 cm^{-1} in Figure 3.12 (b), which is associated to the stretching bands of the nitrate group. These results, taken together with the fact that no band displacement was observed compared to the pure components, allow us to assume that the IL stays entrapped in the polymeric matrix without any chemical change and, thus, is completely free to interact with the species in solution.

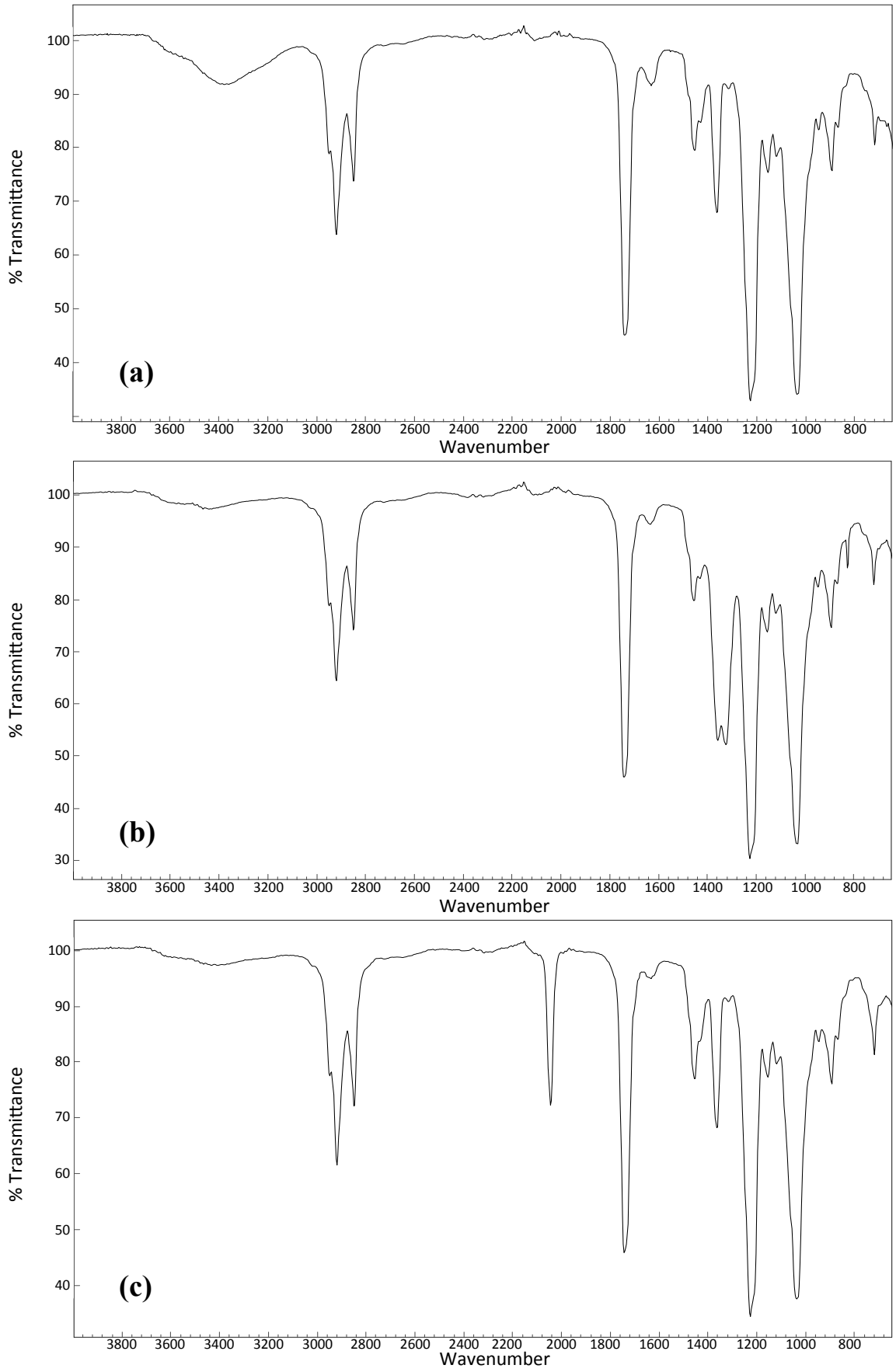

Figure 3.12 IR spectra of (a) 60% AlqCl, (b) 60% AlqNO_3, and (c) 60% AlqSCN PIMs.

To investigate the effect of the anion on the thermal stability of the membrane, a thermal gravimetric analysis was conducted. The analysis indicates the rate of reduction in weight sample by the increase in temperature (see Figure 3.13). As shown, the curves can be divided into three parts. The first part represents a maximum of 4% of the total weight loss, and consists of temperatures up to around 100 °C, at which volatile materials and the water absorbed by membranes are removed. The second part includes temperatures from 137 °C up to 332 °C, and can be attributed to IL thermal decomposition. This decomposition stage presents a different shape depending on the anion in the PIM. For 60% AlqCl and 60% AlqSCN membranes, two steps can be observed starting at 138 and 158 °C, respectively. However, for 60% $AlqNO_3$ only one step can be seen at 191 °C. It is worth pointing out that for 60% $AlqNO_3$ PIM, a positive peak in the DSC was also observed at the same temperature, which is related to an oxidation process catalysed by nitrate anion. Finally, the third part in the TGA curve contains temperatures over 320–330 °C, where the CTA polymer degenerated thermally and the material was carbonized. The weight loss observed in this last part corresponds to the percentage of CTA in the PIM.

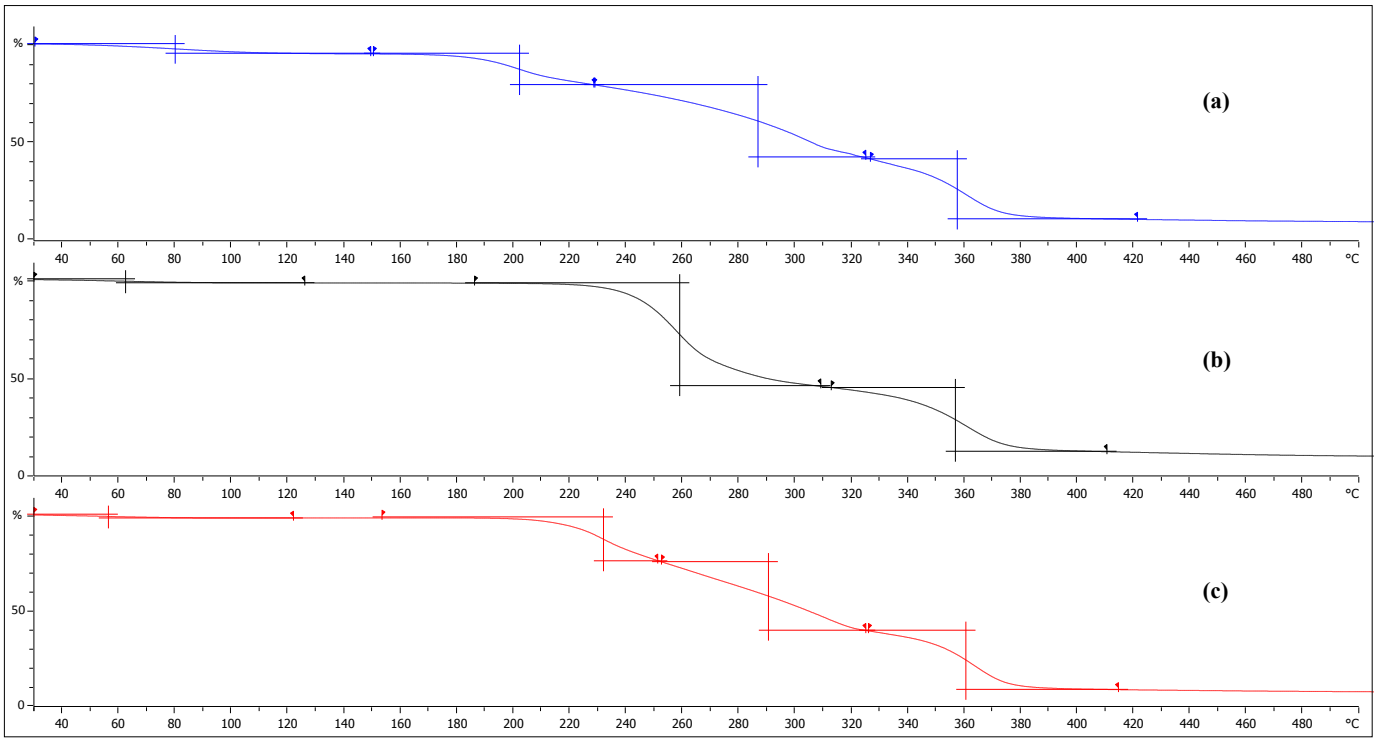

Figure 3.13 TGA curves obtained with the different membranes prepared: (a) 60% AlqCl, (b) 60% $AlqNO_3$ and (c) 60% AlqSCN.

Another parameter of interest related to physicochemical changes in the membrane material is the contact angle, which gives information on their hydrophobic/hydrophilic character. Average values of the contact angle, <ϕ>, obtained for each membrane are presented in Figure 3.14. As can be seen, the hydrophobicity sequence for all membrane formulations is AlqSCN > $AlqNO_3$ > AlqCl, and there is clearly different behaviour depending on the IL content. In particular, PIMs prepared with commercial IL (AlqCl) show a significant reduction (40%) in contact angle value with the increase of the IL content, but this reduction is only of 15% in the case of $AlqNO_3$ whereas the IL content hardly modifies the hydrophobic character of the AlqSCN membranes. These results might be related to the availability of charges of the IL present in the membrane, *i.e.*, with the strength of the ion pair formed between the cationic and anionic part of the IL. Taking into account that the lipophilicity of the anions follows the trend SCN^-> NO_3^-> Cl^-, it is expected that the stability of the ion-pairs formed is AlqSCN > $AlqNO_3$ > AlqCl. These results suggest that the choice of the counter anion can be of paramount importance depending on the PIM characteristics desired, since it is possible to vary the water contact angle from ~25° (60% AlqCl) to ~55% (60% AlqSCN), with the consequent changes in the hydrophobicity of the membrane, and more importantly, only varying the counter-anion accompanying TOMA, it is possible to have more stable membranes [17] than those obtained using the commercial IL Aliquat 336.

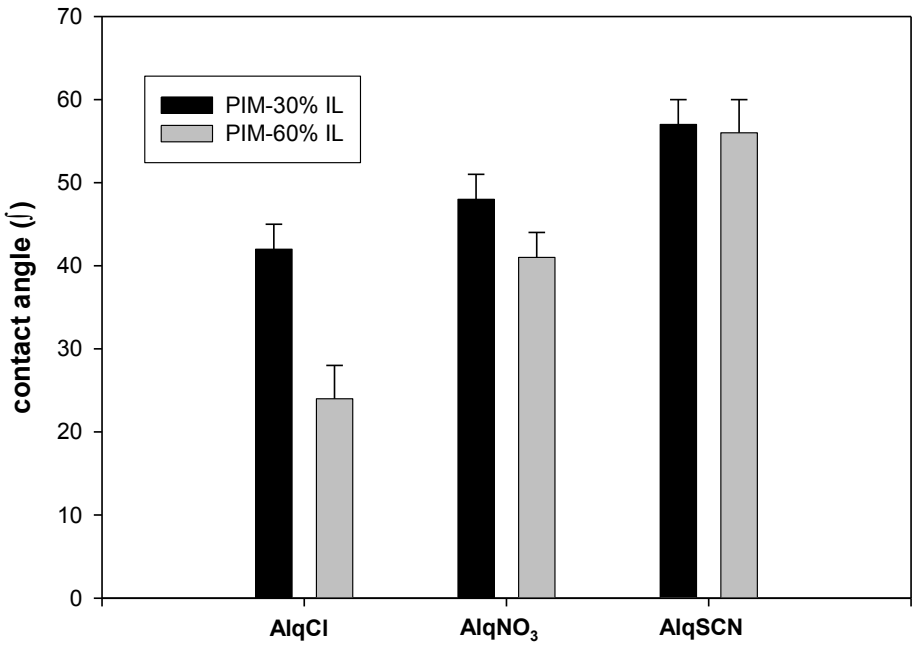

Figure 3.14 Variation of the contact angle of PIM surface in relation to the counter-anion and IL content (n=6).

IS is a non-destructive alternating current technique, which allows the determination of electrical parameters of materials, such as the electric resistance (R) and the capacitance (C), by analysing the impedance plots [27]. Figure 3.15 shows both Nyquist plots ($-Z_{img}$ vs. Z_{real}, Figure 3.15(a) and (b)) and Bode plots ($-Z_{img}$ vs. frequency, Figure 3.15(c) and (d)), where significant differences associated to both the IL and its concentration in the PIM can be observed. In all cases, Nyquist plots show depressed semicircles and the equivalent circuit associated to each one correspond to a parallel association of a resistance and a generalized capacitor [24, 28–30]. PIMs containing AlqSCN differ significantly from those obtained with AlqCl and $AlqNO_3$ for both 30% and 60% IL content; in particular, the maximum in the $-Z_{img}$/frequency curves (Bode plots) for AlqSCN-PIMs appears at lower frequency values, which is usually an indication of a more compact and dense membrane structure.

For the purpose of comparison, the Bode plot obtained for the pure IL AlqCl measurements performed in a different cell [19] is also shown in Figure 3.15(d). As could be expected, clear differences in the electrical response obtained for the IL and PIM (CTA-IL) samples were obtained at low frequency values ($f < 5\times10^3$ Hz), associated to electrode/sample interfacial effects, which is attributed to differences between electrode/ PIM (solid/solid system) and electrode/IL (solid/liquid system). However, at high frequency values all curves show the same shape, with the maximum frequency for 60% AlqCl being practically the same as that obtained with AlqCl IL. The fit of the IS data by using a non-linear program (Z-plot) allowed the determination of the membrane electrical resistance, R_m, and equivalent capacitance, C^{eq}_m. From these results, the conductivity and the dielectric constant of the studied PIMs (σ_m and ε_m, respectively) were obtained from the following expressions (for homogeneous conductors and plane-plate capacitors) [24]:

$$\sigma_m = \Delta x_m/S_m.R_m \quad (3.4)$$

$$\varepsilon_m = C_m.\Delta x_m/S_m.\varepsilon_o \quad (3.5)$$

where ε_o is the vacuum permittivity, while Δx_m and S_m represent the membrane thickness and area, respectively. Table 3.13 shows the σ_m and ε_m values obtained for the different PIMs. As can be observed, doubling IL content in the PIM increases the membrane conductivity by three orders of magnitude. In particular, the value obtained for the conductivity of 60% AlqCl PIM does not differ significantly from pure AlqCl IL conductivity (2.6×10^{-3} $(\Omega\ m)^{-1}$ or 0.026 mS/cm [30]), suggesting that a significant contribution is made by IL in such a formulation. The conductivity values for PIMs with

AlqCl content broadly agree with the results obtained in a previous paper [10], where a detailed analysis of physicochemical parameters was performed using PIMs with five different AlqCl concentrations and two base-polymers (CTA and PVC). On the other hand, much lower conductivity values were obtained for PIMs with AlqSCN. The low dielectric constants found for these PIMs correlates well with the less-polar characteristics of this IL, as expected from the previously shown contact angles.

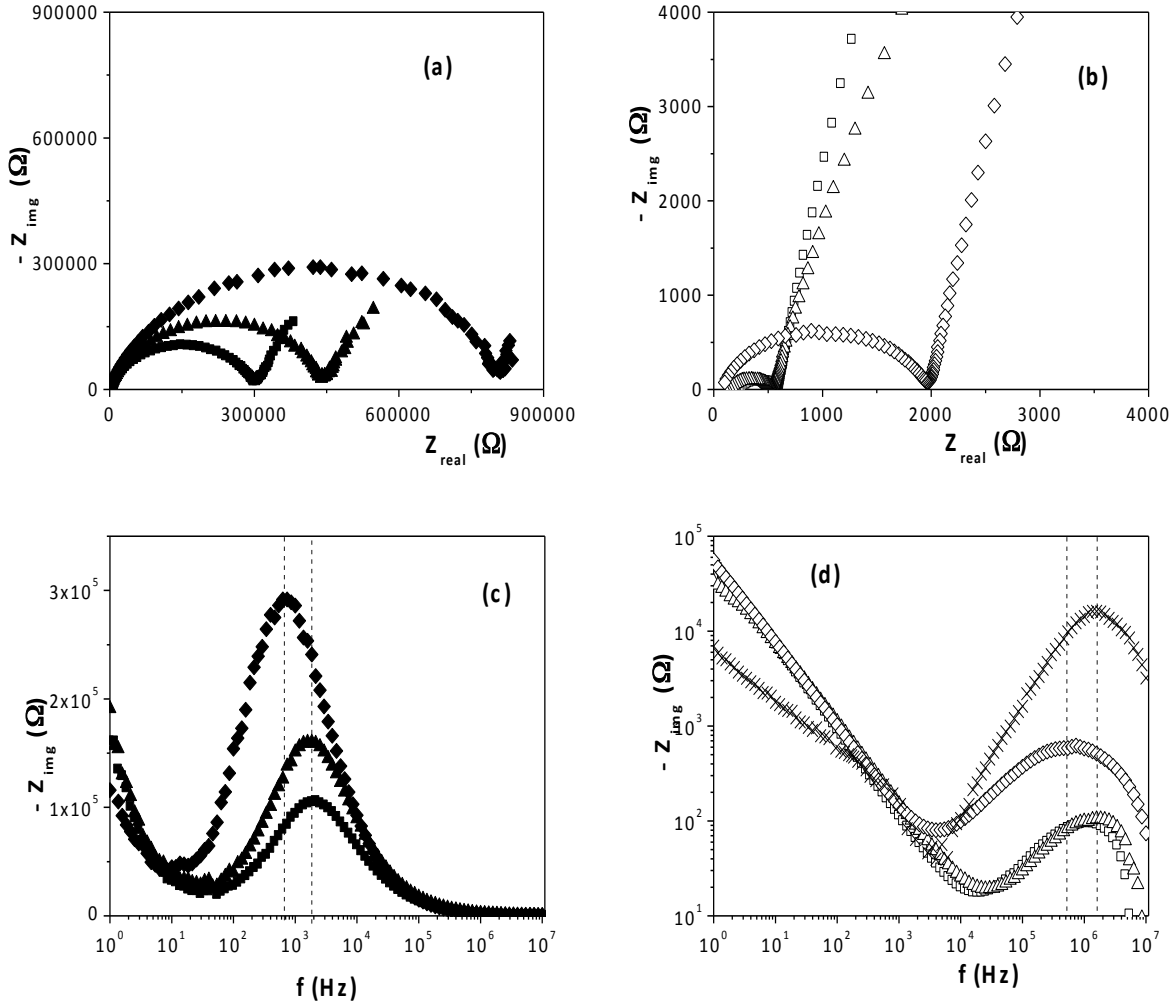

Figure 3.15 Nyquits (a and b) and Bode plots (c and d) for PIMs: 30% AlqCl (■), 30% $AlqNO_3$ (▲), 30% AlqSCN (♦), 60% AlqCl (□), 60% $AlqNO_3$ (Δ), 60% AlqSCN (◊). Pure AlqCl IL (x) Bode plot in (d).

With regards to the dielectric constant values, a similar trend as reported in [10] is also found in the case of PIMs with AlqCl and $AlqNO_3$, *i.e.*, the dielectric constant

increases when the IL content is increased (~75% increase). However, in the case of AlqSCN lower and more similar values are obtained (variation of only ~25%).

Table 3.13 Effect of PIM composition on the conductivity (σm) and dielectric constant (εm) values for dry samples.

PIM		σ_m $(\Omega.m)^{-1}$	ε_m
AlqCl	30%	1.22×10^{-6}	8.2
	60%	1.68×10^{-3}	14.4
$AlqNO_3$	30%	1.11×10^{-6}	7.8
	60%	1.48×10^{-3}	13.6
AlqSCN	30%	3.61×10^{-7}	6.4
	60%	4.48×10^{-4}	8.0

Characterization of the PIMs in contact with electrolyte solution

PIM composition is a key parameter in ensuring an effective transport of the target analyte when applied to separation processes, but other factors, such as the pH and the presence of other ions in the solution could also affect the transport. In the present work, we aimed to investigate whether or not the components of the IL can affect not only the physicochemical characteristics of the membrane, as demonstrated in the previous analysis, but also the passive transport and rejection properties of PIMs. For this reason, two different kinds of experiments were performed. On the one hand, HCl diffusion across all PIMs was investigated by monitoring the pH variation of the receiving solution (ultrapure water). On the other hand, the diffusive transport of ions was studied by means of membrane potentials or equilibrium potentials at both sides of the membranes when separating two solutions of different concentrations (C_v and C_f). These experiments were carried out with NaCl solutions to cover a wide range of concentrations.

Figure 3.16 shows the pH variation in the stripping phase for each PIM after 20 min. As can be seen, PIMs with the IL AlqCl presented the greatest variation in pH, followed by PIMs made of $AlqNO_3$, while PIMs with 30% AlqSCN showed the highest resistance to proton transport. It must be taken into account that Aliquat 336 is known to transport HCl as HCl-Aliquat 336 complex [31], which could partially contribute to the decrease in the pH in the stripping phase. Moreover, in the same study, it is postulated

that water solvates the AlqCl ion pair. Given that the hydrophilic character of the PIMs under study follow the trend 60% AlqCl > 30% AlqCl~60% $AlqNO_3$ > 30% $AlqNO_3$ > AlqSCN, which correlates with the pH variation, it can be assumed that the ILs AlqCl and $AlqNO_3$ allow a solvating environment appropriate for HCl diffusion.

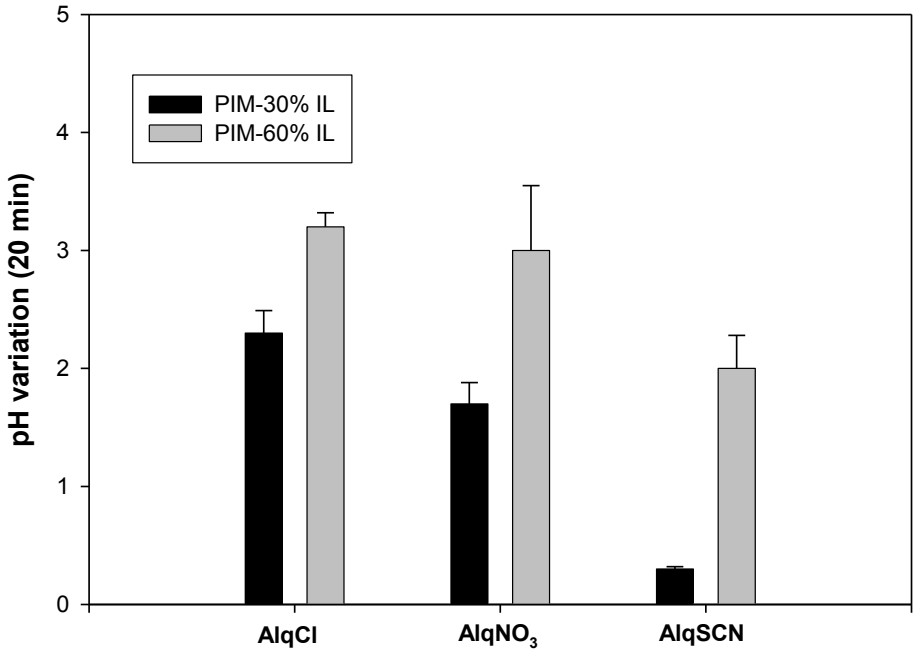

Figure 3.16 pH variation with time depending on the IL nature and content. (a) 30% IL; (b) 60% IL. (n=2).

These results are highly significant since proton transport across membranes is of great importance in many fields, and, depending on the applications, more permeable/impermeable membranes are needed. For example, in the case of microbial fuel cells, which are an emerging technology for the simultaneous treatment of wastewater and energy recovery, the transport of protons plays a crucial role affecting the performance of the cells [21]. In other studies, where the speciation of the analyte to be transported is pH dependent, it is of paramount importance that membranes behave as a barrier for protons; otherwise the speciation in the feed phase can change preventing the analyte transport, as happens in the case of arsenic [25], sulphonamides and tetracyclines [7].

Figure 3.17 shows the membrane potential ($\Delta\Phi_{mbr}$) obtained for the different PIMs as a function of the NaCl solutions concentration ratio and, for the purpose of comparison, the theoretical values for an ideal anion-exchanger (t_+=0, solid line) and the solution

diffusion potentials (dashed line, with $t_{Na^+}°$=0.382 and $t_{Cl^-}°$=0.618, [32]). As can be observed, $\Delta\Phi_{mbr}$ values for the samples obtained with the lower percentage of the three ILs hardly differ from one another and from the solid line representing the ideal anion-exchanger in the whole range of NaCl concentrations studied. However, for the samples with high concentrations of the ILs (60%IL), differences in $\Delta_{\Phi mbr}$ values depending on the IL can be observed for solution concentrations higher than 0.04 M NaCl.

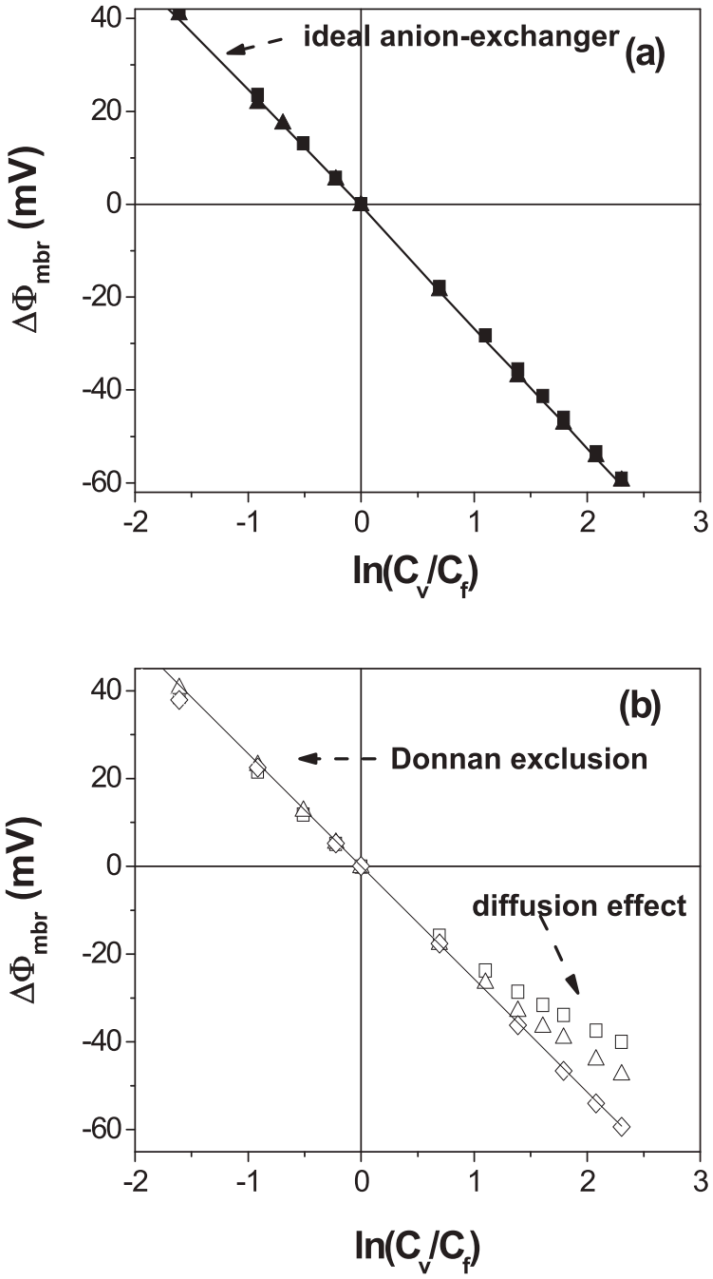

Figure 3.17 Membrane potential as a function of the NaCl variable concentration, Cv, for the studied membranes (Cf=0.01 M). (a) 30% AlqCl (■), 30% $AlqNO_3$ (▲) and 30% AlqSCN (♦); (b) 60% AlqCl (□), 60% $AlqNO_3$ (Δ) and 60% AlqSCN (◊). Membrane potential for an ideal anion-exchanger: solid line; NaCl diffusion potentials: dashed line.

The Teorell-Meyer-Sievers (TMS) model [33,34] considers membrane potentials basically as the sum of two different contributions: i) two Donnan potentials ($\Delta\Phi_{Dn}$), one at each membrane/solution interface, responsible for the exclusion of co-ions (ions with similar charges to that of the fixed charge of the membrane) from the membrane due to electrical interactions and, consequently, its effect can be reduced at high solution concentration values; ii) a diffusion potential in the membrane ($\Delta\Phi_{dif}$) caused by differences in the mobility of the ions diffusing across the membrane, and its contribution usually increases with the concentration gradient in the membrane [35,36]. Taking into account the TMS model, membrane potential results obtained for the 30% IL and the 60% AlqSCN samples seem to indicate almost total exclusion of Na^+ ions from the membranes, although the increase in the hydrophilicity of 60% AlqCl and 60% $AlqNO_3$ membranes could favour the inclusion and diffusive transport of Na^+ ions in these samples at high concentration gradients.

Conclusions

We have demonstrated that new Aliquat 336 derivatives can be successfully prepared by a liquid-liquid exchange process. These new derivatives have been used for the preparation of PIMs at two different concentrations, and the effect on the physicochemical properties of the membranes has been investigated in terms of IL composition and content. The results obtained by XPS and FTIR are in agreement with the expected membrane composition. TGA analysis has not shown differences in the initial decomposition temperature of the membranes, independently of the IL counter-anion present in the PIM. However, higher conductivity and dielectric constants were obtained for membranes containing AlqCl and $AlqNO_3$ compared with those with AlqSCN, and a significant increase in conductivity values (3 orders of magnitude) was observed when the IL concentration was changed from 30% to 60%. It is worth mentioning the differences found in the hydrophilic character of the PIMs, which follows the sequence AlqCl > $AlqNO_3$ > AlqSCN, independently of the IL content. The higher hydrophilicity of the AlqCl membranes supports the results obtained with HCl and NaCl diffusive transport measurements. Consequently, it has been shown that the characteristics of PIMs containing quaternary ammonium salts can be manipulated by varying the corresponding counter anion.

References

[1] L.D. Nghiem, P. Mornane, I.D. Potter, J.M. Perera, R.W. Cattrall, S.D. Kolev, Extraction and transport of metal ions and small organic compounds using polymer inclusion membranes (PIMs), J. Membr. Sci. 281 (2006) 7–41.

[2] C. Fontàs, R. Tayeb, M. Dhahbi, E. Gaudichet, F. Thominette, P. Roy, K. Steenkeste, M.P. Fontaine-Aupart, S. Tingry, E. Tronel-Peyroz, P. Seta, Polymer inclusion membranes: the concept of fixed sites membrane revised, J. Membr. Sci. 290 (2007) 62–72.

[3] M.I.S.G. Almeida, R.W. Cattrall, S.D. Kolev, Recent trends in transport and extraction of metal ions using polymer inclusion membranes (PIMs), J. Membr. Sci. 415–416 (2012) 9–23.

[4] C. Fontàs, R. Tayeb, S. Tingry, M. Hidalgo, P. Seta, Transport of platinum(IV) through supported liquid membrane (SLM) and polymeric plasticized membrane (PPM), J. Membr. Sci. 263 (2005) 96–102.

[5] N. Pont, V. Salvadó, C. Fontàs, Selective transport and removal of Cd from chloride solutions by polymer inclusion membranes, J. Memb. Sci. 318 (2008) 340–345.

[6] C.I. Gherasim, G. Bourceanu, R. Olariu, C. Arsene, Removal of lead(II) from aqueous solutions by a polyvinyl-chloride inclusion membrane without added plasticizer, J. Membr. Sci. 377 (2011) 167–174.

[7] A. Garcia-Rodríguez, V. Matamoros, S.D. Kolev, C. Fontàs, Development of a polymer inclusion membrane (PIM) for the preconcentration of antibiotics in environmental water samples, J. Membr. Sci. 492 (2015) 32–39.

[8] E.A. Nagul, C. Fontàs, I.D. Mckelvie, R.W. Cattrall, S.D. Kolev, The use of a polymer inclusion membrane for separation and preconcentration of orthophosphate in flow analysis, Anal. Chim. Acta 803 (2015) 82–90.

[9] R.L. Gardas, J.A.P. Coutinho, Group contribution methods for the prediction of thermophysical and transport properties of ionic liquids, AIChE J. 55 (2009).

[10] M.I. Vázquez, V. Romero, C. Fontàs, E. Anticó, J. Benavente, Polymer inclusion membranes (PIMs) with the ionic liquid (IL) Aliquat 336 as extractant: effect of base polymer and IL concentration on their physical-chemical and elastic characteristics, J. Membr. Sci. 455 (2014) 312–319.

[11] J.P. Mikkola, P. Virtanen, R. Sjöholm, Aliquat 336 – a versatile and affordable cation source for an entirely new family of hydrophobic ionic liquids, Green Chem. 8 (2006) 250–255.

[12] D. Jogelnig, A. Stojanovic, M. Galanski, M. Groessl, F. Jirsa, R. Krachler, B.K. Keppler, Greener synthesis of new ammonium ionic liquids and their potential as extracting agents, Tetrahedron Lett. 49 (2008) 2782–2785.

[13] Y. Sakai, K. Kadota, T. Hayashita, R.W. Cattrall, S.D. Kolev, The effect of the counter anion on the transport of thiourea in a PVC-based polymer inclusion membrane using Capriquat as carrier, J. Membr. Sci. 346 (2010) 250–255.

[14] I.I. Nasser, F.I.E.H. Amor, L. Donato, C. Algieri, A. Garofalo, E. Drioli, C. Ahmed, Removal and recovery of $Ag(CN)_2$ - from synthetic electroplating baths by polymer inclusion membrane containing Aliquat 336 as a carrier, Chem. Eng. J. 295 (2016) 207–217.

[15] B.N. Mahanty, P.K. Mohapatra, D.R. Raut, D.K. Das, P.G. Behere, Md Afzal, W. Verboom, Polymer inclusion membrane containing a tripodal diglycolamide (TDGA): characterization and sorption isotherm studies, JECE 4 (2016) 1826–1838.

[16] A. Manzak, Y. Yildiz, O. Tutkun, Characterization of polymer inclusion membrane containing Aliquat 336 as a carrier, Membr. Water Treat. 6 (2015) 95–102.

[17] A. Kaya, C. Onac, H.K. Alpoguz, A. Yilmaz, N. Atar, Removal of Cr(VI) through calixarene based polymer inclusion membrane from chrome plating bath water, Chem. Eng. J. 283 (2016) 141–149.

[18] R. Fortunato, C.A.M. Afonso, J. Benavente, E. Rodríguez-Castellón, J.G. Crespo, Stability of supported ionic liquid membranes as studied by X-ray photoelectron spectroscopy, J. Membr. Sci. 256 (2005) 216–223.

[19] R. Fortunato, L. Branco, C.A.M. Afonso, J. Benavente, J.G. Crespo, Electrical impedance spectroscopy characterisation of supported ionic liquid membranes, J. Mem. Sci. 270 (2006) 42–49.

[20] E. Rodríguez de San Miguel, J.C. Aguilar, J. de Gyves, Structural effects on metal ion migration across polymer inclusion membranes: dependence of transport profiles on nature of active plasticizer, J. Membr. Sci. 307 (2008) 105–116.

[21] M.J. Salar-Gacía, V.M. Ortiz-Martínez, A.P. de los Ríos, F.J. Hernández Fernández, A method based on impedance spectrocopy for predicting the behavior of novel ionic liquid-polymer inclusion membranes in microbial fuel cells, Energy 89 (2015) 648–654.

[22] J.F. Moulder, W.F. Stickl, P.E. Sobol, K.D. Bomben, Handbook of X-Ray Photoelectron Spectroscopy, Perkin-Elmer: Eden Prairie, Minneapolis (USA), 1992.

[23] D. Briggs, M.P. Seah, Practical Surface Analysis, 2 ed. Vol I: Auger and X-ray photoelectron spectroscopy, John Wiley & Sons, Chichester, England, 1995

[24] V. Romero, V. Vega, J. García, R. Zierold, K. Nielsch, V.M. Prida, B. Hernando, J. Benavente, Changes in morphology and ionic transport induced by ALD SiO2 coating of nanoporous alumina membranes, ACS Appl. Mater. Interfaces 5 (2013) 152–159.

[25] R. Güell, E. Anticó, S.D. Kolev, J. Benavente, V. Salvadó, C. Fontàs, Development and characterization of polymer inclusion membranes for the separation and speciation of inorganic As species, J. Membr. Sci. 383 (2011) 88–95.

[26] R.M. France, R.D. Short, Plasma treatment of polymers: the effects of energy transfer from an argon plasma on the surface chemistry of polystyrene, and polypropylene. A high-energy resolution X-ray photoelectron spectroscopy study, Langmuir 14 (1998) 4827.

[27] R.J. MacDonals, Impedance Spectroscopy, Wiley, New York (USA), 1987.

[28] K. Asaka, Dielectric properties of cellulose acetate reverse osmosis membranes in aqueous salt solutions, J. Membr. Sci. 50 (1990) 71–84.

[29] M. Algarra, M.I. Vázquez, B. Alonso, C.M. Casado, J. Casado, J. Benavente, Characterization of an engineered cellulose based membrane by thiol dendrimer for heavy metals removal, Chem. Eng. J. 253 (2014) 472–477.

[30] Y. Litaiem, M. Dhahb, Measurements and correlations of viscosity, conductivity and density of an hydrophobic ionic liquid (Aliquat 336) mixtures with a non-associated dipolar aprotic solvent (DMC), J. Mol. Liq. 169 (2012) 54–62.

[31] R.V. Subba Rao, P. Sivakumar, R. Natarajan, P.R. Vasudeva Rao, Effect of Aliquat 336 concentration on transportation of hydrochloric acid across supported liquid membrane, J. Radioanal. Nucl. Chem. 252 (1) (2002) 95–98.

[32] R.A. Robinson, R.H. Stokes, Electrolyte Solutions, Butterworth & Co., London (England), 1959.

[33] K.H. Meyer, J.F. Sievers, The permeability of membranes I – the theory of ionic permeability I, Helv. Chim. Acta 19 (1936) 649–664.

[34] T. Teorell, Transport phenomena in membranes, Discuss. Faraday Soc. 21 (1956) 9–26.

[35] N. Lakshminarayanaiah, Transport Phenomena in Membranes, Academic Press, New York (USA), 1969.

[36] V. Romero, M.I. Vázquez, J. Benavente, Study of ionic and diffusive transport through a regenerated cellulose nanoporous membrane, J. Membr. Sci. 433 (2013) 152–159.

3.2.3 First report on a solvent-free preparation of polymeric membranes with an ionic liquid

Abstract

A novel and environmentally-friendly procedure for the preparation of polymer inclusion membranes (PIMs) containing an ionic liquid is presented for the first time. Traditionally, PIMs are prepared by a solvent casting method and involve the use of harmful organic solvents such as chloroform or dichloromethane. Here we report a new solvent-free procedure based on a thermal-compression technique which involve the melting of the components of the PIM and the application of a high pressure to the melted specimen to form a flat-sheet film. In our study, we have tested different polymers, such as two cellulose derivatives as well as two thermoplastic polymers, polyurethane (TPU) and poli ε-caprolactone (PCL). The ionic liquid (IL) trioctylmethylammonium chloride (Aliquat 336) has been used to produce PIMs with a fixed composition of 70% polymer–30% IL (w/w). From our results, it can be stated that both TPU and PCL polymers provide successful membranes, which have been characterized by elemental analysis, thermogravimetric analysis and scanning electron microscope. Membrane stability was investigated in terms of IL leaching and it is worth mentioning the great stability of PIMs based on the polymer PCL. To test whether the properties of the IL were affected by the preparation conditions, the extraction ability of Aliquat 336 was investigated for both PCL and TPU membranes in terms of Cr(VI) extraction. Satisfactory values (90 % extraction) were obtained for both membranes tested, showing this novel procedure as a green alternative for the preparation of PIMs with ILs.

Introduction

Membrane-based processes have attracted a great attention during the last decades as a valuable alternative for many separation applications [1,2]. Among the different types of membranes, polymeric membranes incorporating ionic liquids (ILs) are under the spotlight due to the satisfactory properties of these compounds. ILs are molten salts liquid at room temperature formed by an organic cation (e.g. dialkylimidazolium, tetralkylammonium, trycaprylmethylammonium, among others) and an organic or inorganic anion. ILs exhibit certain remarkable features such as negligible vapour

pressure, high ion conductivity, low volatility, non-flammability, liquid range of up to at least 300ºC, high potential for recycling, high solvating capacity and high viscosity, etc. [3,4]. However, the use of ILs presents some limitations due to, for example, their high price for synthesis and high energy consumption for recycling, which can be overcome by including them into polymeric membranes, where a less amount of IL is required [4].

Polymer inclusion membranes (PIMs) are a type of polymeric membranes where the extractant is immobilized between the entangled chains of the membrane's base polymer. PIMs have successfully been used in different separation systems, including analytical applications [5], transport of organic compounds [6,7] as well as metallic species [8,9].

The IL trioctylmethylammonium chloride (Aliquat 336) is widely to produce membranes due to its versatility and affordability, and has successfully been employed as a cation source of a new family of hydrophobic ILs [10]. Its ability to extract anionic species has been exploited in several studies concerning either inorganic [11–15] and organic compounds [16,17].

PIMs are conventionally prepared by the solvent casting method, where the polymer and the extractant are properly dissolved in an appropriate volatile solvent, which afterwards, is let to evaporate to form a thin stable polymeric film. Another approach is the phase inversion technique, that involves several steps, such as the dissolution of the polymer and extractant in a solvent, the spreading of this solution onto a substrate, and the solvent removal by immersing the nascent membrane in water [11]. Even though the simplicity of these procedures, they present the important drawback of requiring the use of harmful organic solvents. This is the case when the polymers cellulose triacetate (CTA) or polyvinyl chloride (PVC) are used. In the first case, CTA needs solvents such as chloroform or dichloromethane (10 mL for 0.1 g of polymer) [8,18,19], whereas PVC is dissolved using tetrahydrofuran (5 mL for 0.1 g of polymer) [20,21]. These two polymers, and more recently poly(vinylidine fluoride-cohexafluoropropylene) (PVDF-HFP), which needs to be dissolved in THF, are the most employed polymers to produce PIMs.

Recent research on the preparation of polymeric membranes is focused on the use of polymers that need less harmful reagents such as the case of Pebax 1657, which can be dissolved in a mixture of ethanol and water at a high temperature [22] or in 1-butanol [23]. Membranes prepared with this polymer and the IL based on the cation 1- butyl-3-methyl imidazolium ([Bmim$^+$]) combined with different anions are obtained by the

solvent casting method, and have shown a good efficiency in terms of CO_2 separation. Besides, a review on different non-toxic solvents used for the preparation of polymeric membranes has recently been presented by Figoli et al. [24]. This review highlights the possibility to use less toxic organic solvents such as methyl or ethyl lactate, triethylphosphate, dimethyl sulfoxide or γ-butyrolactone as safer and attractive alternatives to dissolve polymers such as cellulose acetate (CA) or poly(vinylidene fluoride) (PVDF) to produce membranes for ultrafiltration, microfiltration or reverse osmosis processes.

As a further step to achieve greener separation processes based on membranes, we have explored, in this study, a new methodology avoiding the use of hazardous chemicals to prepare PIMs incorporating an IL. This methodology is based on a melt mixing followed by a thermal-compression of the different components. Melt mixing is extensively used as the processing method for the production of polymeric nanocomposites [25,26] or in the preparation of various polymer blends [27]. In our study, this technology has been investigated together with the use of eco-friendly polymers. This is the case of the thermoplastic polymers polyurethane (TPU) and poli ε-caprolactone (PCL). TPUs are linear block copolymers containing hard and soft segments. According to the manufacturer, TPU used in this work is a linear, aromatic bio-polyurethane based on specialty polyol from renewable sources (67% renewable material) with an extremely high crystallization rate and a very high thermoplasticity level. TPU polymers show a wide range of properties, making them suitable for different applications including automotive, electronics, sports goods, footwear and medical applications [28]. The polymer PCL is a biodegradable high molecular weight linear polyester derived from caprolactone monomer with a great potential to be used as an implantable biomaterial in the biomedical field [29,30]. It must be highlighted that the biodegradability of this polymer will reduce its overall environmental impact, such as the formation of microplastics, which is of a great concern nowadays. To the best of our knowledge, this is the first study on the preparation of PIMs incorporating ILs by a thermal-compression procedure.

Experimental

Reagents and solutions

The polymers CTA, cellulose acetate propionate (CAP), cellulose acetate butyrate (CAB) were purchased from Sigma-Aldrich (Steinheim, Germany). Polyurethane Pearlbond ECO D-590 (TPU) was obtained from Lubrizol (Barcelona, Spain) and poli ε-caprolactone (PCL) from Perstorp (Malmö, Sweden). Melting points, chemical structures and processing temperatures of the different polymers are depicted in Table 3.14.

Aliquat 336 (Sigma-Aldrich, Steinheim, Germany) was used as the IL to be incorporated in all polymeric membranes.

A stock solution (1000 mg L^{-1}) of Cr(VI) was obtained from the solid $K_2Cr_2O_7$ (Panreac, Barcelona, Spain) and was used to prepare working solutions containing 10 mg L^{-1} Cr(VI) at pH 4 (adjusted by using HCl (Panreac, Barcelona, Spain)). Calibration standards of Cr were prepared using Reagecon Chromium ICP standard solution. All solutions were prepared using analytical reagent grade chemicals and ultrapure water from a Milli-Q Plus water purification system (Millipore Ibérica S.A., Barcelona, Spain).

Table 3.14 Chemical structures, melting point and processing temperatures of the different polymers and the IL used for PIM preparation.

Polymer	Chemical structure	Melting point (ºC)	Processing Temperature (ºC)
CAP	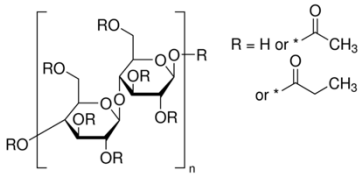	188-210	220
CAB	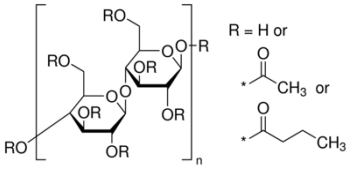	130-160	140
PCL	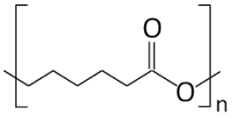	58-60	100

Polymer	Chemical structure	Melting point (ºC)	Processing Temperature (ºC)
TPU	Hard segment (4%): 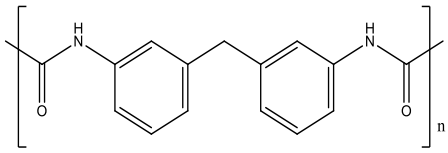 Soft segment (96%): 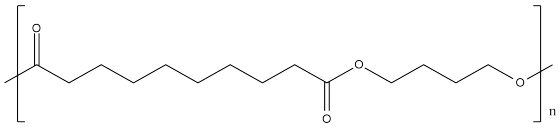	80-84	130

IL	Chemical structure	Melting point (ºC)	Processing Temperature (ºC)
Aliquat 336	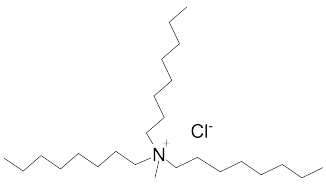	Liquid at room temperature	-

Polymeric membrane preparation

Membrane composition was fixed at 70% polymer and 30% IL (% in mass). This amount of IL has been demonstrated to provide satisfactory results in other studies [20]. Prior processing, the polymers TPU and PCL were dried in an oven at 60°C overnight, following the recommendations of the manufacturer, whereas CAP and CAB were used as received. In all cases, 2.8 g of polymer and 1.2 g Aliquat 336 were mixed by means of a mini-extruder (DSM MICRO 5 cc) under the following experimental conditions: spindle and nozzle temperature were set at the corresponding processing temperature for each polymer (see Table 3.14) and spin speed of the spindle at 100 rpm. The extruded mixture was then placed between two metallic plates (hot-press (Collin P200E)), which were warmed up to the corresponding processing temperature (see also Table 3.14) for 2 minutes before placing the blend on the two metallic plates. After this period, the extruded mixture was placed in the hot press and no pressure was applied for 3 minutes to allow the total melting of the product. An increasingly pressure of 50 bars was then applied

every 15 seconds up to 200 bars, and maintained for 2 minutes. Finally, the system was cooled down to room temperature and a flat membrane was obtained.

For comparison purposes, a membrane made of CTA was also prepared by the solvent casting method [19,31].

Membrane characterization

Elemental analysis of the PIMs was performed using a Perkin Elmer EA2400 instrument. Thermogravimetric analysis (TGA) was done using a Mettler Toledo TGA/DSC combined instrument and a sample amount of about 10 mg. The heating cycle was from 30 to 650 °C at a heating rate of 10 °C/min under nitrogen atmosphere (40 mL min^{-1}). Scanning electron microscope (SEM) images (Hitachi S-2700) were taken from both surface and cross section, obtained by cryogenic fracture, at an accelerating voltage of 15 kV. The samples were placed on a stub and coated with gold.

Membrane stability studies

The stability of the different membranes was investigated by means of mass change. For that, segments of an approximate area of 4 cm^2 (in the mass range of 0.0225 and 0.0326 g) were cut from different parts of the membrane and were placed in polypropylene vessels containing 50 mL ultrapure water, which were shaken using an orbital mixer for 24 h. Before and after the experiment, membrane segments were carefully weighted. Mass loss is calculated by using Eq. (3.6):

$$Mass\ loss\ (\%) = \frac{W_{(0)} - W_{(f)}}{W_{(0)}} \times 100 \qquad (3.6)$$

where $W_{(0)}$ is the initial membrane weight, and $W_{(f)}$ is the final membrane weight after 24 h immersed in ultrapure water. All experiments were carried out at room temperature of 22 ± 1 ºC and were run in triplicate.

Cr(VI) extraction experiments

The efficiency of the different membranes to extract Cr(VI) was investigated using membrane segments of approximately 4 cm^2 size contacted with 25 mL of 10 mg L^{-1} Cr(VI) at pH 4. These conditions ensured an excess of moles of Aliquat 336 over

about three times with regards to moles of Cr(VI) in aqueous sample. To ensure the possibility to quantitatively extract the metal, extraction efficiency (Eq. (3.7)) was evaluated by measuring the metal concentration with a sequential inductively coupled plasma atomic emission spectrometer (ICP-AES) (Liberty RL, Varian, Mulgrave, Vic., Australia).

$$Extraction\ efficiency\ (\%) = \frac{Cr(VI)_{(0)} - Cr(VI)_{(h)}}{Cr(VI)_{(0)}} \times 100 \qquad (3.7)$$

where $Cr(VI)_{(0)}$ is the initial metal in the aqueous solution and $Cr(VI)_{(h)}$ is the metal concentration in the source solution after a certain time.

All experiments were carried out at room temperature of 22 ± 1 ºC and were done by duplicate.

Results and discussion

Preparation of polymeric membranes

As stated in the introduction, PVC and CTA are widely used in the preparation of PIMs. However, both polymers present high melting temperatures and are not appropriate for the thermal-compression method due to the high temperatures required [32] that would lead to the degradation of the IL. Given this, instead of CTA, two cellulose acetate derivatives, CAP and CAB, that have also been used to produce PIMs by the solvent casting method [33,34] were selected due to their more adequate melting points. Moreover, membranes based on TPU and PCL were also tested.

The characteristics of the membranes prepared by the thermal-compression technique are collected in Table 3.15. Due to the high processing temperature needed to prepare membranes using CAP, the resulting film was not mechanically stable. Besides, the brownish colour can be related to the IL degradation. Hence, this polymer was discarded for further experiments. When CAB was employed as the base polymer, the degradation of the IL was not observed, but the resulting membranes presented an oily surface, a lack of flexibility and a brittle behaviour. The presence of oil droplets on the surface is an indicator that the IL is not completely entrapped into the polymeric matrix as a result of a low compatibility between the polymer and the IL [35]. Non-oily and flexible membranes were obtained with both polymers TPU and PCL. Taking into

account that satisfactory membranes are expected to incorporate the IL without its degradation as well as to show a mechanical strength to facilitate the manipulation of the membrane, TPU and PCL were selected as polymers to produce membranes in further experiments.

Table 3.15 Characteristics of the PIMs prepared with thermo-compression procedure.

Membrane composition (w/w)	Characteristics
70% CAP – 30% Aliquat 336	Brownish and fragile
70% CAB – 30% Aliquat 336	Oily, slightly translucent and fragile
70% PCL – 30% Aliquat 336	Non-oily, whitish, translucent and flexible
70% TPU – 30% Aliquat 336	Non-oily, whitish, translucent and flexible

Membrane characterization

Elemental analysis of TPU and PCL membranes was performed and results are presented in Table 3.16. A good agreement was found between the expected values and the experimental ones for the atomic content of C, H and N. It is important to point out that N is only present in the IL in the case of membranes prepared with PCL whereas a 4% of this atom is also present in the formulation of TPU polymer. The fact that N (%) found in the membranes corresponds to the expected values confirms that the IL has been satisfactorily incorporated in the membrane.

Table 3.16 Mass concentration of the characteristic elements of the PIM, presented as the average values percentages (n=2).

Membrane	Elements	Expected (%)	Found (%) (SD)
70% TPU – 30% Aliquat336	N	1.4	1.72 (0.04)
	C	68	67.17 (0.02)
	H	10.4	11.1 (0.2)
70% PCL – 30% Aliquat336	N	1.03	1.1 (0.2)
	C	64.2	64.4 (0.2)
	H	9.6	9.6 (0.2)

PIMs were also investigated by TGA analysis. TGA curves are presented in Figure 3.18 including both obtained for the membrane and the corresponding to the pure components. The TGA curve of the membrane 70% TPU–30% Aliquat 336 clearly shows three parts: a first decrease of the total weight loss (around 4%) at temperatures up to around 100°C, which corresponds to the loss of volatile materials and water absorbed by the membrane. Secondly, the loss starting at a temperature of 180-200ºC that can be attributed to Aliquat 336 thermal decomposition, which is also observed in the Aliquat 336 TGA curve (blue line) and represents a weight loss of 30%. Finally, the third decrease in the membrane TGA curves at temperatures over 320–330°C, which is associated to the thermal degradation of the polymer TPU. These results are in concordance with other studies where PIMs containing Aliquat 336 were prepared by solvent casting [32]. The TGA curve of the membrane 70% PCL–30% Aliquat 336 also presents three parts. However, the weight loss corresponding to the IL represents a 20% of the total value instead of the expected 30%. This result was confirmed by analysing different new segments of the membrane. This fact seems to indicate that Aliquat 336 degradation is shifted to further temperature and cannot be isolated from the polymer decomposition, likely due to some interactions in between the polymer and the IL.

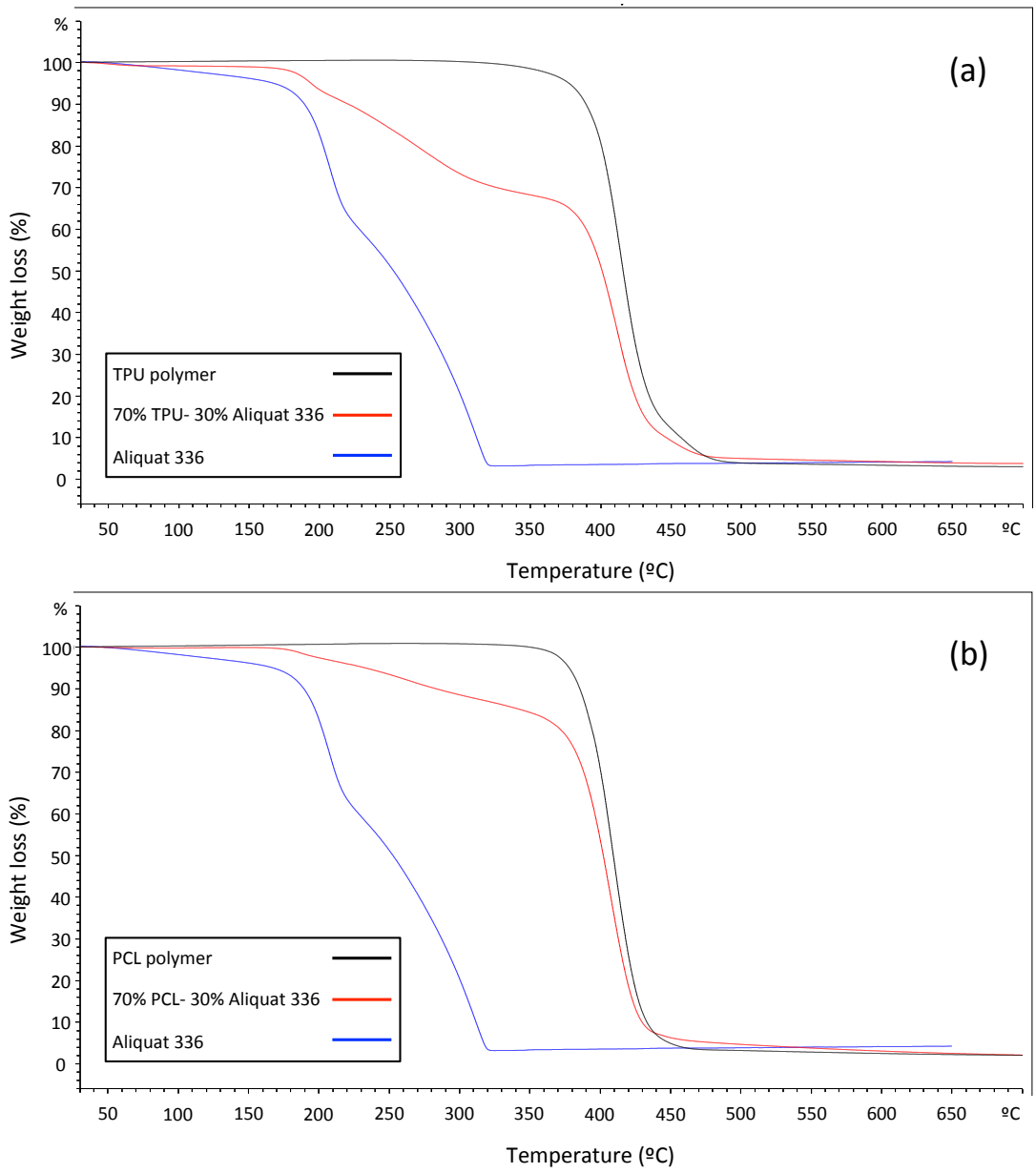

Figure 3.18 TGA curves for 70% TPU – 30% Aliquat 336 (a) and 70% PCL – 30% Aliquat 336 (b).

Morphological characterization of PIMs was performed by SEM analysis. From the surface images of both TPU (Figure 3.19a) and PCL (Figure 3.19c) membranes, it can be observed that all membranes present a uniform surface, dense and with no apparent porosity. However, cross-section images of the membranes revealed a non-homogeneous structure. In the case of TPU membranes, it can be observed a porous structure with nano-pores (Figure 3,19b), whereas a dense structure without pores but presenting some cavities (ranging from 20 up to 50 μm) are found in PCL membranes (Figure 3.19d). It is known that this later polymer forms porous membranes, also distinguishable on surface

images [29,37]. The fact that pores are not present on the surface of membranes containing an IL and prepared by thermo-compression seems to indicate a great entanglement of Aliquat 336 within the polymeric matrix, producing a dense uniform structure. However, the presence of cavities in the body of the membranes can be attributed to tiny air bubbles, which are entrapped into the highly viscous mixture during the mixing step by an extruder.

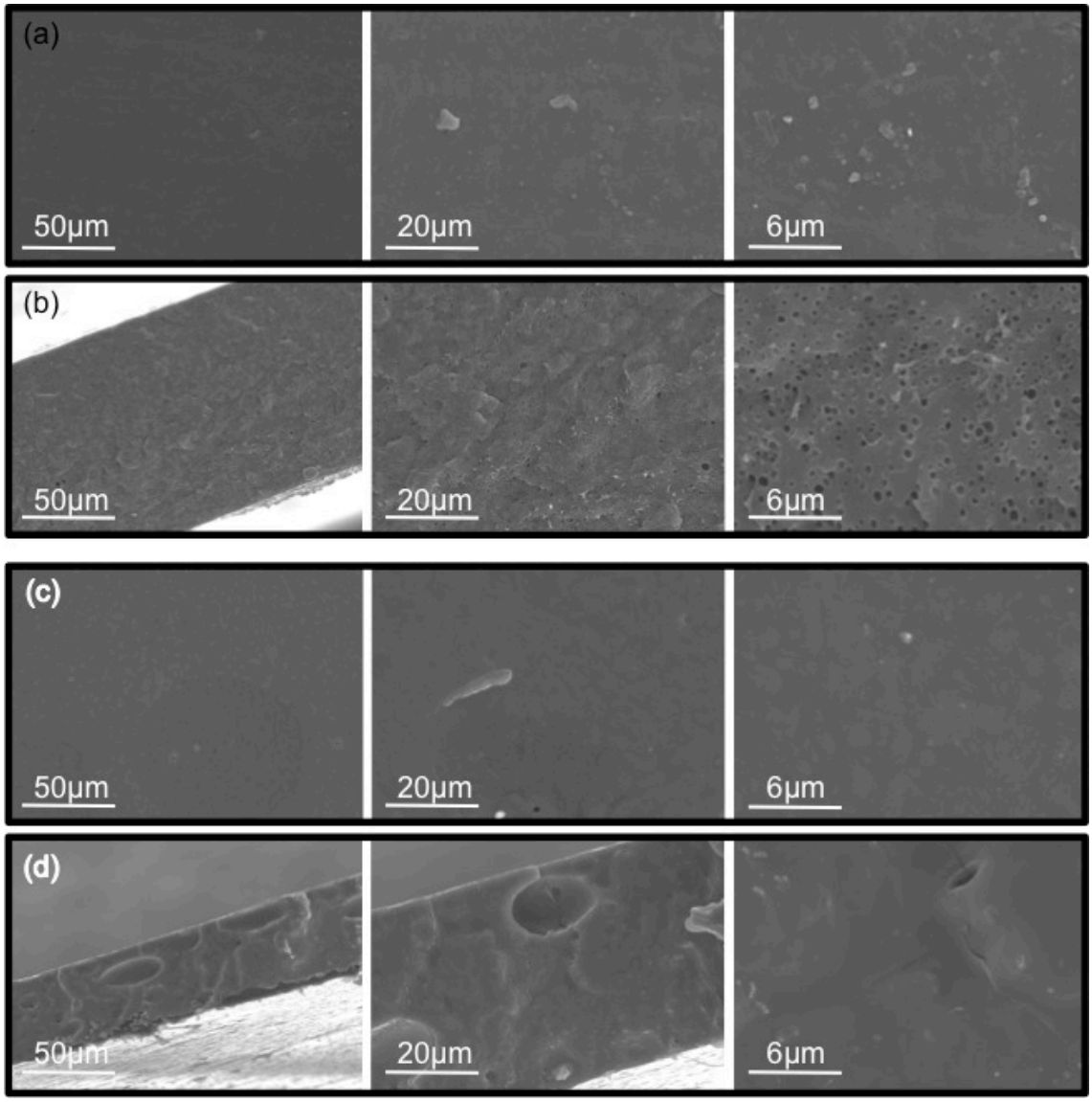

Figure 3.19 SEM images of 70% TPU – 30% Aliquat 336 surface (a), cross-section (b); 70% PCL – 30% Aliquat 336 surface (c), cross-section (d).

Stability studies

It is well-known that an important drawback of PIMs incorporating slightly soluble ILs, such it is the case of Aliquat 336, is their lack of stability due to the solubilisation of these compounds into the aqueous solutions. This fact is strongly related with the loss of efficiency of the membrane. Hence, we investigated the stability of the membranes when contacted in ultrapure water. Membrane's mass loss, which is assumed to correspond to the loss of the IL, was evaluated, and it was found that PCL-based membranes appeared to be the most stable (only a 7.1% ± 0.7 in mass variation). For TPU, the mass loss was 23% ± 2. For comparison reasons, similar experiments were conducted with a membrane composed by 70% CTA – 30% Aliquat 336 and prepared by the solvent casting method. In this case, the mass loss was 19% ± 1. Similar results were found for other PIMs containing the same IL but using PVC as the polymer [38]. The different behaviour of the IL entrapped into the PCL matrix evidences certain interactions between these two components, as it was previously observed in TGA analysis. It is important to highlight that, for the first time, we report the production of PIMs based on a biodegradable polymer using a solvent-free preparation procedure and presenting an outstanding high stability.

Testing membranes efficiency: Cr(VI) extraction

In order to assess whether the high processing temperatures required for the PIM preparation affected the performance of the IL, we tested the extraction abilities of Aliquat 336 towards Cr(VI) anions extraction. Aliquat 336 has been used in different systems such as in a hollow fiber supported liquid membrane (HFSLM) for the removal and preconcentration of Cr(VI) [39] or impregnated in different resins [40–42]. Cr(VI) extraction is based on the formation of an ion-pair, as shown in Eq. (3.8) [13,39]:

$$HCrO_4^- + [Alq^+Cl^-] \leftrightarrow [(Alq^+)\ HCrO_4^-] + Cl^- \quad (3.8)$$

where Alq^+Cl^- represents Aliquat 336.

The extraction of Cr(VI) was evaluated for both PIMs over time, and results are presented in Figure 3.20. It is noticeable the fast and efficient extraction exhibited by TPU membranes, with an extraction value of 60% in only 15 min, being 10% when the polymer was PCL. However, after 5 h of contact time a quantitative extraction was achieved in

both cases. This different behaviour at a short time period supports the fact that the IL is differently entangled depending on the polymer.

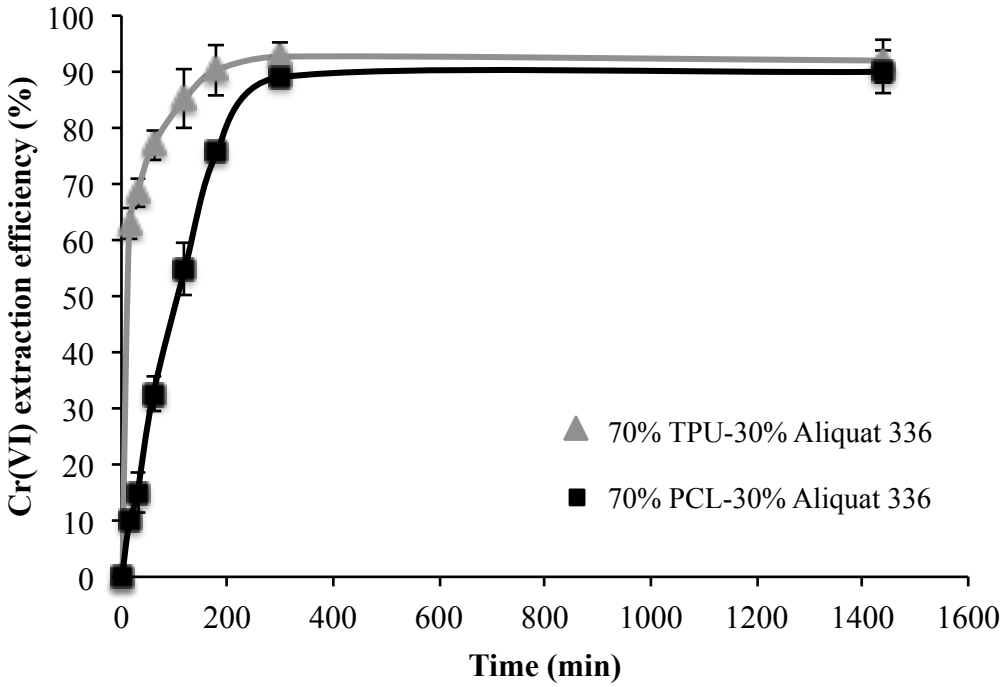

Figure 3.20 Transient Cr(VI) extraction at pH 4 using two different PIM compositions (n=2).

Conclusions

Satisfactory PIMs incorporating an IL have been prepared by a thermal-compression method, avoiding the use of harmful organic solvents. This novel procedure has led to obtain appropriate membranes based on two different thermoplastic polymers, TPU and PCL, and the IL Aliquat 336, with a fixed content of 70% polymer – 30% IL. The characterization of PIMs has revealed that Aliquat 336 was properly included within the polymeric matrix but presenting different interactions depending on the polymer. PCL membranes exhibited a higher stability and a good performance in terms of extraction efficiency, allowing the satisfactory production of high stable membranes based on a biodegradable polymer using a solvent-free preparation method.

References

[1] A.K. Pabby, S.S.H. Rizvi, A.M. Sastre, Handbook of Membrane Separations: Chemical, Pharmaceutical, Food, and Biotechnological Applications, CRC Press, Boca Raton, 2009.

[2] R.W. Baker, Membrane Technology and Applications, 2nd ed., John Wiley & Sons, Ltd., New York, 2004.

[3] R.L. Gardas, J.A.P. Coutinho, Group contribution methods for the prediction of thermophysical and transport properties of ionic liquids, AIChE J. 55 (2009) 1274–1290.

[4] J. Wang, J. Luo, S. Feng, H. Li, Y. Wan, X. Zhang, Recent development of ionic liquid membranes, Green Energy & Environ. 1 (2016) 43–61.

[5] M.I.G.S. Almeida, R.W. Cattrall, S.D. Kolev, Polymer inclusion membranes (PIMs) in chemical analysis - A review, Anal. Chim. Acta. 987 (2017) 1–14.

[6] A. Garcia, A. Alvarez, V. Matamoros, V. Salvadó, C. Fontàs, Development of polymer Inclusion membranes for the extraction of antibiotics from environmental waters, Procedia Eng. 44 (2012) 804–806.

[7] A. Garcia-Rodríguez, V. Matamoros, S.D. Kolev, C. Fontàs, Development of a polymer inclusion membrane (PIM) for the preconcentration of antibiotics in environmental water samples, J. Memb. Sci. 492 (2015) 32–39.

[8] N. Pont, V. Salvadó, C. Fontàs, Selective transport and removal of Cd from chloride solutions by polymer inclusion membranes, J. Memb. Sci. 318 (2008) 340–345.

[9] L. Nghiem, P. Mornane, I. Potter, J. Perera, R. Cattrall, S. Kolev, Extraction and transport of metal ions and small organic compounds using polymer inclusion membranes (PIMs), J. Memb. Sci. 281 (2006) 7–41.

[10] J.-P. Mikkola, P. Virtanen, R. Sjöholm, Aliquat 336®—a versatile and affordable cation source for an entirely new family of hydrophobic ionic liquids, Green Chem. 8 (2006) 250.

[11] Y. O'Bryan, R.W. Cattrall, Y.B. Truong, I.L. Kyratzis, S.D. Kolev, The use of

poly(vinylidenefluoride-co-hexafluoropropylene) for the preparation of polymer inclusion membranes. Application to the extraction of thiocyanate, J. Memb. Sci. 510 (2016) 481–488.

[12] Y. O'Bryan, Y.B. Truong, R.W. Cattrall, I.L. Kyratzis, S.D. Kolev, Electrospun polystyrene / Aliquat 336 for preconcentration and determination of thiocyanate in flow analysis, Electrospinning. (2017) 100–110.

[13] O. Kebiche-Senhadji, S. Tingry, P. Seta, M. Benamor, Selective extraction of Cr(VI) over metallic species by polymer inclusion membrane (PIM) using anion (Aliquat 336) as carrier, Desalination. 258 (2010) 59–65.

[14] A.H. Blitz-Raith, R. Paimin, R.W. Cattrall, S.D. Kolev, Separation of cobalt(II) from nickel(II) by solid-phase extraction into Aliquat 336 chloride immobilized in poly(vinyl chloride), Talanta. 71 (2007) 419–423.

[15] C. Fontàs, R. Tayeb, S. Tingry, M. Hidalgo, P. Seta, Transport of platinum (IV) through supported liquid membrane (SLM) and polymeric plasticized membrane (PPM), J. Memb. Sci. 263 (2005) 96–102.

[16] A. Garcia-Rodríguez, C. Fontàs, V. Matamoros, M.I.G.S. Almeida, R.W. Cattrall, S.D. Kolev, Development of a polymer inclusion membrane-based passive sampler for monitoring of sulfamethoxazole in natural waters. Minimizing the effect of the flow pattern of the aquatic system, Microchem. J. 124 (2016) 175–180.

[17] M. Matsumoto, A. Panigrahi, Y. Murakami, K. Kondo, Effect of ammonium- and phosphonium-based ionic liquids on the separation of lactic acid by supported ionic liquid membranes (SILMs), Membranes (Basel). 1 (2011) 98–108.

[18] R. Vera, S. Insa, C. Fontàs, E. Anticó, A new extraction phase based on a polymer inclusion membrane for the detection of chlorpyrifos, diazinon and cyprodinil in natural water samples, Talanta. 185 (2018) 291–298.

[19] R. Güell, E. Anticó, S.D. Kolev, J. Benavente, V. Salvadó, C. Fontàs, Development and characterization of polymer inclusion membranes for the separation and speciation of inorganic As species, J. Memb. Sci. 383 (2011) 88–95.

[20] C. Fontàs, R. Vera, A. Batalla, S.D. Kolev, E. Anticó, A novel low-cost detection method for screening of arsenic in groundwater., Environ. Sci. Pollut. Res. 21 (2014) 11682–8.

[21] C. Fontàs, I. Queralt, M. Hidalgo, Novel and selective procedure for Cr(VI) determination by X-ray fluorescence analysis after membrane concentration, Spectrochim. Acta - Part B At. Spectrosc. 61 (2006) 407–413.

[22] M. Li, X. Zhang, S. Zeng, L. Bai, H. Gao, J. Deng, Q. Yang, S. Zhang, Pebax-based composite membranes with high gas transport properties enhanced by ionic liquids for CO_2 separation, RSC Adv. 7 (2017) 6422–6431.

[23] E. Ghasemi Estahbanati, M. Omidkhah, A. Ebadi Amooghin, Preparation and characterization of novel Ionic liquid/Pebax membranes for efficient CO_2/light gases separation, J. Ind. Eng. Chem. 51 (2017) 77–89.

[24] A. Figoli, T. Marino, S. Simone, E. Di Nicolò, X.M. Li, T. He, S. Tornaghi, E. Drioli, Towards non-toxic solvents for membrane preparation: A review, Green Chem. 16 (2014) 4034–4059.

[25] I. González, J.I. Eguiazábal, J. Nazabal, Attaining high electrical conductivity and toughness in PA6 by combined addition of MWCNT and rubber, Compos. Part A Appl. Sci. Manuf. 43 (2012) 1482–1489.

[26] A. Granado, J.I. Eguiazábal, Poly(amino ether)/organoclay nanocomposites: Preparation and characterization, J. Appl. Polym. Sci. 132 (2015) 17–20.

[27] N. Aranburu, J.I. Eguiazábal, Compatible blends of polypropylene with an amorphous polyamide, Polym. Eng. Sci. 54 (2014) 2762–2769.

[28] U. Tayfun, M. Dogan, E. Bayramli, Effect of Surface Modification of Rice Straw on Mechanical and Flow Properties of TPU-Based Green Composites, Polym. Compos. 37 (2016) 1596–1602.

[29] S. Sánchez-González, N. Diban, A. Urtiaga, Hydrolytic degradation and mechanical stability of poly(ε-Caprolactone)/reduced graphene oxide membranes as scaffolds for in vitro neural tissue regeneration, Membranes (Basel). 8 (2018) 1–14.

[30] J. Yan, Y. Zhang, Y. Xiao, Y. Zhang, M. Lang, Novel poly(ε-caprolactone)s bearing amino groups: Synthesis, characterization and biotinylation, React. Funct. Polym. 70 (2010) 400–407.

[31] R. Vera, E. Anticó, C. Fontàs, The Use of a Polymer Inclusion Membrane for Arsenate Determination in Groundwater, Water. 10 (2018) 1093.

[32] F.W. Billmeyer, Textbook of Polymer Science, 3rd ed., Wiley, New York, 1984.

[33] A.L. Ocampo, J.C. Aguilar, E. Rodríguez de San Miguel, M. Monroy, P. Roquero, J. de Gyves, Novel proton-conducting polymer inclusion membranes, J. Memb. Sci. 326 (2009) 382–387.

[34] J.S. Gardner, J.O. Walker, J.D. Lamb, Permeability and durability effects of cellulose polymer variation in polymer inclusion membranes, J. Memb. Sci. 229 (2004) 87–93.

[35] S. Kagaya, Y. Ryokan, R.W. Cattrall, S.D. Kolev, Stability studies of poly(vinyl chloride)-based polymer inclusion membranes containing Aliquat 336 as a carrier, Sep. Purif. Technol. 101 (2012) 69–75.

[36] R. Vera, L. Gelde, E. Anticó, M.V.M. De Yuso, J. Benavente, C. Fontàs, Tuning physicochemical, electrochemical and transport characteristics of polymer inclusion membrane by varying the counter-anion of the ionic liquid Aliquat 336, J. Memb. Sci. 529 (2017) 87–94.

[37] N. Diban, S. Sánchez-González, M. Lázaro-Díez, J. Ramos-Vivas, A. Urtiaga, Facile fabrication of poly(ε-caprolactone)/graphene oxide membranes for bioreactors in tissue engineering, J. Memb. Sci. 540 (2017) 219–228.

[38] G. Argiropoulos, R. Cattrall, The study of a membrane for extracting gold (III) from hydrochloric acid solutions, J. Memb. Sci. 138 (1998) 279–285

[39] R. Güell, E. Anticó, V. Salvadó, C. Fontàs, Efficient hollow fiber supported liquid membrane system for the removal and preconcentration of Cr(VI) at trace levels, Sep. Purif. Technol. 62 (2008) 389–393.

[40] N. Kabay, Ö. Solak, M. Arda, Ü. Topal, M. Yüksel, A. Trochimczuk, M. Streat, Packed column study of the sorption of hexavalent chromium by novel solvent

impregnated resins containing aliquat 336: Effect of chloride and sulfate ions, React. Funct. Polym. 64 (2005) 75–82.

[41] B. Saha, R.J. Gill, D.G. Bailey, N. Kabay, M. Arda, Sorption of Cr(VI) from aqueous solution by Amberlite XAD-7 resin impregnated with Aliquat 336, React. Funct. Polym. 60 (2004) 223–244.

[42] N. Kabay, M. Arda, B. Saha, M. Streat, Removal of Cr(VI) by solvent impregnated resins (SIR) containing aliquat 336, React. Funct. Polym. 54 (2003) 103–115.

3.3 Novel applications of PIMs

The contents of this section are based on the following studies:

R. Vera, C. Fontàs, J. Galceran, O. Serra, E. Anticó, Polymer inclusion membrane to access Zn speciation: Comparison with root uptake, Sci. Tot. Environ. 622-623 (2018) 316-324.

R. Vera, S. Insa, C. Fontàs, E. Anticó, A new extraction phase based on a polymer inclusion membrane for the detection of chlorpyrifos, diazinon and cyprodinil in natural water samples, Talanta 185 (2018) 291-298.

3.3.1 Polymer inclusion membrane to access Zn speciation: Comparison with root uptake

Abstract

Metal speciation studies can be performed with a new technique based on a functionalized membrane. The estimation of not only the total amount of metal, but also the metal available to living organisms is very important. In this context, we have investigated the use of a polymer inclusion membrane (PIM) in a new tool for the determination of free metal ion concentration. In order to check the usefulness of PIM devices in metal speciation studies and metal availability to potato plants (*Solanum tuberosum*), Zn has been chosen as a case study. The PIM designed for Zn transport uses polyvinyl chloride (PVC) as polymer and di-(2-ethylhexyl) phosphoric acid (D2EHPA) as carrier, with 0.01M nitric acid in the receiving solution. The stability of the PIM has been demonstrated and good linearity of PIM-device fluxes (JPIM) with free metal concentration was observed for total metal concentrations ranging from 3 μM up to 70 μM. The presence of different ligands, such as ethylenediaminetetraacetic acid (EDTA), humic acid (HA) and citrate, greatly influences the measured J_{PIM} because the formation of metal complexes in the donor phase decreases the free Zn concentration in the sample. Good correlation has been found when comparing PIM fluxes and metal accumulation in potato plants roots in the presence of EDTA. But, the root uptake did not change when adding citrate and HA to the hydroponic medium, so the uptake does not always follows the Free Ion Activity Model (FIAM). These ligands might induce physiological changes in the roots and enhance metal uptake.

Introduction

Dissolved trace metals in environmental water or in pore water of soils and sediments can be found in numerous chemical forms or species, such as free ions, and inorganic or organic complexes. Metal partitioning among the different forms is a dynamic process that depends on different parameters such as type and concentration of ligands, temperature, pH or redox conditions of the medium. It has been established that for cationic metals, the concentration of the free, uncomplexed, metal ion is usually the

best predictor for both metal bioaccumulation and toxicity in most aquatic systems. This general consensus has led to the predominance of the free ion activity model (FIAM), which postulates that the metal uptake by an organism is proportional to the free ion concentration of the metal in the surrounding solution. FIAM relies on the internalisation flux being limiting, rather than the supply of the metal from the solution to the surface of the organism [1].

The biotic ligand model (BLM) is an extension of the FIAM taking into account the competitive binding of cations and protons at the surface of the biological membrane (i.e. the biotic ligand) [2]. Despite being extensively accepted, exemptions to these models have also been reported, and some studies point out that in the case of higher plants, the uptake might be favoured by the presence of organic ligands, which would facilitate the metal uptake at the roots [3-5]. Indeed, apart from internalisation of the free cation [6,7], other mechanisms can contribute to the uptake such as the direct internalisation of intact metal complexes by the organism (simple diffusion across the lipid bilayer or permeation across the lipid bilayer via a ligand transport site).

Different techniques have been developed to measure, not only metal speciation, but also to estimate labile fractions available for organisms [8,9]. This is the case of diffusive gradients in thin films (DGT) technique, for example, consisting of a porous gel matrix attached to a layer of complexing cation exchange beads (Chelex 100). DGT is nowadays widely accepted as a tool to monitor metal availability and to calculate the so-called DGT concentrations [10,11].

Permeation liquid membrane (PLM) techniques are used for the separation and preconcentration of target elements, which are complexed by an organic complexing agent supported in a membrane. This membrane separates two different aqueous solutions: the donor (also called source or feed) phase, containing the sample with the analyte, and the acceptor (also called receiving or stripping) phase, where the analyte is accumulated. The transport is based on liquid-liquid extraction coupled with diffusion. In the nineties, Buffle and Parthasarathy firstly reported PLM for speciation studies as an approach to mimic the processes of metal transport across biological membranes [12]. The metal flux across the membrane is evaluated from the variation of the metal concentration in the acceptor solution as a function of time. Under certain conditions, PLMs measure the free metal ion fraction [13], and PLM has been used as a reliable sensor for free Ni concentrations down to 10^{-7} M as reported by Bayen et al. [14]. Pb availability to freshwater algae was studied by comparing PLM fluxes and Pb biouptake

fluxes [15]. Both, the simplicity of this technique and the large number of available complexing agents render this methodology very attractive. However, a weak point is the poor stability of the membrane due to the leaching of the organic extracting compound into the aqueous adjacent phases [16]. This fact has seriously limited a wider use of PLM.

In this work, we explore for the first time the use of a simple device based on a polymer inclusion membrane (PIM) to determine free ion concentrations in aqueous samples (i.e. specifically targeting one relevant fraction of the total concentration). The principles of this system are similar to those of PLM, since the analyte is transported across the membrane, by means of the carrier, from the donor to the acceptor phase. However, to increase the stability of the membrane, this carrier is entrapped within a polymeric matrix, normally made of cellulose triacetate (CTA) or polyvinyl chloride (PVC). The role of the polymer is to provide mechanical strength to the membrane, and sometimes, besides these components, the addition of a plasticizer is also necessary to improve the elasticity as well as to modify the diffusion characteristics of the membrane [17]. This improved stability, in addition to their easy preparation, low cost, versatility, good chemical resistance and high efficiency, had led to the use of these membranes for separation or preconcentration purposes of different metals or organic compounds [18,19]. PIMs made of PVC and the carrier di-(2-ethylhexyl) phosphoric acid (D2EHPA) have been applied for the determination of the time-weighted average total concentration of Zn [20], but its use as sensor for Zn speciation has -as far as we know- not been described yet. The environmental relevance of this new sensor stems from the crucial role, as stated by FIAM and BLM, of the free ion concentration on the ecotoxicological impact of the considered element.

Zn is one of the essential trace metal micronutrients, required by plants in small amounts for various biochemical reactions and physiological functions such as formation of chlorophyll, photosynthesis and respiration [21,22]. Even though Zn deficiency is more widespread than Zn toxicity, excessive Zn accumulation affects the capacity to maintain homeostasis and can induce oxidative stress.

In this work, PIM fluxes for Zn in the absence and presence of organic ligands forming complexes with different binding strength and charge, such as EDTA, citrate, and humic acids, have been determined using as a donor phase a plant nutrient solution (i.e. a hydroponic medium). Moreover, PIM fluxes have been compared with Zn uptake by potato (*Solanum tuberosum*) roots under the same experimental conditions. Potato plants were chosen for this study because (i) potato is one of the most commonly

consumed vegetable crop worldwide, and (ii) potato plantlets were reproduced asexually using cuttings, reducing the overall variability among samples and contributing to increase the reproducibility of the experiment. Special attention is devoted to elucidate whether the PIM-based sensor (in the current conditions) are determining the free Zn concentration, rather than the total concentration or any other fraction.

Experimental

Reagents and solution

All reagents and solvents used in this study were of analytical grade. The polymer PVC, and the acid 2-(N-morpholino) ethanesulfonic (MES) were obtained from Fluka (Bern, Switzerland). The organic solvent, tetrahydrofuran (THF), was purchased from Panreac (Barcelona, Spain). The carrier, D2EHPA, was provided by Sigma-Aldrich (St Louis,Missouri, USA). For the preparation of the hydroponic solution the following reagents, purchased from Panreac (Barcelona, Spain), were used: ammonium nitrate (NH_4NO_3), boric acid (H_3BO_3), calcium nitrate ($Ca(NO_3)_2 \cdot 4H_2O$), copper sulphate ($CuSO_4 \cdot 5H_2O$), potassium nitrate (KNO_3), potassium dihydrogen phosphate (KH_2PO_4), sodium molybdate ($Na_2MoO_4 \cdot 2H_2O$), sodium hydroxide (NaOH), magnesium sulphate heptahydrate ($MgSO_4 \cdot 7H_2O$), potassium hydroxide (KOH), manganese chloride ($MnCl_2 \cdot 4H_2O$) and zinc sulphate seven hydrate ($ZnSO_4 \cdot 7H_2O$). As iron source the commercial product Kelamix Fe was used (Sicosa, Girona, Spain). Hoagland solution at half strength, used as a nutrient solution and donor medium, is described in Table 3.17. The pH of the solution was adjusted at 6.0 ± 0.1 using 2.5 mM MES. Suprapur grade nitric acid (HNO_3) was obtained from Panreac (Barcelona, Spain). Organic ligands such as L-histidine monohydrochloride monohydrate, humic acids sodium salt (HA, used as received), ethylenediaminetetraacetic acid (EDTA) were provided by Sigma-Aldrich (St Louis, Missouri, USA) and sodium citrate ($Na_3C_6H_5O_7 \cdot H_2O$) was obtained from Scharlau (Barcelona, Spain). Propidium iodide (PI) and Fluorescein di-acetate (FDA) stains were obtained from Sigma and Invitrogen (Thermo Fisher, Waltham, Massachusetts, USA).

Table 3.17 Chemical composition of the nutrient solution corresponding to a half strength Hoagland solution, used as donor medium in all the experiments performed throughout the study.

Chemical compound	Concentration (μM)
KNO_3	2500
$Ca(NO_3)_2.4H_2O$	2500
Fe (in Kelamix)	12
$MgSO_4.7H_2O$	1000
NH_4NO_3	500
KH_2PO_4	250
MES	2500
H_3BO_3	23
$MnCl_2.4H_2O$	4.57
$ZnSO_4.7H_2O$	0.38
$CuSO_4.5H_2O$	0.10
$Na_2MoO_4.2H_2O$	0.25

Calibration standards of Zn were prepared using a 1000 mg L^{-1} stock solution for atomic spectroscopy (Sigma-Aldrich, St Louis, Missouri, USA). The working range was from 0.05 mg L^{-1} to 2.5 mg L^{-1} in the donor solution and 0.3 mg L^{-1} to 15 mg L^{-1} in 0.01 M nitric acid for the analysis of the receiving phase.

Ultrapure water from a MilliQ Plus water purification system (Millipore Ibérica S.A., Madrid, Spain) was used to prepare all solutions.

Instrument and apparatus

An Ethos Plus Milestone microwave with HPR-1000/10S high-pressure rotor and temperature sensor (Sorisole, Bergamo, Italy) was employed for acid digestion of samples. A sequential inductively coupled plasma atomic emission spectrometer, ICP-OES, (Liberty RL, Varian, Mulgrave, Vic., Australia) was used to determine the total concentration of Zn (λ = 213.81 nm) in aqueous solutions and acid plant digestions. The pH values of the aqueous samples were determined with a Crison Model GLP 22 pH meter (Barcelona, Spain).

Fluorescent root plant images were obtained using an epifluorescence BX-41 Olympus microscope that was connected to a DP-73 Olympus digital camera (Olympus, Tokyo, Japan).

Membrane preparation

PIMs were prepared by dissolving 400 mg of PVC in 12 mL of THF and the resulting mixture was stirred for 2 h. Later on, the appropriate amount of carrier D2EHPA (from a 0.5 M D2EHPA solution in THF) was added to the corresponding polymeric solution and stirred again for 1 h in order to obtain the final membrane composition of 70% PVC – 30% D2EHPA or 60% PVC – 40% D2EHPA (% in mass). Finally, the resulting mixture was poured out into a 9.0 cm diameter flat bottom glass petri dish, which was set horizontally and covered loosely. The organic solvent was allowed to evaporate during 24 h at room temperature, and the resulting film (of an approximate thickness of 55 μm) was afterward carefully peeled off from the bottom of the petri dish. Reproducibility of the PIM preparation was routinely checked by means of total weight, IR spectroscopy and thickness measurements.

PIM-device experiments

The designed device (see Figure 3.21), with similarities to those previously reported [20,23] consists of a glass tube with two openings, one at the top (0.9 cm diameter) and another one at the bottom (1.8 cm diameter). The PIM was placed at the bottom opening (1.75 cm^2) and fixed with a screw cap. The opening at the top was closed with a standard screw cap and was used to fill the device with 5 mL of receiving solution. To carry out the experiments using this device, 250 mL of donor nutrient solution spiked with zinc (and organic ligands when indicated) were poured into a glass beaker placed on a magnetic stirrer. The device incorporating the membrane and receiving solution (5 mL 0.01 M HNO_3) was immersed 1 cm in the donor nutrient solution in a vertical position under stirring conditions. After the deployment period, the device was removed from the solution and the receiving solution was taken for analysis. The final concentration in the donor solution was also checked in order to verify that no depletion took place.

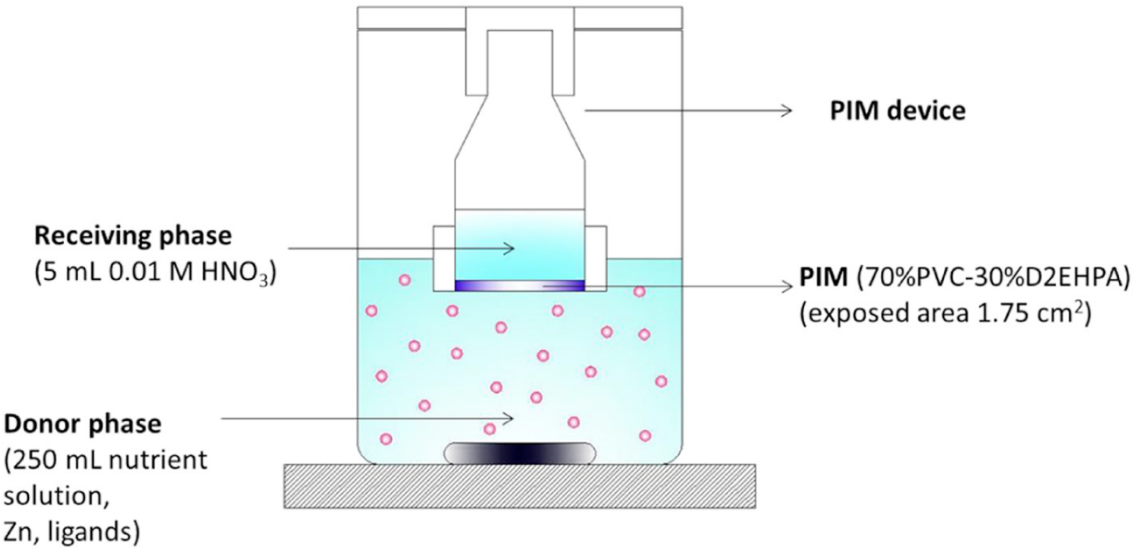

Figure 3.21 Schematics of the PIM device and the whole setup used in the experiments.

Plant growth

Potato plants (*Solanum tuberosum* cv Desireé) were grown in vitro in Murashige and Skoog solid medium (MS) supplemented with 2% sucrose [24]. 1-Node explants without leaves, using only axial gems of four week-old plants, were cultured in vitro in solid MS for three weeks in order to ensure the homogeneity among the different biological replicates. Then, they were transferred to the hydroponic media. Plants in vitro and plants in hydroponics were grown under light/dark photoperiod cycle of 12/12 h at 67 μmol m^{-2} s^{-1} and 25°C and 22°C respectively.

Plant exposure and analysis

Plant exposure to Zn and to the different organic ligands was studied following the experimental design described in Figure S3.27 (in the Supporting Information). From the in vitro plants, fourteen plants (for each treatment) were grown in ten-litter buckets of nutrient solution containing Hoagland's half strength solution (Table 3.17) during two weeks before plant exposure to the metal or the ligand. The treatments include (i) no metal addition (control experiment), (ii) fortified donor medium with 35 μM Zn (no ligand) and (iii) three Zn-fortified media each with an added specific organic ligand at a final concentration of 20 μM of EDTA, 240 μM citrate or 60 mg L^{-1} of HA. The ligand

concentrations for this study were selected so that, for a total Zn concentration of 35 μM, similar free Zn concentrations were reached in all treatments. Plants were exposed for a period of 48 h. After that, plants were removed from buckets and carefully dipped into cold water for 30 s prior to rinsing them with a 5 mM $Pb(NO_3)_2$ solution (Panreac, Barcelona, Spain) to remove Zn from the surface of the roots. Finally, plants were dried in an oven at 60 °C for 5 days [3,25]. Pools of roots from 4 plants were cut into small pieces, dried and weighted before microwave acid digestion. Then, they were transferred to PTFE vessels and digested with 8 mL of nitric acid of suprapure grade (69%) and 2 mL of hydrogen peroxide (30%). The vessels were closed and heated into the microwave following a digestion program consisting of a first step of 5 min to reach 180°C and then 10 min at 180°C. After cooling, digested sample solutions were transferred to a 30 mL flask and brought to volume with ultrapure de-ionized water prior to ICP-OES analysis.

Vital staining of roots

Once the different exposures were finished, a pool of three plants were removed from the buckets and their roots were cut and transferred directly to an aqueous solution containing 5 μg mL^{-1} of PI and 2 μg mL^{-1} of FDA for 15–30 min. The roots were then rinsed twice with water, and mounted on a microscope slide which was subsequently submerged in water [26]. The samples were viewed within 15 min from the staining with a BX-41 Olympus microscope that was connected to a DP-73 Olympus digital camera. For FDA detection, we used the excitation filter B (excitation at 475 nm and emission at 515 nm using a long path filter). For PI detection, we used the excitation filter G (excitation at 530 nm and emission at 610 nm). The same specimen was analysed separately at wavelengths specific to each stain and the two images were merged to give the final image.

Results and discussion

Evaluation of the PIM system

When speciation is of interest, the test sample composition should not be modified, and, in particular, the decrease in analyte concentration in the source solution due to membrane extraction should be negligible (*i.e.* no depletion of the analyte test

sample). These conditions are usually achieved by using a volume of the test solution much larger than the volume of the acceptor phase, e.g. using a hollow fibre geometry [27,28] or with "flowthrough" approaches [20]. Apart from the donor and acceptor volumes, the membrane composition and the acceptor phase acidity can be modulated to ensure no depletion of the analyte in the donor phase. So, we fixed an aqueous volume of 250 mL for the donor solution and of 5 mL for the acceptor solution. We evaluated the effect on metal transport and depletion when the nutrient solution (without MES added) was supplemented with 35 μM Zn(II), and tested two nitric acid concentrations of 0.01 and 0.1M in the acceptor phase and two PIM compositions. Results are presented in Table 3.18, in terms of metal concentration in both the donor and in the receiving solutions after 24 h experiment in each condition. As expected, the better the transport to the receiving solution (*i.e.* higher final concentrations in the acceptor), the larger the variation from the initial Zn concentration in the donor solution is obtained. Given that the use of a PIM made of 70% PVC – 30% D2EHPA and a 0.01 M HNO_3 receiving solution ensures the negligible depletion conditions required to perform our studies, we fixed these conditions for further experiments.

Table 3.18 Effect of PIM and receiving phase compositions on Zn transport and depletion. Contact time: 24 h.

PIM	HNO_3 (M)	Initial [Zn] donor solution (μM)	Final [Zn] donor solution (μM)	[Zn] receiving solution (μM)
70% PVC – 30% D2EHPA	0.1	35.92	35.4	60.1
	0.01	35.92	31.6	120.7
60% PVC – 40% D2EHPA	0.1	35.92	30.1	131.7
	0.01	35.92	20.8	417.7

Stability studies

It has been extensively reported that the lack of stability is the main drawback of PLM [16]. Gramlich et al. [29] described the use of a PLM in hollow fibre configuration consisting of a mixture of a Kryptofix 22DD and lauric acid as carriers dissolved in phenylhexane and toluene (1:1 v/v) as solvents for the transport of free Zn. They found a decrease in the transport capacity of the membrane down to 63% within 8 h after

impregnation. Therefore, it was necessary to use freshly impregnated membranes in all experiments (which lasted 2 h).

To study the stability of the PIM system, we evaluated the variation of Zn flux (J_{PIM} in mol m^{-2} s^{-1}) with time. For that, three experiments were performed contacting the PIM-devices with the corresponding donor solution and retrieved them at different times, from 24 to 48 h. The average flux can be calculated from the number of moles found in the acceptor phase and considering the membrane area and the deployment time. Results are collected in Figure 3.22, where it can be seen that there is not a significant variation in Zn flux for the time period studied, so one can assume the system to be under a steady-state regime [30]. Moreover, the stability of the PIM was also evaluated in terms of membrane mass loss, and it was found only a decline of 2.2 ± 0.4% of total weight after 24 h of immersion (this corresponds to 7% carrier loss).

Hence, these results support the use of PIMs as an attractive alternative to PLM, since they maintain the important features of PLMs such as simplicity, low cost and the possibility to prepare selective membranes, while providing the necessary stability to perform long-term experiments.

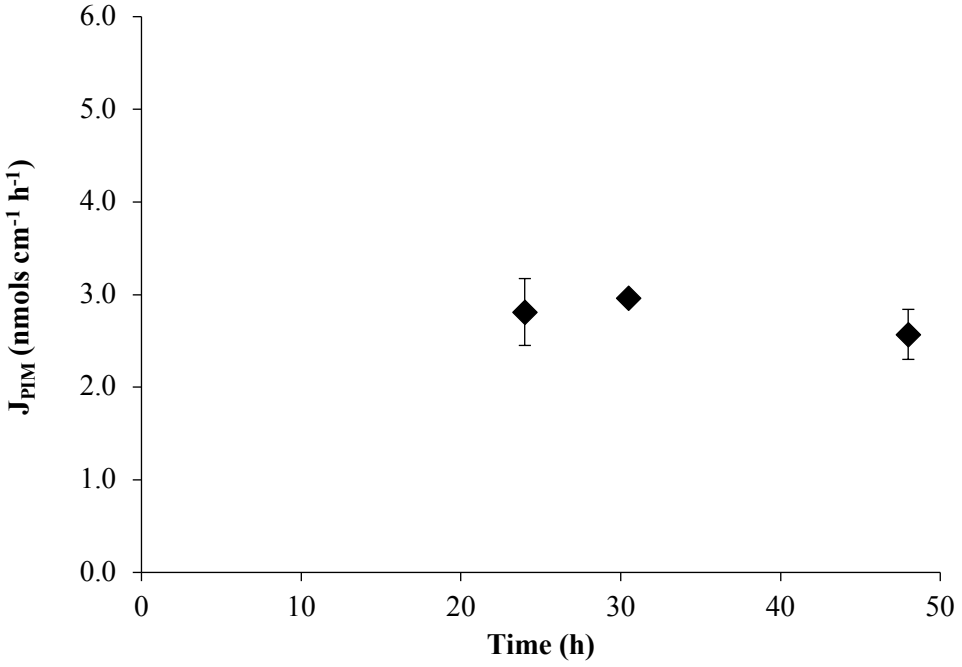

Figure 3.22 Evolution of PIM flux in front of the device deployment time. The initial concentration was 35 μM of Zn. The values show the mean ± SD (n=2).

Measurement of diffusional J_{PIM}

Several experiments were performed to measure JPIM in the absence of organic ligands. The initial total metal concentration in the nutrient solution was varied from 3 μM up to 70 μM. J_{PIM} was calculated as before and, as can be seen in Figure 3.23, it is proportional to the free Zn^{2+} concentration in the donor phase (computed using visual MINTEQ with its standard database, and neglecting the contribution of the complex Kelamix Fe [31]). The equation for a lineal model of J_{PIM} (nmol cm^{-1} h^{-1}) vs. [Zn] (μM) is:

$$J_{PIM} = 0.092(\pm 0.004)\ [Zn]_{PIM} - 0.27(\pm 0.15) \quad (3.9)$$

and $R^2 = 0.9905$.

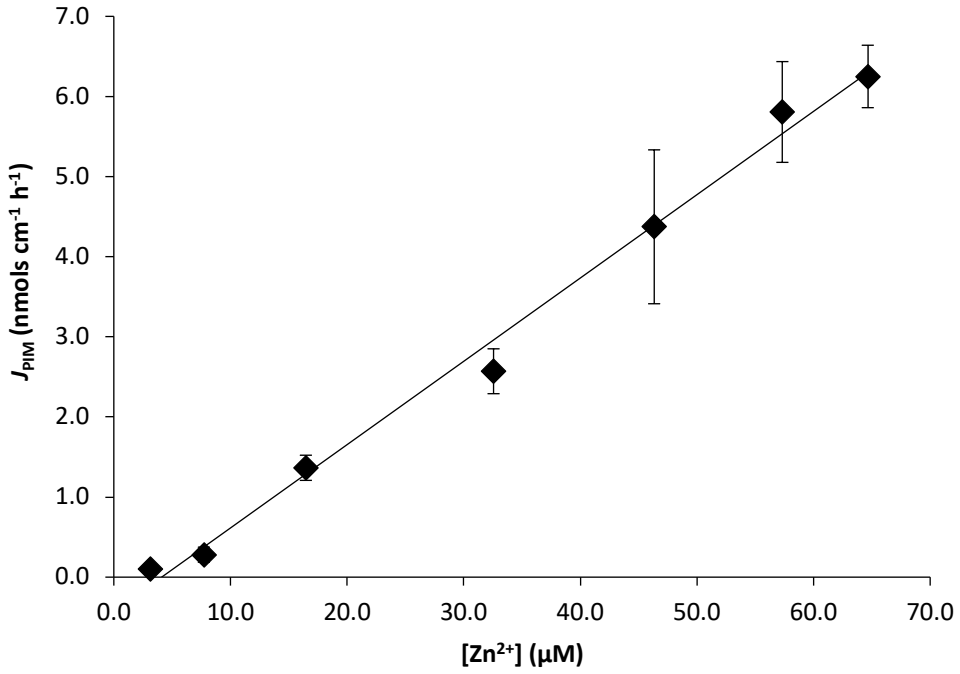

Figure 3.23 J_{PIM} at different free Zn concentrations in the donor phase added to the half strength Hoagland medium. PIM deployment time was 24 h. The values show the mean ± SD (n=3).

To test the real possibilities of PIM as a tool to measure the free ion concentrations, different organic ligands have been used in this work: EDTA, citrate and humic acid. EDTA is a polydentate ligand which forms strong complexes with metals and is used as a ligand to buffer Zn^{2+}, as Zn-EDTA is assumed to barely contribute to Zn uptake [32-34]. Citrate is involved in the storage of Zn in plant vacuoles [35]. Finally, humic acid is a part of the natural organic matter which plays an important role in aquatic

ecosystems by binding trace metals and, thus, influencing their speciation, bioavailability, and toxic effects. Thus, 20 µM of EDTA, 60 mg L^{-1} of HA or 240 µM of citrate were added to the growth medium. J_{PIM} was evaluated in the presence of these ligands at two different total metal concentrations, 35 and 70 µM. We could observe that the addition of organic ligands produced a decrease in all JPIM, which correlates with the reduction of free Zn according to visual MINTEQ calculations. $[Zn^{2+}]_{PIM}$ was determined (using the calibration provided by Figure 3.23 and plotted in Figure 3.24 together with $[Zn^{2+}]_{MINTEQ}$ and the 1:1 line on which both values should match. The good agreement found supports the claim that the sensor is measuring free Zn concentrations. Moreover, the use of PIMs as a new speciation technique (as an alternative to PLM) appears as a promising possibility.

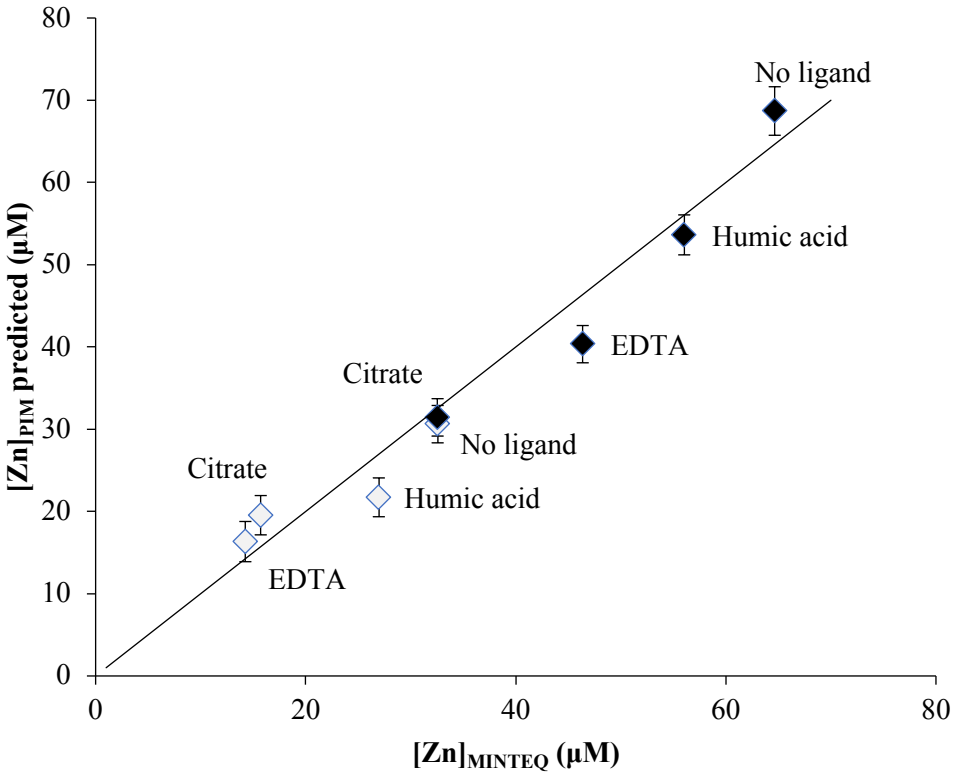

Figure 3.24 Comparison of $[Zn^{2+}]$ determined with the PIM device and the free concentration calculated with MINTEQ for several source solutions consisting of half strength Hoagland medium without and with added ligands (EDTA, HA and citrate). Deployment time was 48 h. Full symbols, 70 µM total Zn; empty symbols, 35 µM total Zn. The values show the mean ± SD (n=3). The solid line is the 1:1 along which $[Zn^{2+}]_{MINTEQ}$ would exactly match $[Zn^{2+}]_{PIM}$.

Modelling the flux of Zn

Separation by means of functionalized membranes is based on the chemical affinity of the target compound towards the ligand or functional group existing inside the membrane. In both, PLMs and PIMs, an appropriate carrier is added to the membrane to interact with the analyte, Zn^{2+} in this study. For this work, the extraction reaction of the metal by D2EHPA (denoted as HL) can be described with the following equilibrium reaction [36]:

$$Zn^{2+}_{(aq)} + 3/2\ (HL)_{2(mem)} \rightleftharpoons ZnL_2 \cdot HL_{(mem)} + 2H^{+}_{(aq)} \quad (3.10)$$

Taking into account our current data and similarly to existing literature on PLM [16], a simple model can be derived from the following hypotheses:

A) Equilibrium at both interfaces.

For the Donor/membrane (indicated as superscript D/m) interface

$$K = \frac{\left[ZnL_2 \cdot HL\right]^{D/m}\left(\left[H^+\right]^{D/m}\right)^2}{\left(\left[(HL)_2\right]^{D/m}\right)^{3/2}\left[Zn^{2+}\right]^{D/m}} \quad (3.11)$$

while for the membrane/Acceptor (indicated as superscript m/A) interface

$$K = \frac{\left[ZnL_2 \cdot HL\right]^{m/A}\left(\left[H^+\right]^{m/A}\right)^2}{\left(\left[(HL)_2\right]^{m/A}\right)^{3/2}\left[Zn^{2+}\right]^{m/A}} \quad (3.12)$$

All concentrations in these section are expressed in mol m^{-3}.

B) diffusion co-limitation of the fluxes, both in the membrane

$$J^{m} = \frac{D^{m}_{ZnL_2 \cdot HL}}{\ell}\left(\left[ZnL_2 \cdot HL\right]^{D/m} - \left[ZnL_2 \cdot HL\right]^{m/A}\right) \quad (3.13)$$

(where ℓ is the thickness of the membrane, in m, and $D^{m}_{ZnL_2 \cdot HL}$ is the diffusion coefficient, in $m^2\ s^{-1}$, of the complexed carrier inside the membrane) and in the Acceptor solution

$$J^{A} = \frac{D_{Zn^{2+}}}{\delta^{A}}\left(\left[Zn^{+}\right]^{m/A} - 0\right) \quad (3.14)$$

(where δ^{A} is the thickness of the diffusion layer in the Acceptor and $D_{Zn^{2+}}$ is the diffusion coefficient of free Zn ion there).

C) Given that the presence of labile ligands (see Figure 3.24) does not relevantly increase J_{PIM} (but rather J_{PIM} is proportional to the free Zn concentration), we assume that there is no limitation by diffusion in the Donor solution

$$\left[Zn^{2+}\right]^{D/m} \approx \left[Zn^{2+}\right]^{*} \tag{3.15}$$

where superscript * indicate the bulk concentration of the sample. This also leads to

$$\left[H^{+}\right]^{D/m} \approx \left[H^{+}\right]^{*} \tag{3.16}$$

D) Steady state is assumed taking into account the lack of variation of J_{PIM} seen in Figure 3.22. In steady-state regime, all fluxes of Zn (be it complexed or free) have to be equal to the resulting flux

$$J^{m} = J^{A} = J_{PIM} \tag{3.17}$$

Simple algebra using previous assumptions leads to

$$J_{PIM} = \frac{\dfrac{K\left(\left[(HL)_2\right]^{D/m}\right)^{3/2}}{\left(\left[H^{+}\right]^{*}\right)^{2}}}{\dfrac{\ell}{D^{m}_{ZnL_2\cdot HL}} + \dfrac{K\left(\left[(HL)_2\right]^{m/A}\right)^{3/2}}{\left(\left[H^{+}\right]^{m/A}\right)^{2}}\dfrac{D^{A}_{Zn^{2+}}}{\delta^{A}}}\left[Zn^{2+}\right]^{*} \tag{3.18}$$

In general, $\left[(HL)_2\right]^{D/m}$ and $\left[(HL)_2\right]^{m/A}$ are not constant, but depend on the loading of Zn, because of the balance of ligand, e.g. at interface Donor/membrane,

$$2\times\left[(HL)_2\right]^{D/m} + 3\times\left[ZnL_2\cdot HL\right]^{D/m} = c_{T,L} \tag{3.19}$$

where $c_{T,L}$ stands for the total D2EHPA (monomer) concentration inside the membrane.

Given the observed linear relationship between flux and free concentrations, we consider "excess of ligand" conditions, i.e. the amount of Zn bound to the carrier is approximately constant:

$$\left[\left(\mathrm{HL}\right)_2\right]^{\mathrm{D/m}} \approx \frac{c_{\mathrm{T,L}}}{2} \approx \left[\left(\mathrm{HL}\right)_2\right]^{\mathrm{m/A}} \tag{3.20}$$

Considering the fast diffusion of protons and their huge concentration (in comparison to Zn)-, one can take

$$\left[\mathrm{H^+}\right]^{\mathrm{m/A}} \approx \left[\mathrm{H^+}\right]^{\mathrm{A}}$$

With these considerations, Eq. (3.18) simplifies to

$$J_{\mathrm{PIM}} \approx \frac{\dfrac{K\left(c_{\mathrm{T,L}}/2\right)^{3/2}}{\left(\left[\mathrm{H^+}\right]^{*}\right)^2}}{\dfrac{\ell}{D^{\mathrm{m}}_{\mathrm{ZnL_2 \cdot HL}}} + \dfrac{K\left(c_{\mathrm{T,L}}/2\right)^{3/2}}{\left(\left[\mathrm{H^+}\right]^{\mathrm{A}}\right)^2}\dfrac{D^{\mathrm{A}}_{\mathrm{Zn^{2+}}}}{\delta^{\mathrm{A}}}}\left[\mathrm{Zn^{2+}}\right]^{*} \tag{3.21}$$

This expression justifies:

i) the linearity of the steady-state flux with free Zn concentration (Figures 3.23 and 3.24) and the lack of impact of labile complexes present in the donor solution. This proportionality is reflected in Eq. (3.9), where the non-null intercept can be attributed to experimental uncertainty as well as to the system having an initial transient regime not considered in Eq. (3.21);

ii) higher fluxes when the acceptor is more acidic, i.e. higher $[H^+]^A$ (in Table 3.18, for instance, in the case of 30% D2EHPA, compare the final accumulated $[Zn^{2+}]$ in the acceptor around 121 μM for 0.1 M HNO_3 with $[Zn^{2+}]$ around 60 μM for 0.01M HNO_3) and

iii) higher fluxes are expected for higher total carrier concentrations, i.e. higher $c_{T,L}$ (in Table 3.18, for instance, in the case of 0.01M HNO_3, compare the final accumulated $[Zn^{2+}]$ around 132 μM for 40% D2EHPA with [Zn] around 60 μM for 30% D2EHPA).

Apart from limitation by diffusion in both the membrane and in the acceptor solutions (as underlying Eq. (3.21)), the accumulation rate of the analyte might be

affected by other processes such as interfacial kinetics (which could become critical for low concentrations of carrier), but this is not considered here given some previous reported results with PIM [37,38] and given that the model agrees with our current data.

Further experiments varying the membrane thickness and the carrier ligand concentration over a range of values [39], can confirm or discard the present model and experimentally tune the PIM to probe the free fraction or others (such a labile one).

Toxicity of the ligands for the roots

According to the FIAM paradigm, biological fluxes are directly proportional to free metal ion concentrations rather than to the total ones [40]. This assumption has been tested using living organisms such as freshwater algae [15,41], microalgae [42] or wheat plants in hydroponics media [43]. Alternatively, fluxes measured with the different speciation techniques (PLM, DGT) have also been correlated with metal bioavailability in some systems [44]. However, it is essential to take into account the intrinsic metal and ligand toxicity before biological fluxes are measured. It has been described that metal chelates at higher concentrations may damage roots, which in turn affects metal uptake [32].

So, we performed viability analyses of the roots of potato plants growing in the different donor solution media with 35 μM Zn and supplemented with the different ligands. Distinction between viable and inviable cells was performed through a double fluorescent staining procedure. FDA is cleaved by esterases present in living cells and fluoresces green after it is cleaved. On the other hand, PI fluoresces red in the nuclei of dead cells. PI also stains most of the cell walls, viable or inviable, which means that PI staining sometimes overlaps FDA staining and appears yellow. In potato plants, young lateral roots are viable when no treatment is applied (Figure 3.25 a) and all the root tips assessed presented green colour. When 35 μM metal content was supplemented in the donor solution, roots succeeded in being stained with FDA and a green colour was obtained in root tips (Figure 3.25 b). Likewise, in treatments where 35 μM metal content and either EDTA, HA or citrate were applied as ligands, cells were metabolically active and thus, green colour was also predominant (Figure 3.25 c–e). Lateral roots treated with the same amount of Zn and histidine ligand, failed to stain with FDA, but were stained with PI (red), suggesting that the cells die as a consequence of the treatment (see Figure 3.25f). Therefore, measurements with histidine as a ligand were not reported in

previous section *Measurement of diffusional J_{PIM}*, and also not considered in what follows.

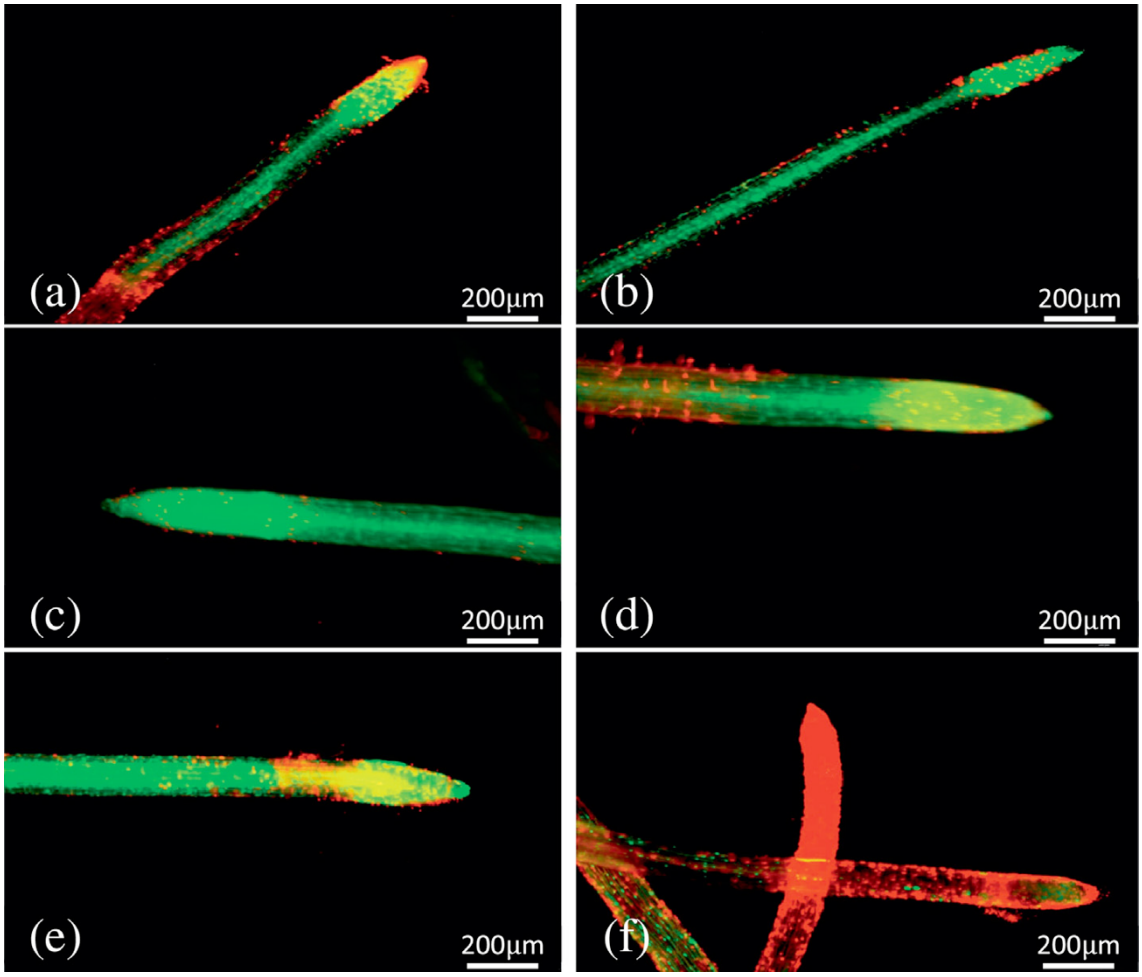

Figure 3.25 Representative epifluorescent micrographs of roots stained with FDA (green nuclei) showing the living cells and PI (red nuclei) showing the dead cells after different treatments: control with no Zn added (a) and 35 µM of Zn content (b) supplemented with 20 µM EDTA (c), 60mg L^{-1} of HA (d), 240 µM citrate (e) and 20 µM of histidine (f).

Plant metal uptake and comparison with J_{PIM}

Predicting availability of metals to plants is a challenge that has been addressed using different approaches. For example, in the case of soil fertility evaluation and risk assessment of soil contaminants, diethylenetriaminepentaacetic acid (DTPA)-extracts and $CaCl_2$ (0.01 M) extractable concentrations are commonly used [45-47]. Moreover, models based on a mechanistic approach have been employed to describe uptake of major nutrients and micro-nutrients, such as Mn and Zn [48,49]. Additionally, DGT and PLM

techniques have been suggested as tools to predict metal bioavailability and different studies have been reported. The limiting transport steps in PLMs and biological plasma membranes have been compared [16,50]. Despite being the transport processes in the test solution almost identical for living organisms and PLM setup, the size and geometry of the systems clearly differ. Also, relevant differences may arise in the transport steps at the water membrane interface or inside the membrane, despite being conceptually similar processes: the nature of the binding sites is different, multistep processes usually account for the transport in biological membranes, and passive diffusion of lipophilic complexes is differently affected by the viscosity and other physical parameters. In any case, PLM has been used to test the FIAM model, and considering the advantages of PIMs compared to PLM, we have performed a series of experiments devoted to compare J_{PIM} with fluxes in plant roots. Thus, the accumulated Zn in the roots was measured and "normalized" fluxes (J_{root}) were computed by using the dry weight of the roots instead of an area. Zn fluxes obtained were in the range 0.56 ± 0.05–1.10 ± 0.05 nmol mg^{-1} h^{-1}. A control experiment with no Zn supplementation, showed also some metal uptake (0.12 ± 0.02 nmol mg^{-1} h^{-1}) due to the presence of just a trace amount of Zn in the donor solution.

The normalized biological fluxes are shown in Figure 3.26 for the different treatments. An ANOVA test was performed and significant differences ($p = 1.92 \times 10^{-10}$) were found among the treatments. As can be seen, in the treatment with EDTA, the obtained root plant uptake was lower compared to the treatment without ligand, which supports that the total concentration of Zn in the solution is not the best indicator for uptake. This tendency can also be observed in Figure S3.28 (Supporting Information), where normalized J_{root}-values are represented in front of J_{PIM}. In the presence of HA and citrate, the found root fluxes are practically identical to the fluxes without ligand. Similar results for citrate were found by other authors [3] and were attributed to the high lability and mobility of these metal-organic complexes that dissociate in the vicinity of the root surface. The direct uptake of undissociated complexes has also been reported. In these situations, FIAM would not apply (*i.e.* the uptake is not proportional to the free concentration).

In the case of HA, we have observed the formation of lateral roots (Figure S3.29 in the Supporting Information), which in turn would increase the exchange area and would yield a metal uptake higher than expected. Moreover, the adsorption of humic substances into biological surfaces can increase their negative surface charge and, thus, enhance their overall electrostatic attraction for cations [6]. The increase of cell

permeability in the presence of humic acids can contribute to metal internalisation as described in Samson and Visser [4], Slaveykova et al. [51] and Vigneault et al. [52]. For higher plants as spinach or wheat, deviations from the FIAM have repeatedly been reported [3,50] pointing out that metal uptake in roots is highly dependent on many factors, such as the plant species, metal concentration and the rate of dissociation of metal complexes, among others.

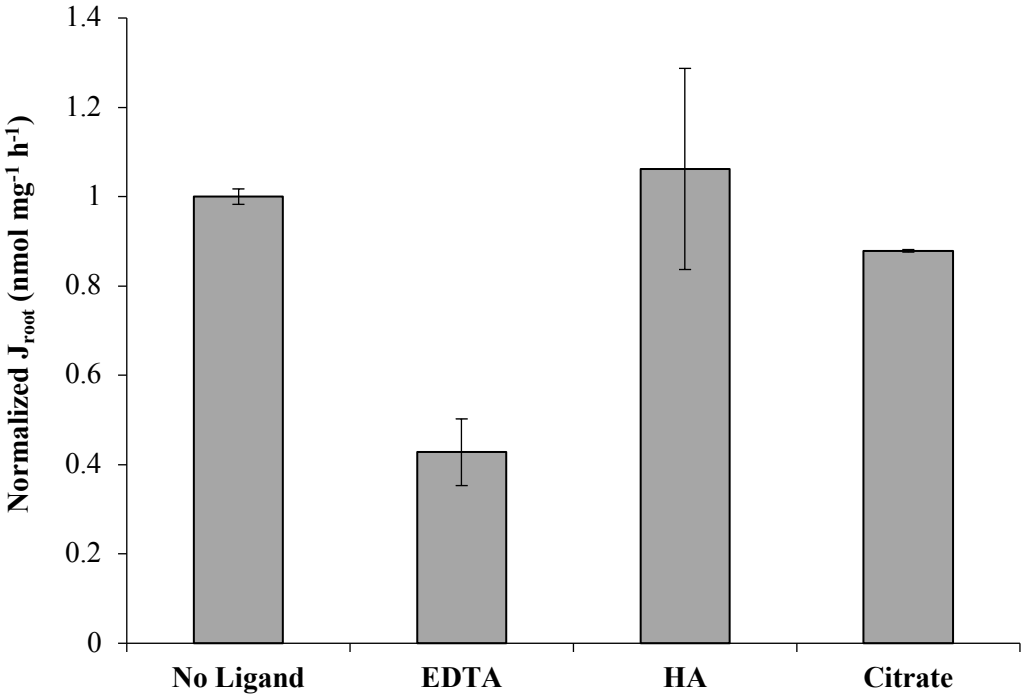

Figure 3.26 Comparison of normalized root fluxes (35 μM Zn treatment and supplemented with EDTA, HA and citrate as ligands). Deployment time was 48 h. The values show the mean ± SD (n=3).

Conclusions

In this study we have developed a simple technique based on a polymer inclusion membrane to assess Zn speciation in a complex nutrient solution. The stability of this type of membrane is substantially improved, rendering this technique suitable for (relatively) long speciation experiments. When a PIM made of 70% CTA and 30% D2EHPA is incorporated in a special device and a 0.01M HNO_3 solution is used as an accep- tor phase, a correlation is found with the free metal, both in absence and in presence of ligands (EDTA, citrate and HA). This correlation is the basis for PIM to

determine [Zn^{2+}] and has been justified with a model consistent with existent evidences. We have also evidenced the need to consider viability and physiological changes of the roots prior to study metal internalisation. Additionally, when comparing J_{PIM} and metal uptake by potato plant roots, different behaviours arise depending on the ligand. In the case of Zn-citrate and Zn-HA complexes we have observed a direct proportionality between total metal and root uptake. However, in the case of EDTA, this relationship is observed for free metal.

References

[1] K.J. Wilkinson, J. Buffle, Critical evaluation of physicochemical parameters and processes for modelling the biological uptake of trace metals in environmental (aquatic) systems. In: H.P. Van Leeuwen, W. Köster (Eds.), Physicochemical Kinetics and Transport at Biointerfaces. John Wiley & Sons, Chichester (UK), 2004, pp. 447–533.

[2] D.M. Di Toro, H.E. Allen, H.L. Bergman, J.S. Meyer, P.R. Paquin, R.C. Santore, Biotic ligand model of the acute toxicity of metals. 1. Technical basis, Environ. Toxicol. Chem. 20 (2001) 2383–2396.

[3] A. Gramlich, S. Tandy, E. Frossard, J. Eikenberg, R. Schulin, Availability of zinc and the ligands citrate and histidine to wheat: does uptake of entire complexes play a role?, J. Agric. Food Chem. 61 (2013) 10409–10417.

[4] G. Samson, S.A. Visser, Surface-active effects of humic acids on potato cell membrane properties, Soil Biol. Biochem. 21 (1989) 343–347.

[5] P. Wang, D.M. Zhou, X.S. Luo, L.Z. Li, Effects of Zn-complexes on zinc uptake by wheat (Triticum aestivum) roots: a comprehensive consideration of physical, chemical and biological processes on biouptake, Plant Soil 316 (2009) 177–192.

[6] C.M. Zhao, P.G.C. Campbell, K.J. Wilkinson, When are metal complexes bioavailable?, Environ. Chem. 13 (2016) 425–433.

[7] F. Degryse, E. Smolders, D.R. Parker, Metal complexes increase uptake of Zn and Cu by plants: implications for uptake and deficiency studies in chelator-buffered solutions, Plant Soil 289 (2006) 171–185.

[8] J. Sierra, N. Roig, G. Giménez Papiol, E. Pérez-Gallego, M. Schumacher, Prediction of the bioavailability of potentially toxic elements in freshwaters. Comparison between speciation models and passive samplers, Sci. Total Environ. 605–606 (2017) 211–218.

[9] A.M. Jones, Y. Xue, A.S. Kinsela, K.M. Wilchen, R.N. Collins, Donnan membrane speciation of Al, Fe, trace metals and REE in coastal lowland acid sulfate soil-impacted drainage waters, Sci. Total Environ. 547 (2016) 104–113.

[10] W. Davison (Ed.), Diffusive Gradients in Thin-films for Environmental Measurements, Cambridge Environmental Chemistry Series. Cambridge University Press, Cambridge (UK), 2016.

[11] W. Davison, H. Zhang, In situ speciation measurements of trace components in natural waters using thin-film gels, Nature 367 (1994) 546–548.

[12] N. Parthasarathy, J. Buffle, Capabilities of supported liquid membranes for metal speciation in natural waters: application to copper speciation, Anal. Chim. Acta 284 (1994) 649–659.

[13] M. Pesavento, G. Alberti, R. Biesuz, Analytical methods for determination of free metal ion concentration, labile species fraction and metal complexation capacity of environmental waters: a review, Anal. Chim. Acta 631 (2009) 129–141.

[14] S. Bayen, K.J. Wilkinson, J. Buffle, The permeation liquid membrane as a sensor for free nickel in aqueous samples, Analyst 132 (2007) 262–267.

[15] V.I. Slaveykova, N. Parthasarathy, J. Buffle, K.J. Wilkinson, Permeation liquid membrane as a tool for monitoring bioavailable Pb in natural waters, Sci. Total Environ. 328 (2004) 55–68.

[16] J. Buffle, N. Parthasarathy, L. Djane, L. Matthiasson, Permeation liquid membranes for field analysis and speciation of trace compounds in waters. In: J. Buffle, G. Hoarvai (Eds.), In Situ Monitoring of Aquatic Systems; Chemical Analysis and Speciation. John Wiley & Sons, West Sussex (UK), 2000, pp. 407–493.

[17] M.I.G.S. Almeida, R.W. Cattrall, S.D. Kolev, Recent trends in extraction and transport of metal ions using polymer inclusion membranes (PIMs), J. Membr. Sci. 415–416 (2012) 9–23.

[18] A. Garcia-Rodríguez, V. Matamoros, S.D. Kolev, C. Fontàs, Development of a polymer inclusion membrane (PIM) for the preconcentration of antibiotics in environmental water samples, J. Membr. Sci. 492 (2015) 32–39.

[19] R. Güell, E. Anticó, S.D. Kolev, J. Benavente, V. Salvadó, C. Fontàs, Development and characterization of polymer inclusion membranes for the separation and speciation of inorganic As species, J. Membr. Sci. 383 (2011) 88–95.

[20] M.I.G.S. Almeida, C. Chan, V.J. Pettigrove, R.W. Cattrall, S.D. Kolev, Development of a passive sampler for Zinc(II) in urban pond waters using a polymer inclusion membrane, Environ. Pollut. 193 (2014) 233–239.

[21] A. Humayan Kabir, A.M. Swaraz, J. Stangoulis, Zinc-deficiency resistance and biofortification in plants, J. Plant Nutr. Soil Sci. 177 (2014) 311–319.

[22] T. Remans, K. Opdenakker, Y. Guisez, R. Carleer, H. Schat, J. Vangronsveld, A. Cuypers, Exposure of Arabidopsis thaliana to excess Zn reveals a Zn-specific oxidative stress signature, Environ. Exp. Bot. 84 (2012) 61–71.

[23] M.I.G.S. Almeida, A.M.L. Silva, R.A. Coleman, V.J. Pettigrove, R.W. Cattrall, S.D. Kolev, Development of a passive sampler based on a polymer inclusion membrane for total ammonia monitoring in freshwaters, Anal. Bioanal. Chem. 408 (2016) 3213–3222.

[24] O. Serra, M. Soler, C. Hohn, V. Sauveplane, F. Pinot, R. Franke, L. Schreiber, S. Prat, M. Molinas, M. Figueras, CYP86A33-targeted gene silencing in potato tuber alters suberin composition, distorts suberin lamellae, and impairs the periderm's water barrier function, Plant Physiol. 149 (2008) 1050–1060.

[25] A.N.N. Cuypers, J. Vangronsveld, H. Clijsters, Peroxidases in roots and primary leaves of Phaseolus vulgaris copper and zinc phytotoxicity: a comparison, J. Plant Physiol. 159 (2002) 869–876.

[26] L.C. John, P.L. Grisafi, G.R. Fink, A pathway for lateral root formation in Arabidopsis thaliana, Genes Dev. 9 (1995) 2131–2142.

[27] L. Tomaszewski, J. Buffle, J. Galceran, Theoretical and analytical characterization of a flow-through permeation liquid membrane with controlled flux for metal speciation measurements, Anal. Chem. 75 (2003) 893–900.

[28] V.I. Slaveykova, I.B. Karadjova, M. Karadjov, D.L. Tsalev, Trace metal speciation and bioavailability in surface waters trace metal speciation and bioavailability in surface waters of the Black Sea coastal area evaluated by HF-PLM and DGT, Environ. Sci. Technol. 43 (2009) 1798–1803.

[29] A. Gramlich, S. Tandy, V.I. Slaveykova, A. Duffner, R. Schulin, The use of permeation liquid membranes for free zinc measurements in aqueous solution, Environ. Chem. 9 (2012) 429–437.

[30] J. Galceran, J. Puy, Interpretation of diffusion gradients in thin films (DGT) measurements: a systematic approach, Environ. Chem. 12 (2015) 112–122.

[31] F. Yunta, S. García-Marco, J.J. Lucena, M. Gómez-Gallego, R. Alcázar, M.A. Sierra, Chelating agents related to ethylenediamine bis(2-hydroxyphenyl)acetic acid (EDDHA): synthesis, characterization, and equilibrium studies of the free ligands and their Mg^{2+}, Ca^{2+}, Cu^{2+}, Fe^{3+} chelates, Inorg. Chem. 42 (2003) 5412–5421.

[32] P.F. Bell, M.J. Mclaughlin, G. Cozens, D.P. Stevens, G. Owens, H. South, Plant uptake of 14 C-EDTA, 14C-Citrate, and 14C-Histidine from chelator-buffered and conventional hydroponic solutions, Plant Soil 253 (2003) 311–319.

[33] J. Hart, W. Norvell, R. Welch, L. Sullivan, L. Kochian, Characterization of zinc uptake, binding, and translocation in intact seedlings of bread and durum wheat cultivars, Plant Physiol. 118 (1998) 219–226.

[34] S.P. Stacey, M.J. McLaughlin, I. Çakmak, G.M. Hettiarachchi, K.G. Scheckel, M. Karkkainen, Root uptake of lipophilic zinc - rhamnolipid complexes, J. Agric. Food Chem. 56 (2008) 2112–2117.

[35] P.J. White, M.R. Broadley, Biofortification of crops with seven mineral elements often lacking in human diets- iron, zinc, copper, calcium, magnesium, selenium and iodine, New Phytol. 182 (2009) 49–84.

[36] S.D. Kolev, Y. Baba, R.W. Cattrall, T. Tasaki, N. Pereira, J.M. Perera, G.W. Stevens, Solid phase extraction of zinc(II) using a PVC-based polymer inclusion membrane with di (2-ethylhexyl) phosphoric acid (D2EHPA) as the carrier. Talanta 78 (2009) 795–799.

[37] C. Fontàs, R. Tayeb, M. Dhahbi, E. Gaudichet, F. Thominette, P. Roy, K. Steenkeste, M.P. Fontaine-Aupart, S. Tingry, E. Tronel-Peyroz, P. Seta, Polymer inclusion membranes: the concept of fixed sites membrane revised, J. Membr. Sci. 290 (2007) 62–72.

[38] S.D. Kolev, A.M St John, R.W. Cattrall, Mathematical modeling of the extraction of uranium(VI) into a polymer inclusion membrane composed of PVC and di-(2-ethylhexyl) phosphoric acid, J. Membr. Sci. 425–426 (2013) 169–175.

[39] H.P. Van Leeuwen, R. Town, J. Buffle, R. Cleven, W. Davison, J. Puy, W. Van Riemsdijk, L. Sigg, Dynamic speciation analysis and bioavailability of metals in aquatic systems, Environ. Sci. Technol. 39 (2005) 8545–8556.

[40] P.G.C. Campbell, Interactions between tracemetals and aquatic organisms: a critique of the free-ion activity model. In: A. Tessier, D. Turner (Eds.), Metal Speciation and Bioavailability in Aquatic Systems. vol. 3. John Wiley & Sons, Chichester (UK), 1995, pp. 45–102.

[41] S. Bayen, I. Worms, N. Parthasarathy, K. Wilkinson, J. Buffle, Cadmium bioavailability and speciation using the permeation liquid membrane, Anal. Chim. Acta 575 (2006) 267–273.

[42] E.A. Rodríguez-Morales, E.R. De SanMiguel, J. De Gyves, Evaluation of the measurement of Cu(II) bioavailability in complex aqueousmedia using a hollow-fiber supported liquid membrane device (HFSLM) and two microalgae species (Pseudokirchneriella subcapitata and Scenedesmus acutus), Environ. Pollut. 206 (2015) 712–719.

[43] A. Gramlich, S. Tandy, E. Frossard, J. Eikenberg, R. Schulin, Diffusion limitation of zinc fluxes into wheat roots, PLM and DGT devices in the presence of organic ligands, Environ. Chem. 11 (2014) 41–50.

[44] P. Bradac, R. Behra, L. Sigg, Accumulation of cadmiumin periphyton under various freshwater speciation conditions, Environ. Sci. Technol. 43 (2009) 7291–7296.

[45] W.L. Lindsay, W.A. Norvell, Development of a DTPA soil test for zinc, iron, manganese, and copper, Soil Sci. Soc. Am. J. 42 (1978) 421–428.

[46] E. Meers, R. Samson, F.M.G. Tack, A. Ruttens, M. Vandegehuchte, J. Vangronsveld, M.G. Verloo, Phytoavailability assessment of heavy metals in soils by single extractions and accumulation by Phaseolus vulgaris, Environ. Exp. Bot. 60 (2007) 385–396.

[47] N.W. Menzies, M.J. Donn, P.M. Kopittke, Evaluation of extractants for estimation of the phytoavailable trace metals in soils, Environ. Pollut. 145 (2007) 121–130.

[48] T. Adhikari, R.K. Rattan, Modelling zinc uptake by rice crop using a Barber-Cushman approach, Plant Soil 227 (2000) 235–242.

[49] U.S. Sadana, N. Claassen, Manganese dynamics in the rhizosphere and Mn uptake by different crops evaluated by a mechanistic model, Plant Soil 218 (2000) 233–238.

[50] F. Degryse, E. Smolders, H. Zhang, W. Davison, Predicting availability of mineral elements to plants with the DGT technique: a review of experimental data and interpretation by modelling, Environ. Chem. 6 (2009) 198–218.

[51] V.I. Slaveykova, K.J. Wilkinson, A. Ceresa, E. Pretsch, Role of fulvic acid on lead bioaccumulation by Chlorella kesslerii, Environ. Sci. Technol. 37 (2003) 1114–1121.

[52] B. Vigneault, A. Percot, M. Lafleur, P.G.C. Campbell, Permeability changes in model and phytoplankton membranes in the presence of aquatic humic substances, Environ. Sci. Technol. 34 (2000) 3907–3913.

Supplementary data

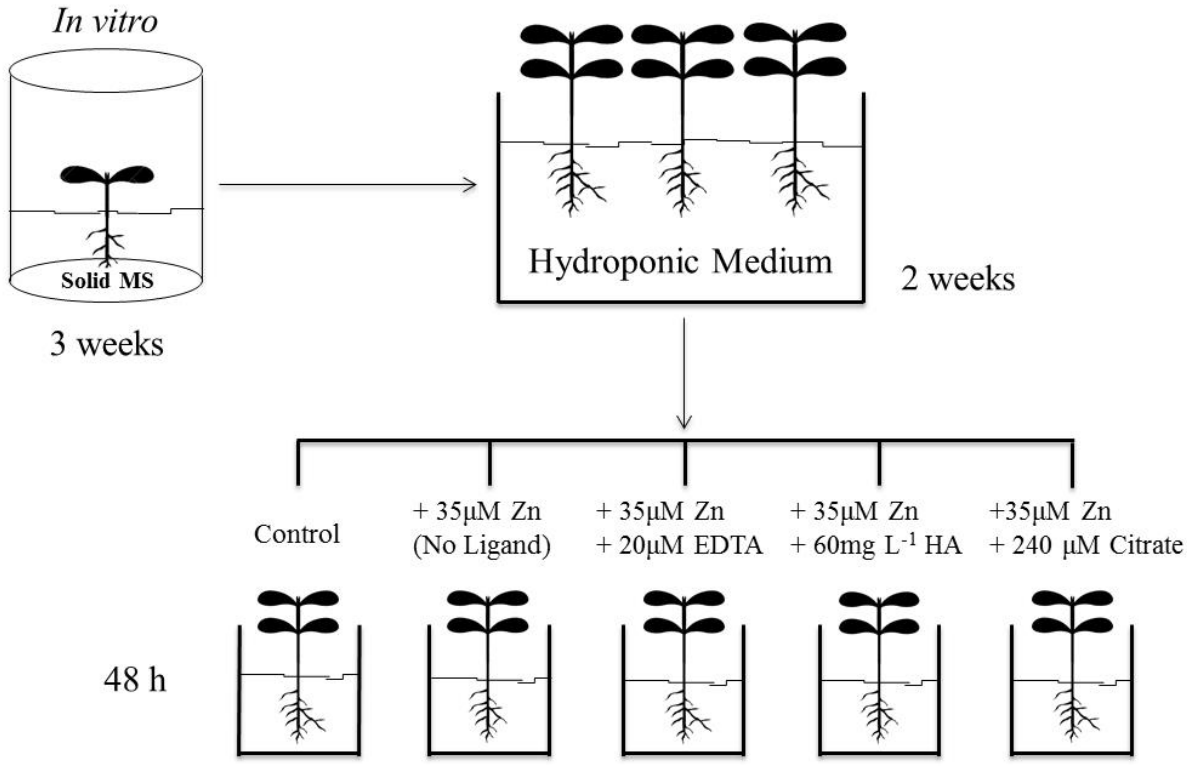

Figure S3.27 Scheme of the experimental design showing the applied treatments (i.e. different donor hydroponic media for the final exposure). MS: Murashige and Skoog solid medium.

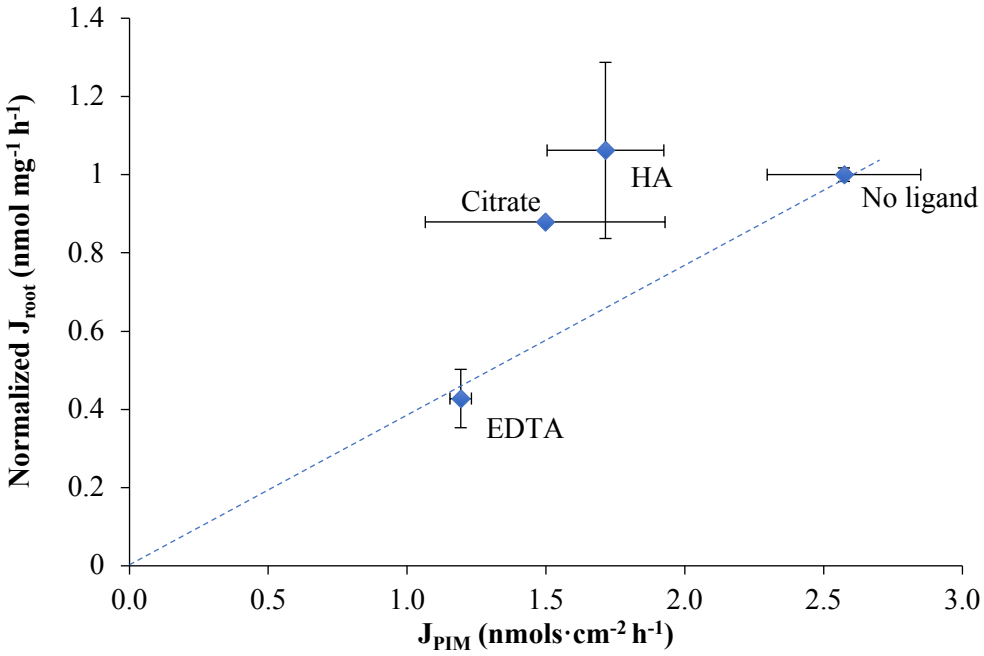

Figure S3.28 Correlation between normalized root fluxes and J_{PIM} (35 µM Zn treatment and supplemented with EDTA, HA and citrate as ligands). Deployment time was 48 h. The values

show the mean ± SD (n=3). The dashed line was plotted to join those points for which both J_{PIM} and J_{roots} are expected to be proportional to the free Zn concentration.

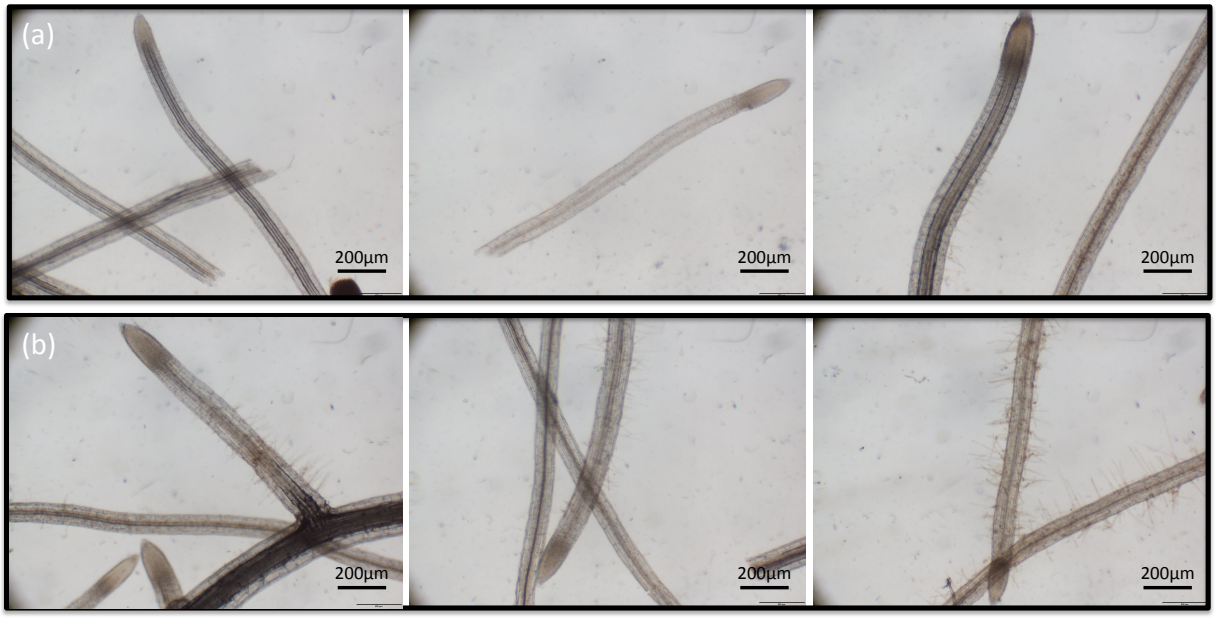

Figure 3.29 Bright field representative micrographs of potato roots grown in hydroponics media supplemented with 35 µM Zn in absence (a) or presence of 60 mg L^{-1} humic acids (b). Note the high abundance of hair cells when humic acids are present in the medium. Scale bar corresponds to 200 µm.

3.3.2 A new extraction phase based on a polymer inclusion membrane for the detection of chlorpyrifos, diazinon and cyprodinil in natural water samples

Abstract

A simple and effective method for the detection of three pesticides (chlorpyrifos, diazinon and cyprodinil) is developed using a polymer inclusion membrane (PIM) prior to gas chromatography and mass spectrometry detection (GC-MS). Analytes are extracted from natural water samples using a 3 cm^2 PIM made of the polymer, cellulose triacetate (CTA), and the plasticizer, nitrophenyl octyl ether (NPOE). Addition of the plasticizer to the CTA matrix is found to be necessary for the extraction of pesticides. After extraction, analytes are recovered from the membrane with 1 mL of acetonitrile and injected into the GC-MS system. The main factors affecting the extraction efficiency are evaluated, including membrane composition, stirring mode, extraction and elution time. Ultrasonic assisted elution of the extracted pesticides is accomplished after 15 min of contact. The PIM assisted extraction method makes it possible for pesticides to be determined in the range of 50–1000 ng L^{-1} with good linearity (coefficient of determination ≥0.995) and suitable recoveries (85–119%) and precision (< 21%, n=3) using 100 mL of a water sample. This methodology is shown to be suitable for the detection of chlorpyrifos in local river waters.

Introduction

An ever-increasing world population placing pressure on global food supplies, energy resources and the environment has led to agrochemicals being used not only to protect crops from pests but also to enhance crop yields [1]. Many pesticides used in agriculture are highly toxic both to the environment and to living organisms when their application is uncontrolled. Storm runoff events can cause pesticides to be mobilized from fields to waterbodies. Due to their highly persistent properties, pesticides bioaccumulate in food and can present a risk to animal and human health [2]. Chlorpyrifos (CP), diazinon (DZ) and cyprodinil (CYP) are three of the most widely used pesticides. CP and DZ belong to the organophophate pesticides chemical family (OPPs). OPPs, like some nerve agents, inhibit a neuromuscular enzyme that is essential for normal function in insects,

humans and many other animals. CP is considered by the World Health Organization to be moderately hazardous to humans and more than 10,000 related human deaths a year are reported. CYP is a fungicide which belongs to the family of aminopyrimidines. Aminopyrimidines play an important role in biological processes, since the pyrimidine ring is present in several vitamins, nucleic acids, and coenzymes. The European Water Framework Directive [3] recognizes CP as a priority pollutant and has set 0.1 μg L−1 as the maximum concentration permitted in fresh waters. Furthermore, a maximum level for individual pesticides of 0.1 μg L^{-1} has been established in water intended to be used for drinking purposes.

Chromatographic techniques have been extensively used as they are powerful separation techniques and enable the analysis of pesticide residues. However, extraction and concentration is needed prior to chromatographic separation and detection to make the sample more amenable to the analytical techniques and to separate the analytes of interest from other interfering species [4]. Sample preparation is therefore an important step in the analytical process. Conventional methods such as liquid–liquid extraction (LLE) and solid-phase extraction (SPE) are labour-intensive and environmentally harmful [5,6]. As a result, considerable effort has been devoted to the development of novel sample preparation methods, such as stir bar sorptive extraction [7], solid-phase microextraction (SPME) [8], membrane assisted liquid-liquid extraction [9], single drop microextraction [10], and dispersive liquid–liquid microextraction [11]. Recently, new sample treatment approaches [12–14] and new materials (sorbents) for pesticide extraction have also been explored. In this respect, magnetic molecularly imprinted polymers [15] and magnetic graphene nanoparticles [16] have been described. Moreover, thin films based on polydimethylsiloxane (PDMS) [17], silicone rods and silicone tubes [18], and microporous polypropylene hollow-fibre (HF) membranes [9] can be used directly as solid sorbents to extract target species based on an adsorption mechanism.

Extraction of the compounds of interest from water samples can also be achieved with a new class of membranes called polymer inclusion membranes (PIM). These new membranes consist of a base polymer, usually polyvinyl chloride (PVC) or cellulose triacetate (CTA) and a plasticizer. The role of the plasticizer is to increase both the flexibility and the softness. Additionally, plasticizers can modify the solubility properties of the sorbent due to their different polarities and dielectric constants. A third component, an organic extractant or carrier, is needed when separation of species relies on a transport mechanism. Ease of preparation, stability, and mechanical strength are noticeable features

of PIMs, which have found many applications in transport systems for the separation and recovery of inorganic species and organic compounds [19,20]. Moreover, membranes made of CTA and the extractant Aliquat 336 have been used as the extraction phase for the preconcentration of trace amounts of several metals such as Cd(II) [21], Cr(VI) [22], Pd(II) and Pt(IV) [23] in complex liquid samples such as electroplating solutions and sea water samples. Once the metals were extracted by the PIM, analysis of the membrane by X-ray fluorescence showed this PIM-assisted extraction to be an easy way to improve the instrumental sensitivity for the detection of these metals. However, the use of PIMs as an extraction phase for organic compounds has yet to be fully exploited.

In this study our intention is to evaluate the use of PIMs as an extraction phase for pesticides prior to their determination using gas chromatography coupled to mass spectrometry. We have studied membranes made of CTA as a polymer and nitrophenyl octyl ether (NPOE), dibutyl sebacate (DBS) and bis (1-butylpentyl) adipate (BBPA) as plasticizers. The extraction efficiency of the different membranes has been evaluated for three pesticides, CP, DZ and CYP. Parameters such as the kinetics of the extraction process as well as elution conditions using different organic solvents such as methanol and acetonitrile (ACN) have also been studied. Moreover, the PIM-assisted extraction for the determination of these pesticides has been validated in a GC-QqQ system. To the best of our knowledge, this work constitutes the first application of a PIM as an extraction phase for the preconcentration of pesticides in river waters.

Experimental

Chemicals and standards

All reagents and solvents used in this study were of analytical grade. CP, DZ and CYP were obtained from Sigma-Aldrich (Steinheim, Germany). The structure and physico-chemical properties of the studied compounds are shown in Figure S3.35 and Table S3.22. Chlorpyriphos-d10 from Dr. Ehrenstorfer GmbH (Augsburg, Germany) was selected as the internal standard (IS). Other reagents (CTA, NPOE, DBS and BBPA), were obtained from Sigma-Adrich (Steinheim, Germany). Sodium chloride was purchased from Fisher Chemical (Fair Lawn, NJ, USA). Ultrapure water from a Milli-Q Plus water purification system (Millipore Ibérica S.A., Barcelona, Spain) was used. All solvents employed in this study were HPLC-hypergradient. Methanol and

trichloromethane were purchased from Panreac (Castellar del Vallès, Spain). ACN was acquired from Fisher Chemical (Fair lawn, NJ, USA).

Stock standard solutions of all pesticides (containing about 500 mg L^{-1}) were prepared in methanol. Intermediate solutions of each pesticide (5 mg L^{-1}) were also prepared in methanol and replaced every week. All these solutions were stored in darkness at 4°C.

Water samples were collected from different rivers in Catalonia (north-east Spain): Riells River (pH of 8.15, a conductivity of 99 μS, and total organic carbon (TOC) of 1.81 mg C L^{-1}), sampled in the Montseny Natural Park; Ter River (pH of 8.08, a conductivity of 628 μS, and TOC of 27.80 mg C L^{-1}), sampled in l'Estartit close to the mouth of the river; Tordera River (pH of 7.99, a conductivity of 624 μS, and TOC of 5.98 mg C L^{-1}), located between the province of Girona and Barcelona; and Llémena River (pH of 8.24, a conductivity of 318 μS, and TOC of 2.16 mg C L^{-1}), in the Garrotxa county. Samples, which were collected during the summer and autumn of 2016, were immediately filtered through a 0.45 μm cellulose acetate membrane filter and stored in darkness at −18°C in glass bottles.

Equipment and chromatographic conditions

GC-ITMS

Preliminary studies, evaluation of extraction conditions and PIM composition were performed using a Trace GC 2000 coupled to a PolarisQ ion trap mass spectrometer detector (Thermo Scientific, Waltham, MA, USA). A TG-5SIL MS capillary column (30m×0.25mm i.d. x 0.25 μm film thickness) (Thermo Scientific) was used and the carrier gas was 99.9990% pure helium (Carburos Metálicos, Barcelona, Spain) at a constant flow rate of 1 mL min^{-1}. The split/splitless injection port was equipped with a 0.75 mm ID liner and operated in splitless mode (maintained for 1 min) at 250°C (270°C and 5 min for SPME experiments).

The oven temperature programme started at 80°C, was held for 2 min; then ramped up to 300°C at 10 °C min^{-1}, and held for 6 min; the total run time was 30 min. Ionization was performed in the electron impact mode at 70 eV. The transfer line temperature was set at 250°C and the ion source temperature at 225°C. MS analyses were conducted in full acquisition mode with an m/z range from 40 to 400 amu. Peak areas of the compounds were obtained from XIC chromatograms with the following m/z ions: 314

and 197 for CP, 225 and 224 for CYP, 304 and 179 for DZ (adapted from Correia et al. [24]). Data analysis was performed using Xcalibur 1.4 software (Thermo Scientific).

GC-QqQ

Method validation and determination of pesticides in river water samples were performed by Trace GC Ultra gas chromatograph equipped with a TriplusTM autosampler coupled to a TSQ Quantum triple quadrupole mass spectrometer system (Thermo Fisher Scientific). Chromatographic separation was performed using a Trace GOLD TG- 5SILMS column from Thermo Fisher Scientific (30m x 0.25mm i.d. x 0.25 μm). The injector was operated in splitless mode (maintained for 1 min) at 250 °C. The oven temperature program was as follows: initial temperature 60°C, held for 2 min; then ramped up to 300°C at 10°C min^{-1}, and held for 6 min; the total run time was 30 min. Mass spectrometric ionization was carried out in electron impact (EI) ionization mode with an EI voltage of 70 eV and a source temperature of 250°C. Detection was performed in Selected Reaction Monitoring mode (SRM), using the ions indicated in Table S3.23. The acquired data were processed by TraceFinder EFS 3.1 software.

Preparation of the PIM

Membranes with a composition of 70% polymer and 30% plasticizer (w/w) were prepared according to the procedure found in the literature [25]. In summary, 200 mg of CTA were dissolved in 20 mL trichloromethane and maintained under stirring for 5 h. 90 mg of plasticizer were then added and the resulting mixture was stirred for 2 h more. Different plasticizers (NPOE, DBS and BBPA) with similar viscosity values but different dielectric constants were tested (see Table S3.24). The mixture was then poured into a 9.0 cm diameter flat bottom glass petri dish, which was set horizontally and covered loosely. The organic solvent was allowed to evaporate over 24 h at room temperature, and the resulting film was then carefully peeled off the bottom of the petri dish. Circular pieces with an area of 3 cm^2 were cut from its central section and used in extraction experiments.

Evaluation of different parameters for pesticide extraction and elution

In preliminary experiments, only CP was evaluated. For this, 100 mL of Llémena River sample was spiked with 2000 ng L^{-1} CP and put in contact with the PIM sorbent. Samples were stirred for different time periods. CP remaining in the aqueous solution was determined by SPME-GC-ITMS. SPME experiments were performed with an SPME Triplus autosampler (Thermo Scientific, Waltham, MA, USA). A previously conditioned commercially available fibre with a 50/30 μm divinylbenzene/ carboxen/polydimethylsiloxane (DVB/CAR/PDMS) coating (Supelco; Bellefonte, PA, USA), was used. Volumes of 15 mL of sample solution were placed in 20 mL glass vials closed with aluminium caps furnished with Teflon-faced septa. The fibre was then immersed in the sample for extraction (50°C for 30 min). Constant stirring was applied during the extraction process. After completion, the fibre was pulled into the needle and the SPME device was removed from the vial and inserted into the injection port of the GC.

Methanol and ACN were evaluated for the elution of CP. To this end, 1 mL of organic solvent was placed into a glass vial closed with Teflon caps and put into contact with a piece of a CP-loaded PIM sorbent that had been previously washed with ultrapure water and carefully dried. The use of an ultrasonic bath to help in the release of retained pesticide and the time needed for the elution step were also investigated. The elution efficiency was evaluated by direct injection of the organic extract in the GC without further evaporation.

Moreover, the influence of PIM composition and the effect of orbital, magnetic and rotary stirring were also checked for the three compounds.

Extraction efficiency and absolute recovery

To study the extraction efficiency of PIMs for the target pesticides at the concentration levels encountered in surface water, a GC coupled to a QqQ system was employed. First, calibration standards were prepared by taking several pieces (one piece for each experiment) of the PIM, which were contacted with 1 mL ACN for 15 min in an ultrasonic bath; the pieces of membrane were then removed and the appropriate amount of the intermediate solution containing the three pesticides was added. The solvent was evaporated to dryness under gentle nitrogen stream and the residue was reconstituted with 1 mL hexane. Fifty μL of the IS solution (100 μg L^{-1}) was finally added. Calibration

curves were obtained for the three pesticides, and the working range of the analytes is presented in Table S3.23, together with the instrumental detection limit (IDL) achieved, based on a signal-to-noise ratio of 3.

Second, the matrix effect (ME), extraction efficiency (EE) and absolute recovery (AR) were studied. For the evaluation of ME, the PIM was contacted for 6 h with different river water samples (Riells, Tordera, Ter, and Llémena River). The membrane was then soaked with 1 mL of ACN, and the three pesticides were added to the solution to obtain a final concentration of 25 μg L^{-1} for each compound. After solvent evaporation, reconstitution with hexane, and the addition of the IS, one μL was injected into the GC. The response signals obtained were compared with the signal in the standard solution in hexane to obtain ME as shown in Eq. (3.22) [26],

$$ME\ (\%) = \left(\frac{B-C}{A}\right) - 1 \times\ 100 \qquad (3.22)$$

where A is the response signal of the analyte(s) recorded for the standard solution, B is the response signal of the analyte recorded for the sample spiked with the target compound after PIM-assisted extraction, and C denotes the response signal of the analyte recorded for a non-spiked sample.

EE was obtained from Llémena water samples at different spiking levels, 100 and 250 ng L^{-1}, and using the Eq. (3.23) [26]:

$$EE\ (\%) = \frac{D-C}{B-D} \times\ 100 \qquad (3.23)$$

where D is the response signal of the analyte recorded for the sample spiked with the target compound before extraction.

AR was calculated using the Eq. (3.24):

$$AR\ (\%) = \frac{D-C}{A} \times\ 100 \qquad (3.24)$$

The response signal in the equations above was obtained through the calibration curve measured as indicated in this section.

Quality parameters of the method

The overall method, including the PIM-assisted extraction, was validated using aqueous standards (100 mL of Llémena River water sample) spiked with a mixture of pesticides at a working range from 50 ng L^{-1} to 1000 ng L^{-1}. After extraction and elution under the final experimental conditions (6 h of extraction time using rotary agitation and subsequent elution with 1 mL of ACN assisted with an ultrasonic bath for 15 min), the GC-MS/MS analysis of the extract was performed. Recovery for the overall method and repeatability (n=3) were calculated by spiking Ter and Llémena River water at two concentration levels (100 ng L^{-1} and 250 ng L^{-1}).

All experiments were run at room temperature (22 ± 1°C).

Results and discussion

Preliminary studies: Influence of contact time on the extraction of chlorpyrifos and the selection of the solvent for elution

Preliminary experiments were performed with only CP and using a PIM with a composition of 70% CTA – 30% NPOE (w/w) prepared following the procedure described in the experimental section. The obtained membrane is a non-porous transparent film, as can be seen in Figure S3.36, that is flexible and has an average thickness of 31 ± 3 μm. The reproducibility of the PIM preparation was routinely checked by means of total weight and thickness measurements.

The kinetics of the extraction was evaluated for this PIM composition at different extraction times, ranging from 30 min up to 480 min. The amount of pesticide remaining in the aqueous phase was determined by means of SPME-GC-ITMS using the experimental conditions described in the section *Evaluation of different parameters for pesticide extraction and elution*. As can be observed in Figure 3.30, the amount of CP in the aqueous phase decreases continuously with time. After 8 h, the extraction is nearly complete, with less than 7% of the initial pesticide concentration remaining in the water sample. It is worth mentioning that when the same experiment was performed using a 100% CTA film, the extraction of CP was not possible. Therefore, the suitability of using a PIM containing NPOE for the extraction of CP is demonstrated.

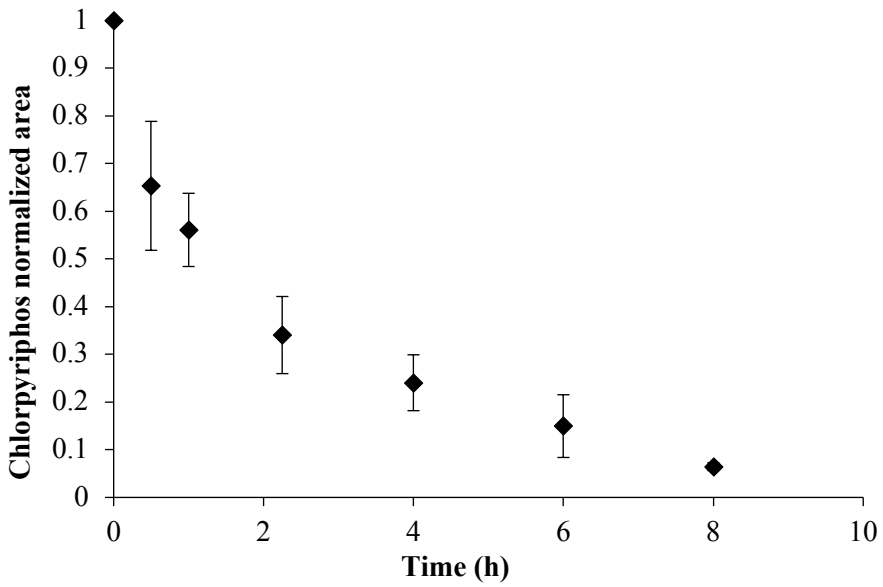

Figure 3.30 Transient amount of CP in the remaining aqueous solution. PIM composition was 70% CTA – 30% NPOE (n=2).

Methanol and ACN (1 mL) were then tested as solvents to recover the analyte from the loaded PIM for GC analysis. Fifteen minutes of elution time was assayed and a greater response was obtained when ACN was used as the solvent. Therefore, methanol was discarded and ACN was selected for further experiments. With the aim of reducing the elution time, ultrasonic assisted elution (UAE) was tested and compared with the previous results (see Figure 3.31). Higher area values were obtained for 5 min and with UAE, compared to other tested conditions, although the results showed lower repeatability. Finally, 15 min and UAE were selected as the working conditions.

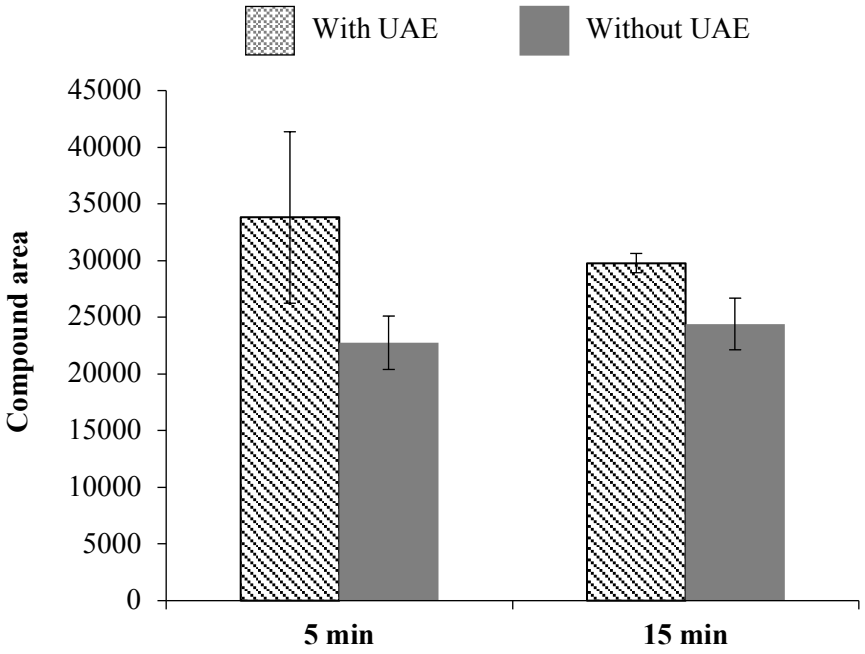

Figure 3.31 Evaluation of CP elution under different experimental conditions: ultrasound assisted elution and time. PIM 70% CTA – 30% NPOE (n=2).

Extraction conditions for the three pesticides

CP, DZ and CYP, which are all currently used in our country, are found at trace levels in river waters [27]. The extraction of the three compounds was studied under different stirring modes (orbital agitation, magnetic stirring and rotary agitation) for extraction times of 2 and 6 h.

As shown in Figure 3.32, slight differences were obtained depending on the agitation mode that was used. Overall, the extraction of pesticides is greater after 6 h than after 2 h. In the case of magnetic stirring, the values obtained are similar to those obtained with the rotary mode, but there were higher standard deviations in the case of all three pesticides. Based on these results, the rotary agitation mode was selected for further experiments and a contact time of 6 h was fixed.

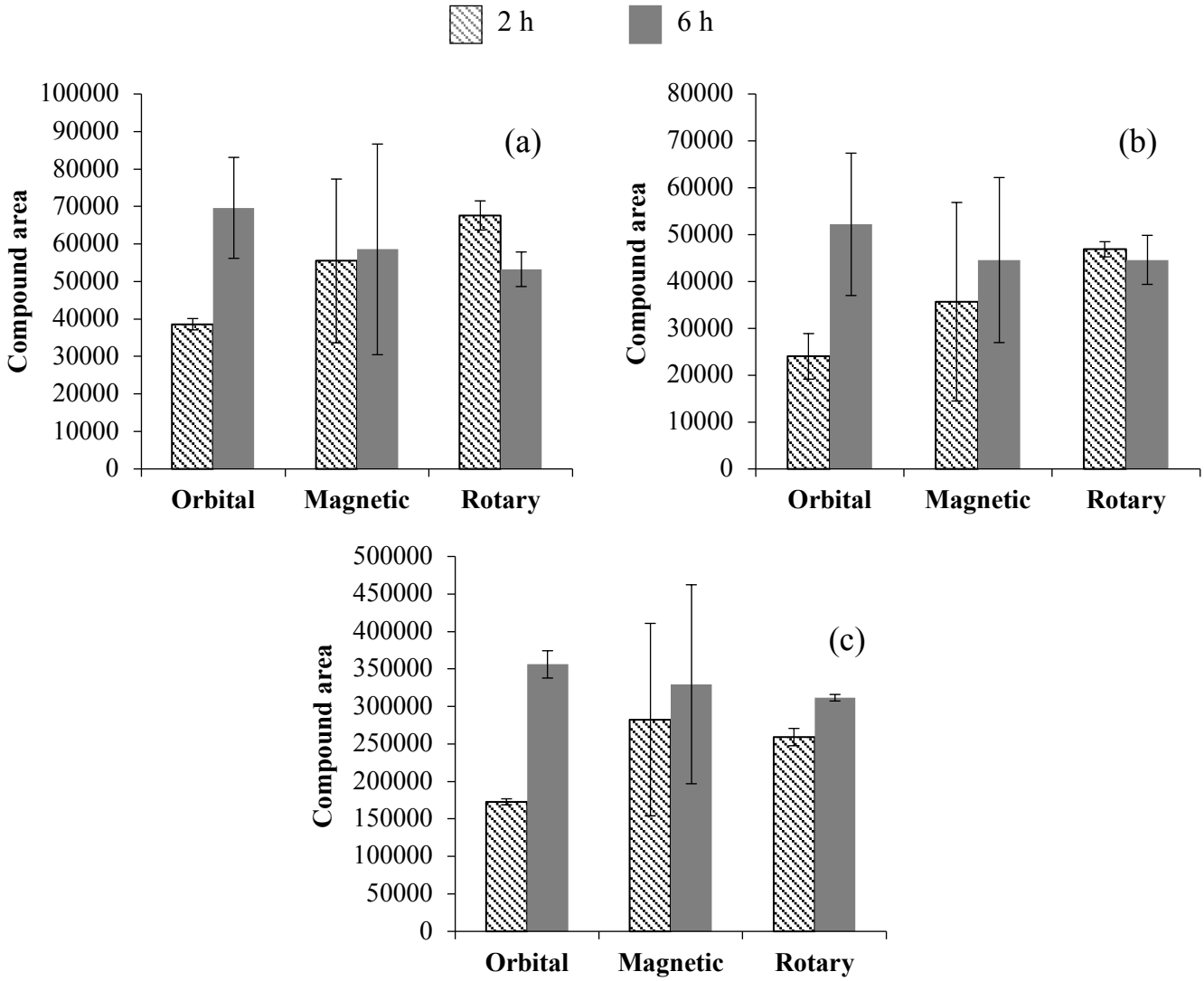

Figure 3.32 Effect of different agitation modes during the extraction step: orbital agitation, magnetic stirring and rotary agitation for pesticides (a) DZ, (b) CP and (c) CYP. PIM: 70% CTA–30% NPOE. Elution was conducted with 1 mL of ACN for 15 min with UAE (n=3).

Evaluation of PIM composition

To investigate the role of plasticizers in this extraction phase, three commercially available compounds were used to prepare CTA-based membranes. The plasticizer content was always 30% (w/w) to avoid undesirable rigidity [23] and extraction was investigated at two different pesticide concentrations. The results are depicted in Figure 3.33 and, in general terms, all three pesticides are better extracted into PIMs containing NPOE. Taking into account that these PIMs do not contain any carrier and that the extraction occurs through solubilisation of the pesticide in the membrane matrix with the

aid of the plasticizer for polar pesticides such as those tested here, membranes with NPOE bearing the higher dielectric constant (see Table S3.24), show better performance. It is worth mentioning that the solubility properties of the PIM can be tuned by changing the plasticizer, allowing low cost materials to be manufactured with different affinities and selectivities.

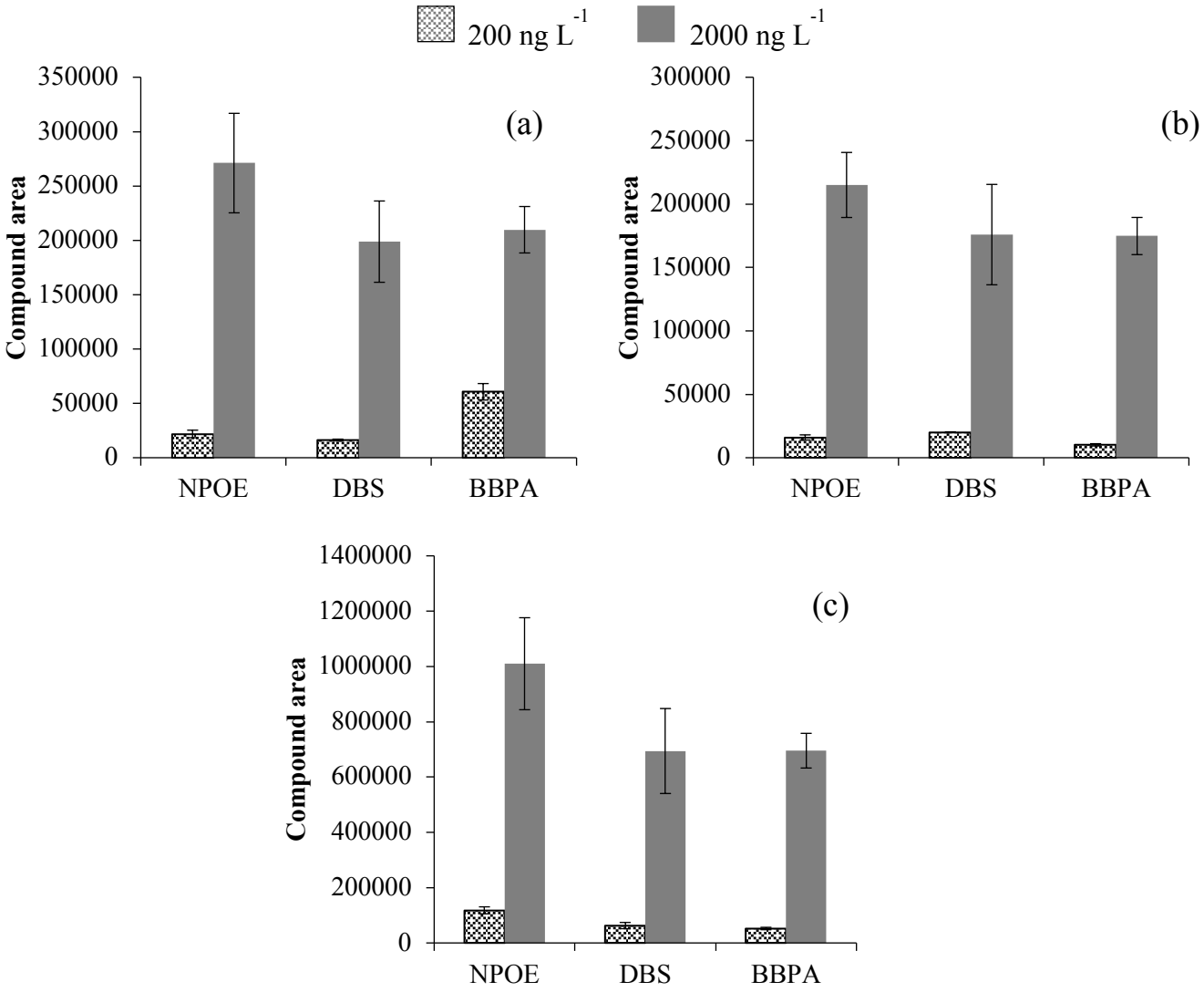

Figure 3.33 Effect of the use of different plasticizers in the extraction of selected pesticides (a) DZ, (b) CP and (c) CYP. PIM: 70% CTA – 30% plasticizer. Elution was conducted with 1 mL of ACN for 15 min with UAE (n=3).

Extraction efficiency and absolute recovery

Extraction efficiency and absolute recovery are key parameters that must be

evaluated when a novel extraction phase is designed and are usually calculated from the experimentally obtained chromatographic signal (peak areas). However, in the case of GC-MS, matrix effects cause signal suppression/enhancement due to the accumulation of non-volatile matrix components in the GC system or blockage of active sites in the injector. ME is used to evaluate the impact of matrix components on the analyte response detector in GC-MS determinations. The EE corresponds to the effectiveness of the PIM-assisted extraction procedure and the AR takes into account the influence of the matrix components (ME) on the whole efficiency. A methodology and a general scheme has been proposed by Caban et al. [26] to evaluate these effects with specially designed experiments and this methodology has been followed in the present work.

For this reason, we focused our efforts on the evaluation of the different interferences and matrix effect arising from the PIM-assisted extraction method with the triple quadrupole MS/MS instrument prior to EE and AR evaluation (Eqs. 3.22 to 3.24). The experimental conditions of the MS/MS system, choice of precursor ions, product ions, and collision energies were adapted from reference [28] and were not optimized.

In Table 3.19 a), ME is presented for Tordera, Riells, Llémena and Ter river water samples. Values in the range of −1% to −3% were found for DZ and CP, and higher for CYP (−8.6% and −15.2%, for Tordera and Riells samples, respectively). Higher values for the Ter River correlate with the higher TOC of this water. Considering the different characteristics of the tested river waters, it is noticeable that the proposed method suffers from little interference due to a matrix effect, which is an advantage compared to SPE where extensive clean up procedures are needed.

Water from the Llémena River was selected for the evaluation of EE and AR, which was undertaken at two different concentration levels (100 and 250 ng L^{-1}). As shown in Table 3.19 b), values of AR between 36% and 46% for CYP, 42% and 45% for DZ, and 68-70% for CP were found. The higher AR for CP agrees with the log K_{ow} values, CP bearing the higher value and may be related to the affinity of the compound towards the plasticizer NPOE.

The AR results obtained in the present work are in concordance with others reported in the literature for new extraction phases [29]. Moreover, the AR values found encourage us to evaluate a quantification method for the determination of the selected pesticides based on PIM-assisted extraction as preconcentration step.

Table 3.19 Evaluation of matrix effect (ME), extraction efficiency (EE) and absolute recovery (AR) for the different river waters. PIM: 70% CTA – 30% NPOE. Standard deviations are given in parentheses.

a) Effect of river water on ME (spiked concentration of 25 ng L^{-1}, n=2).

	Tordera River TOC 5.98 mgC L^{-1}	**Riells River TOC 1.81 mgC L^{-1}**	**Ter River TOC 27.80 mgC L^{-1}**	**Llémena River TOC 2.16 mgC L^{-1}**
Diazinon	-2 (2)	-1.7 (0.7)	-4 (7)	-0.8 (0.5)
Chlorpyrifos	-2.05 (0.00)	-3 (1)	-7 (2)	0.7 (0.1)
Cyprodinil	-8.06 (0.6)	-15 (4)	-13 (6)	-1.6 (0.9)

b) b) EE and AR Llémena River evaluated at two levels (n=2).

	100 ng L^{-1}		**250 ng L^{-1}**	
	%EE	**%AR**	**%EE**	**%AR**
Diazinon	43 (3)	42 (3)	45.5 (0.1)	45.1 (0.1)
Chlorpyrifos	67 (5)	68 (5)	70 (5)	70 (5)
Cyprodinil	34 (2)	36 (2)	40 (8)	46 (8)

Quality parameters for the PIM-assisted extraction method

Under final working conditions of 6 h extraction with rotary agitation and a subsequent elution step of 15 min UAE with 1 mL ACN, the optimized PIM-assisted extraction method was validated in terms of quality parameters, including lineal range, correlation coefficients and limits of detection and quantification for the three pesticides. Linearity was evaluated with samples taken from the Llémena River spiked at increased concentrations between 50 and 1000 ng L^{-1}. The spiked samples were extracted and analysed with the GC-QqQ system. Correlation coefficients for the corresponding calibration curves ranged from 0.997 to 0.999. Method detection limits (MDLs) of 3 ng L^{-1}, 2 ng L^{-1} and 23 ng L^{-1} for DZ, CP and CYP, respectively, were obtained using a S/N ratio equal to 3. Method quantification limits (MQLs), which were determined using the

S/N ratio equal to 10 but also taking into account the error in the calibration curve, are set out in Table 3.20. In Table 3.21, MDLs from our method are compared with other extraction methods reported in the literature for the determination of CP, DZ and CYP in waters, such as liquid-liquid extraction combined with GC-FPD, GC-NPD and GC-ECD [30–33], liquid-solid extraction combined with GC-MS [34], solid-phase microextraction combined with GC-ECD and GC-MS/MS [35,36], dispersive liquid-liquid microextraction combined with GC-MS [37], and other microextraction techniques [2,15,38–41]. As shown in the table, the MDLs of the present method are much lower than those of EPA methods, and comparable to those of other extraction- based systems.

Recovery test and real water analysis

Water samples from the Ter (sample from November 2016) and Llémena rivers were fortified at two concentration levels, 100 ng L^{-1} and 250 ng L^{-1}, to determine the overall method recovery by comparing the concentration obtained using the calibration curve with the initial spiked level. The selection of the fortified levels was based on the regulated values according to the Water Framework Directive. In Figure 3.34a), the chromatographic peaks obtained for the three fortified pesticides are depicted. Satisfactory recoveries were found ranging from 85% to 119% for the three compounds. Intra-day precision was determined and we found RSD from 2% to 21%, the latter value for DZ. These values can be considered satisfactory for the ng L^{-1} concentration range [42].

The practical applicability of the PIM-assisted extraction method was demonstrated by determining the concentration of CP, DZ and CYP in water samples from the Ter, Tordera, Llémena and Riells rivers. As shown in Figure 3.34b), only in the case of the Ter River water (sample from July 2016) was CP found at a concentration of 36 ng L^{-1}. Traces of DZ can also be observed below the MQL. As has been mentioned, CP is a pesticide that is commonly used today in our country and which has been found in other river water samples in Catalonia. For example, in the Llobregat River water, a maximum value of 6.23 ng L^{-1} was determined in 2010 and of 13.65 ng L^{-1} in 2011 [24].

Table 3.20 Quality parameters for the PIM-assisted extraction method.

	Working range (ng L^{-1})	R^2	MQL (ng L^{-1})	Ter River (n=3)				Llémena River (n=2)			
				Recovery (%)		RSD (%)		Recovery (%)		RSD (%)	
				100 ng L^{-1}	250 ng L^{-1}	100 ng L^{-1}	250 ng L^{-1}	100 ng L^{-1}	250 ng L^{-1}	100 ng L^{-1}	250 ng L^{-1}
Diazinon	50-1000	0.9988	56	111	85	21	4	115	107	6	2
Chlorpyrifos	50-1000	0.9999	30	93	102	18	7	113	118	6	5
Cyprodinil	80-1000	0.9972	76	106	113	9	11	119	115	5	13

Table 3.21 Comparison of the PIM-assisted extraction method with others previously reported for the studied pesticides.

Method	Instrument	Pesticide	MDL (μg L^{-1})	Sample volume	Final volume	Ref.
LLE (EPA 622 method)	GC-FPD	CP DZ	0.3[a] 0.6[a]	1000 mL	5 mL	[30]
LLE (EPA 614 method)	GC-FPD	DZ	0.012[a]	1000 mL	5 mL	[31]
LLE (EPA 507 method)	GC-NPD	DZ	0.13[a]	1000 mL	5 mL	[32]
LLE	GC-ECD	CP DZ	0.05 0.05	500 mL	2 mL	[33]
LSE (EPA 525.2 method)	GC-MS	CP DZ	0.044[a] 0.11[a]	1000 mL	0.5 mL	[34]
SPME	GC-ECD	CP	0.073	10 mL	-	[35]
SPME	GC-MS/MS	CP	0.001	20 mL	-	[36]
DLLME	GC-MS	CP DZ	0.0025 0.0039	5 mL	0.05 mL	[37]
BAμE–LD/LVI	GC–MS	CYP	0.004	25 mL	0.2 mL	[38]
VAM-IL-DLLME	HPLC-UV	CYP	0.02	8 mL	0.05 mL	[39]
HF-LPME	GC/ITMS	DZ	0.006	20 mL	0.0035 mL	[40]
SFODME	GC-ECD	CP	0.043	10 mL	0.01 mL	[41]
SDME	GC-FPD	CP DZ	0.004 0.004	5 mL	0.001 mL	[2]
Magnetic MIP	HPLC-UV	DZ	5	10 mL	0.2 mL	[15]
PIM-assisted extraction	GC/QqQ	CP DZ CYP	0.002 0.003 0.023	100 ml	1 mL	This work

LSE: Liquid-solid extraction (C18 Cartridge).
SPME: Solid-phase microextraction.
DLLME: Dispersive liquid-liquid microextraction.
BAμE–LD/LVI: Bar adsorptive microextraction.
VAM-IL-DLLME: Vortex-assisted magnetic ionic liquid dispersive liquid-liquid microextraction.
HF-LPME: Hollow fibre liquid phase microextraction.
Magnetic MIP: Magnetic molecularly imprinted polymer.
SFODME: Solidified floating organic drop microextraction.
SDME: Single drop microextraction.
LLE: Liquid-liquid extraction.

[a] Method detection limit (MDL) is defined as the statistically calculated minimum amount that can be measured with 99% confidence that the reported value is greater than zero.

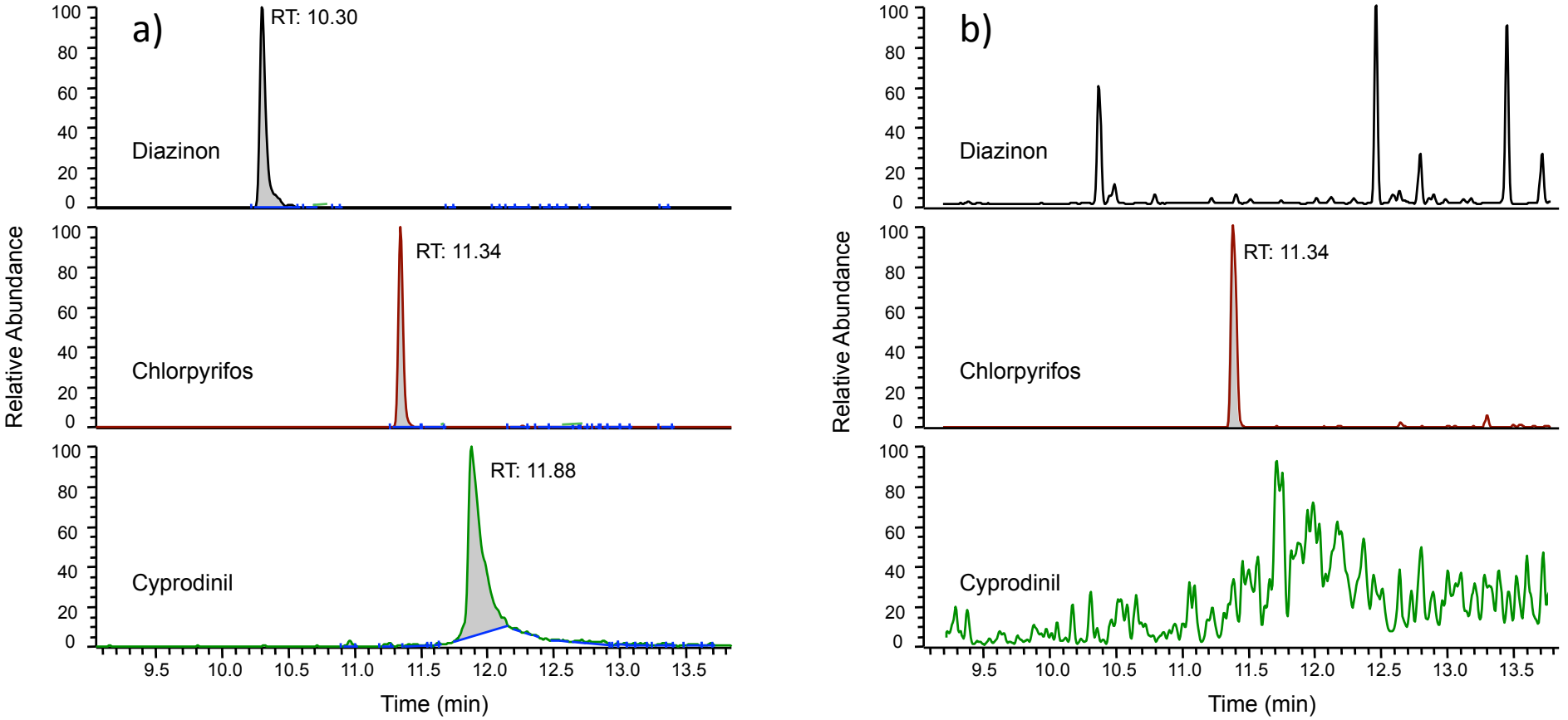

Figure 3.34 SRM chromatograms of the pesticides obtained after application of the PIM-assisted extraction in spiked Ter River water (a) and non-spiked Ter River water (b).

Conclusions

A PIM made of the polymer CTA and the plasticizer NPOE has been proposed as a novel and affordable extraction phase for the determination of three pesticides commonly used in crop protection in Catalonia river waters. Under optimized conditions, the PIM-assisted extraction method has provided good analytical performance for CP, DZ and CYP, including low detection limits of 2–23 ng L^{-1} for a 100:1 volume ratio, a suitable linearity and satisfactory precision. The proposed method has been successfully applied to different river waters and has allowed the detection of CP in a river water sample at a low ng L^{-1} level.

References

[1] F.P. Carvalho, Agriculture, pesticides, food security and food safety, Environ. Sci. Policy 9 (2006) 685–692.

[2] F. Ahmadi, Y. Assadi, S.M.R.M. Hosseini, M. Rezaee, Determination of organophosphorus pesticides in water samples by single drop microextraction and gas chromatography-flame photometric detector, J. Chromatogr. A 1101 (2006) 307–312.

[3] Directive, 2000/60/EC of the European parliament and of the council of 23 October establishing a framework for Community action in the field of water policy, 2000.

[4] J. Stocka, M. Tankiewicz, M. Biziuk, J. Namie, Green Aspects of Techniques for the Determination of Currently Used Pesticides in Environmental Samples, Int. J. Mol. Sci. (2011) 7785–7805.

[5] R.M. González-Rodríguez, B. Cancho Grande, J. Simal-Gándara, Multiresidue determination of 11 new fungicides in grapes and wines by liquid-liquid extraction/ clean-up and programmable temperature vaporization injection with analyte protectants/ gas chromatography/ion trap mass spectrometry, J. Chromatogr. A 1216 (2009) 6033–6042.

[6] J.B. Baugros, B. Giroud, G. Dessalces, M.-F. Grenier-Loustalot, C. Cren-Olivé, Multiresidue analytical methods for the ultra-trace quantification of 33 priority

substances present in the list of REACH in real water samples, Anal. Chim. Acta 607 (2008) 191–203.

[7] C. Margoum, C. Guillemain, X. Yang, M. Coquery, Stir bar sorptive extraction coupled to liquid chromatography-tandem mass spectrometry for the determination of pesticides in water samples: method validation and measurement uncertainty, Talanta 116 (2013) 1–7.

[8] Q. Wu, C. Feng, G. Zhao, C. Wang, Z. Wang, Graphene-coated fiber for solid-phase microextraction of triazine herbicides in water samples, J. Sep. Sci. 35 (2012) 193–199.

[9] R. Montes, I. Rodríguez, E. Rubí, M. Ramil, R. Cela, Suitability of polypropylene microporous membranes for liquid- and solid-phase extraction of halogenated anisoles from water samples, J. Chromatogr. A 1198– 1199 (2008) 21–26.

[10] J.P. dos Anjos, J.B. de Andrade, Simultaneous determination of pesticide multiresidues in white wine and rosé wine by SDME/GC-MS, Microchem. J. 120 (2015) 69–76.

[11] L. Fu, X. Liu, J. Hu, X. Zhao, H. Wang, X. Wang, Application of dispersive liquidliquid microextraction for the analysis of triazophos and carbaryl pesticides in water and fruit juice samples, Anal. Chim. Acta 632 (2009) 289–295.

[12] P. Liang, F. Wang, Q. Wan, Ionic liquid-based ultrasound-assisted emulsification microextraction coupled with high performance liquid chromatography for the determination of four fungicides in environmental water samples, Talanta 105 (2013) 57–62.

[13] Y. Wen, J. Li, F. Yang, W. Zhang, W. Li, C. Liao, et al., Salting-out assisted liquidliquid extraction with the aid of experimental design for determination of benzimidazole fungicides in high salinity samples by high-performance liquid chromatography, Talanta 106 (2013) 119–126.

[14] H. Farahani, Y. Yamini, S. Shariati, M.R. Khalili-Zanjani, S. Mansour-Baghahi, Development of liquid phase microextraction method based on solidification of floated organic drop for extraction and preconcentration of organochlorine pesticides in water samples, Anal. Chim. Acta 626 (2008) 166–173.

[15] F. Zare, M. Ghaedi, A. Daneshfar, A. Ostovan, Magnetic molecularly imprinted polymer for the efficient and selective preconcentration of diazinon before its determination by high-performance liquid chromatography, J. Sep. Sci. 38 (2015) 2797–2803.

[16] Z. Li, M. Hou, S. Bai, C. Wang, Z. Wang, Extraction of Imide Fungicides in water and juice samples using magnetic graphene nanoparticles as adsorbent followed by their determination with gas chromatography and electron capture detection, Anal. Sci. 29 (2013) 325–331.

[17] E. Boyaci, K. Goryńksi, C.R. Viteri, J. Pawliszyn, A study of thin film solid phase microextraction methods for analysis of fluorinated benzoic acids in seawater, J. Chromatogr. A 1436 (2016) 51–58.

[18] A. Martin, C. Margoum, J. Randon, M. Coquery, Silicone rubber selection for passive sampling of pesticides in water, Talanta 160 (2016) 306–313.

[19] A. Garcia-Rodríguez, V. Matamoros, S.D. Kolev, C. Fontàs, Development of a polymer inclusion membrane (PIM) for the preconcentration of antibiotics in environmental water samples, J. Membr. Sci. 492 (2015) 32–39.

[20] L. Nghiem, P. Mornane, I. Potter, J. Perera, R. Cattrall, S. Kolev, Extraction and transport of metal ions and small organic compounds using polymer inclusion membranes (PIMs), J. Membr. Sci. 281 (2006) 7–41.

[21] E. Marguí, C. Fontàs, K. Van Meel, R. Van Grieken, I. Queralt, M. Hidalgo, High-Energy Polarized-Beam Energy-Dispersive X-ray Fluorescence Analysis Combined with Activated Thin Layers for Cadmium Determination at Trace Levels in Complex Environmental Liquid Samples, Anal. Chem. 80 (2008) 2357–2364.

[22] C. Fontàs, I. Queralt, M. Hidalgo, Novel and selective procedure for Cr (VI) determination by X-ray fluorescence analysis after membrane concentration, Spectroch, Acta 61 (2006) 407–413.

[23] C. Fontàs, E. Marguí, M. Hidalgo, I. Queralt, Improvement approaches for the determination of Cr(VI), Cd(II), Pd(II) and Pt(IV) contained in aqueous samples by conventional XRF instrumentation, X-Ray Spectrom. 38 (2009) 9–17.

[24] M. Correia, C. Delerue-Matos, A. Alves, Multi-residue methodology for pesticide screening in wines, J. Chromatogr. A 889 (2000) 59–67.

[25] R. Güell, E. Anticó, S.D. Kolev, J. Benavente, V. Salvadó, C. Fontàs, Development and characterization of polymer inclusion membranes for the separation and speciation of inorganic As species, J. Membr. Sci. 383 (2011) 88–95.

[26] M. Caban, N. Migowska, P. Stepnowski, M. Kwiatkowski, J. Kumirska, Matrix effects and recovery calculations in analyses of pharmaceuticals based on the determination of β-blockers and β-agonists in environmental samples, J. Chromatogr. A 1258 (2012) 117–127.

[27] A. Masiá, J. Campo, A. Navarro-Ortega, D. Barceló, Y. Picó, Pesticide monitoring in the basin of Llobregat River (Catalonia, Spain) and comparison with historical data, Sci. Total Environ. 503– 504 (2015) 58–68.

[28] S. Walorczyk, Development of a multi-residue screening method for the determination of pesticides in cereals and dry animal feed using gas chromatography-triple quadrupole tandem mass spectrometry, J. Chromatogr. A 1165 (2007) 200–212.

[29] S.S. Lakade, F. Borrull, K.G. Furton, A. Kabir, R.M. Marcé, N. Fontanals, Dynamic fabric phase sorptive extraction for a group of pharmaceuticals and personal care products from environmental waters, J. Chromatogr. A 1456 (2016) 19–26.

[30] M. US EPA, method 622: the determination of organophosphorus Pesticides in municipal and industrial wastewater. https://www.epa.gov/sites/production/files/2015−10/documents/method_622_1992.pdf (accessed 26 October 2016).

[31] M. US EPA, method 614: the determination of organophosphorus pesticides in municipal and industrial wastewater. https://www.epa.gov/sites/production/files/2015−10/documents/method_614_1992.pdf (accessed 26 October 2016).

[32] M. US EPA, method 507: determination of nitrogen - and phosphorous-containing pesticides in water by gas chromatography with a nitrogen-

phosphorous detector. ⟨https://www.epa.gov/sites/production/files/2015 07/documents/epa-507.pdf⟩ (accessed 26 October 2016), 1995.

[33] M.I.R. Mamun, J.H. Park, J.-H. Choi, H.K. Kim, W.J. Choi, S.-S. Han, et al., Development and validation of a multiresidue method for determination of 82 pesticides in water using GC, J. Sep. Sci. 32 (2009) 559–574.

[34] M. US EPA, test method 525.2: determination of organic compounds in drinking water by liquid-solid extraction and capillary column Gas Chromatography/Mass Spectrometry (accessed 26 October), (2016) ⟨https://www.epa.gov/sites/ production/files/2015-06/documents/epa-525.2.pdf⟩ (accessed 26 October).

[35] K. Korba, L. Pelit, F.O. Pelit, K.V. Ozdokur, H. Ertaş, A.E. Eroğlu, et al., Preparation and characterization of sodium dodecyl sulfate doped polypyrrole solid phase micro extraction fiber and its application to endocrine disruptor pesticide analysis, J. Chromatogr. B 929 (2013) 90–96.

[36] D. García-Rodríguez, A.M. Carro, R. a Lorenzo, F. Fernández, R. Cela, Determination of trace levels of aquaculture chemotherapeutants in seawater samples by SPME-GC-MS/MS, J. Sep. Sci. 31 (2008) 2882–2890.

[37] A.C.H. Alves, M.M.P.B. Gonçalves, M.M.S. Bernardo, B.S. Mendes, Validated dispersive liquid-liquid microextraction for analysis of organophosphorous pesticides in water, J. Sep. Sci. 34 (2011) 1326–1332.

[38] C. Almeida, J.M.F. Nogueira, Comparison of the selectivity of different sorbent phases for bar adsorptive microextraction–Application to trace level analysis of fungicides in real matrices, J. Chromatogr. A 1265 (2012) 7–16.

[39] M. Yang, X. Xi, X. Wu, R. Lu, W. Zhou, S. Zhang, et al., Vortex-assisted magnetic β- cyclodextrin/attapulgite-linked ionic liquid dispersive liquid-liquid microextraction coupled with high-performance liquid chromatography for the fast determination of four fungicides in water samples, J. Chromatogr. A 1381 (2015) 37–47.

[40] P.-S. Chen, S.-D. Huang, Determination of ethoprop, diazinon, disulfoton and fenthion using dynamic hollow fiber-protected liquid-phase microextraction

coupled with gas chromatography-mass spectrometry, Talanta 69 (2006) 669–675.

[41] F.O. Pelit, L. Pelit, C. Alaca, H. Ertaş, F.N. Ertaş, Preconcentration and determination of Endocrine disruptor pesticides in well, Water Solidi. Float. Org. Drop Micro., CLEAN - Soil, Air, Water 42 (2014) 1284–1291.

[42] AOAC Official Methods of analysis, Guidelines for standard method performance requirements Appendix F, AOAC International, 2012, pp. 1–17.

Supplementary data

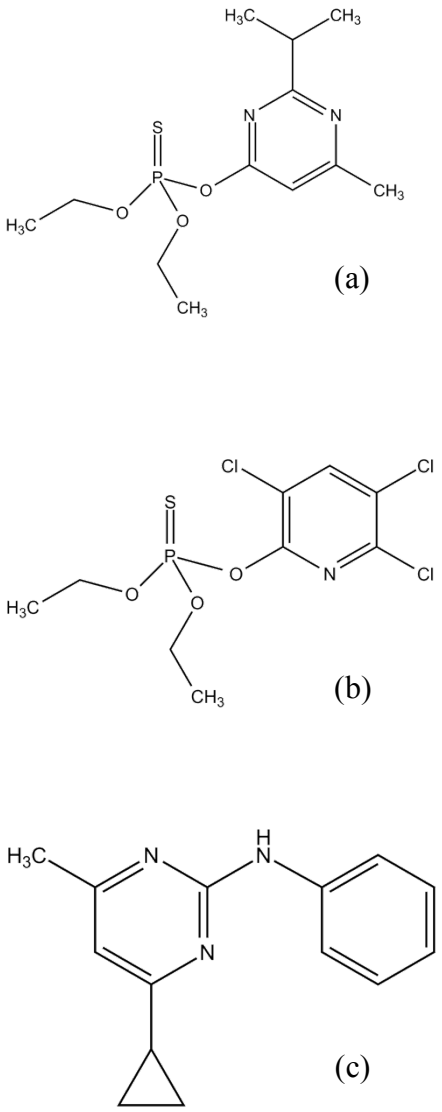

Figure S3.35 Pesticide chemical structures, (a) Diazinon, (b) Chlorpyrifos and (c) Cyprodinil.

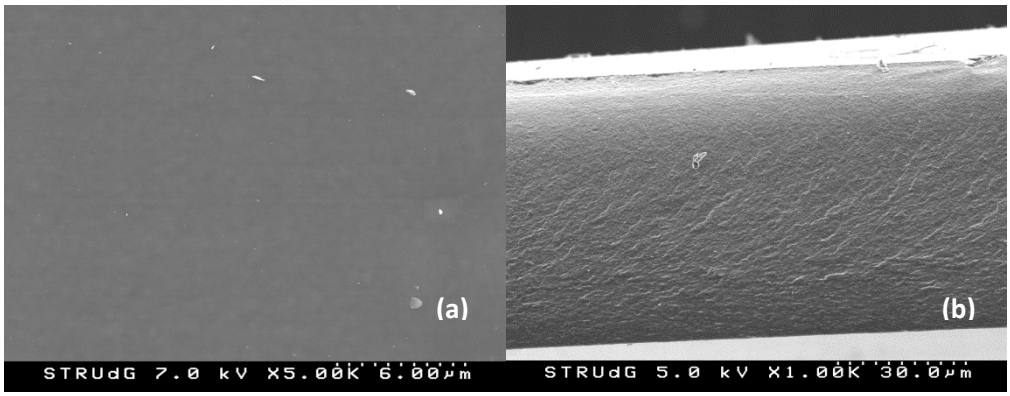

Figure S3.36 SEM images of a PIM (70% CTA – 30% NPOE) surface (a) and cross section (b).

Table S3.22 Physicochemical of the pesticides selected for study[1]

Pesticide	Chemical group	Molecular weight	log K_{ow}- pH 7, 20ºC	Water solubility- 20ºC (mg L^{-1})
Diazinon	Organophosphorous	304.35	3.69	60
Chlorpyrifos	Organophosphorous	350.58	4.7	1.05
Cyprodinil	Anilinopyrimidines	225.29	4	13

[1]http://sitem.herts.ac.uk/aeru/ppdb/en/atoz.htm

Table S3.23 Mass spectral characterization and quality parameters of the instrumental method (GC-QqQ) for the studied pesticides.

	RT (min)	Precursor Ion (m/z)	SRM1 (m/z)	SRM2 (m/z)	Collision energy	IDL (µg L^{-1})	R^2	Working range (µg L^{-1})
Diazinon*	10.28	304	179	162	10	0.15	0.9991	1.0-50.0
Chlorpyrifos*	11.34	314	258	286	12	0.16	0.9999	1.2-61.6
Cyprodinil**	11.95	225	224	208	20	2.68	0.9997	3.0-54.4

*SRM1 ion used for quantification, SRM2 ion used for identification

**SRM2 ion used for Quantification

IDL, instrumental detection limit

Table 3.24 Chemical structure and physical properties of plasticizers used in this study.

Name	Structure	Viscosity Pa·s (cP)	Dielectric constant (ε)
2-nitrophenyl octyl ether (NPOE)	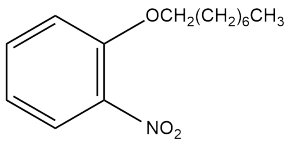	$12.8 \cdot 10^{-3}$	23.1
Bis (2-ethylhexyl) sebacate (DEHS)	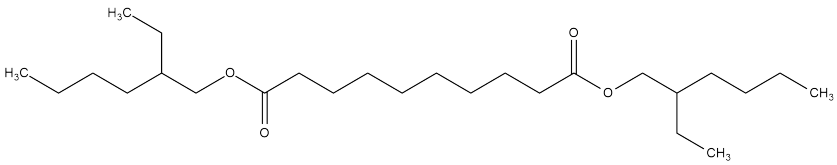	$9.5 \cdot 10^{-3}$	4.5
Bis (1-butylpentyl) adipate (BBPA)	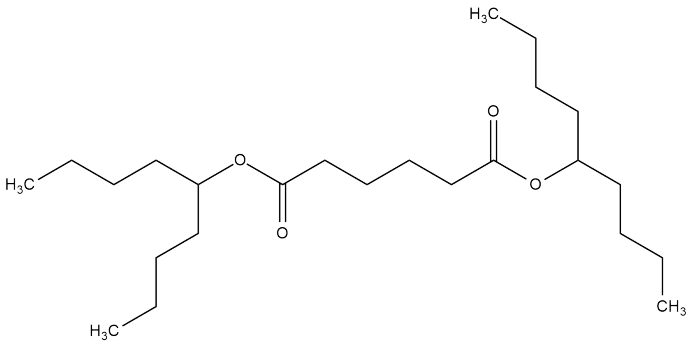	$14 \cdot 10^{-3}$	4

CHAPTER 4

General discussion and future perspectives

4.1 Development of new analytical methodologies for arsenic determination

As mentioned in the introduction of this thesis, the presence of arsenic is a major problem in many different regions around the world. In consequence, it is of paramount importance to progress towards simple, robust and cost-effective methodologies to facilitate its detection. Despite the large number of studies published for the determination and speciation of arsenic in natural waters, there is still a need for simple methodologies to allow the easy detection of this hazardous element in water samples.

As a result of this thesis, three different methodologies are presented for the easy determination of arsenic in water samples. In one case, we have developed a PIM to be incorporated in a special device to allow the preconcentration of As(V) and, thereby, facilitate its later determination by colorimetric reaction. In another approach, this kind of membrane has been coupled in a flow analysis (FA) system for the online preconcentration of arsenate followed by the formation of arsine that finally causes discoloration of a permanganate solution. The third methodology here investigated, is the use of a commercial adsorbent based on TiO_2 (Adsorbsia As600) to preconcentrate both As(V) and As(III) species, prior to their detection by ICP-OES.

The ion-exchanger Aliquat 336 has been chosen as the carrier for the studies concerning PIMs to extract As(V) species, since this form is present as anions in the pH of natural waters. At neutral pH, As(III) is present as an uncharged species, and, therefore, cannot be extracted by an ion-exchange mechanism. In order to measure the total arsenic content using this PIM, previous oxidation of As(III) should be conducted.

PIM-preconcentration studies using the device were done with the aim of improving the performance of a previous study in which a PIM made up of 70% PVC – 30% Aliquat 336 was used [1]. That system allowed the preconcentration of As(V) contained in 100 mL of water to a 5 mL 0.1 M NaCl solution (used as stripping phase) after 24 h, and detection was done using the molybdenum blue colorimetric method. However, apart from the long time needed to preconcentrate arsenate, the system was not effective for the analysis of waters bearing high conductivity. Consequently, with the aim of improving these results, in this thesis we have evaluated different parameters, such as membrane composition, stripping phase characteristics, and membrane thickness, to use a PIM system for the effective preconcentration of arsenate in complex natural waters in a shorter period of time. We found that a PIM made up of 52% CTA as the base

polymer and 48% Aliquat 336 gave effective arsenate transport, and that the use of a solution ratio of 50 mL feed /2.5 mL stripping (i.e. 50/2.5) instead of 100/5 was effective enough to achieve the required LOD for the intended application in the more convenient time scale of 5 hours. Moreover, the use of a 2M NaCl solution as stripping phase, instead of 0.1M, allowed effective As(V) transport despite the presence of other major anions in the groundwater. The analysis of different spiked water samples resulted in recoveries ranging from 79% to 124%, and showed good agreement with results obtained with ICP-OES. The developed PIM system was useful to effectively analyse groundwater samples containing naturally occurring arsenic from the north-east area of Catalonia (Spain).

The other methodology we developed responds to the demand for analytical methods providing high-throughput, cost-effectiveness, simplicity, sample and reagent economy and respect towards the environment, leading to the automation and miniaturization of chemical analysis. To this end, new set-ups which include the different steps of the analytical process have been envisaged relying on flow techniques, like the one presented in this thesis. Since their first appearance in 1957, when Skeggs developed a segmented flow analysis (SFA) [2,3], flow techniques have garnered great attention for clinical, industrial and environmental purposes, as they permit reproducible fast determination, as well as incorporating automated sample treatment stages to achieve different purposes, such as sample preparation (e.g. dissolution, disaggregation, extraction, filtration, etc.) for the preconcentration of trace analytes or interference removal. Moreover, there is a wide variety of automatic methods with very particular features that make them great alternatives for use in particular applications in different areas. For instance, methods based on FA have been employed for the satisfactory determination of arsenic [4,5], zinc [6,7] or chromium species [8,9].

Taking into account previous encouraging results using a PIM for the preconcentration of As(V) species, in this study we developed for the first time the on-line coupling of a PIM in a FA system in order to minimize sample handling and to increase sensitivity for As(V) determination. The developed system consisted of the sample passage through the PIM cell for 15 min, while the acceptor stream was stopped to allow arsenate preconcentration. After that, arsenate was reduced to arsenite by merging the acceptor stream with a reductant solution stream, generating arsine which was transported across a hydrophobic membrane, placed in a gas-diffusion cell (GDC), to a permanganate solution where it was oxidized, producing a decrease in permanganate absorbance, which was continuously monitored.

The same carrier as used in previous works, Aliquat 336, was incorporated in the PIM, which was placed in an extraction cell and used for the on-line preconcentration of As(V). We evaluated the effect of the polymer in preparing the PIM and, among the different available polymers, PVC and PVDF-HFP, the latter was chosen since it exhibited the highest As(V) transport as derived from the signal value shown in Table 4.1.

Table 4.1 Effect of PIM composition on the analytical signal.

Membrane composition (% w/w)	Replicates	Signal	Average (sd)
70 PVC – 30 Aliquat 336	1	0.009	0.007 (0.003)
	2	0.008	
	3	0.003	
70 PVC – 20 Aliquat 336 – 10 1-TD	1	0.041	0.03 (0.01)
	2	0.017	
	3	0.023	
70 PVDF-HFP –30 Aliquat 336	1	0.173	0.1723 (0.0006)
	2	0.173	
	3	0.172	

1-TD: 1-tetradecanol

In order to enhance the sensitivity of this methodology, several FA parameters were optimized, such as the effect of the different flow streams of the system, the reaction coil length, the composition of the acceptor stream and the membrane composition of the GDC, among others. The highest arsine diffusion in the GDC was obtained with both PTFE and Surevent® membranes. However, only the latter did not compromise baseline stability. This methodology provided a remarkable LOD of 3 μg L^{-1}, and enabled the analysis of different spiked drinking waters by the standard addition method with acceptable repeatability.

In general terms, PIM-based methods have demonstrated satisfactory results for the determination of arsenic in water samples. However, each methodology possesses specific characteristics that make them suitable for different purposes. In the case of the PIM-based device, thanks to its simplicity and cost-effective characteristics, it would be a good choice to be applied in remote areas as a sort of testing field kit. Conversely, the FA method possesses distinct features related to flow methods, particularly the fact that preconcentration and detection are performed in an integrated mode. This feature results in the minimization of error associated with sample treatment and also increases sample

throughput, which could be of interest for analytical laboratories devoted to the detection of arsenic in waters.

As an alternative methodology, in this thesis we have also investigated the use of the commercial sorbent Adsorbsia As600, which is specially designed for the removal of arsenic in waters, for analytical purposes. This sorbent is based on TiO_2, the crystalline form of anatase with a small proportion of gypsum, and an average size of 7 nm.
The experimental capacity of the sorbent was evaluated under batch conditions, obtaining values of 0.14 mmol g^{-1} (10.1 mg g^{-1}) for As(V) and 0.21 mmol g^{-1} (16.5 mg g^{-1}) for As(III), at pH of 7.3, demonstrating the good performance of this material to adsorb both inorganic forms of arsenic present in natural waters. The fact that no previous oxidation of As(III) to As(V) is needed exposes this methodology as an attractive possibility to be taken into account when the aim is to determine total arsenic content in water.

The presence of major anions commonly found in natural waters did not disturb the efficiency of the system, as happens when sorbents based on an ion exchange mechanism are used. Only the presence of 100 mg L^{-1} of silicate clearly diminished arsenic adsorption, demonstrating that this sorbent is less sensitive to anionic interferences.

Even though it is stated by the manufacturer that Adsorbsia As600 cannot be regenerated, we investigated the elution of retained arsenic species to allow its detection by ICP-OES. Among the elutants tested, only NaOH provided good results, although the elution was not quantitative and deteriorated the sorbent. Percolating 50 mL of solution through a minicolum packed with 60 mg of sorbent and using 2 mL of 0.5 M NaOH as elutant, an LOD of 40 μg L^{-1} of arsenic was obtained. This LOD could be easily decreased by using a larger amount of sample due to the high capacity of the sorbent.

The good results in terms of As adsorption using this TiO_2 based sorbent could be further explored, using, for example, this sorbent for the online preconcentration of both inorganic arsenic species in a FA system or as a material to be incorporated into PIMs in order to modify their properties. In the literature, different examples of the addition of inorganic nanoparticles into polymeric membranes can be found, such as the inclusion of gold [10], palladium [11] or SiO_2 nanoparticles [12].

4.2 Advances on PIMs

Despite the attractive features of PIMs, such as simplicity in preparation and handling, different improvements are required to boost the applicability of this technique. On the one hand, it is of utmost importance to explore new carriers to further enhance stability of the membrane, and on the other, to develop new preparation routes avoiding the use of harmful chemicals. In addition, focusing on a green membrane process, not only the reduction of organic solvents is desirable, but the use of biodegradable or renewable materials to replace oil-derived plastics is advisable.

To evaluate how slight differences on the components of the PIM affected the physicochemical and electrical characteristics as well as membrane stability and efficiency, we prepared Aliquat 336 derivatives to be incorporated as carriers in PIMs. Hence, we obtained the derivatives $AlqNO_3$ and AlqSCN and they were used to prepare PIMs, along with the commercial compound AlqCl, with a composition of 30% or 60% (w/w) in CTA. PIMs were fully characterized by different techniques. The morphology of the resulting membranes was evaluated by means of SEM images. As shown in Figure 4.1, PIMs containing 30% of IL (see Figure 4.1 a1, b1 and c1) presented a dense, smooth surface. Likewise, the same morphology was obtained for a PIM containing 60% of the IL AlqCl (see Figure 4.1 a2), whereas PIMs based either on $AlqNO_3$ or AlqSCN presented spherical deposits on the surface (see Figure b2 and c2, respectively). This appearance can be due to an aggregation of the IL, maybe due to low compatibility with the polymer CTA, which is not observed in the case of AlqCl. Despite the presence of these deposits on the surface, apparently none of the membranes presented an oily texture, which indicated the totality of the IL was incorporated in the PIM.

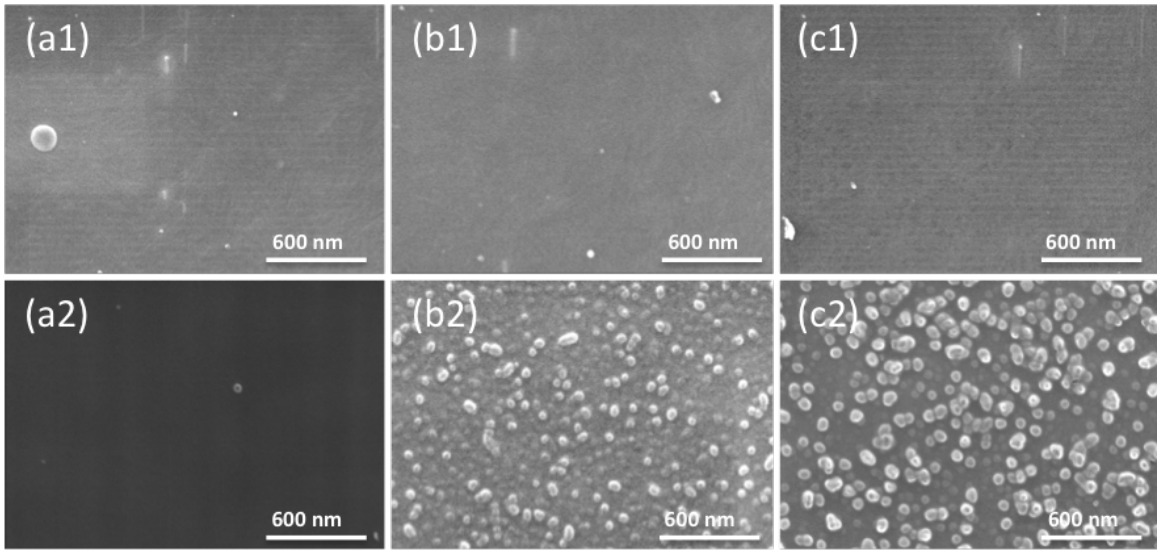

Figure 4.1 Surface SEM images of different PIM compositions: (a1) 70% CTA – 30% AlqCl, (b1) 70% CTA – 30% $AlqNO_3$, (c1) 70% CTA – 30% AlqSCN and (a2) 40% CTA – 60% AlqCl, (b2) 40% CTA – 60% $AlqNO_3$, (c2) 40% CTA – 60% AlqSCN.

PIMs were also analysed by means of other techniques to characterize the bulk material. XPS measurements showed that despite the nature of the counter-anion, all ILs were present on both surfaces of the membrane, ensuring the availability of the carrier for the extraction reaction that takes place in the interface aqueous solution-membrane. Likewise, FTIR measurements also confirmed the suitability of the PIM preparation procedure providing information about the bulk composition, and showed that no band displacement was observed compared to the FTIR analysis of the pure compounds. Moreover, TGA measurements also demonstrated the suitability of the membrane preparation procedure.

It was also important to evaluate how the modified ILs could have an impact on parameters such as hydrophobicity and electrochemical behaviour. Moreover, acid transport was also measured to investigate the passive transport of species. Table 4.2 collects the values of contact angle measurements, IS and acid diffusion (indicated as pH variation) for each of the investigated membranes.

Table 4.2 Effect of PIM composition on different membrane parameters. Standard deviation is given in parentheses based on three replicates.

PIM	% IL	Contact angle (º)	σ_m $(\Omega.m)^{-1}$	ε_m	pH variation
AlqCl	30	42 (3)	1.22×10^{-6}	8.2	2.3 (0.2)
	60	24 (4)	1.68×10^{-3}	14.4	3.3 (0.1)
$AlqNO_3$	30	48 (3)	1.11×10^{-6}	7.8	1.7 (0.2)
	60	41 (3)	1.48×10^{-3}	13.6	3.0 (0.6)
AlqSCN	30	57 (3)	3.61×10^{-7}	6.4	0.38 (0.02)
	60	56 (4)	4.48×10^{-4}	8.0	2.1 (0.3)

As shown in Table 4.2, PIMs containing 60% of the different IL displayed higher membrane conductivity by three orders of magnitude compared to PIMs with a lower IL content. PIMs containing the IL AlqSCN had less polar characteristics and, as expected, the lowest conductivities. In terms of dielectric constant, PIMs containing AlqCl or $AlqNO_3$ revealed similar values, whereas the lowest values were obtained when using IL AlqSCN.

Contact angle values were in concordance with the hydrophobicity of the counter anion used in the corresponding IL-based PIM, following the trend $SCN^- > NO_3^- > Cl^-$. However, relevant differences were observed depending on the IL content. In the case of the commercial IL AlqCl, a 40% reduction in the contact angle was obtained with the increase in IL content, while a 15% decrease was found in the case of $AlqNO_3$. When the IL was AlqSCN, the hydrophobic character of the PIM was only slightly modified because of the high stability of the ion-pair formed using this IL. To correlate the hydrophobicity of the PIM with its stability, some experiments were conducted to investigate the possible leaching of the IL to the aqueous solutions. PIM stability was investigated by measuring the mass change of segments when contacted (for 24h under agitation) with either 25 mL of ultrapure water or a 0.1 M NaCl solution. Results are presented in Table 4.3, which shows that stability follows the trend AlqCl < $AlqNO_3$ <

AlqSCN, and that, as expected, PIMs are less stable in ultrapure water than in a saline solution. The fact that stability follows this trend can be attributed to the formation of more stable ion pairs between the cation trioctylmethyl ammonium (Alq^+) and the more lipophilic anions, and thus, it is in concordance with contact angle measurements.

Table 4.3 Mass loss of PIMs after being immersed in ultrapure water or 0.1M NaCl solution for 24 h. Standard deviation is given in parentheses based on three replicates.

		Mass loss average (SD)	
PIM	**IL %**	**Ultrapure water**	**0.1 M NaCl**
AlqCl	30	18.5 (0.6)	3.7 (0.9)
	50	38.5 (0.7)	11 (6)
$AlqNO_3$	30	10.5 (0.9)	6 (2)
	50	17 (1)	8 (2)
AlqSCN	30	3 (1)	1.9 (0.3)
	50	5 (2)	3 (1)

The diffusive transport of HCl across the membranes follows the same trend as the hydrophilic character of the PIMs studied: 60% AlqCl > 30% AlqCl ~ 60% $AlqNO_3$ > 30% $AlqNO_3$ > AlqSCN. The more hydrophilic the membrane is, the higher the solvating capacity of the IL to form a complex with HCl.

To evaluate not only the diffusive but the effective transport of a species by interacting with the IL, we conducted transport experiments with As(V) at pH 7 using the PIMs with 50% $AlqNO_3$ to be compared with results obtained with a PIM with 50% AlqCl [13]. The stripping phase consisted of a 0.1 M solution of the corresponding sodium salt (i.e. $NaNO_3$ or NaCl) in order not to modify the IL composition of the PIM. The transient As(V) concentration profiles in both the feed and stripping solutions for both PIMs are shown in Figure 4.2. As can be seen, transport is strongly affected by the IL used. In the case of AlqCl, As(V) is quantitatively transported to the stripping phase while in the case of $AlqNO_3$, transport efficiency is only 10%. This fact seems to indicate that the ion pair formed by Alq^+ and NO_3^- is more stable than the ion pair needed to extract As(V) (which can be represented as Alq^+ $H_2AsO_4^-$), and hence, extraction/transport, is

less favourable. This result indicates that the use of more stable membranes can lead to a loss of efficiency, which is not acceptable.

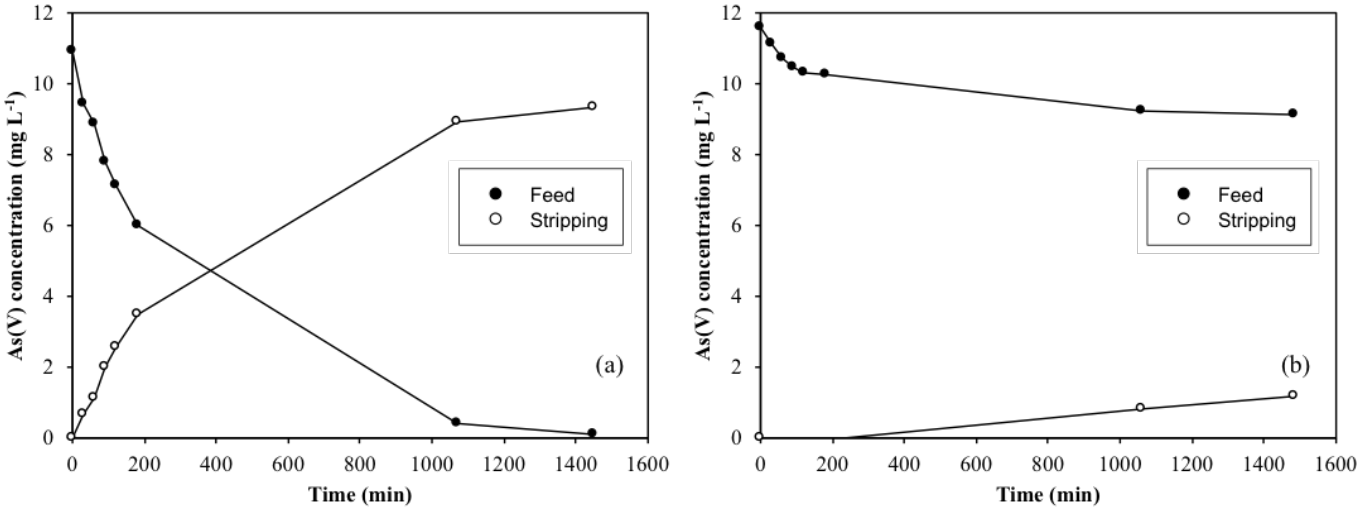

Figure 4.2 Transient concentration curves in As(V) transport experiments involving 50% (w/w) CTA – 50% (w/w) AlqCl (a) and 50%(w/w) CTA – 50%(w/w) $AlqNO_3$ (b). (Experimental conditions: feed solution: 10 mg L^{-1} As(V), pH = 7; stripping solution: 0.1 M NaCl in (a) and 0.1M $NaNO_3$ in (b)).

Given this, we investigated the efficiency of a PIM made up of 50% CTA – 50% AlqCl used repeatedly in successive experiments for the transport of As(V) during 6 cycles of 24 h each. An average transport efficiency of 75 ± 9% was obtained, which shows that even though the use of AlqCl can lead to some losses of the carrier, the PIM is very effective in terms of transport and can be used for long-term experiments.

The other approach investigated in this thesis is based on the preparation of PIMs. Membranes are traditionally prepared by dissolving the corresponding amount of polymer in a certain volume of organic solvent. Despite the simplicity of this procedure, it requires the use of harmful organic solvents, which is an important drawback. So far, PVC and CTA have been the polymers most used by researchers for the preparation of PIMs. CTA needs solvents such as chloroform or dichloromethane (10 mL for 0.1 g of polymer), whereas PVC is dissolved using tetrahydrofuran (5 mL for 0.1 g of polymer). Therefore, in this thesis we have explored the possibility of reducing the impact on the environment through a solvent-free procedure to obtain PIMs based on a thermal-compression procedure. The thermal-compression procedure consists of mixing the membrane components in a molten state and subsequently compressing the mixture to

obtain a thin film. The main consideration to be taken into account when using this procedure, is the thermal stability of membrane components. PVC or CTA are not advisable polymers due to the very high temperatures required to reach the melting point. Hence, two thermoplastic polymers were tested with good feasible characteristics, namely TPU and PCL. A high percentage of the polymer TPU is produced from renewable sources, whereas PCL is a biodegradable polymer that can decompose in the media after its use. Membranes were prepared by mixing these polymers with Aliquat 336 at 30% content (w/w) by the thermal compression technique, and the obtained films were characterized by elemental analysis, TGA and SEM. Elemental analysis results correlated with the expected composition of the membranes. However, when TGA analysis was conducted in the case of membranes based on PCL, it was shown that a partial decomposition of Aliquat 336 shifted to higher temperatures, which could be explained by certain interactions between the IL and the polymeric matrix.

With regard to the SEM images, TPU-based membrane presented a porous structure with the presence of nano-pores, whereas the membrane constituted by PCL showed a dense structure with some cavities. Nevertheless, the presence of these nano-pores or cavities in both membrane compositions, did not affect the extraction abilities of Aliquat 336, which was tested using a PIM segment immersed in a Cr(VI) solution. It is well known that chromate is extracted by Aliquat 336 by an ion-exchange mechanism, and in our study, both PIMs made of PCL and TPU effectively extracted the metal. Moreover, the stability of the PIMs was also investigated, and it was found that PCL-based membranes are the most stable and thus, can be an attractive polymer to be taken into account to prepare more eco-friendly and stable PIMs.

We have proved in this thesis the possibility of tuning PIM characteristics by changing the counter-anion of a quaternary ammonium IL that can be of a great interest depending on its application. Besides, a promising scenario towards greener membrane preparation is opened using eco-friendly materials and avoiding the use of harmful reagents, drastically reducing their impact on the environment.

4.3 Novel PIM applications

As presented in the previous sections, PIM systems are commonly employed for the extraction, transport or removal of different analytes by using appropriate carriers in

a mechanism based on the facilitated transport of target analytes against their concentration gradient. However, new applications are yet to be explored. Thus, in this thesis we have evaluated PIMs for speciation studies, measuring the free metal fraction in the presence of different organic ligands.

To this end, we explored the use of PIMs for the first time for measuring metal speciation in aqueous solutions, in particular, zinc, in the absence and presence of organic ligands. We then compared the obtained flux measurements to the metal uptake by a living organism (*i.e.* a potato plant), as a tool to predict plant exposure. Metals can be found in the media in different chemical forms, such as free ions, and inorganic or organic complexes with different stabilities and charges. If we consider that the metal flux through the membrane depends on the different species, flux measurements can provide information about metal speciation. This hypothesis has been previously explored with supported liquid membranes (SLMs) [14–16], but not yet with PIMs. Thus, we studied the flux of zinc from a nutrient solution using a PIM composition of 70% PVC – 30% D2EHPA and a receiving composition of 0.01M HNO_3. In contrast to the previously mentioned ion-exchanger, Aliquat 336, the carrier D2EHPA presents great selectivity towards Zn^{2+} and often acts as a carrier following a counter-transport mechanism; in this case, a crossed transport of protons and metallic ions takes place [17]. No significant variations in terms of zinc flux were observed between 24 and 48 h of deployment time, demonstrating that the system was under steady-state regime and also highlights the great stability that PIMs present compared to other types of liquid membranes, such as SLM, making the use of PIMs a suitable technique for long-term experiments. No depletion of the analyte was observed either.

The J_{PIM} was evaluated by varying total metal concentration (ranging from 3 up to 70 μM) without the addition of organic ligands. Results showed a linear correlation to the free metal concentration, according to MINTEQ calculations, in the donor phase. In addition, we tested two zinc concentrations 35 and 70 μM in the presence of different organic ligands namely EDTA, citrate and HA. Our results showed that J_{PIM} was decreased in all cases due to the presence of the organic ligands as there was a reduction in the free metal fraction. This fact supports that PIM measurement can be used as a speciation technique for the determination of free zinc concentrations.

Considering the obtained results and taking into account different hypotheses we managed to formulate a simple model for J_{PIM} as shown in the following equation (Eq. 4.1):

$$J_{\mathrm{PIM}} \approx \frac{\dfrac{K\left(c_{\mathrm{T,L}}/2\right)^{3/2}}{\left(\left[\mathrm{H}^{+}\right]^{*}\right)^{2}}}{\dfrac{\ell}{D^{\mathrm{m}}_{\mathrm{ZnL_2 \cdot HL}}} + \dfrac{K\left(c_{\mathrm{T,L}}/2\right)^{3/2}}{\left(\left[\mathrm{H}^{+}\right]^{\mathrm{A}}\right)^{2}} \dfrac{D^{\mathrm{A}}_{\mathrm{Zn^{2+}}}}{\delta^{\mathrm{A}}}} \left[\mathrm{Zn}^{2+}\right]^{*} \qquad (4.1)$$

This equation justifies the linearity of the steady state with Zn^{2+} concentration and the lack of impact of labile complexes present in the donor solution. Moreover, a higher flux is expected with an increase in the acidity of the acceptor phase as well as with an enhanced total carrier concentration. In addition, some other information can be derived from the previous equation such as a certain limitation by diffusion in both the membrane and in the acceptor solutions. If membrane thickness and the carrier concentration are evaluated over a range of values, PIM could be used to measure labile fractions or again the free fraction.

On the other hand, we wanted to correlate the resulting J_{PIM} obtained in the presence of the different ligands compared to the plant metal uptake in the same media. Other authors have also performed metal uptake studies using higher plants, such as wheat [18] or spinach plants [19,20]. Hence, we used the potato plant (*Solanum tuberosum*) as another alternative. Before conducting flux measurements, we wanted to demonstrate root viability to ensure that root cells were still alive after being in contact with the different medias (i.e. EDTA, HA, citrate or histidine). Only the ligand histidine caused toxicity to the roots reducing the number of living cells, and therefore, further experiments were not conducted using this ligand.

When comparing J_{PIM} and J_{root}, a non-satisfactory correlation was observed in the presence of the different organic ligands. These results suggest that metal uptake in roots is highly dependent on many factors, which can result in a higher than expected metal uptake, as shown in Figure 4.3.

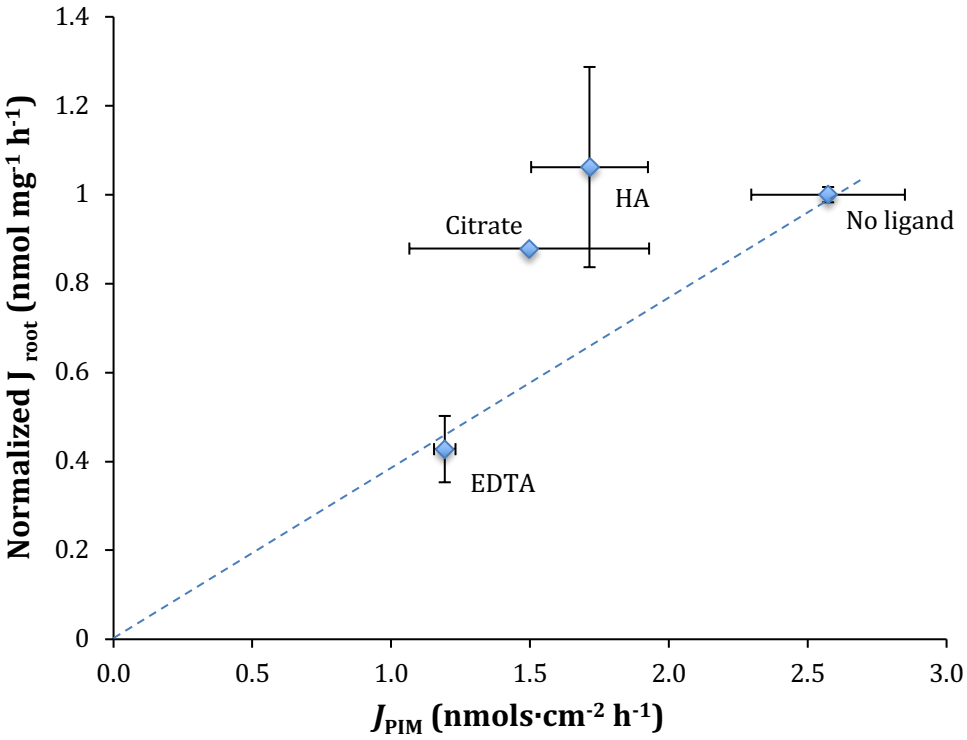

Figure 4.3 Correlation between normalized J_{root} and J_{PIM} (35 µM Zn treatment and supplemented with EDTA, HA and citrate as ligands).

When either HA or citrate were added into the media, similar metal plant uptakes were obtained compared to the fluxes without ligand. In the case of citrate this expected metal internalization is attributed to dissociation of metal complexes in the surroundings of the root, leading to a higher uptake. Likewise, the presence of HA induced the formation of more lateral roots enhancing the surface area and, in consequence, the metal uptake. Viability and physiological changes of roots lead to different behaviours, which are not taken into account when PIM is used as a predicting tool for metal internalization in plants.

These results show that a PIM-based system can be suitable for the measurement of free metal species, Zn^{2+} in this case. However, as reported in other studies [18-20], the comparison of obtained results with metal accumulated in higher plants is still a big challenge to be addressed and, therefore, other different living organism systems should be used in future experiments to facilitate comparison.

A different use of PIMs has been presented, related to their use in sample preparation as a microscale extraction approach where no exhaustive extraction is needed

(microextraction techniques). For the first time, this methodology has been explored for the determination of selected pesticides (e.g. chlorpyrifos or CP, diazinon or DZ and cyprodinil or CYP) using GC-MS.

In contrast to previous PIM systems, in which a carrier was required in order to achieve transport through the membrane, the PIM-assisted extraction method does not require the addition of a carrier as the mechanism is based on sorption/solubilization and only a base polymer plus a plasticizer are needed (i.e. 70% CTA – 30% NPOE).
Preliminary extraction and elution experiments were conducted with CP, showing that only 7% of the initial pesticide remained in the solution after 8 h of extraction, which means that quantitative extraction into the membrane was achieved. Better elution results and repeatability were obtained using 1mL of ACN and 15 min using UAE. Ultrasounds clearly helped to release the retained pesticide into the organic solvent reducing the total elution time.

In terms of extraction efficiency, only slight differences were obtained using different agitation modes for the three pesticides tested. Rotary agitation was selected for further experiments due to higher reproducibility. Since extraction occurs by the solubilization of pesticides into the membrane matrix with the aid of the plasticizers, different plasticizers were incorporated in membranes (i.e. DBS, BBPA and NPOE) and evaluated. NPOE, bearing the highest dielectric constant, allows better solubilization of polar pesticides than the ones studied. Therefore, NPOE was selected to conduct extraction experiments.

In terms of method validation, the PIM-assisted extraction method only showed small matrix effect (ME), which is a clear advantage if compared to other methods where an extensive clean-up must be carried out in order to remove interferences. Indeed, the absolute recovery (AR), is greater for CP (68 ± 5 at 100 ng L^{-1} and 70 ± 5 at 250 ng L^{-1}) as is the pesticide with the highest log K_{ow} value and therefore, presenting a major affinity towards NPOE.

PIM-assisted extraction methods showed comparable MDL to other existing extraction methods and improved EPA methods, as summarized in Table 4.4. The method detection limits (MDLs) of the PIM-assisted extraction method were below the ones reported in the EPA methods. Moreover, it would be expected that this value could be further reduced if a greater sample volume had been used to conduct the extraction experiments.

Table 4.4 Comparison of the PIM-assisted extraction method with EPA methods.

Method	Instrument	Pesticide	Method detection limit (μg L^{-1})	Sample Volume (mL)	Final Volume (mL)
LLE (EPA 622)	GC-FPD	CP	0.3	1000	5
		DZ	0.6	1000	5
LLE (EPA 614)	GC-FPD	DZ	0.012	1000	5
LLE (EPA 507)	GC-NPD	DZ	0.1	1000	5
LSE (EPA 525.2)	GC-MS	CP	0.044	1000	0.5
		DZ	0.11		
PIM-assisted extraction	GC-QqQ	CP	0.002	100	1
		DZ	0.003		
		CYP	0.023		

Our results revealed that this method successfully allowed the detection of CP in river water at trace level demonstrating its efficiency and feasibility for the analysis of real environmental samples. It must be highlighted that this method demonstrates the suitable use of a membrane sorbent, which can easily be prepared and modified, by choosing the plasticizer, in order to achieve the desired selectivity towards the target analyte.

4.4 Future perspectives

Considering all the previous studies presented in this thesis, and evaluating their advantages and drawbacks, different endeavours can be defined for future exploration.
In the case of arsenic measurements, the FA method should be explored for the determination of As(V) in other samples such as river water and groundwater. In addition, the use of an extraction cell with a different configuration, such as LOD and sample throughput, should be tested with the aim of enhancing the analytical features of the

methodology. Moreover, the As(III) analysis could be achieved by incorporating an oxidation step before introducing the sample into the system. One of the simplest options would be the use of ozone to achieve this oxidation, although the total method cost would be increased. In addition, another novel FA system including a PIM as a preconcentration step could be developed for the online high-throughput analysis of different target compounds, such as nutrients, metals or relevant organic compounds (i.e. pesticides, endocrine disruptors, among others).

With regard to further improving stability and membrane performance, PIMs based on the polymer PVDF-HFP have appeared as an attractive alternative to conventional polymers. Moreover, they can be combined with PEG-DMA, allowing the fabrication of cross-linked PIMs by ultraviolet irradiation. The high degree of entanglement of the polymeric matrix in crosslinked PIMs leads to a significant increase in both membrane stability and permeability, as reported in the literature [21]. Therefore, a wide range of possibilities are yet to be fully explored.

Future PIM studies must consider sustainability during the fabrication of the membrane itself by exploring more eco-friendly materials, and reducing or eliminating waste generation. To this end, an improvement in the solvent-free preparation of polymer inclusion membranes with an ionic liquid must be conducted and endeavours to find new polymers are recommended.

Considering the better stability of PIMs compared to other types of liquid membranes (i.e. PLMs), which have traditionally been employed for this purpose, it would not be unreasonable to think that several future studies will further explore metal speciation based on the use of PIMs, as presented for the first time in this thesis.

The full potential of PIMs to be used as a sorbent appears to be a very competitive alternative to other traditional techniques, such as SPE, due to their low cost, easy preparation and high selectivity. PIMs can be used in future studies for the extraction of new contaminants or other compounds by simply tuning their affinity towards the target of interest.

References

[1] C. Fontàs, R. Vera, A. Batalla, S.D. Kolev, E. Anticó, A novel low-cost detection method for screening of arsenic in groundwater., Environ. Sci. Pollut. Res. 21 (2014) 11682–8.

[2] V. Cerdà, L. Ferrer, J. Avivar, A. Cerdà, Chapter 1 - Evolution and Description of the Principal Flow Techniques, in: V. Cerdà, L. Ferrer, J. Avivar, A.B. Cerdà (Eds.), Elsevier, Boston, 2014: pp. 1–42.

[3] L. Skeggs, An Automatic Method for Colorimetric Analysis, Am. J. Clin. Pathol. 28 (1957) 311–322.

[4] L.O. Leal, R. Forteza, V. Cerdà, Speciation analysis of inorganic arsenic by a multisyringe flow injection system with hydride generation-atomic fluorescence spectrometric detection, Talanta. 69 (2006) 500–508.

[5] Y. Zhang, M. Miró, S.D. Kolev, Hybrid flow system for automatic dynamic fractionation and speciation of inorganic arsenic in environmental solids, Environ. Sci. Technol. 49 (2015) 2733–2740.

[6] L.L. Zhang, R.W. Cattrall, S.D. Kolev, The use of a polymer inclusion membrane in flow injection analysis for the on-line separation and determination of zinc, Talanta. 84 (2011) 1278–1283.

[7] D.S. De Jesus, R.J. Cassella, S.L.C. Ferreira, A.C.S. Costa, M.S. De Carvalho, R.E. Santelli, Polyurethane foam as a sorbent for continuous flow analysis: Preconcentration and spectrophotometric determination of zinc in biological materials, Anal. Chim. Acta. 366 (1998) 263–269.

[8] E. Punrat, C. Maksuk, S. Chuanuwatanakul, W. Wonsawat, O. Chailapakul, Polyaniline/graphene quantum dot-modified screen-printed carbon electrode for the rapid determination of Cr(VI) using stopped-flow analysis coupled with voltammetric technique, Talanta. 150 (2016) 198–205.

[9] B. Lešniewska, L. Trzonkowska, E. Zambrzycka, B. Godlewska-Zyłkiewicz, Multi-commutation flow system with on-line solid phase extraction exploiting the ion-imprinted polymer and FAAS detection for chromium speciation analysis in sewage samples, Anal. Methods. 7 (2015) 1517–1526.

[10] Y.Y.N. Bonggotgetsakul, R.W. Cattrall, S.D. Kolev, The preparation of a gold nanoparticle monolayer on the surface of a polymer inclusion membrane using EDTA as the reducing agent, J. Memb. Sci. 379 (2011) 322–329.

[11] Y.Y.N. Bonggotgetsakul, R.W. Cattrall, S.D. Kolev, A method for coating a polymer inclusion membrane with palladium nanoparticles, React. Funct. Polym. 97 (2015) 30–36.

[12] X. Zuo, S. Yu, X. Xu, J. Xu, R. Bao, X. Yan, New PVDF organic-inorganic membranes: The effect of SiO_2 nanoparticles content on the transport performance of anion-exchange membranes, J. Memb. Sci. 340 (2009) 206–213.

[13] R. Güell, E. Anticó, S.D. Kolev, J. Benavente, V. Salvadó, C. Fontàs, Development and characterization of polymer inclusion membranes for the separation and speciation of inorganic As species, J. Memb. Sci. 383 (2011) 88–95.

[14] A. Gramlich, S. Tandy, V.I. Slaveykova, A. Duffner, R. Schulin, The use of permeation liquid membranes for free zinc measurements in aqueous solution, Environ. Chem. 9 (2012) 429–437.

[15] V.I. Slaveykova, N. Parthasarathy, J. Buffle, K.J. Wilkinson, Permeation liquid membrane as a tool for monitoring bioavailable Pb in natural waters., Sci. Total Environ. 328 (2004) 55–68.

[16] S. Bayen, I. Worms, N. Parthasarathy, K. Wilkinson, J. Buffle, Cadmium bioavailability and speciation using the permeation liquid membrane, Anal. Chim. Acta. 575 (2006) 267–273.

[17] M. Resina, J. Macan, J. De Gyves, M. Mu, Zn(II), Cd(II) and Cu(II) separation through organic–inorganic Hybrid Membranes containing di (2-ethylhexyl) phosphoric acid or di-(2-ethylhexyl) dithiophosphoric acid as a carrier, J. Memb. Sci. 268 (2006) 57–64.

[18] A. Gramlich, S. Tandy, E. Frossard, J. Eikenberg, R. Schulin, Availability of zinc and the ligands citrate and histidine to wheat: Does uptake of entire complexes play a role?, J. Agric. Food Chem. 61 (2013) 10409–10417.

[19] F. Degryse, E. Smolders, R. Merckx, Labile Cd complexes increase Cd availability to plants, Environ. Sci. Technol. 40 (2006) 830–836.

[20] F. Degryse, E. Smolders, H. Zhang, W. Davison, Predicting availability of mineral elements to plants with the DGT technique: A review of experimental data and interpretation by modelling, Environ. Chem. 6 (2009) 198–218.

[21] Y. O'Bryan, Y.B. Truong, R.W. Cattrall, I.L. Kyratzis, S.D. Kolev, A new generation of highly stable and permeable polymer inclusion membranes (PIMs) with their carrier immobilized in a crosslinked semi-interpenetrating polymer network . Application to the transport of thiocyanate, J. Memb. Sci. 529 (2017) 55–62.

CHAPTER 5

Conclusions

The general main conclusions extracted from the research conducted in this thesis are summarised as follows:

- A simple and cost-effective analytical methodology based on the use of a PIM consisting of CTA and Aliquat 336, placed in a special device, has been used for the satisfactory arsenate preconcentration of a 2 M NaCl solution after 5 h of contact time. This methodology has allowed the determination of arsenate from different groundwater samples.

- A FA system has been developed for the first time, implementing an on-line preconcentration and extractive separation of arsenate (using a PIM made of 70% PVDF-HFP – 30% Aliquat 336), and subsequently reduced to arsine, which is spectrophotometrically detected after its on-line gas-diffusion separation. The method allowed the determination of arsenate at the low μg L^{-1} level by the multi-point standard addition method, making it an attractive methodology for arsenic determination in drinking waters.

- The determination of both inorganic arsenic species has been accomplished using the TiO_2-based sorbent Adsorbsia As600, that has been used, for the first time, for analytical applications. We have established the setup and the experimental conditions for using this sorbent for As(V) and As(III) preconcentration prior to its determination with ICP- OES and good recoveries and reproducibility were obtained. A detection limit of 40 μg L^{-1} for a sample volume of 50 mL was obtained using 2 mL of 0.5 M NaOH as elutant.

- We have demonstrated that new Aliquat 336 derivatives can be successfully prepared by a liquid-liquid exchange process. Impedance spectroscopy and membrane potentials have been used for the electrochemical characterization that PIMs prepared with the new ionic liquids. Higher conductivity and dielectric constants were obtained for membranes containing AlqCl and $AlqNO_3$ compared to those with AlqSCN.

- The hydrophilic character and transport efficiency of PIMs was found to follow the sequence AlqCl > $AlqNO_3$ > AlqSCN, whereas stability followed the opposite order.

- Greener PIM preparation strategies have been presented for the first time, dismissing the use of toxic organic solvents for their preparation as well as employing more eco-friendly polymers. Membranes consisting of the biodegradable polymer PCL, showed great stability without compromising good performance in terms of Cr(VI) extraction.

- A simple device based on a PIM consisting of 70% PVC – 30% D2EHPA has been used for the first time, for the determination of free zinc concentrations in aqueous samples in the absence and presence of the organic ligands: EDTA, citrate and HA. J_{PIM} fluxes were compared to metal uptake by potato root plants, showing that in the case of citrate and HA, direct proportionality between total metal and root uptake was obtained, whereas in the presence of EDTA this relationship was observed for the free metal fraction.

- A simple and novel microextraction methodology based on the use of a 70% CTA – 30% NPOE PIM as a sorbent for the effective preconcentration of three pesticides, namely CP, DZ and CYP. An extraction time of 6 h and elution using 1 mL of ACN allowed the detection of CP in river water at a concentration of 36 ng L^{-1}.